THESE de doctorat en Cotutelle

Pour obtenir le grade de Docteur délivré par

Université de Lille

Ecole Doctorale Sciences de la Matière, du Rayonnement et de l'Environnement

Université Libanaise

Ecole Doctorale Sciences et Technologie

Spécialité: Chimie

Présentée et soutenue publiquement par

ADHAMI Wissal

le 17 Décembre 2020

Synthèse verte de polymères dans un système en flux

Dr Christian ROLANDO	Directeur de recherche émérite au CNRS, Université de Lille	Directeur de thèse
Pr Youssef BAKKOUR	Professeur, Université Libanaise	Directeur de thèse
Pr Christelle DELAITE	Professeur, Université de Haute-Alsace	Rapporteur, Présidente
Pr Sandra VAN VLIERBERGHE	Professeur, Université de Ghent	Rapporteur
Dr Abdelkarim EL OMAR	Professeur, Université Libanaise	Examinateur
Dr Mohamad EL ETER	Professeur, Beirut Arab University	Examinateur

© 2020 Tous droits réservés.

lilliad.univ-lille.fr

OUTLINE

The aim of this work is to highlight the green chemistry in polymers' synthesis (especially for polyesters) in a flow system. To this purpose, we used a tubular reactor made of fluorinated ethylene propylene (FEP), where kinetic studies were developed in order to show improvements in polymerization compared to the case in batch reactors already present.

Chapter 1 introduces the different polymers synthetic pathways and microflow technology; explaining how this latter evolves the progress of polymerization.

Chapter 2 focuses on the enzymatic ring opening polymerization (*e*-ROP) of lactones. These reactions were catalyzed by immobilized lipase Novozyme 435® after being introduced into the tubular reactor.

Chapter 3 presents a second catalytic route for ROP of lactones, in which we used phosphazene superbases (PBs) instead of the lipase. The effect of the catalyst's basicity on the progress of lactones ROP is as well further detailed.

Chapter 4 develops the polycondensation of diacids or diesters with diols in batch using organo-based catalysts that present hydrophobic parts in their structures.

Chapter 5 provides controlled photopolymerization of methyl methacrylate in flow using the organocatalyst Eosin Y and green LEDs.

Chapter 6 resumes the main conclusions of the previous chapters.

Chapter 7 describes the experimental parts of the work as well as the characterization of synthetized polymers by Mass Spectrometry (MS), Nuclear Magnetic Resonance (NMR) and Gel Permeation Chromatography (GPC).

© 2020 Tous droits réservés.

lilliad.univ-lille.fr

ACKNOWLEDGMENTS

And here we begin with the emotional section in this long report. In September 2017, I had the acceptance of what has been until now the most important experience lived through in my life to the moment my PhD thesis enrolment. I left my hometown "Tripoli" and I reached "Lille" that became my second country, where I lived unforgettable moments. Words are not enough to express my highest gratitude for all people who stood up with me during the past three years of challenges, stress, laugh, cry and finally success.

First of all, I would like to thank my supervisor in France, **Dr. Christian Rolando** for all his guidance and support. I was so lucky doing my PhD project with an expert like you, and it was an honor to achieve my success under your supervision. Thank you so much for giving me the chance to be a member of your team.

My supervisor in Lebanon, **Pr. Youssef Bakkour** who trusted me and who was the reason that brought me to the MSAP lab starting from the master internship. Thank you for your trust and support during this challenging period. Your supervision was a credit for the work.

Pr. Ahmed Mazzah, the MSAP lab director, thank you for your prompting and support. Your intentions are always highly appreciated.

Pr. Fawaz El Omar, the LCA lab director, I appreciate your hard work to improve the scientific research in Lebanon. Thank you so much for your great efforts.

I am deeply grateful to have the external jury members **Pr. Christelle Delaite** (University of Haute-Alsace), **Pr. Sandra Van Vlierberghe** (University of Ghent), **Dr. Abdelkarim El Omar** (Lebanese University) and **Dr Mohamad El Eter** (Beirut Arab University). Thank you for your precious time that you gave for the evaluation of this work. I appreciate having such bright scientists as members of my dissertation committee.

© 2020 Tous droits réservés.

lilliad.univ-lille.fr

Special thanks to **Dr. Nathalie Azaroual, Mr. Alexandre Rech, Dr. Vincent Darcos, Mme. Aurélie Malfait** and **Dr. Julien Molina** for their contributions in polymer analysis.

I would like to thank the great chemists in the MSAP Lab **Dr. Maël Penhoat** and **Dr. Laetitia Chausset-Boissarie**. I appreciate every advice, discussion and encouragement that you gave me.

Mr. Christophe Penverne, I deeply appreciate your efforts, you have never delay to help, and we missed your touches in the Lab.

A special thanks goes to **Dr. Fabrice Bray**, who is not directly related to the work, but he is a source of positive vibes that can recharge you to continue your mission to the end.

I would like to thank **Ziad Mahmoud**, my colleague in the MSAP lab, who doesn't hesitate to help or cooperate when needed.

Big thanks to the wonderful MSAP team members including those who left: **Mélanie**, **Violaine**, **Amandine**, **Stéphanie**, **Stanislas**, **Katia** and **Wael**.

I would like to thank additionnally the trainees that I had the chance to work with and who gave me additional motivation with their high passion in research: **Amira**, **Rayan**, the excited **Isabel**, **Maïssa** and **Ogata**.

Manal and **Ranin**, we spent a lot of time together, strong moments in research, difficulties and good talks. Thank you so much for your permanent support. **Lamees,** the most adorable girl, I was lucky to spent even if less than a year with a girl like you in our lab. Be happy, there is no more “tjannabini”.

My big fans “paris girls”: my cousins **Sabine** and **Maya**, **Riham**, **Chayma** and **Iman**. With you girls I forgot that I am abroad. From “*Lahloubet al Masareh*”- the title you gave me - thank you so much for such moments.

© 2020 Tous droits réservés.

lilliad.univ-lille.fr

My friends in Lille: **Siveen**, **Nour** and **Mohamad**, I spent my quality time with you guys. You endured my madness and enjoyed my laughs. Thank you for every shared moment that we had, I love you so much.

And what can I say to the craziest girl I have ever met!! **Marie**, an expert partner in kitchen crimes, I will miss your exceptional laugh, our words and your instant understanding. Thank you so much for your listening, help and support all the time with much of love.

Uncommon and deep thanks goes to my oldest friendship **Rim,** I want to use our words: we were and will be always "side by side". From Lebanon to France, the distance didn't affect your support and deeply love. You are the best and I love you so much.

Thanks from the heart to my biggest supporters. The one and only, a real man and a big brother **Ahmad** and the two great men **Rabii** and **Khalil**.

People who nobody can be like them are my big family, the eternal love of my life. Sisters and brother: my second mom **Racha**, caring **Ghina**, Crazy **Mariam,** lovely **Soumayraa** and our man, my backbone **Abdelrahman.** And yeah, there is an additional member – The first grandchild, our king – **Abdallah.** Without you guys, I wouldn't be able to reach my goals. Thank you so much for all your care, love, interest and your undescriptive support. One day I will tell your little angels, the prince **Tarek, Zeina, Zaynab, Roukaya, Laureen, Mahmoud and Omar** that they played an emotional role in this project pathway.

And last but not least, Mom and Dad, for me "*Zanzoun*" and "*Abou l abed*". You both are the reason for what I am today. I really can't find the words to express what I feel towards you. You are the unique example of unconditional love; you were the source of my power, my energy and my determination. For the moment, I don't have more than "Thank you and I love you so much" to tell you.

© 2020 Tous droits réservés.

lilliad.univ-lille.fr

To my Family

© 2020 Tous droits réservés.

lilliad.univ-lille.fr

TABLE OF CONTENTS

© 2020 Tous droits réservés.

lilliad.univ-lille.fr

© 2020 Tous droits réservés.

lilliad.univ-lille.fr

© 2020 Tous droits réservés.

lilliad.univ-lille.fr

© 2020 Tous droits réservés.

lilliad.univ-lille.fr

© 2020 Tous droits réservés.

lilliad.univ-lille.fr

© 2020 Tous droits réservés.

lilliad.univ-lille.fr

LIST OF ABBREVIATIONS

3

3-phenyl-1-propanol..... *PP*

A

AAc .....*adipic acid*

ACN..... *Acetonitrile*

AIBN .....*Azobisisobutyronitrile*

ATRP ..... *atomic transfer radical polymerization*

B

BA*Buthylacrylate*

BDO.....*1,4-butanediol*

BTPP.....*P1-t-Bu-tris(tetramethylene)*

C

CA ..... *Candida cylindracea*

CALB.....*lipase B from Candida. Antarctica*

CC *Candida Cylindracea*

CLRP .....*controlled/living radical polymerization*

CRP ..... *Controlled Radical Polymerization*

CSA..... *Camphorsulfonic acid*

CTPB.....*Cyclic Trimeric Phosphazene Base*

Cu ..... *Copper*

D

Đ .....*Dispersity*

DCM..... Dichloromethane

DDL *12-dodecano-lide*

DMAEMA .....*2-(dimethylamino)ethyl methacrylate*

DMF .....*dimethylformamide*

DMSO.....*Dimethyl sulfoxide*

DP ..... *Degree of polymerization*

DPAT .....*diphenylammonium triflate*

© 2020 Tous droits réservés.

lilliad.univ-lille.fr

E

EBiB.....*ethyl α-bromoisobutyrate*

EBPA ..... *ethyl α-bromophenylacetate*

EM.....*Enzyme Activated Monomer, enzyme activated monomer*

e-ROP.....*Ring Opening Polymerization*

F

FEP..... *Fluorinated Ethylene Propylene*

G

GL ..... *Glycolic acid*

GPC..... *Gel Permeation Chromatography*

H

HDL *16-hexadecanolide*

HEMA..... *2-hydroxyethyl methacrylate, 2-hydroxyethyl methacrylate*

HiC ..... *Humicola insolens*

HPLC..... *High Performance-Liquid Chromatography*

I

i.d ..... *Internel diameter*

L

LED.....*Light Emitting Diode*

L-LA..... *L-lactide*

M

MADIX.....*Macromolecular Design via the Interchange of Xanthates*

MALDI-FT-ICR..... *Matrix-assisted laser desorption/ionization Fourier transform ion cyclotron resonance*

MALDI-FTICR-MS .... Matrix-assisted laser desorption/ionization Fourier transform ion cyclotron resonance mass spectrometry

MALDI-TOF..... *Matrix assisted laser desorption ionization-time of flight*

MeCN..... *Acetonitrile*

MHD..... *magnetohydrodynamic*

MLs ..... *macrolactones*

MMA..... *methyl methacrylate*

M_n *Number-average molecular weight*

© 2020 Tous droits réservés.

lilliad.univ-lille.fr

MOHEL.....*3-methyl-4-oxa-6-hexanolide*

MS ..... *Mass Spectrometry*

Mw.....*Weight Average Molecular Weight*

N

N435 ..... *Novozym 435*

NMP ..... *Nitroxide-mediated polymerization*

NMR..... *Nuclear Magnetic Resonance Spectroscopy*

NMRP..... *Nitroxide-mediated radical polymerization*

O

o-ROP..... *Organo RingOopening Polymerization*

P

PAs.....*Polyamides*

PBA ..... poly(butyl acrylate)

PBMA..... *Poly(butyl methacrylate)*

PBs..... *Phosphazene bases*

PBS.....*poly(butylene succinate)*

PC .....*Pancreatic*

PCL..... *poly(ε-caprolactone)*

PDI ..... *Polydipersity Index*

PDL.....*ω-Pentadecalactone*

PDMS .....*polydimethylsiloxane*

PEs ..... *Polyesters*

PET.....*poly(ethylene terephthalate)*

PF .....*Pseudomonas fluorescens*

PHB .....*poly(β-hydroxybutyrate)*

pI .....*Isoelectric point*

PLA.....*poly(lactic acid)*

PMMA..... *poly-methylmethacrylate*

PTCL.....*Polythiocaprolactone*

PTFE .....*PolyTetraFluoroEthylene*

PTH *10-phenylphenothiazine*

PTMC ..... *Poly(trimethylene carbonate)*

PTS..... *p-toluenesulfonic acid*

PVL..... *poly(δ-valerolactone)*

© 2020 Tous droits réservés.

lilliad.univ-lille.fr

R

rac-LA..... *racemic-latide*

RAFT..... *Addition–Fragmentation Chain Transfer Polymerization*

ROCP..... *ring opening copolymerization*

ROP.....*Ring Opening Polymerization*

RP .....*Radical Polymerization*

RT .....*Room temperature*

RTD ..... *residence time distribution*

S

SLs..... *small lactones*

T

TCC.....*triclocarban*

TEMPO.....*2,2,6,6- tetramethylpiperidinyl-1-oxy*

THF .....*Tetrahydrofuran*

TMC ..... *Trimethylene carbonate*

TOF ..... *Time of Flight*

U

UDL *11-undecanolide*

B

β-BL..... β-*butyrolactone*

β-PL.....*β-propiolactone*

Γ

γ-BL.....*γ-Butyrolactone*

γ-VL..... *γ-valerolactone*

Δ

δ-VL.....*δ-valerolactone*

E

ε-CL.....*ε-caprolactone*

© 2020 Tous droits réservés.

lilliad.univ-lille.fr

LIST OF TABLES

© 2020 Tous droits réservés.

lilliad.univ-lille.fr

© 2020 Tous droits réservés.

lilliad.univ-lille.fr

LIST OF FIGURES

© 2020 Tous droits réservés.

lilliad.univ-lille.fr

© 2020 Tous droits réservés.

lilliad.univ-lille.fr

© 2020 Tous droits réservés.

lilliad.univ-lille.fr

© 2020 Tous droits réservés.

lilliad.univ-lille.fr

© 2020 Tous droits réservés.
lilliad.univ-lille.fr

© 2020 Tous droits réservés.

lilliad.univ-lille.fr

© 2020 Tous droits réservés.

lilliad.univ-lille.fr

© 2020 Tous droits réservés.

lilliad.univ-lille.fr

© 2020 Tous droits réservés.

lilliad.univ-lille.fr

© 2020 Tous droits réservés.

lilliad.univ-lille.fr

© 2020 Tous droits réservés.

lilliad.univ-lille.fr

© 2020 Tous droits réservés.

lilliad.univ-lille.fr

LIST OF SCHEMES

© 2020 Tous droits réservés.

lilliad.univ-lille.fr

© 2020 Tous droits réservés.

lilliad.univ-lille.fr

Abstract

Green chemistry is an attractive field which has evolved over the past twenty years and aims to develop products that do not harm the environment using eco-responsible syntheses. This work focuses on the green synthesis of polyesters which are considered as important synthetic polymers due to their biocompatibility and biodegradability. Polyesters are obtained by two main routes: polymerization by polycondensation of diacids with diols which is the most widely used route, and polymerization by ring opening of lactones, lactides or cyclic carbonate (Ring Opening Polymerization, ROP). Polycondensation requires harsh reaction conditions to promote the condensation reaction by removing a water molecule between the acid and alcohol functional groups in order to achieve high conversions. Recently, flow synthesis techniques have allowed better control of organic synthesis and polymerization reactions. We have studied the enzymatic ring-opening polymerization (*e*-ROP) of lactones using Novozym® 435 lipase as a catalyst immobilized on porous beads in flow to develop controlled polymerization that respects the principles of green chemistry. The porous beads were introduced into a tubular reactor made of fluorinated ethylene propylene (FEP) with an internal diameter = 1.55 mm. We were able to polymerize ε-caprolactone (ε-CL) with a 100 % conversion rate (conv) and a dispersity (*Đ)* of 1.3 and δ-valerolactone (δ-VL) (conv = 93%, *Đ* = 1.27). Copolymers have also been synthesized. We have also studied the catalysis of ring-opening polymerization by phosphazenes which are organic superbases. The basicity of phosphazene governs the reaction: the highest basicity lead to the highest yield in spite of poorer dispersity. The best yields were obtained using *t*- P_4Bu (pK = 41.9) as catalyst for polymerizing ε-CL and δ-VL at room temperature, with values of 96% and 93% respectively. When *t*-BuP_2 (pK = 33.5) was used, a lower conversion of 45% was obtained but with a very good dispersity *Đ* = 1.08. We also worked on polycondensation using new organic catalysts with hydrophobic parts in their structures allowing the elimination of water or alcohol co-products which limit the course of the reaction. Thus we have studied the polycondensation between diols and diacids or diesters catalyzed by diphenylammonium triflate (DPAT) or pentafluorophenylammonium triflate (PFPAT) in batch. We obtained polymers by polyesterification between succinic acid and butanediol using DPAT or PFPAT as catalysts with conversions of 76% and 92% respectively.

© 2020 Tous droits réservés.

lilliad.univ-lille.fr

Finally, we investigated photo-induced atomic transfer radical polymerization (ATRP) in a flow system using Eosin Y, an inexpensive organic compound that absorbs in the green (530 nm) to catalyze the polymerization of methyl methacrylate (MMA) which can be synthesized with a 91% conversion rate and a dispersity *Đ* of 1.42. The lively appearance of these polymers has been demonstrated by the success of subsequent copolymerizations. In conclusion, we have shown that flow chemistry allows polymer synthesis with better control of polymerization compared to flask synthesis. This better control makes it possible to obtain polymers with high yield, low dispersity and a molar mass close to the theoretical value.

© 2020 Tous droits réservés.

lilliad.univ-lille.fr

Résumé

La chimie verte est un domaine attractif qui s'est développé depuis une vingtaine d'année et qui vise à la mise au point de produits ne nuisant pas à l'environnement à l'aide de synthèses écoresponsables. Ce travail est centré sur la synthèse verte de polyesters qui sont des polymères synthétiques importants en raison de leur biocompatibilité et de leur biodégradabilité. Les polyesters sont obtenus par deux voies principales de synthèse : la polymérisation par polycondensation de diacides avec des diols constituant est la voie la plus couramment utilisée, et la polymérisation par ouverture de cycle de lactones, lactides ou carbonate cyclique (Ring Opening Polymerisation, ROP). Les polycondensations exigent des conditions réactionnelles dures pour favoriser la réaction de condensation en éliminant une molécule d'eau entre acide et alcool afin d'atteindre des conversions élevées. Récemment les techniques de synthèse en flux ont permis un meilleur contrôle des réactions de synthèse organique et de polymerisation. Nous avons étudié la polymérisation enzymatique par ouverture de cycle (e-ROP) de lactones en utilisant comme catalyseur la lipase Novozym® 435 immobilisée sur des billes poreuses en flux pour développer des polymérisations contrôlées et respectueuses des principes de la chimie verte. Les billes poreuses ont été introduites dans un réacteur tubulaire en éthylène propylène fluoré (FEP) de diamètre interne = 1,55 mm. Nous avons pu polymériser la ε-caprolactone (ε-CL) avec une conversion de 100% et une dispersité de $Đ$ = 1,3 et la δ-valérolactone (δ-VL) (conv = 93%, $Đ$ = 1,27 respectivement). Des copolymères ont également été synthétisés. Nous avons également étudié la catalyse de la polymérisation par ouverture de cycle par les phosphazènes qui sont des superbases organiques. La basicité du phosphazène gouverne la réaction : les plus basiques conduisent au rendement le plus élevé mais au dépit de la dispersité. Les meilleurs rendements ont été obtenus en utilisant le *t*-BuP_4 (pK = 41,9) comme catalyseur pour polymériser les ε-CL et δ-VL à température ambiante, avec des rendements de 96% et 93% respectivement. Avec le *t*-BuP_2 (pK = 33,5), une conversion plus faible de 45% a été obtenue mais avec une très bonne dispersité $Đ$ = 1,08. Nous avons également travaillé sur la polycondensation en utilisant de nouveaux catalyseurs organiques qui présentent dans leurs structures des parties hydrophobes permettant de favoriser l'élimination des coproduits eau ou alcool qui limitent l'avancement de la réaction. Ainsi nous avons étudié la polycondensation

© 2020 Tous droits réservés.

lilliad.univ-lille.fr

entre les diols et les diacides ou les diesters catalysée par le triflate de diphénylammonium (DPAT) ou le triflate de pentafluorophénylammonium (PFPAT) en batch. Nous avons obtenu des polymères par polyesterification entre l'acide succinique et le butanediol en utilisant DPAT ou PFPAT comme catalyseurs avec des conversions de 76% et 67% respectivement. Enfin, nous avons étudié la polymérisation radicalaire par transfert atomique (ATRP) photo-induite dans un système en flux en utilisant l'Eosine Y, un composé organique peu coûteux absorbant dans le vert (530 nm) pour catalyser la polymérisation du méthacrylate de méthyle (MMA) qui peut être synthétisé avec une conversion de 91% et une dispersité $Đ$ de 1,42. L'aspect vivant de ces polymères a été démontré par le succès des copolymérisations ultérieures. En conclusion, nous avons montré que la chimie en flux permet une synthèse de polymères avec un meilleur contrôle de la polymérisation comparée à la synthèse en ballon. Ce meilleur contrôle permet d'obtenir des polymères avec un rendement élevé, une faible dispersité et une masse molaire proche de la valeur théorique.

© 2020 Tous droits réservés.

lilliad.univ-lille.fr

0. INTRODUCTION

The importance of polyesters comes from their wide applications in our daily life. Due to their non-toxicity and biocompatibility, they are employed in sophisticated causes such as medical and pharmaceutical areas.[1] Ring Opening Polymerization (ROP) is mainly adopted to produce poly(esters) and many other polymers from corresponding cyclic monomers.[2,3]

Many metal based catalysts were utilized in polyesters synthesis like aluminium, tin and zinc, and the most used was tin (II) octanoate catalyst. However metal based catalysts still represent an inconvenient in catalyzing the synthesis of biodegradable polyesters destined for biomedical uses.[4]

Green chemistry is actually a very attractive field; it represents a new chemistry approach regarding the benefit from different green products that respect the environment during synthesis including: catalysts, starting materials, solvents… as well as many other implicated factors which are employed without damaging the environment.[5] In our case we are focused on the synthesis of green macromolecules.

As green catalysts, enzymes proceed clean reactions with no side products providing a high selectivity with respect to enantio-, regio- and chemo-selectivities.[6–8]. They are also considered as nontoxic, renewable, natural and free metal compounds. Furthermore, enzymes are recyclable and can be reused for many times. Finally, they allow the polymerization to undergo in green solvents such as water or supercritical carbon dioxide and not necessarily in organic solvents.[9,10] All these advantages cannot be offered usually by conventional catalytic systems.

One of the most used enzymes in the enzymatic polymerization field according to literature is Lipase which belongs to the family of hydrolase enzymes.[4,5,7,8] Novozym 435® is an extensively studied and widely used lipase in polymer synthesis. It's also readily and commercially available.

A second nontoxic and efficient catalyst was applied and it is organic based. In the last decade, more efforts have been made to develop this kind of catalytic systems. Actually, a wide range of organic molecules tolerate an appropriate catalyst for each specific synthetic task.[11] In term of green polymer synthesis, we are also interested in this type of catalyst.

© 2020 Tous droits réservés.
lilliad.univ-lille.fr

More specifically, phosphazenes bases (PBs) catalysts have been our choice for ROP of lactones. These catalysts are characterized by a strong basicity compared to nucleophilic ones, good solubility in many organic solvents and high thermal stability, all making them a good choice as organic catalysts.[12,13]

On the other hand, the classical method used in esterification is the direct condensation of carboxylic acids with alcohols in the presence of small amounts of catalyst. However, this method is limited by several difficulties preventing our interest to reach high yields. Those latter include the need to remove water, to add an excess amount of one of the reagents and to optimize reaction conditions, in addition to the catalyst contamination problem. To overcome these problems, chemists started to use organo-catalysts in order to promote esterification. These catalysts offer many advantages such as self-separation from the reaction mixture, mild reaction conditions and the use of equimolar reagents' amounts. Besides, due to the catalyst structure containing hydrophobic parts, the reaction can progress in presence of water, which makes the reaction system less complicated. Thereafter, organo-catalysts such as diphenylammonium triflate (DPAT)[14] and pentafluorophenylammonium triflate (PFPAT)[15] are the catalysts to be investigated in polycondensation reactions.

On the other hand, we studied the photo-induced atom transfer radical polymerizations (ATRP) of MMA (methylmethacrylate) as well as its copolymerization in a flow system. Photo-induced controlled radical polymerization was observed while carrying out a Cu mediated living radical polymerization of methyl acrylate (MA) in a flow system, whereby this experiment, a slow but effective polymerization was obtained.[16]

In order to determine the optimal wavelength, many light sources were tested covering the UV-VIS spectrum. The best results were recorded under a UV lamp with $\lambda max \approx 360$ nm.[17]

In fact, metal contamination was a drawback in atom transfer radical polymerization.[18,19] To overcome this drawback, a significant focus has been directed toward lowering catalyst loading[20] and/or working on nullifying residual metals present in the mixture.[21,22] Although these established methods minimizing the quantity of metal are encouraging, they are still not practical and ambitious enough. So, a much more viable solution was suggested: the development of a metal free catalyst system for ATRP .[23]

Recently, a combination between the organic syntheses and microscale technology in flow was established to reach high performances. Many advantages are provided in using such

© 2020 Tous droits réservés.
lilliad.univ-lille.fr

system including high surface to volume ratio of microreators and the short diffusion paths. This statement allows a more efficient heat and mass transfer compared to conventional platforms.[24–27] In continuous microreator, the simple variation of the flow rate of reagents solution or the micro-channel length, contributes to adjust the reaction time. As an example, we cite the pioneer work employing immobilized enzyme in continuous flow system achieved by Gross *et al* to polymerize ε-caprolactone.[28] In comparison to batch system, they yielded higher number-average molecular weight (M_n) of polycaprolactone (PCL) in less reaction time. In addition, "saturated water" conditions did not affect the conversion or the end group fidelity.[29] Afterwards, several applications to the polylactones synthesis were developed in microflow system.[30–32] The end fidelity was well tested also via enzymatic ring opening polymerization of δ –Valerolactone in flow mode as well as its copolymerization with interesting results compared to the batch.[33]

As summary, in order to improve the polymer green chemistry, we should combine the advantages of micro-flow system, green catalysts and synthetic polymers pathways. Herein, the first aim of our work is the synthesis of polyesters via ring opening polymerization or polycondensation, as well as their copolymers using microflow devices. All these syntheses cited above will be carried out in micro-flow devices with different dimensions of tubular reactors, in which the reactions will progress due to the action of green catalysts such as immobilized enzymes like Novozym 435 (CALB N435, lipase B from *Candida Antarctica*), and organic based catalysts like phosphazenes bases for the ring opening polymerizations. In addition, diphenylammonium triflate (DPAT) and pentafluorophenylammonium triflate (PFPAT) are the catalysts chosen for polycondensations in batch and for their attempts in flow system.

The second aim is to carry out a photo-induced atom transfer radical polymerizations (ATRP) in a flow system as well as the atom transfer radical copolymerization, using an organic-based photoredox catalyst in a lab designed tubular microreator (L = 3.37 m; i.e. = 800 μm) placed in direct contact with green LEDs. The focus will be on the synthesis of poly-methylmethacrylate (PMMA) using EosinY as a metal free catalyst that absorbs in the green region (530 nm) in addition to its copolymerization with Styrene and Butylacrylate (BA).

A large study of each reaction's different parameters will be fulfilled, including: reaction time, solvents, temperature, initiators… etc. In addition, kinetic studies were performed. To characterize the formed polymers, we will use various analytical methods like ^{1}H nuclear

© 2020 Tous droits réservés.
lilliad.univ-lille.fr

magnetic resonance spectroscopy (NMR), mass spectrometry (MS) and gel permeation chromatography (GPC).

© 2020 Tous droits réservés.
lilliad.univ-lille.fr

1. CHAPTER ONE: STATE OF THE ART

1.1. Living polymerization

By definition, living polymerization is a polymerization reaction where no undesired side reactions such as transfer or termination occur, and where all polymer chains are simultaneously initiated.[34] Thus, the growing ends of polymer chains are active indefinitely for further polymerization. Consequently, the term of living/controlled polymerization is applied to reactions where termination and chain transfer are negligible compared to the propagation step and where molecular weight distributions are narrow. In theory, the production of polymers with polydipersity index (PDI) of 1.0 performs the ideal living polymerization system. In reality, no such reactions have been found, nevertheless this goal is not so far to attain following the development of some systems, where a PDI as small as 1.05 was reported.[35,36]

A living polymerization has the following features.[37]

- The kinetics of the reaction are first order with respect to the monomer.
- The percentage of conversion is directly proportional to the monomer to initiator ratio (known by the degree of polymerization (DP)).
- Narrowly dispersed polymers are obtained.
- The formed polymers continue to be reactivated for further polymerization.

Living polymerizations have opened up a whole new world of possibilities concerning the design of new polymeric architectures and compositions, which explains their interest from both a scientific and an industrial point of view. The main types of living polymerization will be presented in the following subsections.

1.1.1. Ionic Polymerization

1.1.1.1. Anionic Polymerization

The oldest living polymerization method was the living anionic polymerization discovered in 1956 by M. Szwarc.[38] In this reaction, the active intermediate that initiates the polymerization should be negatively charged. Classical initiators used include sodium in liquid ammonia,

© 2020 Tous droits réservés.
lilliad.univ-lille.fr

Grignard reagents and triphenylmethyl sodium [$(C_6H_5)_3C$-Na]. However, the common initiator used is the alkyl lithium reagents such as butyl lithium that gives after its decomposition a positively charged lithium ion Li^+ and a negatively charged carbanion. This active carbanion will attack a carbon of the monomer's C=C group. This will allow the movement of the "π" electrons and settlement on a carbon out of the C=C carbons, thus forming the initiator of the anionic polymerization which is a carbanion (Figure 1-1). This form of polymerization is favored with monomers having an anion-stabilizing group like nitrile (–CN) or chloride (-Cl), which stabilize the carbanion formed throughout the polymerization. Examples of these monomers: acrylonitrile [CH_2=C(CN)], vinyl chloride [CH_2=C(Cl] and methyl methacrylate [CH_2=C(CH_3)$COOCH_3$].[39] Narrow dispersed polymers (<1.1) are obtained using this technique mainly adapted by industry for thermoplastic elastomers' production.[40]

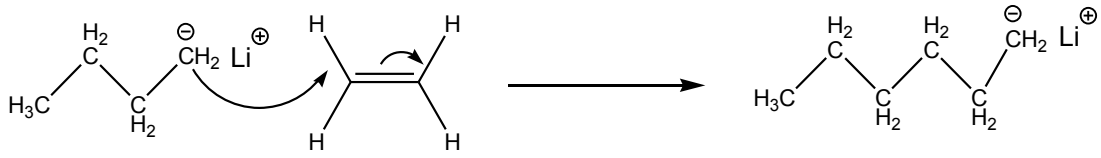

Figure 1-1 Initiation of Anionic Polymerization

© 2020 Tous droits réservés.

lilliad.univ-lille.fr

1.1.1.2. Cationic polymerization

After the discovery of anionic polymerization, it was obvious to work on cationic polymerization development. Effectively, living cationic system has succeeded in polymerizing isobutyl vinyl ether as detailed by T. Higashimura and co-workers in 1984.[41] In cationic polymerization, an electron deficient compound is used as active species in the initiation step. This compound will be attacked by the π electrons of the monomer's C=C bond, forming the cationic intermediate (Figure 1-2), and generates the initiation. In the propagation step, another monomer reacts with the cationic active species which produces another carbocation but with an additional monomer, and the same process is repeated along with the increase in the polymer's chain size. Termination arises after losing a proton H^+ or reacting with an anion. The common initiators used in cationic polymerization are aqueous aluminum chloride or borontrifluoride. An efficient reaction occurs with monomers that stabilize the cationic reactive site like methyl propylene and phenyl styrene.[42]

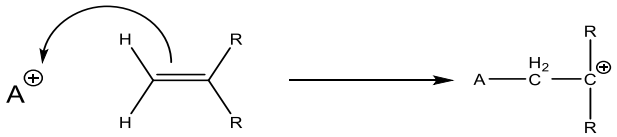

Figure 1-2 Initiation of cationic polymerization, A^+ is the active species

© 2020 Tous droits réservés.
lilliad.univ-lille.fr

1.1.2. Radical polymerization

Although controlled ionic polymerization presents a powerful way for polymers design, it shows some limitations in terms of monomers' choice and reaction conditions, as well as the apparition of side reactions in presence of protic solvents or polar functional groups. These limitations oriented the development of radical polymerization which consists in the formation of a radical as an active site for the initiation.[43]

Polymer science was enhanced by controlled/living radical polymerization (CRP); it enables the polymer synthesis with definite molar masses, low distributions, diverse compositions and architectures.[44] A wide variety of functional groups can be incorporated into polymers using this type of polymerization. In this way, polymers acquired new properties rendering their usage in new applications such as nanotechnology, biomedicine, energy and defense. Radical polymerization is considered one of the most attractive industrial polymerization technologies. By estimation, this method produces about 40-45% of all synthetic polymers.[45] This is due to the advantages of the radical polymerization which can progress with wide range of monomers with polar functional groups and polar solvents including water, in addition to the high reactivity of the radical.[46]

The formation of the radical initiator can be induced thermally or photochemically.

The emerging radical will form a bond on the monomer's C=C . This will allow the transfer of "π" electrons and the settlement on a carbon out of the C=C carbons. The formed radical compound containing the initiator and a monomer motif is considered the active radical intermediate.

The major problem in radical polymerization is the high reactivity of radicals, which facilitates termination reactions between two active chains by coupling/disproportionation. In this case, polydisperse macromolecules with a broad PDI are probably obtained due to the difficulty in controlling these properties. In contrast, this is not the case in ionic polymerization where electrostatic repulsion prevents a reaction between two cations or two anions. However, by using conventional RP, no pure block co-polymers nor polymers with controlled architecture can be produced.[43] Controlled/living radical polymerization methods have been developed to overcome these difficulties. The strategy for the above-mentioned termination reactions elimination has been addressed to ensure that only a fraction of the polymer in question is activated at a short time. This can be done by the presence of the least

© 2020 Tous droits réservés.
lilliad.univ-lille.fr

amount possible of active radical chains in progress, while the majority of macromolecules are in a dormant/inactivated state. The existing of such equilibrium guarantees the uniform growing of polymers. Thus, the short activated period will eliminate unwanted reactions as transfer and termination, one of the most important reasons leading to broad molecular weight distributions, and control obtainement over the polymerization.[35,47]

Three main controlled radical polymerization systems have been widely investigated consisting of : nitroxide-mediated radical polymerization (NMP),[48,49] atom-transfer radical polymerization (ATRP),[35,47,50,51] and reversible addition-fragmentation chain transfer radical polymerization (RAFT).[52–54]

© 2020 Tous droits réservés.

lilliad.univ-lille.fr

1.2. Synthesis of polyesters: ROP and polycondensation

Polyesters is the fourth mostly found family in nature after the three biomacromolecules of nucleic acids (DNA and RNA), proteins (polypeptides), and polysaccharides.[1] The importance of polyesters comes from their wide applications in our daily life, and their non-toxicity and biocompatibility, making them suitable for sophisticated causes such as medical and pharmaceutical areas. We can cite as examples of polyesters: poly(ethylene terephthalate) (PET) as an aromatic polyester, poly(butylene succinate) (PBS), poly(ε-caprolactone) (PCL), and poly(lactic acid) (PLA) as aliphatic polyesters. The two first are produced in industry via condensation polymerization (polycondensation) (Scheme 1-1 (B)) and the two remaining others via ring opening polymerization (Scheme 1-1(A)).

In 1930s, and after his invention of nylon66, Carothers achieved the synthesis of aliphatic polyesters via condensation polymerization between dicarboxylic acid and glycol. But unfortunately these polymers had low molecular weight and melting point which made their commercialization difficult.[55] However, the aromatic polyester PET was successfully produced and it has been widely considered as an excellent polymer material for that period. The commercial production of aliphatic polyesters was developed. Owing to environmental considerations, scientists focused on avoiding the usage of fossil resources and they were more interested to explore materials based on renewable resources, in addition to the development of new production processes using non-toxic substances for the catalysis. This is the response to "green chemistry".[56]

The enzymatic polymerization for the production of polysaccharides, polyesters, poly(aromatic)s and so on, is well known in the literature.[57–64] Lipase-catalyzed polyester synthesis was mainly studied by different groups in order to emphasize "green polymer chemistry".[57,60,63,64]

© 2020 Tous droits réservés.

lilliad.univ-lille.fr

(A) Ring-Opening Polymerization

(1) Cyclic Ester (Lactone) Monomer

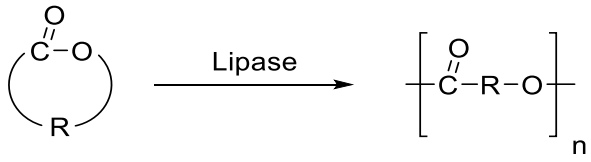

(B) Condensation Polymerization (Polycondensation)

(2) Oxyacid or its Ester

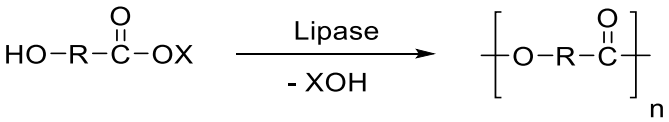

X: H, (halo)alkyl, vinyl, etc

(3) Carboxylic Acid or its Ester and Diol

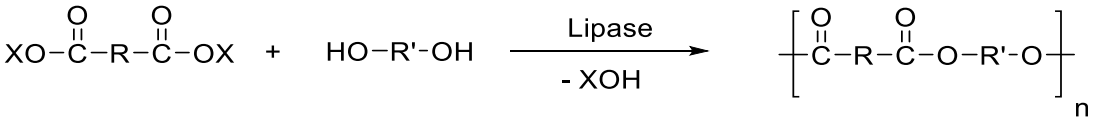

X: H, (halo)alkyl, vinyl, etc

(C) Ring-Opening Addition-Condensation Polymerization

(4) Carboxylic Anhydride and Diol

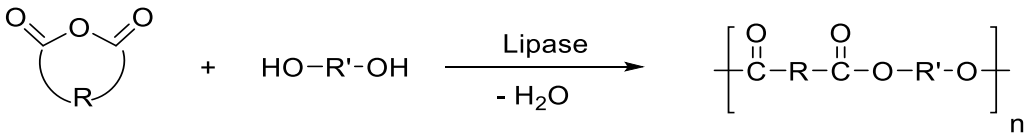

Scheme 1-1 Main reaction modes of lipase-catalyzed polyester synthesis.[7]

© 2020 Tous droits réservés.

In general, the ester molecule is obtained from four fundamental esterification or transesterification reactions (Scheme 1-2). All these reactions are reversible, that's why an intervention action is mandatory to shift the equilibrium to the product side and to accelerate the reaction. To this end, small molecules produced, like water or alcohol should be eliminated from the reaction media or reduced.[63]

- Esterification

(a) Dehydration

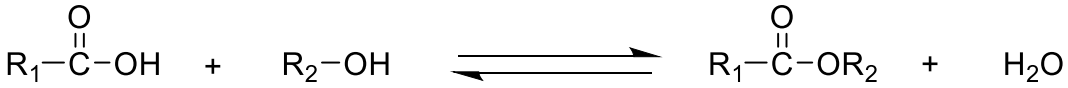

- Transesterification

(b) Alcoholysis

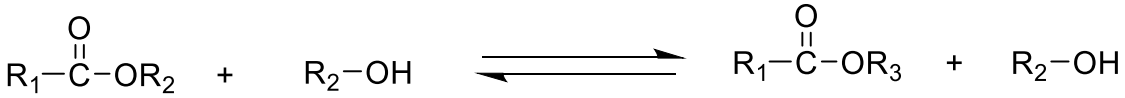

(c) Acidolysis

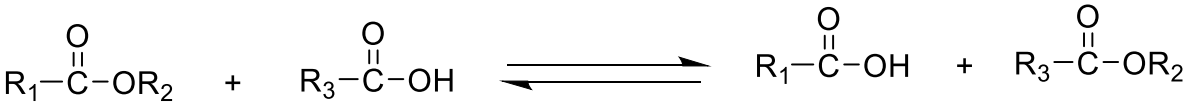

(d) Intermolecular esterification

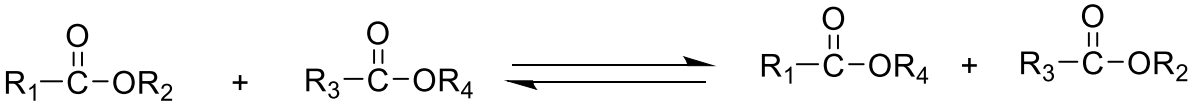

Scheme 1-2 Esterification and transesterifications for ester synthesis.

© 2020 Tous droits réservés.

lilliad.univ-lille.fr

1.3. Ring opening polymerization of lactones

Based on the process nomenclature, ring opening polymerization consists in an opening of a cyclic monomer followed by its polymerization. A large number of cyclic monomers have been polymerized especially by enzyme catalysts. Figure 1-3 shows some examples of monomers that can be divided into two classes: cyclic esters (Lactones) and other cyclic monomers.[1] We will present in this report two catalytic systems that promote ROP which are the enzymatic ring opening polymerization (*e*-ROP) (chapter 2) and organo ring opening polymerization (*o*-ROP) (3).

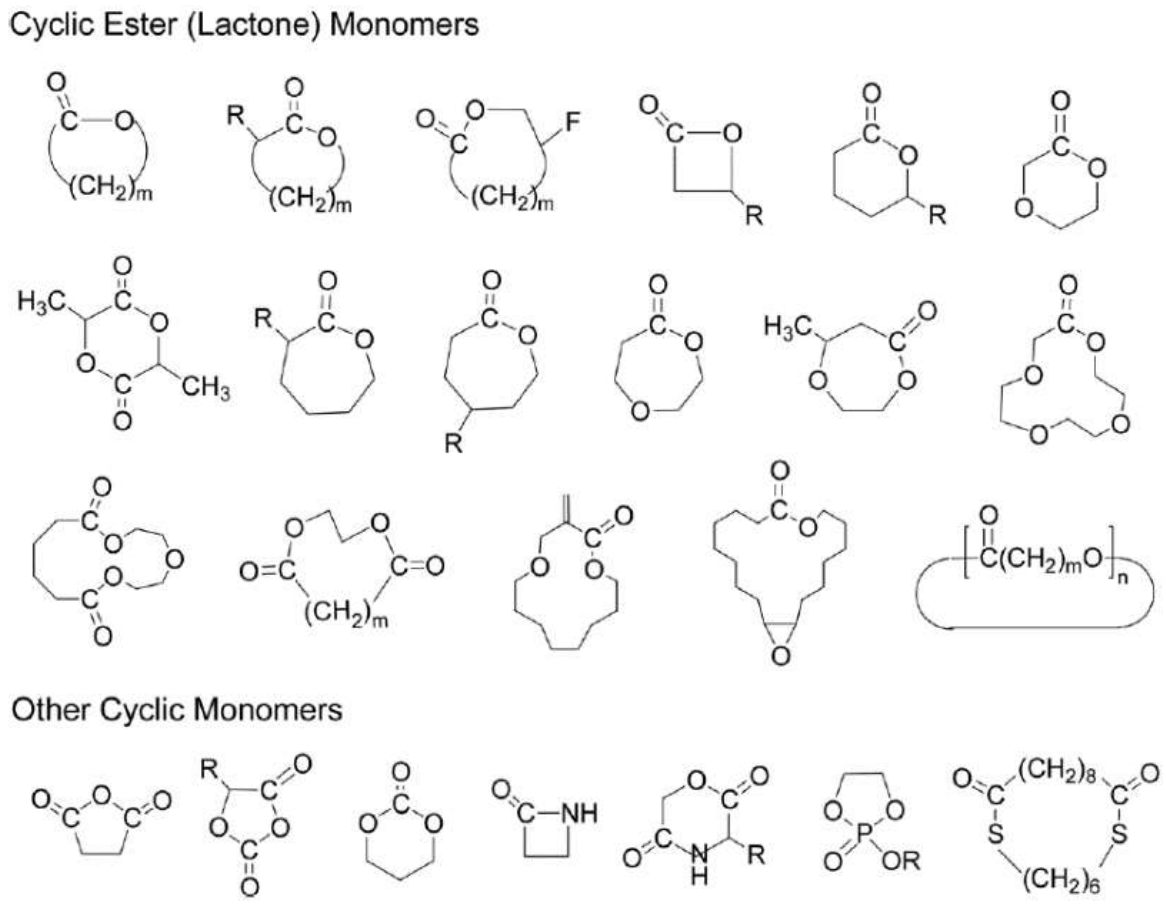

Figure 1-3 Typical examples of cyclic monomers for enzyme-catalyzed ring-opening polymerizations (ROP).

© 2020 Tous droits réservés.
lilliad.univ-lille.fr

1.4. Enzymatic ring opening polymerization

1.4.1. *e*-ROP: Enzymes and enzymatic catalysis

Enzymes are found in living cells where they play a very important role by catalyzing metabolic reactions *in vivo* to give biomacromolecules that maintain the living system. This enzymatic catalytic function was attractive and got much interest in research. The first type of enzymes was found by A. Payen and J. F. Persoz in 1833,[65] which was the diastase (amylase). After this work, the most attractive and investigated topics in literature of science were related to the catalytic aspect of enzymes, so that a new field of enzymology has emerged. A good effort of research was focused on enzymatic functions and more than thousand types of enzymes were found.[66] Enzymes are used in polymer synthesis and even more for its modification, and this can be performed with selective reactions that give access to new functionalities in polymer chains.

There are six classes of enzymes (Table 1-1). Many of them are used for the industrial production implicated in a wide range of fields like: food, pharmacology, medicine and textile industries etc. Table 1-1 presents the classes of enzymes that are typically used for the enzymatic polymerization as well as for polymers modification.

class	enzymes	example enzymes	macromolecules synthesized	macromolecules modified
1.	oxidoreductases	peroxidase, laccase, tyrosinase, glucose oxidase	polyphenols, polyanilines, polythiophene, vinyl polymers	polysaccharides, polypeptides (proteins)
2.	transferases	phosphorylase, glycosyltransferase, acyltransferase	polysaccharides, cyclic oligosaccharides, polyesters	polysaccharides, polypeptides (proteins)
3.	hydrolases	glycosidase (cellulase, amylase, xylanase, chitinase, hyaluronidase), lipase, protease, peptidase	polysaccharides, polyesters, polycarbonates, polyamides, poly(amino acid)s, polyphosphates, polythioesters	polysaccharides, polypeptides (proteins)
4.	lyases	decarboxylase, aldolase, dehydratase		
5.	isomerases	racemase, epimerase, isomerase		
6.	ligases	ligase, synthase, acyl CoA synthase		

Table 1-1 Classification of typical enzymes and macromolecules examples synthesized by enzymatic polymerization as well as modified by enzymatic reaction.[9]

To explain the enzymatic catalysis, there are two issues to be referred. The first one was proposed by E. Fischer in 1894 under the term of "key and lock" theory, in which enzyme and substrate present specific relationships.[67] These relationships are based on recognition of the substrate molecules by the enzyme. For example, in the case of *in vivo* reactions (cycle A, Figure 1-4), an enzyme-substrate complex is formed once the enzyme recognizes specifically

© 2020 Tous droits réservés.
lilliad.univ-lille.fr

the desired substrate that fits. A supramolecular interaction permits the formation of a complex and makes the substrate active to undergo the reaction with high selectivity. The recognition of substrate with "key and lock" relationship followed by the complex formation is a must for the reaction to be realized. On the other hand, this process is simulated *in vitro* (cycle B, Figure 1-4), in which an artificial substrate can be recognized by the enzyme to form the artificial substrate-enzyme complex followed by the substrate activation required for the reaction occurrence, giving access to the desired product with high selectivity. The key step for a successful reaction is based on the optimization of substrate design to be recognized by the enzyme.

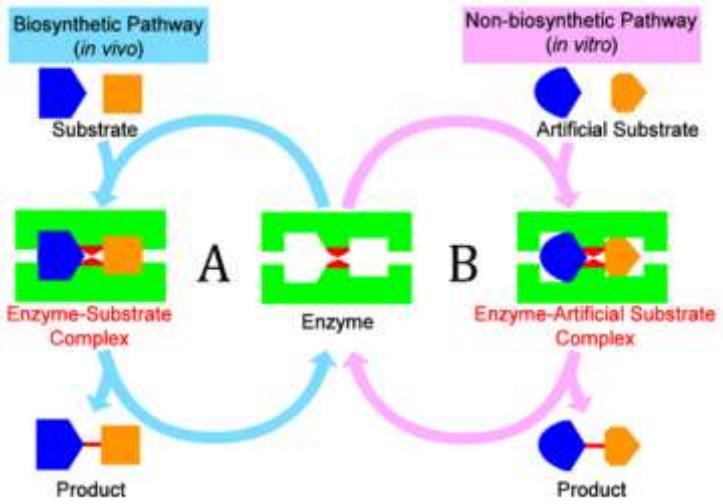

Figure 1-4 Schematic expression for "key and lock" theory for *in vivo* enzymatic reactions via biosynthetic pathway (cycle A) and for *in vitro* enzymatic reactions via non-biosynthetic pathway (cycle B).[9]

Second, the explanation for enzymes ability to catalyze reactions under mild conditions, like in living cells, was suggested in 1946 by L. Pauling.[68,69] A complex (ES) is formed by key and lock interaction between an enzyme (E) and a substrate (S), thus activating the substrate and generating a transition state [$(ES^{\ddagger})$] for the reaction to occur. Following this route, the activation energy ($\Delta G_{enz}^{\ddagger}$) is reduced by the action of the enzyme giving a more stable state in comparison to that obtained ($\Delta G_{no}^{\ddagger}$) passing through a transition state [$S^{\ddagger}$] of a reaction in absence of the enzyme action (Scheme 1-3).

© 2020 Tous droits réservés.
lilliad.univ-lille.fr

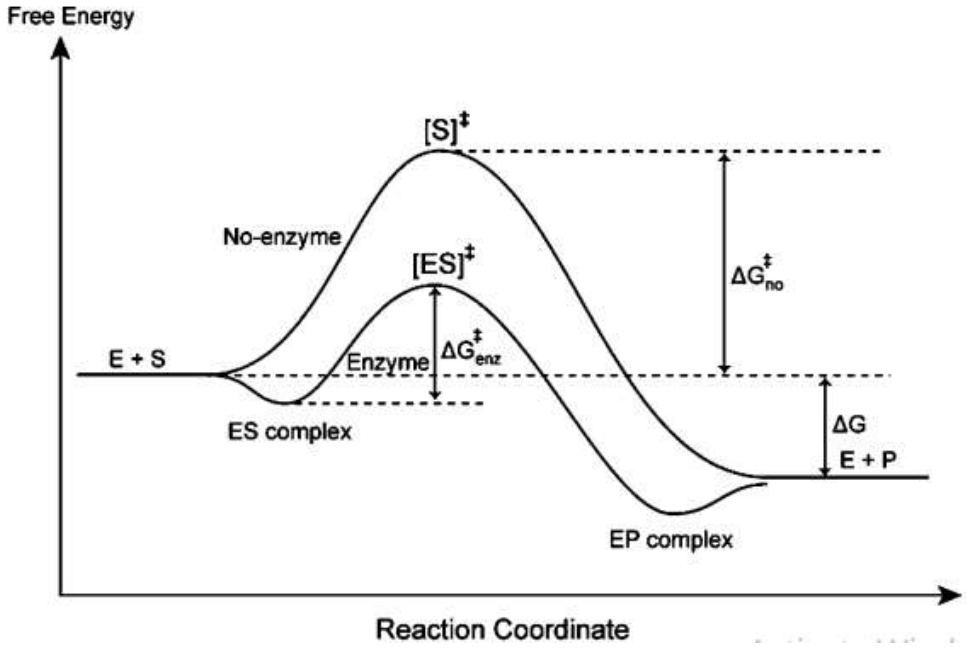

Scheme 1-3 Energy diagram for a chemical reaction. Comparison between an enzyme-catalyzed reaction and a reaction without enzyme.[63] copyright 2009 American Chemical Society.

Normally, enzymes lead an acceleration rate from 10^6 up to 10^{12} fold. Even a 10^{20} fold was previously reported.[70]

In vitro, enzymatic catalysis was first developed by a polish chemist in 1930s using esterase as a catalyst and an organic solvent for ester synthesis and it didn't take much interest.[71] Later on during 1980s, the production of aliphatic esters was extensively studied via enzymatic esterifications or transesterification.

These previous reactions indicate that the relationship given by the key and lock theory between the enzyme and the substrate is not totally strict but it presents flexibility to some extent. And this is the reason why enzymes have the ability to catalyze reactions *in vitro*. Once the substrate is recognized by the enzyme, the reaction can be performed. It is important to mention that supramolecular chemistry performs very well during the enzymatic reaction steps, especially in the transition states. These arguments are proved to be valid for all macromolecules synthesis catalyzed by enzymes.[9]

1.4.2. Mechanism: lipase catalyzed lactones polymerization

The *e*-ROP of lactones proceeds via several steps including the passage by the intermediate form of an acyl-enzyme.[58,60,63,72]

© 2020 Tous droits réservés.
lilliad.univ-lille.fr

It's well known that the lipase Ser-His-Asp triad contains the active catalytic site which is the $–CH_2OH$ group of Ser residue. The key step of the reaction between lactone and lipase catalyst is the acylation of the latter, it proceeds by two steps; the formation of an enzyme-lactone complex followed by the ring-opening of lactone, thus the formation of acyl-enzyme intermediate (enzyme activated monomer, EM). Then, the nucleophile which is the initiator will attack the intermediate acyl carbon, and that corresponds to the initiation step that produces the shortest propagating species (ω-hydroxycarboxylic acid (n = 1)). In the propagation, the terminal hydroxyl group of the propagating chain will nucleophilically attack the EM to elongate the polymer chain for one more monomer unit. The two steps of initiation and propagation have the same behaviour and correspond to a deacylation of the enzyme. So, the mechanism of this polymerization proceeds via an "activated monomer".

The above mechanism is proved by in-depth studies based on organic chemistry, in addition to the 3D X-Ray crystallographic analysis done in the 1990s to determine the lipase structure.[73,74]

Several studies were realized on the ROP polymerizability of lactone monomers.[1,71] It was suggested that the reactivity of lactones ring opening is managed primarily by the ring strain, which was similarly observed in organic reactions, for example: alkaline hydrolysis and the polymerization of lactones via anionic ROP. Nevertheless, the reactivity of enzymatic ring opening polymerization of lactones is totally different. The polarity of monomers is indicated by their dipole moment value. This latter is taken also as a measurement of monomers' ring strain. The dipole moment value of CL is higher than that of macrolides which are close to an acyclic fatty acid ester (butyl caproate), propounding smaller ring strain of the latter. Actually, with macrolides, alkaline hydrolysis and anionic polymerization using NaOMe initiator exhibit smaller rate constants than those of CL. Consequentially, macrolides are considered less reactive and less polymerizable than CL via anionic ring opening polymerization.

In 1997, the kinetic of lipase catalysed ring opening polymerization of CL and 12-dodecanolide (DDL) was studied for the first time based on Michaelis–Menten equation. It was found that DDL is more reactive than CL by 1.9 times.[75,76] Based on these results, it was suggested that the rate of the overall reaction is determined by the formation of an acyl intermediate (EM in Scheme 1-4), because the intermediate reactivity should be high and accordingly the following steps are rapid.

© 2020 Tous droits réservés.
lilliad.univ-lille.fr

Acylation of enzyme

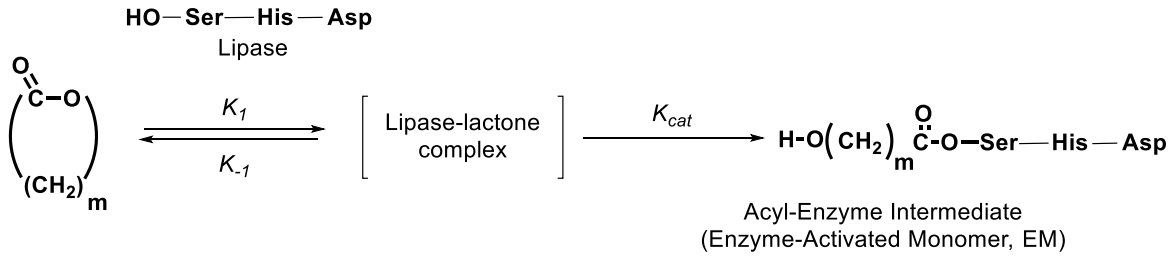

Initiation

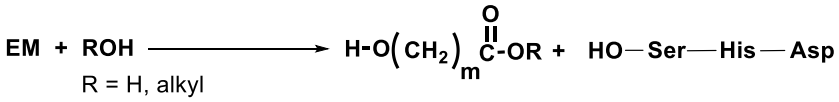

Propagation

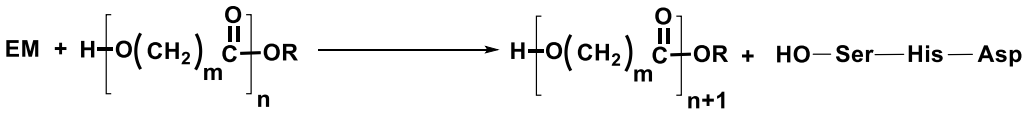

Scheme 1-4 Plausible mechanism of lipase-catalyzed ROP of lactone.

K_m, V_{max} and V_{max}/K_m (S^{-1}) are the michaelis-Menten parameters that reflect the overall rate of *e*-ROP and are presented in Table 1-2.[75–83] With lipase PF catalyst, the larger is the lactone size, the larger the polymerization rate is in one order magnitude difference. That high rate in the formation of EM is the reason of the higher polymerizability of macrolides. The values of Michaelis–Menten constant K_m ($K_m = [(K_{-1}+K_{cat})/K_{+1}$ mol.l^{-1}]) are close to each other and variate between 0.61 and 1.1. However, it is the opposite for V_{max} (V_{max} = (K_{cat} $[E]_0$, mol.l^{-1}.s^{-1})) values, where the range is 0.66 to 7.2.[75] At the end, it can be considered that PDL (16-membered) is more reactive than CL (7-membered) by 7.4 times using Lipase PF (column A,)[75] and by 6.7 times using CALB (Novozym 435) (column B,Table 1-2).[83] Based on these results, it was suggested that the polymerization rate is governed greatly by the larger values of V_{max}. So, the key step in the lipase-catalyzed ROP is the intermediate EM formation from the lipase lactone complex (Scheme 1-4). However, the reactivity of lactones is totally opposite in Zn-catalyzed anionic polymerization. In this case, macrolides have similar reactivity, which is way lower than VL and CL for 2500 and 330 times respectively (Table 1-2) In conclusion here, the polymerizability is conducted by the ring strain. In the propagation step, the rate is determined by the SN_2 reaction; the

© 2020 Tous droits réservés.
lilliad.univ-lille.fr

propagating Zn-alkoxide species will undergo a nucleophilic attack at its carbonyl carbon followed by the scission of the acyl-oxygen bond to form another time the alkoxide species (Scheme 1-4).[77]

		Rate constant		**Relative rate of polymerization**	
Lactone (ring size)	Dipole moment (C.m)	Alkaline hydrolysis[a] ($L\ mol^{-1}s^{-1}$, $\times10^4$)	Propagation[b] (s^{-1} , $\times10^3$)	Enzymatic Polymerization A[c] B[d]	Zn-catalyzed polymerization[e]

Table 1-2 Dipole moment values and ROP rate data of unsubstituted lactones of different ring size.[7]

© 2020 Tous droits réservés.

lilliad.univ-lille.fr

VL (6)	4.22	55,000		0.10 0.07	2500
CL(7)	4.45	2550	120	0.10 0.15	330
HL (8)	3.70	3530		3.8	
OL (9)	2.25	116		0.45	21
NL (10)	2.01	0.22		0.04	
DL (11)	1.88	0.53		0.02	
UDL (12)	1.86	3.3	2.2	0.13 0.06	0.9
DDL (13)	1.86	6.0	15	0.19 0.37	1.0
PDL (16)	1.86	6.5		0.74 1.0	0.9
HDL (17)				1.0	1.0
Butyl caproate	1.75	8.4			

[a]With alkaline of NaOH in 1,4-dioxane/water at 0°C
[b]Anionic ROP by NaOMe catalyst in THF at 0°C
[c]Lipase PF as catalyst in diisopropyl ether at 60°C; the relative rate is given by normalizing the Vmax/Km values with respect to HDL
[d]CALB as catalyst in toluene at 45°C; the relative rate is given by normalizing the Vmax/Km values with respect to PDL
[e]Zn(Oct)2 initiator in bulk polymerization at 100°C; the relative rate is given by normalizing the initial rate constants with respect to HDL

© 2020 Tous droits réservés.
lilliad.univ-lille.fr

1.4.3. End functional polyester synthesis

Lipase can be used to catalyze the synthesis of end-functionalized polymers, macromonomers and telechelics, which are important actors in macromolecular chemistry. A good control of the polymers' terminal structure is required in such syntheses. End-functionalized polyesters are well produced by lipase catalysis and well validated by single-step synthesis.[7]

1.4.3.1. Initiator method

The initiation of lactones ROP catalyzed by lipase needs a nucleophile species like water or alcohol. ROP of CL and DDL was catalyzed by lipase CC in the presence of functional alcohol following the initiator method.[84] (meth) acryroyl- polyester macro-monomers were synthesized using alcohols like 2-hydroxyethyl methacrylate (HEMA), 5-hexen1-ol and 5-hexyn-1-ol (Scheme 1-5.a) as initiators. The production of graft co-polymers or comb polymers can be readily done by radical or homo-polymerization of the obtained macro-monomers.

1.4.3.2. Terminator method

The polymerization of DDL catalyzed by Lipase was implemented to give end-functionalized polyesters by a single step in the presence of vinyl esters.[85–87] During the polymerization, a termination action occurs between a hydroxyl group and the vinyl ester; where this latter is considered as terminator. The introduction of (meth)acryloyl group was quantitatively carried out using vinyl (meth)acrylate as terminator and gives a macromonomer which is the (meth)acryloyl polyester with M_n 2000–4000 Da and functionality > 0.95. ω-alkenyl macromonomer was obtained using the vinyl 10-undecanoate as terminator (Scheme 1-5.b). The addition of divinyl sebacate to the system, gives access to telechelics with carboxylic acid extremities and characterized by M_n 2900 and functionality of 1.95 (Scheme 1-5.c).[86]

© 2020 Tous droits réservés.
lilliad.univ-lille.fr

Macromonomer by Initiator method

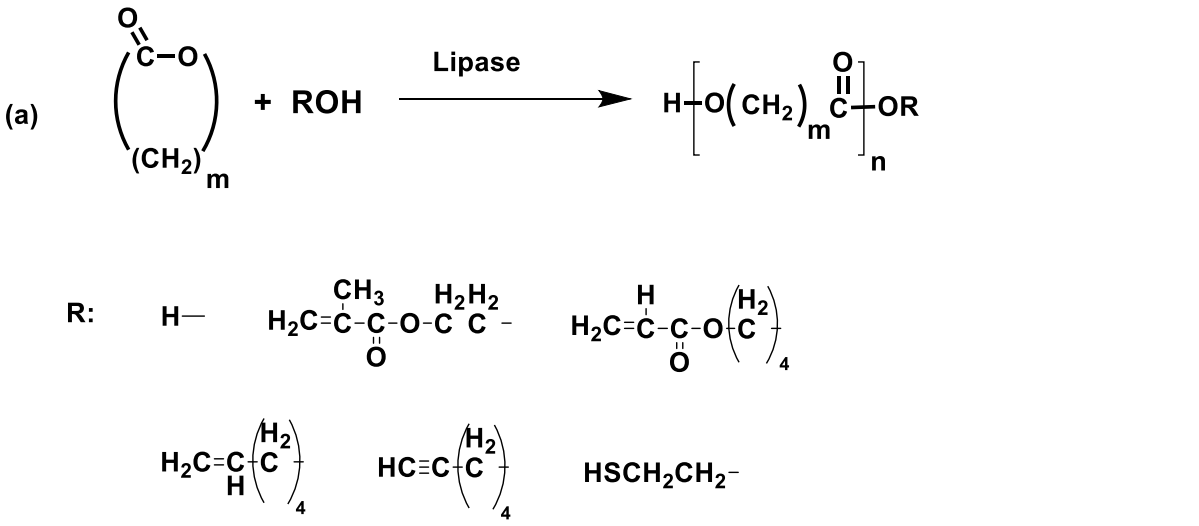

Macromonomer by Terminator Method

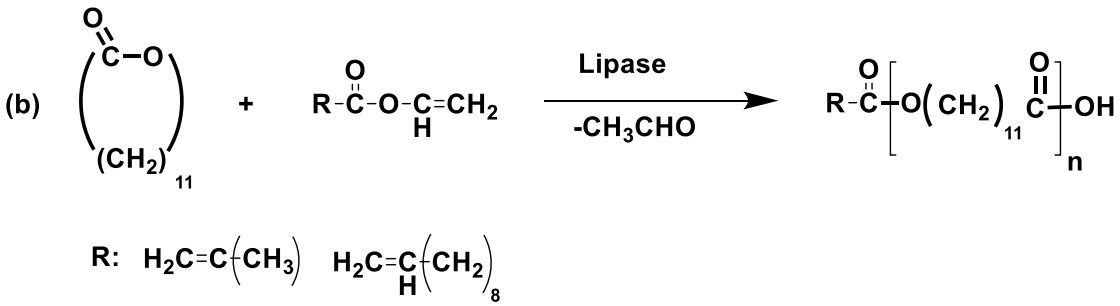

Telehelics by Terminator Method

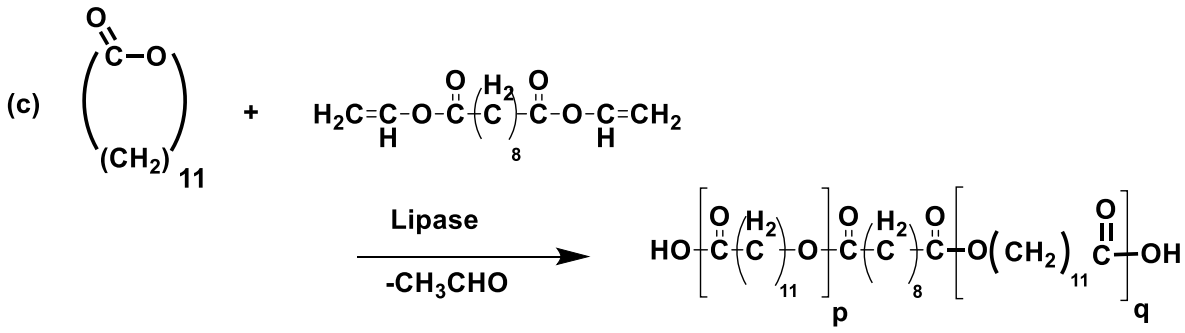

Scheme 1-5 Initiator and terminator methods to afford various macromonomers and telechelics

© 2020 Tous droits réservés.

1.4.4. Chemoselective polymerization

In contrast of anionic and radical polymerization, Lipase catalyzed chemoselectively the ring opening polymerization of 2-methylene-4-oxa-12-dodecanolide to give a polymer chain with maintaining the exo-methylene group (Scheme 1-6). Different groups exist in the structure of α-methylene-macrolides like aromatic, ether or amine groups. The polymerization of such macrolides was performed via enzymatic, anionic and radical polymerization. The selectivity towards lactones was afforded by lipase catalyst. On the other hand, the two other ways induce the polymerization of vinyl group. In addition, the produced polyester was a good target to undergo a radical crosslink through its methylene group.[85,88]

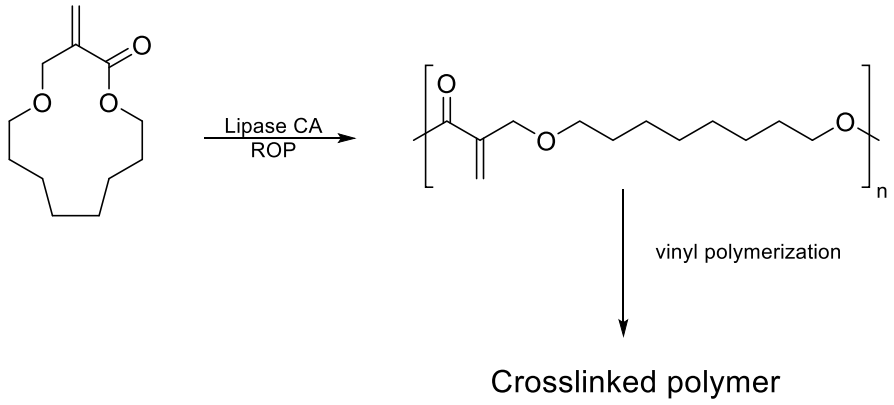

Scheme 1-6 Chemoselective ROP of α-methylene-macrolide

1.4.5. Enantioselective polymerization

Lipase PC catalyzed enantio-selectively the ROP of 3-methyl-4-oxa-6-hexanolide (MOHEL) in bulk at 60 °C (Scheme 1-7).[80] A powerful enantioselective polymerization occurred towards the racemic monomer (MOHEL), where the reaction rate of *(S)*-isomer was larger than the second isomer by seven times. The enantio-selectivity was also proved for copolymerization reactions catalyzed by Lipase CC to copolymerize β-butyrolactone (β-BL) with DDL,[78] and δ-VL with achiral lactones.[79] In addition, further studies were performed to describe the use of Lipase catalyst promoting regio-selective polymerizations to give specific polyesters.

© 2020 Tous droits réservés.
lilliad.univ-lille.fr

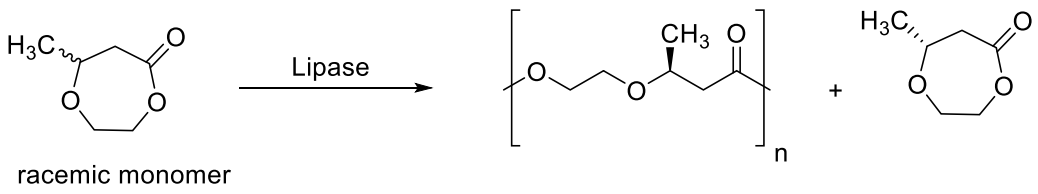

Scheme 1-7 Enantioselective ROP of MOHEL.

1.4.6. *e*-ROP: Green aspects of enzymatic polyester synthesis

Our work is considered to be involved under the headtitle of green polymer chemistry. So it's important to present the different green aspects of the enzymatic route for polymer synthesis. The green character of enzymatic catalysis in polymer synthesis was widely developed in literature.[1,57,60,63,64,72,89] The purpose of such development is to realize and maintain a green sustainable society. Polyesters syntheses were well proved using Lipase as a catalyst, in which, the characteristics of green polymer synthesis are addressed, such as: clean-process, energy saving natural resources problems, carbon dioxide emission, etc. The advantages of green chemistry will be applied to mitigate our environmental problems.

1.4.6.1. Reagents and products

Biobased chemicals are used as starting materials. They are obtained from the fermentation and/or further treatments of various biobased sources such as: corn, sugar cane, cassava, etc. The feedstocks that are needed for the production of polyesters include: lactic acid, itaconic acid and anhydride, succinic anhydride, 1,4-butanediol, sorbitol, sebacic acid, glycerol, etc.

The majority of produced polyesters are biodegradable non accumulated in the nature. Specific designed and functionalized polyesters can be applied in sophisticated biomedical and pharmaceutical areas..[7]

1.4.6.2. Nature of catalyst

Lipase is the most used enzyme to catalyze polyester synthesis. It presents attractive features; it is a non-toxic compound, cost effective compared to other enzymes and it gives access to high molecular weight polyesters. Lipase is available in immobilized form, which permits its recycling and reusing. Lipase can be combined with another type of catalyst opening a chemo-enzymatic catalytic process.[7]

© 2020 Tous droits réservés.
lilliad.univ-lille.fr

1.4.6.3. Reaction features

The polymerization catalysed by lipase can be performed under mild conditions in term of low temperature, neutral pH and atmospheric pressure. And due to the high enantio-, regio- and chemo- selectivities of lipase, the production of by-products is prevented or negligible. These important and attractive features are not given by the classical catalytic systems used for polyester synthesis.[7]

1.4.6.4. Solvents

A wide range of solvents can be used with lipase catalyst; they are not limited to organic ones, but also water, supercritical carbon dioxide, ionic liquids and others are considered as green solvents. These expand the practical route of polyesters production.[7]

1.4.6.5. Recycle of polyester

The formation of ester bonding is easy; and so is the reversible breaking action. Polyesters are chemically recycled by the reversible process offered by lipase catalysis,[90–92] where the latter is selective for ester function like acid. So actually, we are in front of high ability of reversible action during ROP of lactones, where linear polymers are able to be transformed to cyclic oligomers, and this can be limited by finding optimum reaction conditions.

© 2020 Tous droits réservés.
lilliad.univ-lille.fr

1.4.7. Degradation of polylactones by enzymes

Biodegradation is defined as a process by which organic substances such as polymers are decomposed into smaller compounds by living microorganisms' involvement like: fungi, bacteria and algae. These transformations are made through metabolic processes.[93,94] Biochemical processes take place into the micro-organisms cells. However, polymers are unable to penetrate the cell walls due to their macromolecular structure and water insolubility; thus, during polymers biodegradation, enzymes are produced by microorganisms to reduce the molar mass of polymers, so they can be transported through their cells, introduced into the metabolic pathway and consequently employed as carbon and energy sources. It's well known that polyesters require the presence of ester hydrolysis to produce water soluble products. Therefore, the biodegradation of polyesters can be applied by microorganisms producing hydrolyses.[95]

Polymers are largely recycled for efficient uses. In the case of polyesters, lipases can catalyze the formation of ester bond as well as its cleavage. So, polyesters can be recycled by this depolymerization process resulting in cyclic oligomers. The degradability of polymers is useful to prevent or minimize environmental pollution, due to the ability of polymer waste to be recycled or reused.[94]

Lipase B from yeast *Candida antartica* (CALB) can degrade polyesters in organic and aqueous solvents (Scheme 1-8).

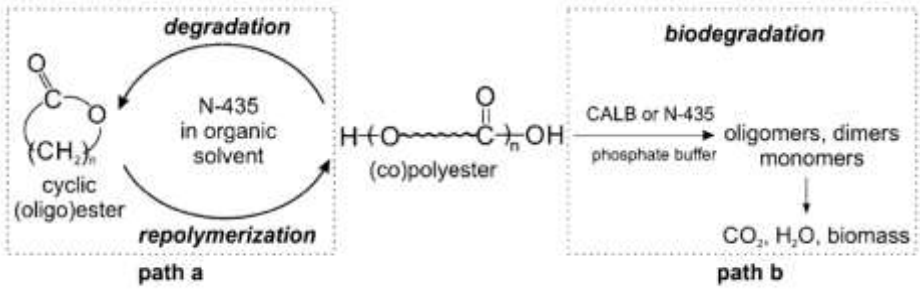

Scheme 1-8 Enzymatic degradation of polyesters in organic solvent (path a) or in aqueous solution (path b) by CALB lipase.[94]

The formation of cycle oligomers is concerned in the first pathway of Scheme 1-8, path a, and they are used in further polymerization reactions. The recycling of polymer chains was well performed in the presence of N435:we can cite as examples the degradation of PLA,[96] PBA, PBS,[97] PCL,[90,98] PHB,[99] and PTCL.[100]

© 2020 Tous droits réservés.
lilliad.univ-lille.fr

The degradation of PHB[99] and PCL[90] to give cyclic oligomers with M_n less than 500 g mol^{-1} was applied in the presence of toluene at temperature below 100 °C. These two polymers cited above were also depolymerized under continuous flow conditions in the presence of toluene and through N435 packed column.[98,101] At 40 °C, depending on the polymer concentration and the flow rate, the yield of cyclic oligomers obtained ranged between 87% and 99%.

The recycling of PTMC contributed in majority to the formation of TMC monomer while linear and cyclic oligomers were negligible.[102] The reaction was carried out in acetonitrile and catalyzed by N435 for 148 h to reach a yield of 80%. The monomer obtained was then successfully repolymerized through ring opening polymerization and catalyzed by N435, which gave a conversion of 60% after 80 h.

As mentioned before, N435 can catalyze the degradation of polyester films in buffer solution (Scheme 1-8, path b). The ability of N435 to depolymerize homopolymer PTMC was demonstrated with 98% broken mass after 9 days[103] and a decrease of molar mass from 117 kg mol^{-1} ($Đ$ = 1.8) to 6.90 kg mol^{-1} ($Đ$ = 16.7) was recorded after 5 days. However, the degradation of copolymer formed by TMC and GL did not behave similarly, where the loss of mass did not pass the 5.8%.

An interesting method for PCL films degradation was suggested in 2009 by Gross et al.[104] CALB was solubilized in toluene in the presence of surfactant pairing with sodium bis(2-ethylhexyl)sulfosuccinate and then mixed with PCL-toluene and flip into films. With 1.6% of catalyst concentration in the polymer matrix and after 19 days, a total film degradation was reached. The biodegradation rate was accelerated almost 17 times, when they increased four times the catalyst concentration, in addition, after 20 h of the process, the molar mass of PCL decreased from 120 to 24.7 kg mol^{-1}. In 2012, experiments were repeated by the same group but this time in continuous flow conditions.[105] The biodegradation rate was increased about six times as the autocatalysis caused by acidic degradation products accumulated in the films external media was avoided. On the other hand, the degradation rate of PCL can be improved by a copolymerization with other lactones[106] so that the copolymers of CL including VL and DL-lactide as second monomers performed higher hydrolysis rates.[107]

© 2020 Tous droits réservés.
lilliad.univ-lille.fr

1.5. Atom Transfer Radical Polymerization (ATRP)

1.5.1. Similarities and differences between RP and CRP.

Basically, conventional RP and CRP progress via similar radical mechanism, exposed to the same chemo-, regio- and stereo-selectivities, and are feasible with the same range of monomers. However, a lot of differences between RP and CRP subsist highlighting the importance of the latter.[43]

1. The lifetime of radical chains in CRP is protracted to more than 1 h due to the participation of dormant species and intermittent reversible activation, in contrast it is in the range of 1 s in RP.
2. In conventional RP the free radical initiator is often left unconsumed at the end because of slow initiation, which is the opposite case in CRP, where near instantaneous growth of all chains can be achieved due to the fast initiation ensuring the control over chain architecture.
3. Almost all chains are dead in RP, whereas in CRP activated chains count more than 90%.
4. Basically, polymerization takes more time in CRP than in RP. However, the rates could be equivalent in certain cases (e.g., when the M_W intended to obtain in CRP is relatively low)
5. In the two systems a steady state radical concentration is established, but reached by different mechanisms. In RP this state is based on the comparable rates of initiation and termination, whereas in CRP it is based on establishing a balance between the rates of activation/deactivation.
6. Termination usually occurs between long chains and new chains permanently generated in RP. In CRP systems based on PRE, all chains own a comparable length from the beginning till the end of polymerization.

The three most used CRP systems will be detailed in the following:

© 2020 Tous droits réservés.
lilliad.univ-lille.fr

1.5.2. Nitroxide mediated CRP

In 1980, nitroxides -stable free radicals- were used in the free radical polymerization in order to control.[108] In such polymerization, an interaction between transient radicals and persistent (stable) radicals is established. Following this combination, dormant adducts will be produced. In the dormant state, the two radicals exist in a trapped form and unable to interact with other radicals. However, the recurrence of both radical species is feasible by the controlled dissociation of dormant adducts. The transient radical will form an active radical intermediate after being combined to one of the monomers. This is followed by successive addition of monomers to the growing transient radical obtained during this step. When the concentration of nitroxide radical is high, the equilibrium will be shifted to the deactivation of transient radical, a result of the recombination of both radical components. During this phase, the polymer is considered as a dormant species where the concentration of the transient one is in decline, which leads to the reduction of termination reaction. In this case, we can talk about controlled living free radical polymerization.[48]

Using nitroxide engaged system eliminates the demand for catalyst since it can be active as initiator without any auxiliary. 2,2,6,6- tetramethylpiperidinyl-1-oxy (TEMPO) based are the most commonly used.[9,32] A thermal decomposition at the C-O bond generates two radicals (Figure 1-5). The nitroxide is the stable (persistent) one, while the other vinylic is highly reactive making it the transient radical. The latter can react with monomers like styrenes, acrylamides and methacrylates and contribute to the propagation step. The control of the process is explained by the maintenance of alternation of dissociation and capping between the two form of persistent radical and transient radicals at the polymer's end. And as it is expected, molecular weights of low dispersity are obtained.[48,49] In addition, based on this technique, an efficient co-polymerization producing block copolymers was reported.[109]

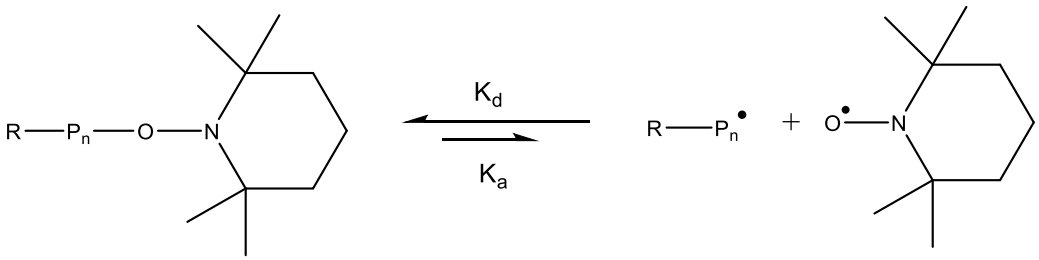

Figure 1-5 Nitroxide Mediated CRP

© 2020 Tous droits réservés.
lilliad.univ-lille.fr

1.5.3. Reversible Addition-Fragmentation Transfer Polymerization (RAFT)/ Macromolecular Design via the Interchange of Xanthates (MADIX)

RAFT was introduced in 1998 by E. Rizzardo and G. Moad.[52] In parallel, MADIX was developed by Zard's group.[110] Both of RAFT and MADIX progress following the same mechanism. However, MADIX is limited by using exclusively xanthates, whereas RAFT covers thiocarbonyl thio compounds in general (Figure 1-6).[111]

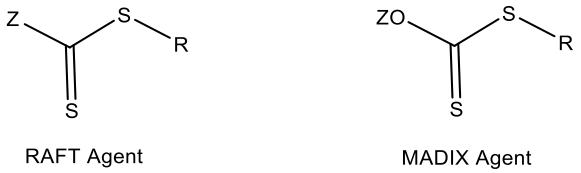

Figure 1-6 RAFT and MADIX Agents

During the reaction, a radical propagating species is produced through an interaction between a radical – that resulted from decomposition of radical initiator (like AIBN) and the monomer. The latter could be carboxylic acids, amides and tertiary amines. The RAFT/MADIX agent will be added to this species to form a RAFT/MADIX radical adduct. This adduct will decompose into a new active radical and a dormant polymer-thiocarbonyl thio species (Figure 1-7). Depending on the released active species nature, we can envisage two possibilities: the onset of new polymer chain with R•, or the continuation of growing polymer chain with Pn•. It is of great importance to guarantee a rapid transfer of the RAFT/MADIX agent between different dormant and active radical species on which is based the homogeneous growth of the polymers.[35,38,54] Fundamentally, we should have a much faster exchange reaction than the propagation one, and this is affected by the choice of the RAFT/MADIX agent (X) which must be perfectly chosen. The formation of polymers of well controlled masses and dispersity is favored under best conditions where the optimum initiator and RAFT/MADIX agent are used.[52,54,112]

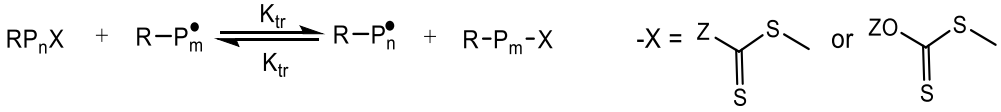

Figure 1-7 RAFT/MADIX polymerization

© 2020 Tous droits réservés.
lilliad.univ-lille.fr

1.5.4. Atom Transfer Radical Polymerization (ATRP)

ATRP, one of the topics of our work, has emerged as the most widely applied CRP with more than 11,000 publications from1995 to 2011[35] . This is due to readily available reagents use, robust implementation, and functional group tolerance.[113]

The ATRP system started by carrying out reactions using metal catalyst in combination with aromatic ligands yielding well-controlled structures and narrow molecular weight distributions. This work was developed during the same period in 1995 by two research groups headed by K. Matyjaszewski who coined the name atom transfer radical polymerization,[114] and M. Sawamoto who termed it Metal Catalyzed Living Radical Polymerization.[115]

ATRP has been successfully mediated by a variety of metals, including those from Groups 4 (Ti),[116] 6 (Mo),[117,118] 7 (Re),[119] 8 (Fe,[120,121] Ru,[51,122] Os[123]), 9 (Rh,[124] Co[125]), 10 (Ni,[126,127] Pd[128]), and 11 (Cu).[47,129] Cu complexes were considered the most effective catalysts in ATRP for a wide range of monomers in various media.[43]

In ATRP system, the control of polymerization is based on strict regulation of equilibrium between a dormant alkyl halide and an active propagating radical species. Such regulation ensures the minimization of radical concentration in order with the undesirable bimolecular termination reactions.[130] The transition metal ligand complex undergoes an oxidation and a single electron will be offered to the alkyl halide (dormant species) forming a highly reactive organic radical (transient species). The latter, undergoes the propagation step with the unsaturated monomer used. The metal fails to keep the combination with the halide which will be abstracted by the polymer transient radical, thus forming a dormant polymer and leading to the control of polymer's length.[47]

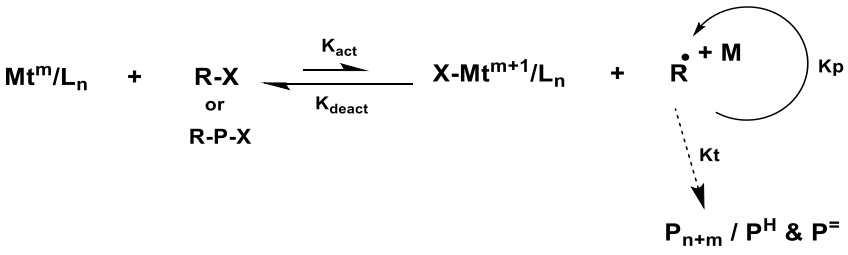

Figure 1-8 ATRP mechanism in the presence of metal catalyst

© 2020 Tous droits réservés.
lilliad.univ-lille.fr

The general mechanism is shown in (Figure 1-8).[57,90,124] In such a mechanism, the control is achieved by metal catalyzed activation/deactivation cycle, in the presence of alkyl halide as initiator or dormant species. An alkyl radical –produced by homolytic cleavage- and an oxidized transition metal/ligand (deactivator) are generated after an interaction between the transition metal/Ligand of low oxidation state (activator) and the alkyl halide. This process takes place with a rate constant k_{act} which is by far less than that of deactivation process k_{deact}. The small amount of active radical species present in the reactor undergoes the propagation step following the classical addition to the unsaturated polymer already known in conventional radical polymerization with rate constant k_P. the cycle returns to reform the dormant alkyl halide and the activator, and this is after the deactivation of alkyl radical by the high oxidation state metal complex. Despite maintaining control over the system, termination reactions are not totally eliminated, and can occur with rate constant K_t by coupling or disproportion. But these reactions are immediately prevented by the increase of metal/ligand quantities leading to shifting towards the deactivation process. The repetition of activation/deactivation cycles for all dormant species allows the uniform growth of all polymer chains. As a result, an auto-regulation system is obtained which guarantees the living nature of ATRP.

The key reaction behind ATRP is known to be the atom (halogen) transfer responsible of the homogeneous growth of polymer chains. This requires a fast initiation and a rapid deactivation process. At the end, a linear relationship is provided between the degree of conversion and the mass of the obtained polymer.

© 2020 Tous droits réservés.
lilliad.univ-lille.fr

1.5.5. ATRP components

As a multicomponent system, ATRP comprises a monomer, an initiator with a transferable halogen and a catalyst which is composed of a metallic species and a suitable ligand. For a successful ATRP, other factors, such as temperature / light source (depending on induction method) or the solvent should be taken into consideration.

1.5.5.1. Monomer

A wide range of monomers have been successfully polymerized using ATRP technique. Typical monomers used contain substituents stabilizing propagating radicals like: styrenes, (meth)acrylates, (meth)acrylamides, and acrylonitrile (Figure 1-9). Note that under the same conditions using the same catalyst, each monomer performs with its own equilibrium k_{act} and k_{deact} constants.[37,47]

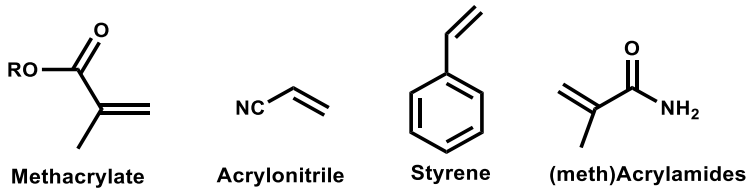

Figure 1-9 Structures of common ATRP monomers

1.5.5.2. Initiators

The mass of polymer to be obtained is strongly affected by the initiator. ATRP is characterized by a fast initiation, where the number of growing chains is equal to the initiator's initial concentration with negligible termination reactions. Thus, an elevated concentration of initiator contributes to decrease the degree of polymerization and subsequently decrease the theoretical molecular weight as the Equation 1-1 shows below:[47]

$$DP = \frac{[M]0}{[initiator]0} \times conversion$$

Equation 1-1

Typical initiators used in ATRP are alkyl halides (Figure 1-10) (RX), where the alkyl halide group migrates between the metal complex and the growing radical during the activation and

© 2020 Tous droits réservés.
lilliad.univ-lille.fr

deactivation processes. In general, the presence of activating substituents such as aryl, carbonyl, or allyl groups, on the α-carbon of any alkyl halide, allows to use it as ATRP initiator. Thus far, the best molecular weight control is obtained when X is either bromine or chlorine.[47] In copper-mediated ATRP, Iodine works well for acrylate polymerizations,[131] and for styrene polymerization in ruthenium- and rhenium-based ATRP.[119,131,132] Fluorine is not used as initiator, Since the C-F bond is too strong, it is difficult to achieve its homolytic cleavage. In addition, successful polymerization of acrylates and styrenes was reported using pseudohalogens, such as thiocyanates.[47]

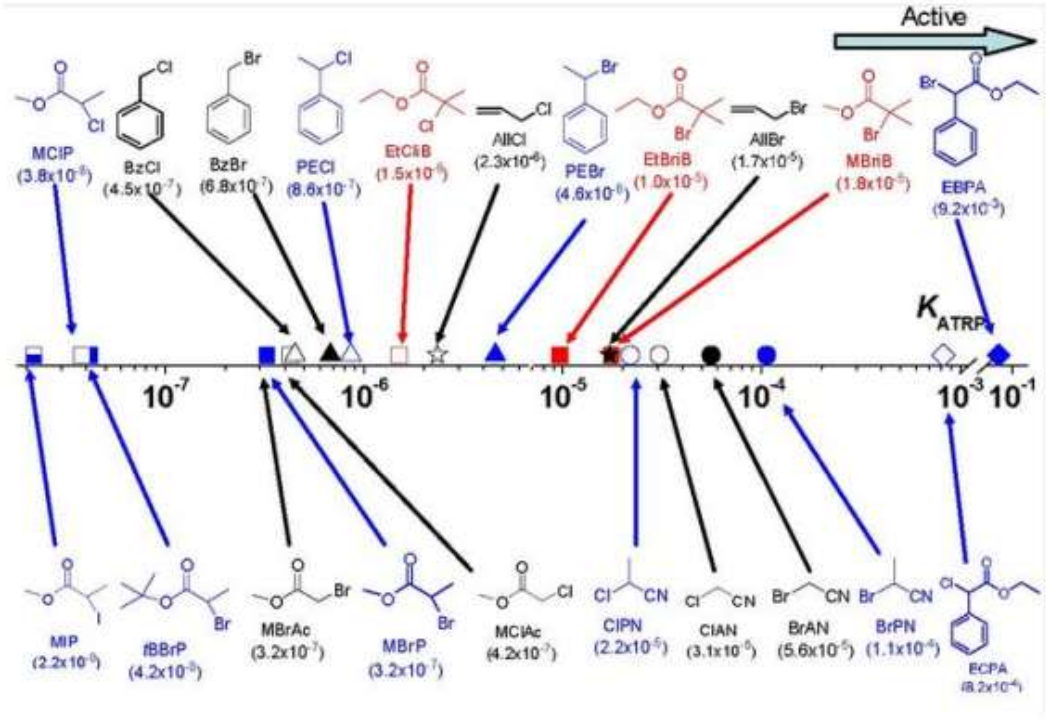

Figure 1-10 Activities of various alkyl halide initiators used in ATRP[133]

1.5.5.3. Catalysts

One of the most important component in ATRP system is the catalyst as it determines the position of the atom transfer equilibrium and the dynamics of exchange between the dormant and active radical states. An efficient catalyst should meet several prerequisites:[35,47,134]

- All the chains should start the polymerization at the same time, and the initiation should be more rapid than the propagation.
- In order to prevent the excess of active radical species leading to termination, the equilibrium between the dormant and the active radical states should be strongly shifted toward the dormant side.

© 2020 Tous droits réservés.
lilliad.univ-lille.fr

- The homogeneity of polymers' growth rate should be ensured by the rapid process of deactivation by which the halogen is transferred to the active radical deactivating it.
- Any side reactions like oxidation, reduction or H abstraction of the radical should be limited.

So the choice of the metal based complex is important, and it should meet the following considerations:

- The metal center should have at least two oxidation states separated by one electron.
- The coordination sphere around the metal should be expandable upon oxidation in order to ensure the accessibility of the halogen into it.
- A strong interaction should be exhibited between the halogen and the metal.
- The metal should have an affinity towards halogens.

The choice of the complex ligands is also of great importance. The role of the ligand is to solubilize the metal catalyst in the reaction mixture in addition to its involvement in regulating the redox potential of the catalyst.[47,135]

1.5.5.4. Solvent

The solubility of PMMA was studied by Evchuk and al using a temperature ranging from 30 to 70 °C in 12 different organic solvents: benzene, toluene, o-xylene, m-xylene, trichloromethane, trichloroethylene, 1, 4-dioxane, cyclohexanone, acetophenone, ethyl acetate, pentyl acetate, and dimethyl formamide. As a result, trichloroethylene was found to be the best solvent for PMMA, while trichloromethane was the poorest. Acetate and cyclohexanone as polar solvents were found to be good for PMMA, but the more polar dimethylformamide solvent -that we used- dissolved slowly this polymer. Practically, tetrahydrofuran (THF) dissolve PMMA at room temperature faster than most of the 12 organic solvents mentioned in this study. Note that the tacticity of PMMA was not taken into consideration.[136]

1.5.6. Copolymerization

Not so far after ATRP discovery, the development was directed towards the synthesis of block copolymers while taking advantage of the variety of monomers, conservation of end groups, and control over molecular weights and polydispersities. The synthesis of polymethyl acrylate-b-polystyrene and polystyrene-b-polymethylacrylate was the first example reported.[129,137]

© 2020 Tous droits réservés.
lilliad.univ-lille.fr

Indeed, a halogen group exists at the produced polymer chain's end, which allows its utilization to initiate a subsequent polymerization. This presents an efficient tool for the preparation of a wide range of copolymers, such as block, gradient, and hyperbranched polymers.[138]

Block copolymer can be synthesized using ATRP following two ways.[139,140] The first method is based on adding a second monomer to the reaction mixture after the near termination of the first polymerization. The second one consists of the utilization of the formed polymer as a macro-initiator after its isolation and purification. The first method is easy to operate, but the second resulting block is usually not pure.[141]

Many articles mentioned the synthesis of block copolymers using acrylic monomers such as *n*-butyl acrylate (BA) and methyl methacrylate (MMA) using ATRP.[139,141,142] A copolymerization of poly- (methyl methacrylate)-*block*-poly(*n*-butyl methacrylate) (PMMA-*b*-PBMA) by ATRP was also reported.[138]

1.5.7. Limitations of ATRP

Monomers with ionic or carboxylic acid groups alter the equilibrium of ATRP by reacting with the catalyst, thus they are not suitable for this system. Vinyl acetate and halogenated alkenes are also not favored in ATRP and this is due to their corresponding unstable radical formed.[143]

Traditionally, the equilibrium of ATRP system is mediated by transition metal catalyst, which ultimately contaminates the polymer product and restricts its potential application, especially in electronic applications,[113] and in bio-applications where even ppm levels of transition metal residues might be detrimental.[144,145] However, the current drawback is the absence of an efficient method to remove or recycle the catalyst.[21]

Significant progress makes possible the use of lower levels of transition metal catalysts[146,147] and increased capability of polymer purification.[21,148] Different removal methods were achieved using alumina columns, precipitation of polymer to a non-solvent, or precipitation of the Cu complex with NaOH or Na_2S. Although these methods are efficient, the use of alumina column to purify a viscous polymer mixture presents a limitation especially on large scale (>10 g). Additionally, significant amounts of solvent are required for repeated precipitations.[21] Also, after immobilizing the catalyst on a solid support, it can be potentially recycled,[149,150] but the polymerization process control can be limited.[151]

© 2020 Tous droits réservés.
lilliad.univ-lille.fr

Recently a more ambitious and viable approach has arisen to entirely eliminate metal contamination of the polymer product. It is the organocatalyzed ATRP (*O*-ATRP).[152,153]

© 2020 Tous droits réservés.
lilliad.univ-lille.fr

1.6. Characterization of Polymers

1.6.1. Degree of Conversion

The degree of conversion is an important factor indicating the amount of monomers that have effectively undergone ATRP. This factor can be determined by ^{1}H NMR or gravimetrically. Polymer chemists aim to have a high % of conversion within small reaction times in order to save energy and time.

1.6.2. Molecular Weight

The molecular weight is another important factor for polymers. The increase of degree of polymerization induces the linear increase of M_n of the formed polymers:

$$M_n = \text{Mmonomer} \times \text{conversion} \times \text{DP}^{47}$$

Equation 1-2

This factor is linked to many physical properties like transition temperatures of different stages (liquid, wax, rubber & solid) and mechanical properties like strength, viscosity, viscoelasticity.[154] From many types of molecular weight, number average molecular weight M_n and mass average molecular weight M_w are the two parameters that can give an indication about the polymer's dispersity.

1.6.3. Number average molecular weight M_n

Under the conventional definition of average value, M_n is the ratio of the total weight of the polymer to the number of polymer molecules. M_i denotes the possible molecular masses of the polymers. N_i is the number of these different macromolecules whose masses are M_i. So the total mass will be designed by $N_i \times M_i$.

Thus the number average molecular weight M_n is presented as in Equation 1-3

$$\overline{M_n} = \frac{\sum_{i=1}^{\infty} N_i \times M_i}{\sum_{i=1}^{\infty} N_i} = \frac{Total\ weight}{Number\ of\ polymers}$$

Equation 1-3

1.6.4. Weight average molecular weight M_w

Weight average molecular weight depends on the mass or the size of the polymers along with their number (Equation 1-4). in this equation the weight of a polymer chain is $w_i = N_i \times M_i$.[155,156]

© 2020 Tous droits réservés.
lilliad.univ-lille.fr

M_w, is strongly affected by the large molecules that greatly contribute to its value because of the square function in its formula. So the M_w is sensitive to changes in the number of large molecules more than that of small molecules. Nevertheless, low mass polymers contribute greatly to M_n because for small molecules, a certain mass includes a large number of molecules.

$$\overline{M_w} = \frac{\sum_{i=1}^{\infty} N_i \times {M_i}^2}{\sum_{i=1}^{\infty} N_i \times M_i}$$

Equation 1-4

To mention that the conversion of monomers and the molar mass of the polymer values can be calculated by ^{1}H NMR, which is detailed in section 7.2.

1.6.5. Polydispersity index (PDI)

Chemists are permanently working on yielding polymers that include molecules of similar and ideally identical mass values. This can be represented by the weight distribution plot. A broad plot indicates the presence of dispersed polymer. So to reach the desired objective, this plot should be the subtlest possible. In ATRP case, the values of average molecular weights M_n and M_w are almost identical and this is due to the fact of simultaneous initiation of all polymers with the same rate, thus, the distribution is too steep.

The value of polydispersity index is used to indicate homogeneity of the synthesized polymers. It is the ratio of the weight average molecular weight over the number average molecular weight (Equation 1-5). In the ideal case, the two components of this equation are identical, which gives a PDI of 1.0. the smallest PDI reported was 1.05 which presents a continuous progress in this field.[35,36]

Gel Permeation Chromatography is used to determine the values of M_n, M_w and PDI. A calibration by standard polymers of known molecular weight is required using this method. A comparison between the the polymer retention time and that of standards should be realized in order to determine the M_n, M_w and PDI.[157] Dosy NMR is also used to determine M_n and PDI[158] whereas 1H NMR allows to determine M_n.[159]

$$PDI = \frac{M_w}{M_n}$$

Equation 1-5

© 2020 Tous droits réservés.
lilliad.univ-lille.fr

1.7. Microreactor technology

For high performance manufacturing technology, as a key green engineering method, a combination between bio-catalysis and microscale technology in flow was established for production processes. Many advantages are provided in using such a system including high surface to volume ratio of microreactors and the short diffusion paths. This allows a more efficient heat and mass transfer compared to conventional platforms.[24–27] In continuous microreactor, the simple variation of the flow rate of reaction mixture or the micro-channel length contributes to adjust the reaction time.[28]

Microreactor technology started to gain interest among chemists during the past two decades following the work effectuated by Ley[160,161] that showed the possibility of using this technology for complex organic molecules synthesis. Nowadays, it is believed that almost all the ordinary batch reactions can be carried out in flow reactors.[162]

A microreactor is characterized by its miniaturized confined space where a reaction takes place. Generally, it is made of a tubular system with microscale dimentions.[163] The operation consists of a continuous feeding of reagents and recovery of products in highly controlled way. Microreators exist in a wide range of volumes. And they are called mesoscale reactors when their volume is above 5 ml.[164]

1.7.1. Continuous Flow system

The flow system should be composed of two or three main parts: the flow reactor, an injection system and for photochemical reaction a light source. In some cases, additional parts can be found such as: mixer and online analytical or purification systems.(Scheme 1-9).[165]

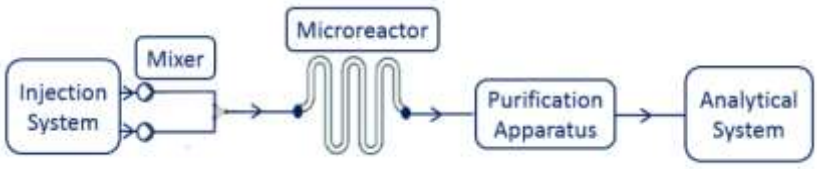

Scheme 1-9 Set-up of a microreactor assembly

© 2020 Tous droits réservés.
lilliad.univ-lille.fr

1.7.1.1. Injection system

The continuous flow control is provided by injection systems based on mechanical or non-mechanical pumps. The first type is commonly used in form of syringe pumps, peristaltic pumps and High Performance-Liquid Chromatography (HPLC) pumps (Figure 1-11).

The reaction mixture is stored within syringes. With peristaltic pumps, flexible tubes are used to host the reaction media. The mixture is expelled out of the tube by the compressing force applied by the rotation of the rotor.[166] For HPLC pumps, there is a piston inside that forces the liquid to flow through tubular reactors at specific flow rates.

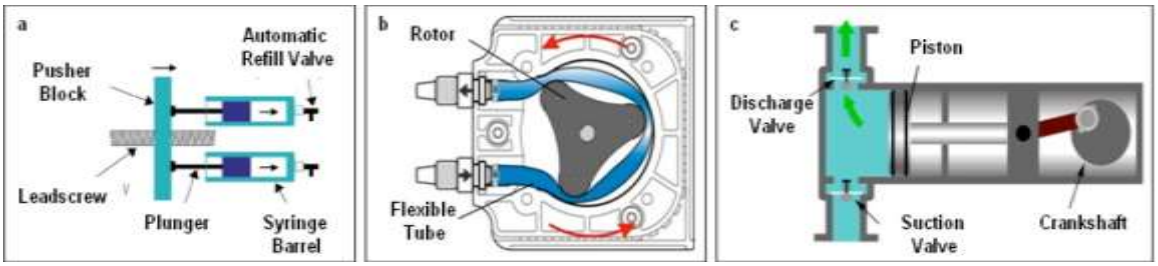

Figure 1-11 Mechanical pumps: (a) syringe pump; (b) peristaltic pump; (c) HPLC pump[167]

Non-mechanical pumps comprise those that function based on electricity such as the electro-hydrodynamic pump. This kind of pumps own electrodes to provide the generation of an electric field that accelerates charged molecules and consequently form a flow.[167]

To insure the connection of the different parts in a continuous flow system assembly, tubing, fittings, connectors and sleeves are used.[165]

1.7.1.2. Mixing systems

The scale-up of microreactors varies according to the processes in the microreactors, their compatibility with chemicals and the products economics. To design a reaction in a batch system, the reactor design and scale-up challenges should be overcome to meet industrial requirements. One of the most important advantage of microreactors is their ability to perform complex reactions with higher control in term of kinetics and product properties due to the enhanced synthetic conditions. In general, these complex reactions involve multiple phases that are immiscible. They can be aqueous-organic liquids[168,169] and gas-liquid reactions.[170] However, mixing takes place by advection and employs laminar flow. The efficiency of mixing in microreactors can be improved by different designs. Depending on the presence of mechanical agitation and external forces, mixers are divided in two categories either active or passive. In active micromixers, a perturbation energy is involved in form of electrokinetic, dielectrophoretic, acoustic/ultrasound, and magnetohydrodynamic (MHD)

© 2020 Tous droits réservés.
lilliad.univ-lille.fr

energy; nevertheless; their fabrication called for special techniques.[171–173] In passif micromixers, a lamination of multiple fluid streams is created that increases the interfacial area for diffusion.[172–174] Although the good efficiency of multi-lamination, high pressure drops can be created by the narrow micro-channels. In general, passive mixing is the one used in multiphase flow systems to prevent any foul after extended operation. Figure 1-12 presents the simple continuous flow and the system with passive mixing forms. Furthermore, the flow in microreactors can be also categorized as continuous or segmented flow. In addition, the segmented one, can be classified into two categories:gas-liquid or liquid-liquid segmented flow (Figure 1-12).[175]

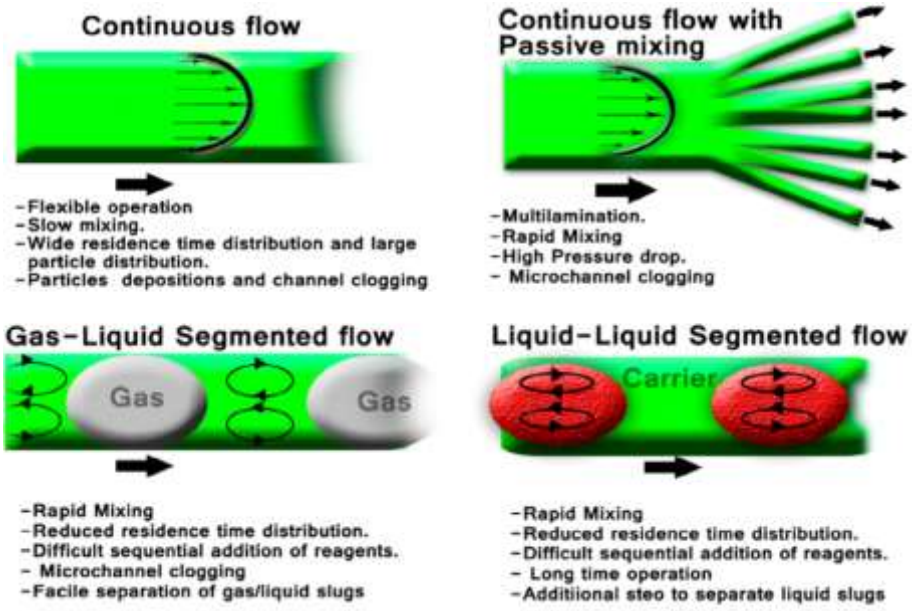

Figure 1-12 Comparison of different microreactor flow systems.[176]

Compared to batch reactors, simple continuous flow without passive mixing permits an easy change of experimental conditions and gives better homogenous solution during the synthetic process. Usually, the mixing is obtained by molecular diffusion of the species within the laminar region.[176]

1.7.1.3. Types of microreactors

Reactors with microscale dimensions can be fabricated based on a wide range of materials: polymers, silicon, metals, stainless steel, glass, and ceramics. Microreactors can be fabricated as microcapillaries and chips (presented in Figure 1-13) through simple methodologies

© 2020 Tous droits réservés.
lilliad.univ-lille.fr

improved in microfluidics technology. Microcapillary reactors are fabricated from suitable tubing of determined length and material, whereas chip-based reactors engage glass, silicon or plastics that are fabricated by several methods such as micromachining, wet etching, and soft lithography techniques.[177,178]

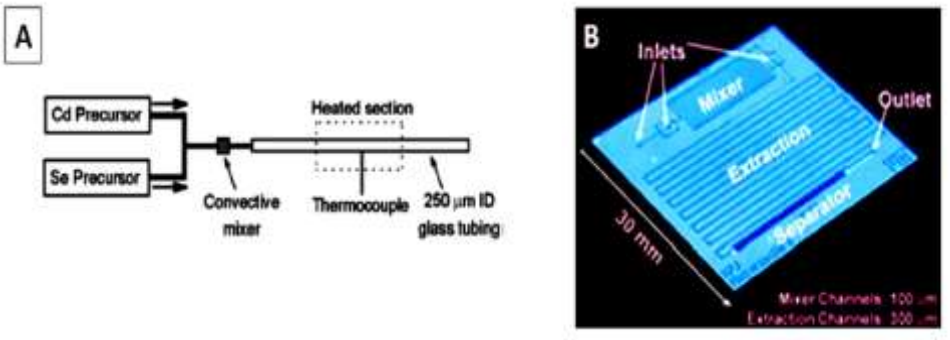

Figure 1-13 (A) Schematic of a capillary-type microreactor for the synthesis of CdSe nanocrystals[179] and (B) chip-type multiprocess microreactor capable of mixing, extraction, and phase separation[180]

In principle, microcapillary reactors are used for chemical reactions in order to reach high yields and conversions.[181,182] In addition, microreactors employ better heat and mass transfer during the reaction. Yen *et al.* prepared CdSe colloidal nanocrystals using a flow capillary microreactor presented in Figure 1-13-A, which comprises a convective mixer and a heated glass reaction channel in the form of a capillary.[179]

Regarding the chip type of microreactor, it employs easy microfluidics control and it is well integrated with many processes into one device. Using this type of microreactors, series of miniature channels can be connected in a specific geometry in order to control the special and temporal alteration of small volume of fluid. Thus, the synthesis of compounds by multistep process is feasible now on the miniaturized reaction networks fabricated onto a chip.[183,184] Kralj *et al.* developed a device able to mix and separate organic-aqueous and fluorous-aqueous liquid –liquid system (Figure 1-13-B).[180]

1.7.2. Materials for microreactors fabrication

A wide range of materials are used for the fabrication of microreactors like: glass, ceramics, perfluoroalkoxy (PFA), silicone, polymers and steel.[185–189] Table 1-3 shows the advantages and disadvantages of typical materials used for microreactor fabrication. Several points should be addressed to select the appropriate material, aong of which we cite: operating conditions (pressure and temperature), physical properties of reaction mixture (pH, viscosity, phase and reactivity), cost, mass production capacity and fabrication simplicity. Silicone is

© 2020 Tous droits réservés.
lilliad.univ-lille.fr

widely available and this is one of the most used materials for microreactors. Numerous industrially liquid-gas phase reactions can be performed in silicon microreactors.[190–192] Nowadays, microreactors based on polymer material attract much attention. Polymeric microreactors offer many advantages like adjustable properties, elastic flexibility, effective cost, easy to fabricate and they have a good availability. Polymers. Polymeric material can be divided into broad categories: polydimethylsiloxane (PDMS) and its modified versions and thermoplastic polymers such as polyvinyl chloride (PVC), polystyrene (PS), polycarbonate (PC), poly(methyl methacrylate) (PMMA), polyimide (PI), and olefin-based polymers.[193–197] Although that glass microreactors are difficult to handle, they are considered as a popular choice for organic syntheses since they allow electroosmotic flow with the most used polar solvents.[198]

Material	Advantages	Disadvantages
Silicon	• Cheaper • Well-characterized material • High-precision fabrication	• Expensive fabrication techniques • Clean-room required
Glass	• Visualization of reaction and flow • Electroosmotic flow (EOF) possible • Withstands high operating pressures	• Difficulty in creating high aspect ratio structures
Polymer	• Low cost • Various fabrication techniques • Tunable properties • Disposable microreactors possible	• Chemical compatibility • Thermal stability
Metal	• No clean-room required • Durable materials • Well-established fabrication techniques	• Replacement with noble metals possible • Issues with variable pressure drop

Table 1-3 Advantages and disadvantages of typical materials used for microreactors fabrication[198]

1.7.3. Photomicroreactors

Limited are the choices of materials for photo-reactors fabrication, since they should be transparent to the desired irradiation wavelength. Therefore, just certain types of polymers, glass, silicon and ceramics can be suitable materials for photo-reactors.[165] The cheapest and easiest reactors to be fabricated are those polymers-based ones. Polymethyl methacrylate (PMMA), polydimethylsiloxane (PDMS), perfluoroalkoxyalkane (PFA), and fluorinated ethylene propylene (FEP) polymers are used for photomicroreactors due to their high light transmissions. However, PMMA and PDMS are swollen by organic solvents, thus their usage is limited to aqueous reactions. In contrast, FEP and PFA are inert towards most reagents and solvents even under extremely acidic or alkaline conditions. They have great flexibility and transparency to UV and visible light making them a favorite choice for tubing used as photo-reactors.[199]

© 2020 Tous droits réservés.
lilliad.univ-lille.fr

Many types of glass are used in the fabrication of photomicroreactors because of their light transparency, such as: Quartz (cut off < 170 nm), Pyrex (< 275 nm), Corex (< 260 nm) and Vycor (< 220 nm). In addition, they can filter the undesired wavelength emitted from a polychromatic light source. They present the best inert properties compared to other materials, but they are difficult to be fabricated and to handle. Ceramic behaves similarly. Silicone is not compatible with alkaline conditions and expensive.[199]

1.7.4. Light sources

Typical Hg lamps are used for photochemical reactions in microfluidic systems. They are perfectly suited when tubular reactors are coiled around them. these lamps should be placed outside reactors since their dimensions are larger than those of the reactors.[165]

Recently, light emitting diodes (LEDs) are gaining much attention in continuous flow photochemistry field. The LEDs can produce narrow emission spectra (20 nm) and by using them, side reactions are reduced compared to other types of light sources that are broadband emitters. In addition, the photon flux efficiency and the reaction's yield are improved using the LEDs, since they can be matched to the maximum absorption wavelength of the chromophore. Furthermore, they don't require a high power input and they manifest minimal heat loss, which makes the system cooling very easy to provide. They are also low cost light source and their relative small dimensions makes them suitable to be placed on the microreactor.[200,201]

High power LEDs are good alternative for mercury lamps for applications requiring more power, they are characterized by their stable power, fast warm up time, long life (over 10,000 hours) and precise adjustment. However, the very low optical power (few $\mu W.cm^{-2}$) of developed UVB LEDs (315 – 280 nm) makes their use limited in photochemistry. The use of LEDs in UV photochemistry is focused on the near UVA LEDs range (365-400 nm) for which suitable high power LEDs (up to 12 $W.cm^{-2}$) are developed.[202–206]

1.7.5. Biocatalysts in flow reactors

Biocatalysis is considered to be a reliable tool aiming to develop green and intensified chemistry, since proper reactors are well designed. Usually biocatalysis is used in batch reactors with good flexibility and simplicity. On the other hand, it has been found that in continuous flow reactors, biocatalysis can be performed in a more productive, controlled and environmentally sustainable process.[186,207]

© 2020 Tous droits réservés.
lilliad.univ-lille.fr

The switch from batch to continuous flow in micro- and meso-reactors implies two key concepts which are: green chemistry and process intensification.[208] In a flow process, biotransformations are accelerated due to an improved mass transfer, and give an economic large scale production using smaller equipment. Besides a significant decrease of reaction time is provided, from hours to few minutes. The reaction parameters are more easily controlled enhancing thus yields and productivities.[209] With a good control of the reaction, the reaction waste generation will be reduced. The scale up in flow system is provided by adding flow reactors in series and/or in parallel.

Biocatalysts were used in their free form in flow reactors as shown in Figure 1-14-1. However, a combination of immobilized biocatalysts with flow reactors was an interesting approach considering its importance to facilitate biocatalyst reuse and the addition of extra processes downstream. This latter approach has been well reviewed and detailed.[210] Figure 1-14 shows the different ways to combine flow reactors with enzymes:

1- The immobilization of biocatalyst on beads packed in the reactor - as applied in our study - which allows high enzyme load but with attention paid to excessive back-pressure (Figure 1-14-2).[211]
2- The immobilization of biocatalyst on the inner surface of the reactor (kind of coating) (Figure 1-14-3).[212]
3- The immobilization of biocatalyst on a monolith contained in the reactor to reduce the limitation of the previous two forms 2 and 3 (Figure 1-14-4).[213]
4- The immobilization of biocatalyst on a membrane (Figure 1-14-5).[214,215]

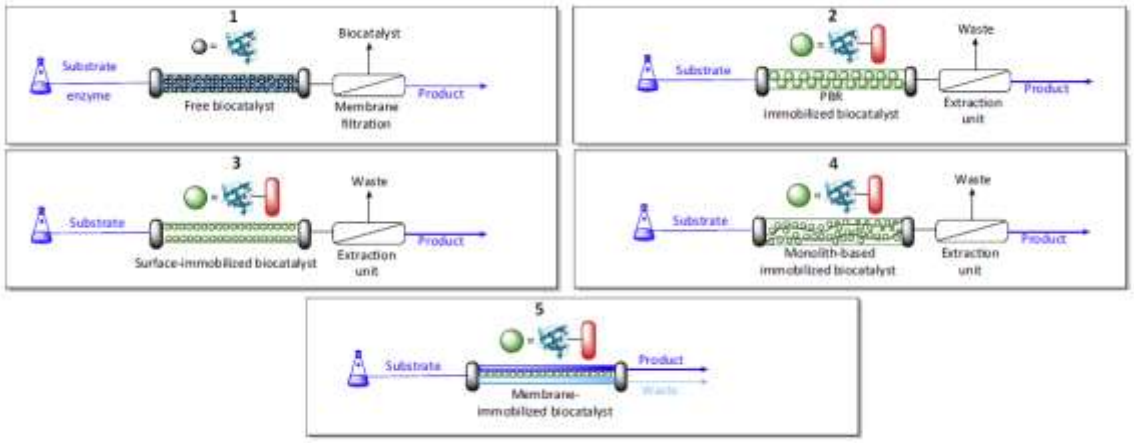

Figure 1-14 (1) Free biocatalyst. (2) biocatalyst immobilized in a packed bed reactor. (3) Biocatalyst immobilized on the inner surface of the channel. (4) Biocatalyst immobilized on a monolith. (5) Biocatalyst immobilized on a membrane.[210]

© 2020 Tous droits réservés.
lilliad.univ-lille.fr

1.7.6. Batch vs flow in scaling up

The application of flow processes on a large scale is an important issue to discuss. For reactions carried out in batch, the scale affects the efficiency of the mass and heat transfer within the system, which imposes the necessity to re-optimize reaction conditions. Apparently, the scale-up of microreactors seems simple, but the cost of a given type of individual microreactor and the challenge of pumping the reaction mixture throughout the channel can be considered as a limitation for this approach. The use of mesoreactors was the way to overcome these limitations and turn into production from g/h to tons/year. And this allowed the scale-up of different types of reactors like: chip microreactors, single tubular reactors or parallel capillary reactors.[25,216–218] For given flow rates and reactor volumes, the amount of generated product can be determined by the duration over which the entire flow process is operated.

1.7.7. Solvent constraints

When using microreactors, additional attention should be paid to solvent choice. In such a system, the reagents should be totally dissolved to avoid any solid precipitation within the microfluidic system. Otherwise, the device will be clogged.[164]

1.7.8. Purification apparatus and analytical systems

Microfluidic technology offers a very important option, which is the ability to adjust an online purification and monitoring systems to the assembly. Tools that can be added downstream the microreactor are the following: microextractor,[180] a porous membrane that selectively wets an organic solvent,[219] distillation apparatus,[220] purification column[180] and another reactor for scaling up.

Several analytical systems can be integrated too, providing the possibility for reactions' rapid screening. This system can be an automotive measurement of tempretaure and pressure, HPLC, IR, UV, spectrometer, etc.[221,222]

1.7.9. Why to use photochemistry in flow

1.7.9.1. Photon flux

The photon flux is defined as the number of photons yielded to the reaction mixture in a process per unit of time. It might be used to determine the quantum yield of a reaction.[164] Chemical actinometry can be used to determine the photon flux.[165] In fact, several factors may engender a reduction of photons' transmitted amount delivered by the irradiation system

© 2020 Tous droits réservés.
lilliad.univ-lille.fr

to the reaction, such as refraction and incompatibility between the reactor's dimensions and geometries and the light source.

Since the photon flux affects greatly reaction kinetics, Loubière and co-workers compared the photon flux received by a batch reactor and a flow reactor.[223] The photon flux received was 4.44×10^{-4} Einstein.min^{-1} in batch reactor compared to 2.46×10^{-4} Einstein.min^{-1}.

When dividing the photon flux value to the reactor volume, we obtain the photon flux density. In that case, the corresponding value obtained for the microreactor was 301 Einstein.m^{-3}.min^{-1} vs 1.98 Einstein.m^{-3}.min^{-1} for the batch reactor, indicating that the amount of photons received by the microreactor is 150 times higher than that received by the batch reactor. And this explains the fact that reaction kinetics in flow reactors are accelerated.[164,223]

1.7.9.2. Photonic efficiency

Photonic efficiency is another factor that can characterize a photochemical reaction. As a definition, it is the ratio of reaction rate to the photon flux Q (Equation 1-6).[164]

$$\xi = \frac{reaction\ rate}{Q}$$

Equation 1-6

It was reported that this value in batch reactor varies between 0.0086 and 0.0042.[224] On the other hand, Noël and co-workers showed that in microscale irradiation, this value can be enhanced up to 0.66.[225]

1.7.10. Examples of Polymerization reactions in microflow reactors

Microreactor technology is starting to gain interest in polymer science. Even though flow polymerizations are previously reported, the development in this field is still ongoing. The major improvements and developments in flow polymer synthesis are resumed in several reviews.[30,226,227]

Numerous controlled radical polymerization strategies have been performed under continuous flow conditions in microreactor scale systems or larger reactors tubing. As an example, reversible addition−fragmentation transfer (RAFT) polymerizations were carried out in flow and showed a good efficiency in producing homopolymers with narrow dispersities and desired molar mass.[228,229] Junkers and co-workers developed the photo-induced controlled polymerization of MMA in tubular reactor which gave polymers with low dipersities and controlled molar masses. Second, the produced polymer was used as a macro-

© 2020 Tous droits réservés.
lilliad.univ-lille.fr

initiator to initiate a subsequent copolymerization.[230] Even more, thermoplastic elastomers composed of styrene and isoprene monomers were synthesized by ultrafast photo-RAFT in flow system.[231]

Zhenping Cheng and Lifen Zhang have described the extension of polymer chain by RAFT polymerization in continuous flow mode, where block polymers of 3- sulfopropyl methacrylate potassium salt and poly(ethylene glycol) methyl ether methacrylate were produced without need to isolate the first synthesized polymer.[232] In addition, block and multiblock copolymers in single stream continuous microreactor were successfully produced, and the efficiency of flow system has been proved for such preparations.[233,234] Light mediated RAFT polymerizations were also so efficient in flow mode and ensured homogeneous reaction conditions.[235] It was successfully scaled up for 10 m tubular reactor to give a reactor volume around 8.7 ml.[236]

The preparation of poly (n-butyl acrylate)-block- poly(styrene) copolymers synthesis by nitroxide-mediated radical polymerization (NMRP) was accomplished in two serial continuous microtubular reactors.[237] The tubular reactors were coupled to a multi- lamination micromixer that improved the control of copolymerization reaction generating polymers with narrowest molecular weight distributions.

Photoredox organic ATRP (*O*-ATRP) was carried out in continuous flow mode to produced homo and copolymers.[113] One of the first reports that described the controlled radical polymerization by ATRP in continuous production was set by Beers and co-workers.[238] This pioneer work translated CRP from batch to flow using metal-based either metal free catalysts.[239,240]

And recently, our group managed to implement *O*-ATRP catalyzed by metal free catalyst in continuous flow tubular reactor , a work intended to be discussed further in this report.[241]

Lately, the ROP of lactones started to be investigated in continuous flow mode. A typical metal-based catalyst, $Sn(OTf)_2$ was used in flow mode ROP using PTFE tubing, showing a better control of ε-caprolactone polymerization.[242,243] Kai Guo and co-workers have studied the copolymerization of poly(δ-valerolactone) (PVL) and poly(ε-caprolactone) (PCL) catalyzed by organo-based catalysts.[244] The pioneer work of emloying immobilized enzyme in continuous flow system was achieved by Gross *et al* in order to polymerize ε-caprolactone.[28] In comparison with batch system, they yielded higher number-average

© 2020 Tous droits réservés.
lilliad.univ-lille.fr

molecular weight (M_n) of PCL in less reaction time. In addition, "saturated water" conditions did not affect the conversion or the end group fidelity.[29] Following these studies, several applications to polylactones synthesis were developed in microflow system aiming to produce homo and block polyleactones using enzymatic catalysis, organic catalysis or the combination of these two catalytic systems. A wide range of monomers was used in copolymerization reactions and it covered lactone monomers, including D,L-lactide (LA) and cyclic carbonates.[30–32] The end fidelity was well tested also via enzymatic ring opening polymerization of δ –Valerolactone in flow mode as well as its copolymerization with interesting results compared to the batch.[33] Through the organo-ring opening polymerization 1,5,7- triazabicycloij4.4.0]dec-5-ene (TBD) has been a good catalyst that promoted valerolactone polymerization in flow mode.[245]

The recycling character of enzymes allowing its reuse was enhanced using microreactor technology and in presence of green solvent like water and supercritical carbon dioxide, without necessarily organic ones.[9,10]

Furthermore, it was found that the profile of the fluid flowing into a tubular reactor has an effect on the produced polymer structure, molar mass, composition and dispersity.[246] The relationships between polymer residence time distribution (RTD) and its structure were established.[247,248] RTD is the residence time taken by the fluid to fully pass through the tubular reactor.

© 2020 Tous droits réservés.
lilliad.univ-lille.fr

2. CHAPTER TWO: ENZYMATIC RING OPENING POLYMERIZATION (*e*-ROP) OF LACTONES IN FLOW SYSTEM

2.1. Lipase B from *Candida Antarctica*

Enzymatic ring opening polymerization is a way to obtain biodegradable polyesters. This clean process can be managed by different lipases derived from different microorganisms like: bacteria (*Pseudomonas fluorescens,*[249] *Burkholderia cepacia*),[250,251] yeast species (*Yarrowia lipolytica*),[252] lipases of animal origin (porcine pancreas),[253] as well as thermophilic lipase/esterase family enzyme from the archaeon *Archaeoglobus fulgidus*.[254,255] Even so, the most studied enzyme for this purpose was lipase B from the yeast *Candida antartica* (CALB).[94]

The molecular weight of CALB is 33 KDa, with a pI of 6.0. CALB belongs to α/β protein and owns almost the same features of other lipases. The structure of CALB involves a Ser-His-Asp triad, which includes the catalytic active site with a very small cover which cannot close totally the active center.[74,256] This small cover doesn't affect the ability of CALB to be adsorbed on hydrophobic surfaces, thus, it remains as an interfacial enzyme. That is why, CALB is still considered a true lipase, even that its closed form is not totally similar to other lipases.[257,258] But this fact makes its handling simpler compared to other lipases, as it doesn't present the same high tendency to form dimeric aggregates like other lipases.

CALB is considered as the most stable lipase in its commercial form,[259,260] that has been widely used in a broad range of reactions, and it is almost the most used lipase.[73,261,262] It was investigated in almost all areas suitable to lipases' uses like: the production of polymers and biodiesel, the modification of polymers and triglycerides in addition to many other reactions.[263]

2.2. Immobilized Lipases

Enzymes are preferable to be in immobilized form for the most of industrial uses especially those requiring high temperatures. Immobilization of enzymes can improve their features, making them reusable, more active and efficient biocatalysts. Through immobilization, all

© 2020 Tous droits réservés.

these features can be applied to lipases.[263] Moreover, free lipases have less storage stability than the immobilized counterparts. In fact, immobilized lipases own a full activity over a long time, exhibiting an excellent stability of biocatalyst. Following this concept, the overall costs with that of immobilization process can be requite. Actually, we are not interested in immobilization methods and procedures, because the lipase used in our study is already commercially available.[264]

But it is of interest to mention some important points to be considered for immobilized lipases. First, after immobilization on porous supports, the enzyme will not be exposed to external interfaces anymore. This fact presents an advantage and a limitation. The first concerns enzymes' inactivation that cannot occur with these interfaces. However, interfacial activation will be impossible if the enzyme is inside the porous support, except when using anhydrous media able to enter to the porous system. Second, as mentioned before, Lipases have the tendency to form dimeric aggregates which contain two lipase molecules. And so on, the immobilization can occur for the dimeric enzyme instead of the monomeric one; and if it is the case, the dimeric lipase will be an undesired form that presents altered properties and lower activity than the monomeric lipase form. but this problem-and some others- was well resolved by using detergent during immobilization process blocking dimers formation.[263]

The ability of lipases to be adsorbed on hydrophobic surfaces, makes their immobilization on these latter the best strategy to apply. The advantages of such a strategy are the following: 1- immobilization, purification and stabilization are merged in one-step process. the enzyme stabilization is engendered by its open and adsorbed form, 2- Lipase remains in its open and monomeric form, (Figure 2-1) , 3- finally, immobilized lipases are more resistant to reaction conditions because there is no conformational equilibrium to be adapted. Lipases immobilized by interfacial adsorption maintain their activity even under ionic strength. On the other hand, the conventionally immobilized enzymes don't resist these conditions and their active center will be closed. However, this method presents some problems that could be overcome. Thus, the immobilization of lipases *via* interfacial activation is considered the most used process.[263]

© 2020 Tous droits réservés.

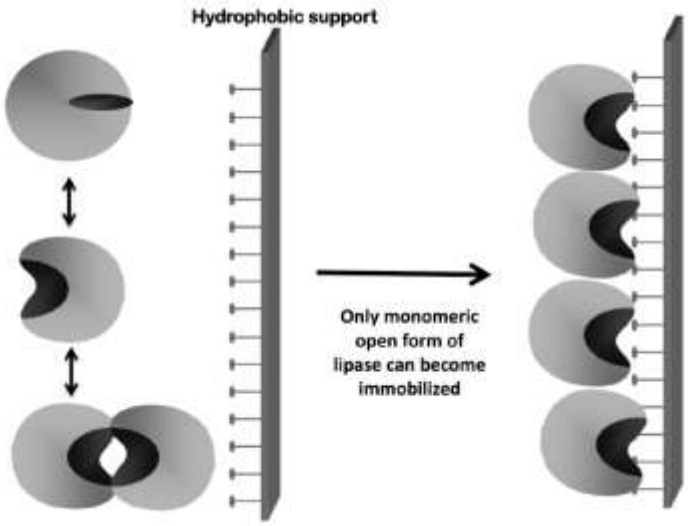

Figure 2-1 Immobilization of lipases on hydrophobic supports at low ionic strength *via* interfacial activation: immobilization of monomeric and open forms of lipases[263]

2.3. Novozym 435

Novozym 435 (N435) is the immobilized form of CALB provided by Novozymes™. The first use of N435 was reported in 1992. CALB was supported on Lewatit VP OC 1600 via interfacial activation, which is a macroporous acrylic polymer resin. The N435 support, Lewatit VP OC 1600, is composed of spherical beads morphology which forms a macroporous matrix. This organic carrier is based on poly(methyl methacrylate) crosslinked with divinylbenzene, and commercially known by Lewatit VP OC 1600. The synthesis of Lewatit support was not detailed. But it is presumed that the copolymer (the polymethacrylate divinylbenzene) is obtained via condensation polymerization or addition between methacrylic esters and divinylbenzene. This kind of support is suitable for enzyme immobilization, especially for lipase, due to its relative hydrophobicity.[263]

Many advantages are offered by the use of N435 as a catalyst, as:[263]

1- The selectivity with multifunctional substrates,
2- Its great performance under anhydrous conditions as well with moisture sensitive substrates,
3- Its activity in a mild range of temperatures (20-110 °C),
4- Its suitability for the two reaction systems: batch and continuous reactors,
5- Its recycling (up to 10 times) depending on reaction conditions,

© 2020 Tous droits réservés.

6- Its intensive use for industrial production.

2.4. Enzymatic ring opening polymerization of lactones: lipase catalyzed ROP of lactones

In the 1980s, the first *in vitro* enzymatic synthesis of polyesters via condensation polymerization was noted using lipase as a catalyst to produce oligomers.[265] However, the enzymatic polyesters synthesis really began in 1993, when two independent groups developed the ring opening polymerization (ROP) of lactones (cyclic esters) using lipase as a catalyst.[266–268]

Lipase catalyzed ROP of ε-caprolactone (CL), a seven membered cyclic ester, in bulk at 75°C for ten days of reaction and yielded 92% of poly-ε-caprolactone with M_n = 7700 Da and polydispersity index of PDI = M_w/M_n = 2.4 (Scheme 2-1 (a)). Similarly, δ-valerolactone (δ-VL), a six membered cyclic ester was produced at 60°C with M_n = 1900 Da and PDI = 3.0.[268] These polyesters have two terminal structures on each extremity, one is a carboxylic acid group and the other is a hydroxyl group. So, the initiation and termination steps were suggested to be achieved by water molecules present in the reaction medium. ε-CL was then polymerized using methanol as an initiator in hexane for more than 26 days to reach total conversion of monomer giving PCL and dilactone as a by-product.[266] Furthermore, lipase catalyzed ring opening copolymerization (ROCP) between ε-CL and δ-VL and produced a random copolyester structure of M_n = 3700 and PDI = 2.9 (Scheme 2-1 (b)). In addition, the copolymerization was applied between CL and two lactones which are 15-pentadecanolactone (PDL) and D-lactide.[267]

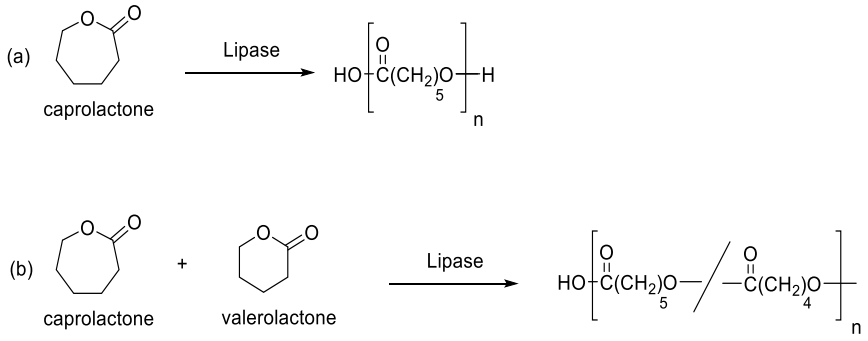

Scheme 2-1 Lipase-catalyzed ROP of Caprolactone (a), and ROCP between Caprolactone and valerolactone (b)

© 2020 Tous droits réservés.

These results encouraged the studies of enzymatic polyesters synthesis, where the polymerizations or copolymerizations of wide range of lactones ring-size, substituted or not, were developed using lipases of different origin as a catalyst.[58,63,72,265–271]

In Scheme 2-2, 4 to 17 membered cyclic lactone monomers are presented.[76,80,82,83,272,273] They are susceptible to be polymerized or copolymerized by lipase catalysis to give good yielded polyesters.

In 1996, lipase successfully catalyzed the ROP and ROCP of the four membered β-propiolactone (β-PL) and its substituted form in Bulk and gave linear polyester with M_n up to 2×10^4.[273]

γ-butyrolactone (γ-BL), a five membered lactone, was well known as a non-polymerizable monomer because of its low strain energy.[274–277] But it was found that it can be copolymerized by lipase catalyst[278] or by metal based catalysts to give oligomers and copolymers.[279,280] However, it was showed that ROP can proceed the conversion of this monomer by choosing the suitable catalyst. Thus, at atmospheric pressure and temperature of -40 °C, a high conversion of 90 % was successfully reached for polymers with more than 30 kg mol^{-1} of molecular weight, controlled linear or cyclic topologies, and presenting a good recyclability.[281] The use of amino compounds to promote the ROP was more efficient than the metal based catalysts, and it was able to polymerize γ-valerolactone -a substituted form of γ-butyrolactone(BL)- also known as a difficult monomer to be polymerized for the same reason of the former.[282]

δ-valerolactone (δ-VL), a six membered cyclic ester was polymerized first,[266–268] and α-methyl-VL was catalyzed by lipase CA (*Candida cylindracea*) and gave polyester with M_n=8400 and a yield of 93%.[283] Copolyester with M_n=1900 was produced from copolymerization between VL and 16 membered cyclic ester pentadecalactone (PDL).

The seven membered cyclic lactone is the most one studied in the literature among others. Many articles were reported on the ROP or ROCP of this monomer using different types of lipases as a catalyst.[76,80,83,91,266,267,272,283–286] A wide range of lipase was examined as catalyst for the polymerization of lactones. *Candida antarctica* (lipase CA or CA lipase B (CALB)) was found the most effective lipase for the ROP of lactones. It is an immobilized lipase on an acrylic resin, commercially available as Novozym 435.[287] An important evolution was observed using Novozym 435 compared to other lipases, where it contributed to decrease

© 2020 Tous droits réservés.

lilliad.univ-lille.fr

reaction time from 10 days to less than 10 hours in bulk at 60 °C with a reduction of catalyst's quantity from 50% to 1%. A molecular weight of 25000 of polyesters was reached in toluene at 70°C. The high catalytic activity of Novozym 435 remains with macrolactones 12 and 13-membered (UDL and DDL, respectively). α-methyl-CL was polymerized using lipase CA as a catalyst in bulk at 60°C for 24 hours, and yielded a polyester (74%) with M_n = 11400 and PDI=1.9.[273] For unsubstituted α-, γ-, and ω-methyl-CL monomers, low polymerizability was observed using lipase catalysis.[284]

Novozym 435 catalyzed the ring opening polymerization of the eight membered lactone, HL, at 45 °C to produce the corresponding polyester with M_n = 23600 and PDI=2.8.[83] With the nine membered lactone, OL, it gave polyester with M_n = 16000 at 75°C. Note that the copolymerization of the later was also examined.[288]

In addition, Novozym 435 catalyzed the polymerization of 10 and 11-membered lactones, NL and DL, to give respectively polyesters with M_n=16000 and 20000 withPDI =2.1 and 3.2.[83]

Furthermore, macrolides which are bigger ring size lactones: 12, 13, 16 and 17 membered lactones respectively UDL, DDAL, PDAL and HDL (Scheme 2-2) were successfully polymerized with lipase catalyst.[76,80,82,266,287–291] By using lipase PF as a catalyst, poly(UDL) of M_n = 23000 and PDI=2.6 was quantitatively obtained in bulk at 75°C, and by using the lipase CC (*Candida cylindracea*) the same monomer gave a polyester of M_n = 25000 and PDI=2.2 with a yield of 95%. These results present a higher polymerizability of the macrolides than that of CL. By using cutinase (HiC) as a catalyst, PDL was polymerized and gave quantitatively the corresponding polyester with M_n = 44600 and PDI =.7 in toluene at 70°C.[292]

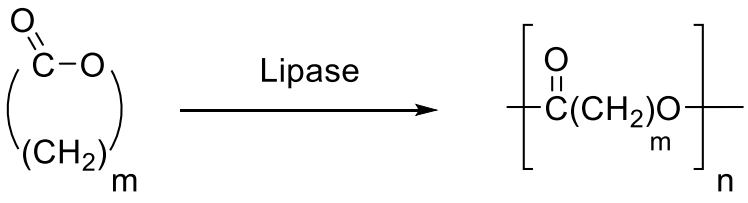

m=2 : PL
m=4 : VL
m=5 : CL
m=6 : HL
m=7 : OL
m=8 : NL
m=9 : DL
m=10 : UDL
m=11 : DDL
m=14 : PDL
m=15 : HDL

© 2020 Tous droits réservés.

Scheme 2-2 Unsubstituted lactone monomers for lipase-catalyzed ROP.[7]

The largest unsubstituted ring size lactone was the 17 membered one (HDL). Various lipases were used to catalyze the ring opening polymerization of HDL at 45-75°C in bulk for 5 days. With high yields, the corresponding polyester was obtained and reach M_n of 5800 and a PDI of 2.0.[289] The 16 and 17 membered di-ester monomers were well polymerized by lipase CA catalysis and polyesters of M_n up to 4100 (PDI 2.2) were obtained in high yields.[293] PDL (16 membered) was randomly copolymerized with four lactones monomers of different ring sizes (4, 5 ,10 and 11 membered) and this reaction was carried out in bulk at 60 °C and was catalyzed by lipase PF or lipase PC to give polymers with M_n of 1200-6300, which are nonrandom structured polymers (Scheme 2-3).

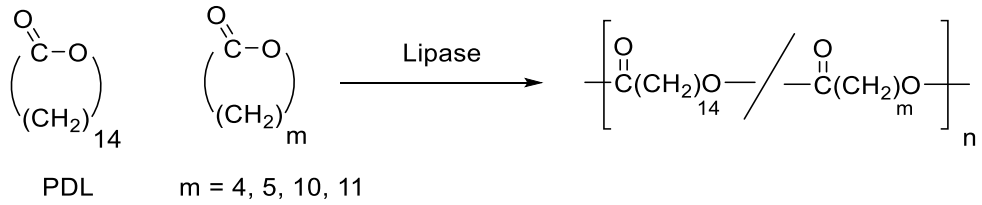

Scheme 2-3 Ring-opening copolymerization (ROCP) of PDL with four lactones of different ring sizes.[7]

Green chemistry is actually a very attractive field presenting a new point of view of chemistry regarding the usage of different green products inclunding: catalysts, starting materials, solvents… and many other factors which are used without damaging our environment.[5] In our case, we concentrated on macromolecules green synthesis.

© 2020 Tous droits réservés.

2.5. Results and discussion

2.5.1. Poly-(ε-caprolactone) synthesis

To the best of our knowledge, *e*-ROP of lactones is not widely investigated in flow mode, but it is in active progress. The pioneer work concerning the *e*-ROP of ε-CL in microreactor was accomplished by Gross *et al.*[28,29] They used aluminium microchannel reactor covered with kapton film, in which the polymerization took place. With this system, they proved the advantages of using N435 in a microreactor to catalyze the ROP of ε-CL. Based on this work, we aimed to perform the *e*-ROP of lactones in flow mode but in FEP tubing as mentioned in the experimental part (section 7.4.3).

First, we studied the *e*-ROP of ε-CL. To this end, we showed the variation of yield percentage (Scheme 2-4) in function of the residence time for the *e*-ROP of ε-CL using the equivalents 20/1/40 respectively for ε-CL, 3-phenyl-1-propanol ((PP) the initiator) and toluene (solvent). 100 mg of N435® were immobilized into the tubular reactor, which is equivalent to 10% of the monomer mass.

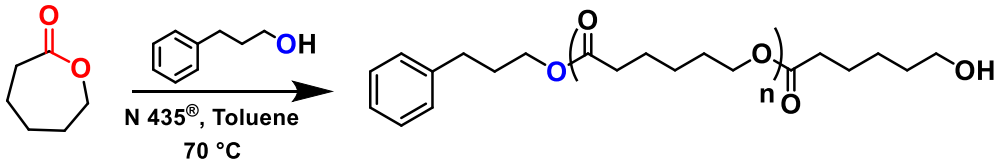

Scheme 2-4 Enzymatic ring opening polymerization of ε-caprolactone

First, we performed this study at RT. As Table 2-1 shows, the conversion of ε-CL increased from 15% to 94% with the increase of the residence time from 0.5 min to 8 min, and above 8 min the conversion remains at 94% (Figure 2-2). The polymerization follows a first-order kinetics during the whole course of the reaction with an equation of y = 0.2494x for $\ln([M]_0/[M]_t)$ vs. irradiation time (min). The rate constant is 0.2494 min^{-1} (Figure 2-3). The linear shape of the kinetic plot presented in Figure 2-3 shows the good control of the polymerization and indicates that during the propagation step the concentration of active centers is not altered and that no termination reactions occurred.[294] The Matrix assisted laser desorption ionization-time of flight (MALDI-TOF) spectrum (Figure 2-4) presented a well-regulated shape reflecting a good dispersity of the polymer chains initiated by PP and proved by the dispersity (*Đ)* calculated obtained through GPC (*Đ* = 1.35) A negligible quantity of macrocycles was detected. The *e-ROP* of ε-CL was performed at 60 °C in flow mode using PTFE tubing with internal diameter *i.d.*= 3.8 mm, in which N435 beads were introduced.[32] In

© 2020 Tous droits réservés.

our case, we aimed to miniaturize the reactor and we used a FEP tubing with *i.d.* = 1.55 mm. Such a system was efficient to give narrow polymer chains with the estimated molar masses as the results showed even at RT, so with energy saving.

Table 2-1 Conversion and molar mass of poly(ε-caprolactone) produced by e-ROP in flow versus the residence time (min) at room temperature.

Residence time (min)	0.5	1.0	1.5	2.0	4.0	6.0	8.0	10	12
Conv (%)[a]	15	25	31	42	55	77	86	94	94
$M_n \times 10^{-3}$ (g/mol)[a]	-	-	-	1.9	3.0	2.1	1.9	2.3	2.1

[a] Determined by ^{1}H NMR

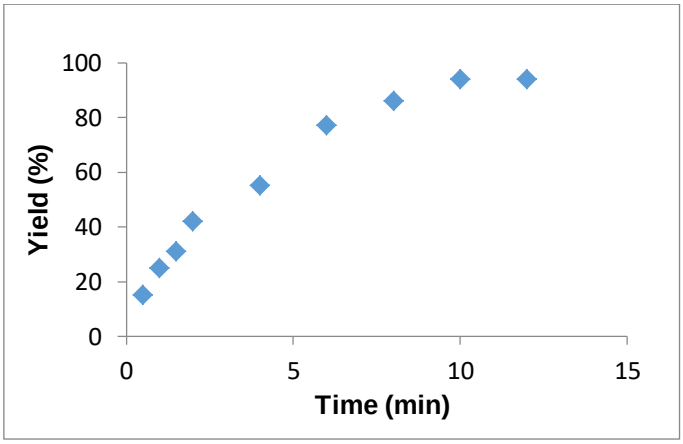

Figure 2-2 Yield percentage (%) of poly-ε-caprolactone in function of residence time (min) at room temperature.

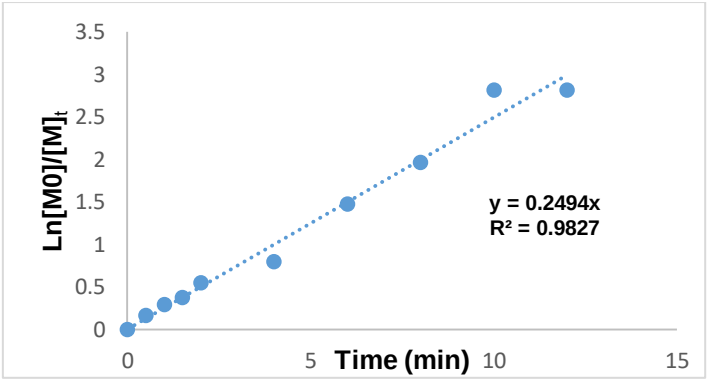

Figure 2-3 Kinetic plot of ε-caprolactone polymerization in flow: Ln[M0]/[M]$_t$ in function of residence time (min) at room temperature

© 2020 Tous droits réservés.

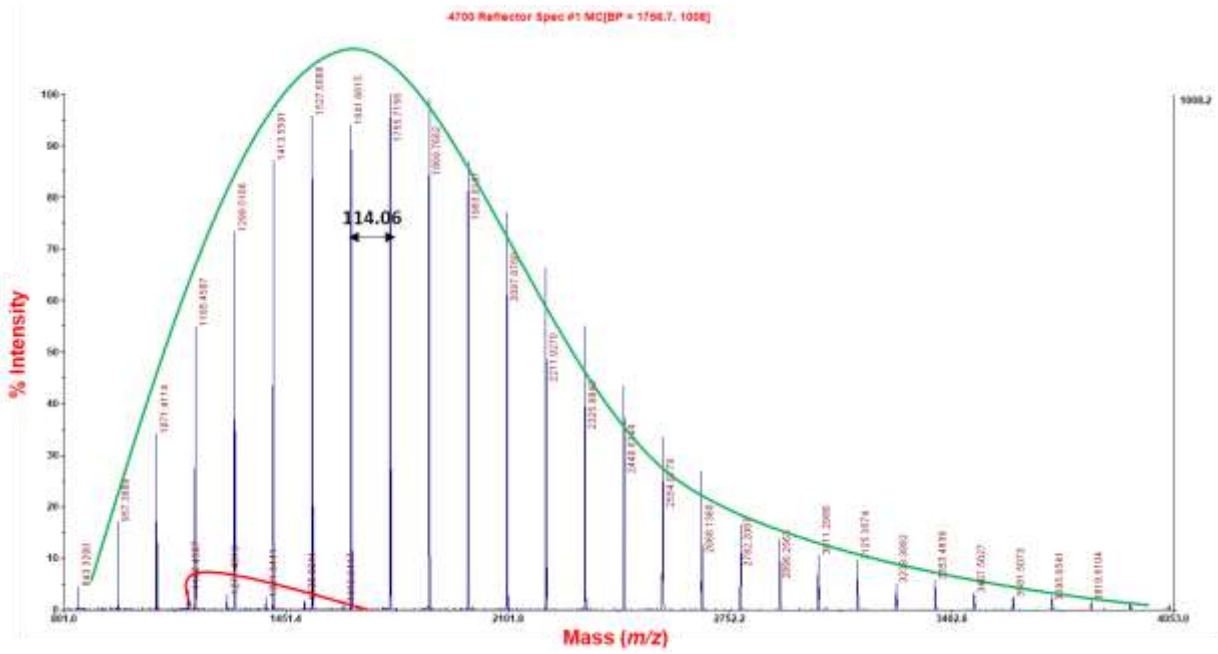

Figure 2-4 MALDI-TOF spectrum of poly-ε-caprolactone produced following 10 min of residence time via e-ROP in flow at RT. Green curve: chains initiated by the initiator (PP) M = ($M_{monomer}$ × number of repetition) + $M_{phenylpropanol}$ + M_{Na^+}, Red curve: Macrocycles M = ($M_{monomer}$ × number of repetition) + M_{Na^+}. The difference between the peaks is the molecular mass of ε-caprolactone = 114.06.

Second, we repeated the same study but at 70 °C. As indicated in Table 2-2 , the conversion of ε-CL increased from 30% to 100% with the increase of residence time from 15 s to 240 s, and above 240 s the yield percentage remains at 100% (Figure 2-5). So, in this reaction system, a low residence time was enough to reach the highest conversion. The linear shape of the kinetic plot presented in (Figure 2-6) showed the well-controlled character of the polymerization. The regulated shape of MALDI-TOF spectrum (Figure 2-7) showed the presence of well dispersed polymer chains and this was proved further by the GPC analysis ($Đ$ = 1.3). Two other species of ε-PCLs were detected: macrocycles and chains with H_2O extremity, but the overwhelming majority remains for PP end chains (Figure 2-8).

Table 2-2 Conversion and molar mass of poly(ε-caprolactone) produced by e-ROP in flow versus the residence time at 70°C.

Residence time (s)	15	30	60	90	150	210	240	360	600
Conv (%)[a]	30	37	51	62	79	81	100	100	100
$M_n \times 10^{-3}$ (g/mol)[a]	-	-	2.8	2.4	2.5	2.3	3.0	2.3	2.2

[a] Determined by ^{1}H NMR.

© 2020 Tous droits réservés.

lilliad.univ-lille.fr

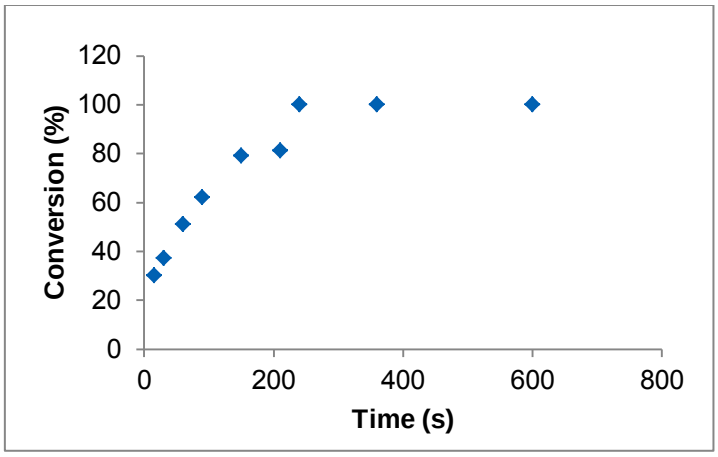

Figure 2-5 Variation of conversion (%) of poly(ε-caprolactone) in function of residence time (s) at 70 °C.

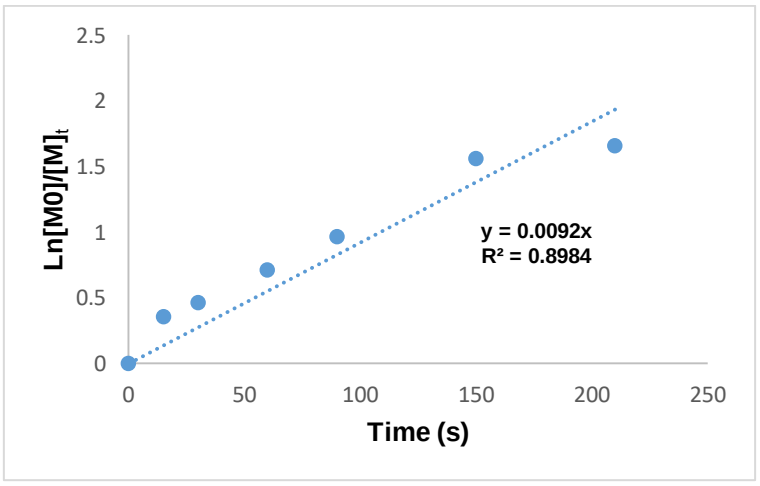

Figure 2-6 Kinetic plot of ε-caprolactone polymerization: $Ln[M0]/[M]_t$ in function of residence time (s) at 70°C.

© 2020 Tous droits réservés.

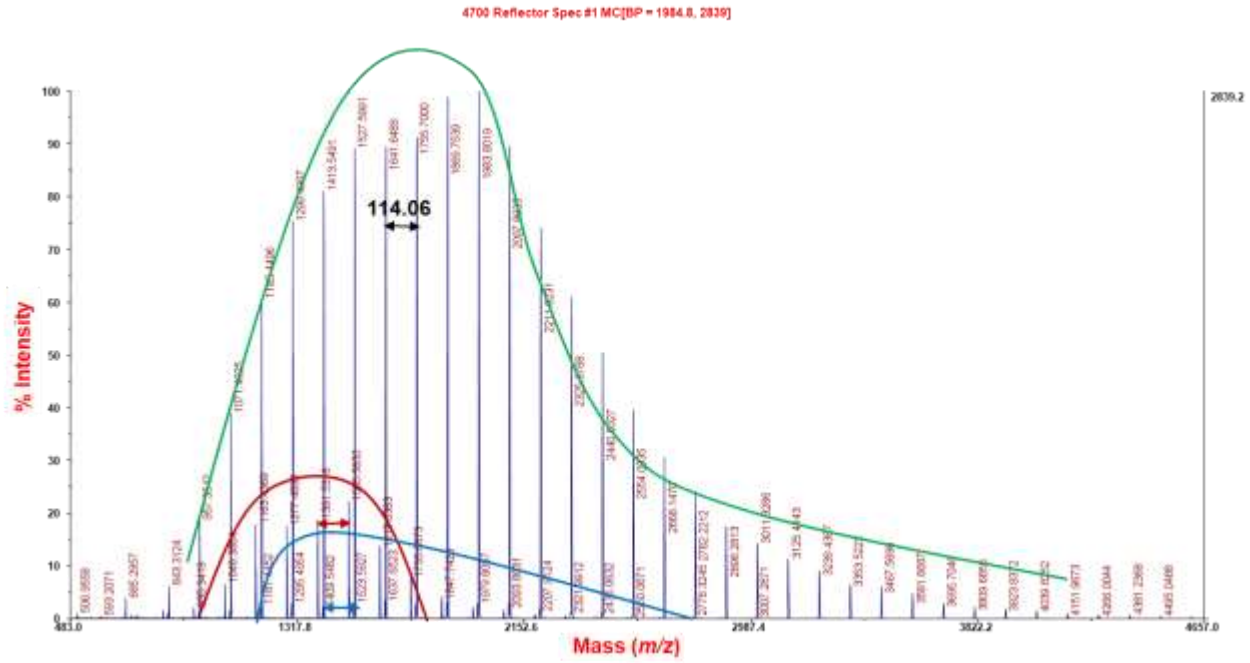

Figure 2-7 MALDI-TOF spectrum of poly-ε-caprolactone produced following 240 s of residence time via e-ROP in flow at 70 °C. Green curve: chains initiated by the initiator (phenylpropanol) M = ($M_{monomer}$ × number of repetition) + $M_{phenylpropanol}$ + M_{Na^+}, Red curve: Macrocycles M = ($M_{monomer}$ × number of repetition) + M_{Na^+}, Blue curve: water end chain M = ($M_{monomer}$ × number of repetition) + M_{water}+ M_{Na^+}. The difference between the peaks is the molecular mass of ε-caprolactone = 114.06.

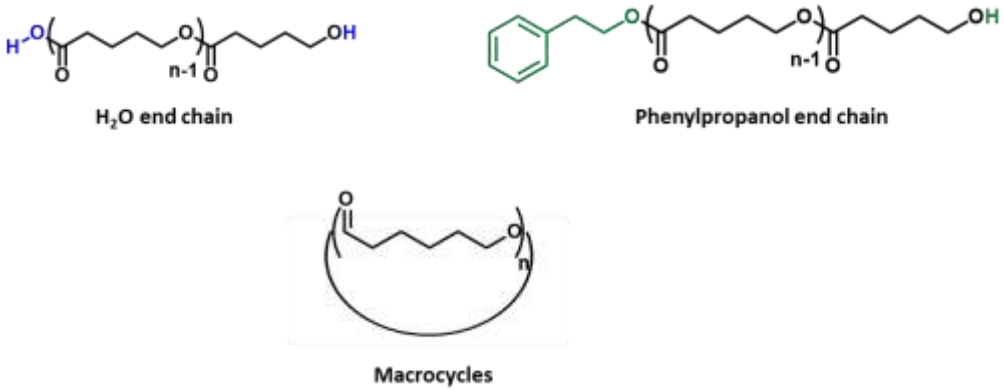

Figure 2-8 Poly-ε-caprolactones with different end chains.

© 2020 Tous droits réservés.

2.5.2. Poly-(δ-valerolactone) synthesis.

The same study realized previously with ε-caprolactone was repeated using another cyclic monomer which is six membered lactone; the δ-valerolactone (δ-VL) (Scheme 2-5), a more difficult monomer to be polymerized compared to ε-CL. This time, we followed the variation of the yield percentage in function of residence time at 60°C using 200 mg of N435® which is equivalent to 22 % of the monomer mass. The reagent mixture followed the equivalents 20/1/40 respectively for ε-CL, PP (initiator) and toluene (solvent). As observed in Table 2-3 , the conversion of δ-VL polymerization increased from 12% to 93% with the increase of residence time from 20 s to 214 s (Figure 2-9). It is important to mention here that the use of tubular reactor of *i.d.*=1.55 mm improved the progress of this reaction, since in literature they used a PTFE tubular reactor of *i.d* = 3.8 mm and a higher residence time was needed to reach the highest conversion: 12 and 20 min of residence time were required for a mixture of [δ-VL]/[initiator] = 10 and 30 respectively.[295] In contrast, 214 s (3.5 min) was enough in our case ([δ-VL]/[initiator] = 20) to reach the highest conversion.

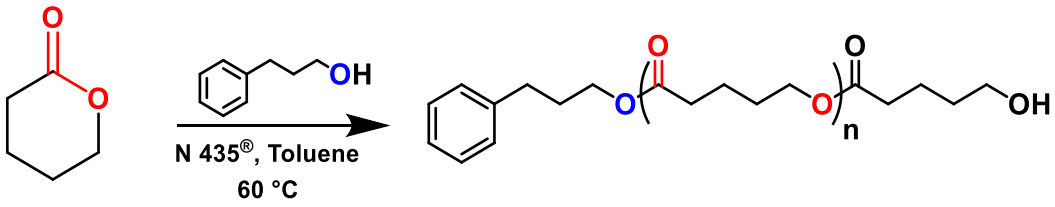

Scheme 2-5 Enzymatic ring opening polymerization of δ-caprolactone.

Table 2-3 Conversion and molar mass of poly(δ-valerolactone) produced by e-ROP in flow versus the residence time at 60 °C.

Residence time (s)	20	40	85	214	330	420
Conv (%)[a]	12	30	48	93	86	95
$M_{n,} \times 10^{-3}$ (g/mol)[a]	0.3	0.6	2.0	2.2	1.7	1.5

[a] Determined by ^{1}H NMR.

© 2020 Tous droits réservés.

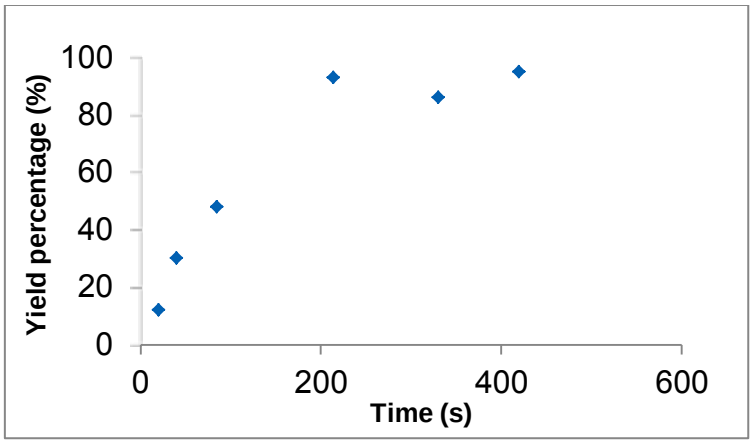

Figure 2-9 Variation of Yield percentage (%) of poly(δ-valerolactone) in function of residence time (s) at 60 °C.

After 214 s, the molar mass decreased and this can be explained by the apparition of transesterification side reactions at this stage. The linear shape of the kinetic plot presented in (Figure 2-10) shows the well-controlled progress of the polymerization. The MALDI-TOF spectrum (Figure 2-11) demonstrates a good dispersity of the polymer chains from its regulated shape and this is proved also by GPC analysis ($Đ$ = 1.27). Two other species of poly-δ-valerolactone were detected by MALDI-TOF spectrum: Macrocycles and chains with water extremity. But the overwhelming majority remains again for PP end chains.

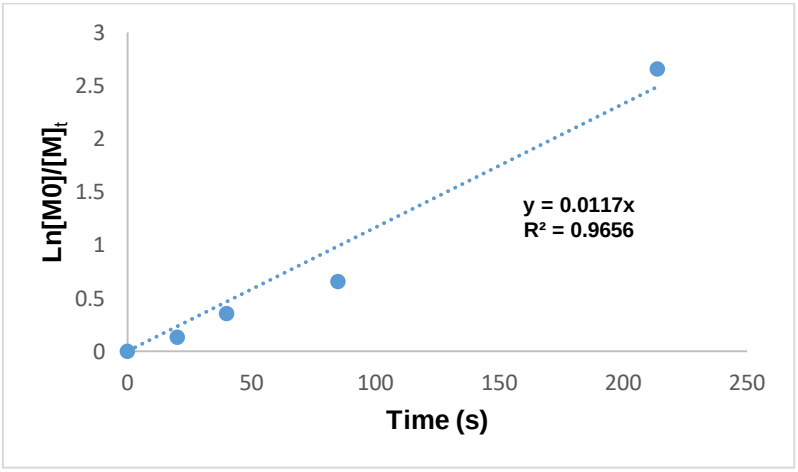

Figure 2-10 Kinetic plot of δ-valerolactone polymerization: Ln[M0]/[M]$_t$ in function of residence time (s) at 60°C.

Moreover, we carried out the polymerization of δ-valerolactone at RT (Table 2-4). Always with 200 mg of N435®, we tried to find here the residence time needed to obtain the highest conversion. In 10 min, we were able to have 100% of conversion (Table 2-4, Run 2), which was not reachable at high temperature. And the MALDI-TOF spectrum of this product

© 2020 Tous droits réservés.

presents a good Gaussian shape that indicates a very good dispersity of the polymer chains (Figure 2-12), and interestingly a *Đ* of 1.28 was recorded by GPC. Thus, we can see that at high and at room temperatures we had the same control of δ-VL polymerization (*Đ* = 1.27 and 1.28 respectively). This result showed the ability of polymerizing δ-VL with saving energy by decreasing the temperature from 60 °C to the room temperature (23 °C) but with increasing the residence time from 2.4 min to 10 min. Hence, a compromise between the residence time and the temperature should be established to conserve the same result.

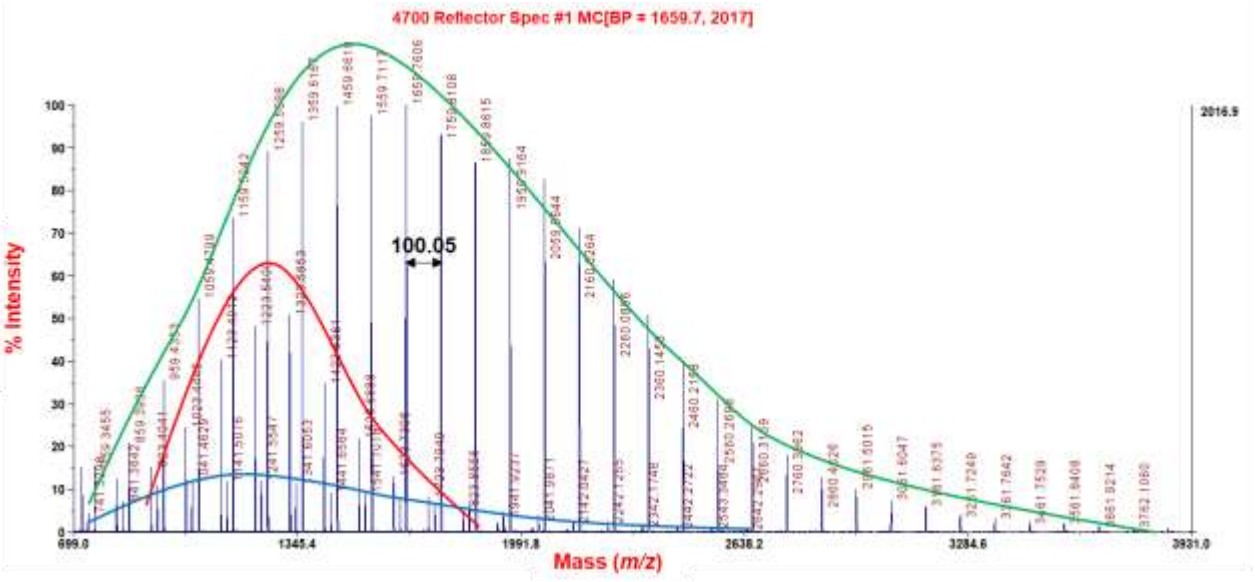

Figure 2-11 MALDI-TOF spectrum of poly-δ-valerolactone produced following 214 s of residence time via e-ROP in flow at 60 °C. Green curve: chains initiated by the initiator (phenylpropanol) M = ($M_{monomer}$ × number of repetition) + $M_{phenylpropanol}$ + M_{Na^+}, Red curve: Macrocycles M = ($M_{monomer}$ × number of repetition) + M_{Na^+}, Blue curve: water end chain M = ($M_{monomer}$ × number of repetition) + M_{water}+ M_{Na^+}. The difference between the peaks is the molecular mass of δ-valerolactone = 100.05.

Table 2-4 Conversion and molar mass of δ-valerolactone in flow at room temperature.

Run	Residence time (min)	$M_{n,theo}$ × 10^{-3} (g/mol)[a]	$M_{n,}$ × 10^{-3} (g/mol)[b]	Conv (%)[b]
1	8	1.9	2.5	97
2	10	2.3	2.0	100

[a] Calculated from ([M]/[I]) Conv.× M_W(VL)+M_W(PP).
[b] Determined by ^{1}H NMR

© 2020 Tous droits réservés.

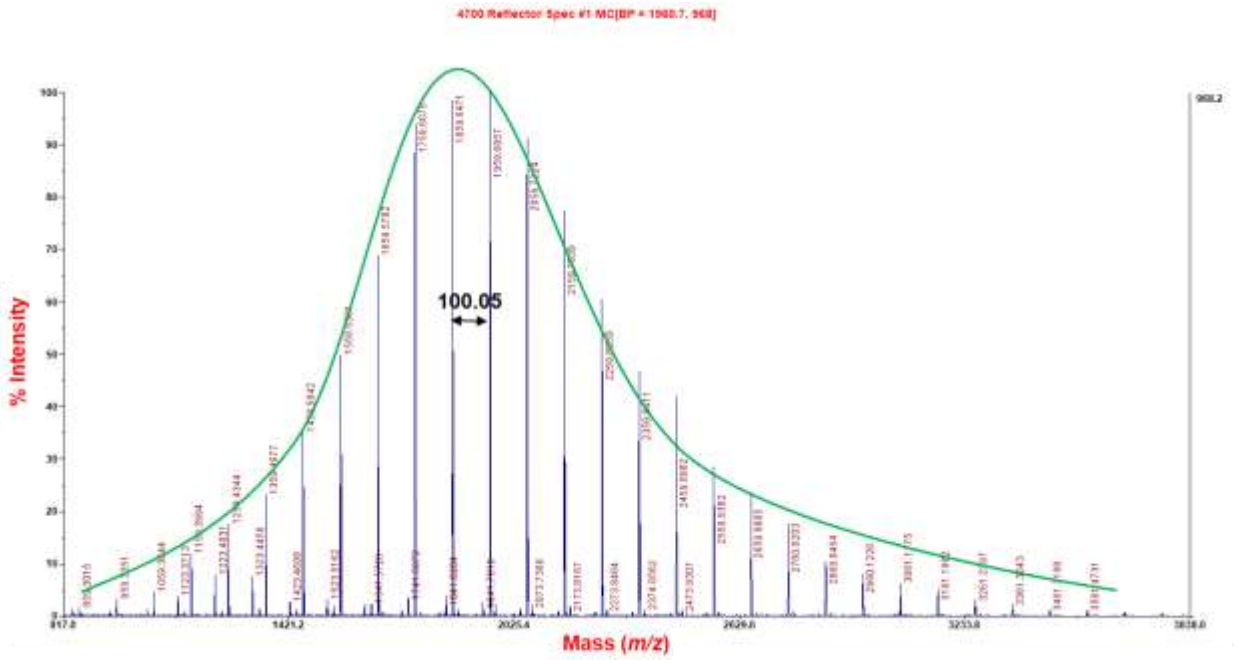

Figure 2-12 MALDI-TOF spectrum of poly-δ-valerolactone produced following 10 min of residence time via e-ROP in flow. Green curve: chains initiated by the initiator (phenylpropanol) M = ($M_{monomer}$ × number of repetition) + $M_{phenylpropanol}$ + M_{Na^+}. The difference between the peaks is the molecular mass of δ-valerolactone = 100.05.

2.5.3. Effect of initiators on enzymatic ring opening polymerization (*e*-ROP)

A second study was performed, where different alcoholic initiators were used to polymerize ε-CL and δ-VL as shown by Table 2-5. The effect of these initiators on polymers molar mass as well as on their polydispersity index was detected. All reactions were carried out following the same equivalents: 20/1/40 respectively for ε-CL or δ-VL/initiator/toluene within 4 min of residence time.

When using the secondary alcohol (4-phenyl-2-butanol) as an initiator to polymerize ε-CL, the presence of two species of macrocycles and chains initiated by the initiator was detected by MALDI-TOF analysis (Figure 2-14.a). In addition, the use of cholesterol (secondary alcohol) contributed just to the formation of macrocycles (Figure 2-14.b) where polymers in form of cotton were obtained (Figure 2-13) reflecting the high molecular mass of the product proved by GPC (Table 2-5). And after testing the polymerization of δ-VL using cholesterol as an initiator, only macrocycles formation was recorded again (Figure 2-14.c). For the rest of initiators used, MALDI-TOF spectra behave almost similarly and reveal the presence of two major species: chains with initiator extremity and macrocycles (Figure 2-15 to Figure 2-19), where the former is much more abundant. So, we can conclude that primary alcohols are

© 2020 Tous droits réservés.

more efficient to initiate the ring opening polymerization of lactones than the secondary alcohols.

In term of *Đ* (Table 2-5), 1.6 was the highest value recorded using cholesterol (secondary alcohol) for ε-CL polymerization. The rest of values vary in a range between 1.23 and maximum 1.44 when using pyrenebutanol which is a bulky primary alcohol. These results indicate the good control of the *e*-ROP performed in a flow system.

In addition, the *e*-ROP of ε-CL and δ-VL initiated by PP but at RT required an increase of residence time from 4 min to 10 min to reach high conversions. The *Đ* remains almost the same compared with those of polymerizations done at high temperature using the same initiator, which means that these polymerizations can be performed with energy save but with few minutes' increase of residence time.

Figure 2-13 ε-PCL obtained from *e*-ROP in flow by using cholesterol as an initiator

© 2020 Tous droits réservés.

lilliad.univ-lille.fr

Table 2-5 Enzymatic ring opening polymerization of ε-caprolactone (CL)[a] and δ-valerolactone (VL)[b] with different alcohols as initiators in a flow system[c].

Initiator	Monomer	$M_n \times 10^{-3}$ (g/mol)[d]	$M_w \times 10^{-3}$ (g/mol)[d]	$Đ$[d]	Conv (%)[e]
1-octanol	CL	5.2	6.5	1.28	95
1-propanol	CL	5.1	6.3	1.24	88
3-methyl-1-butanol	CL	3.7	5.2	1.40	-
4-phenyl-2-butanol	CL	5.7	7.0	1.24	90
3-phenyl-1-propanol	CL	5.1	6.6	1.30	100
3-phenyl-1-propanol[f]	CL	3.4	4.6	1.34	94
3-phenyl-1-propanol	VL	4.1	5.2	1.27	93
3-phenyl-1-propanol[f]	VL	3.7	4.8	1.28	100
Pyrenebutanol	CL	3.3	4.8	1.44	96
Pyrenebutanol	VL	3.7	3.8	1.39	90
Cholesterol	CL	19	23.4	1.23	91
Cholesterol	VL	6.3	10.1	1.60	78

[a] Reaction temperature is 70 °C, in toluene, [M]/[I](mol) = 20, 100 mg of N435
[b] Reaction temperature is 60 °C, in toluene, [M]/[I](mol) = 20, 200 mg of N435
[c] Reactions in flow system with residence time of 4 min
[d] Determined by GPC
[e] Determined by ^{1}H NMR
[f] Reactions at room temperature

© 2020 Tous droits réservés.

lilliad.univ-lille.fr

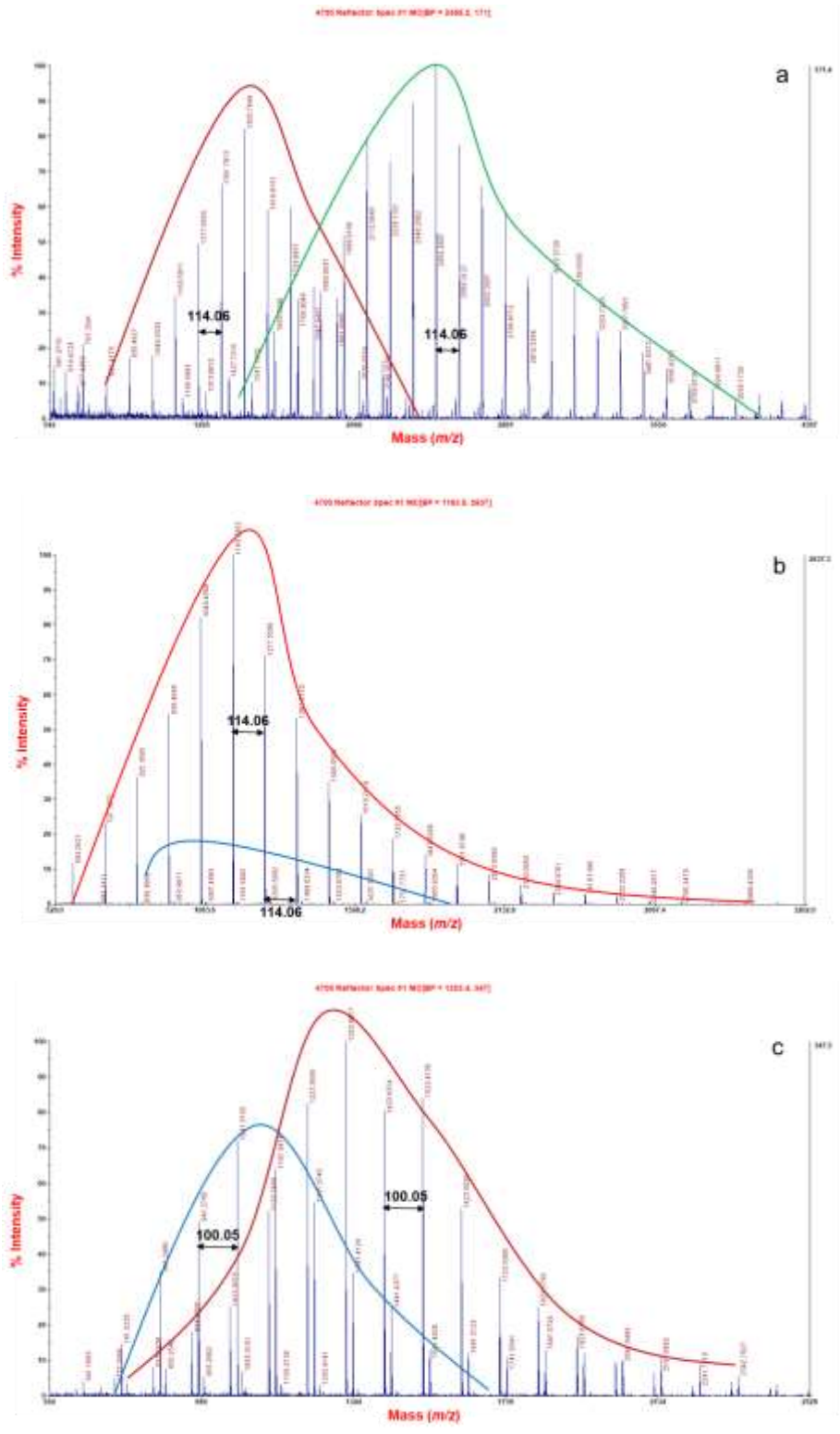

Figure 2-14 MALDI-TOF spectra of (a) poly- ε-caprolactone and (b) poly-δ-valerolactone produced through *e*-ROP in flow using cholesterol as an initiator and (c) 4-phenyl-2-butanol as an initiator. Green curve: chains initiated by the initiator M = ($M_{monomer}$ × number of repetition) + $M_{initiator}$ + M_{Na^+}, Red curve: Macrocycles M = ($M_{monomer}$ × number of repetition) + M_{Na^+}, Blue curve: water end chain M = ($M_{monomer}$ × number of repetition) + M_{water}+ M_{Na^+}. The difference between the peaks is the molecular mass of the used monomer δ-valerolactone = 100.05 or ε-caprolactone = 114.06.

© 2020 Tous droits réservés.

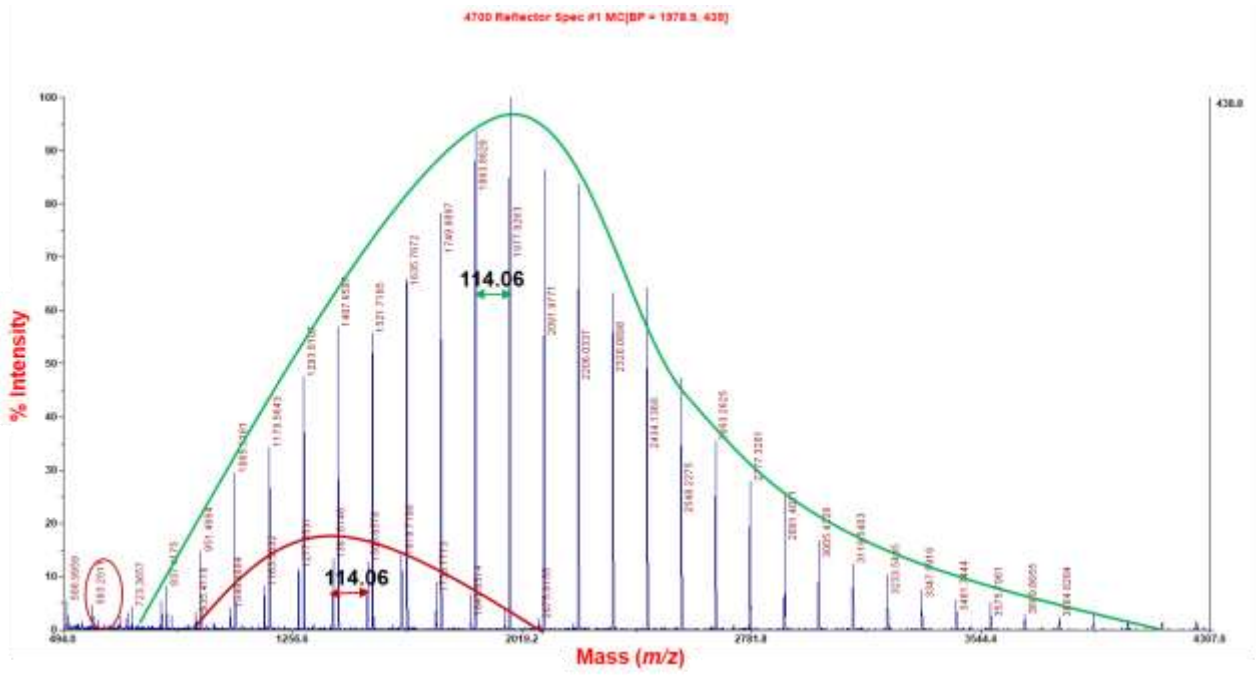

Figure 2-15 MALDI-TOF spectrum of poly-ε-caprolactone produced through *e*-ROP using 1-octanol as an initiator in flow. Green curve: chains initiated by the initiator (1-octanol) M = ($M_{monomer}$ × number of repetition) + $M_{octanol}$ + M $_{Na}^{+}$, Red curve: Macrocycles M = ($M_{monomer}$ × number of repetition) + M $_{Na}^{+}$, Blue curve: water end chain M = ($M_{monomer}$ × number of repetition) + M_{water}+ M $_{Na}^{+}$. The difference between the peaks is the molecular mass of ε-caprolactone = 114.06.

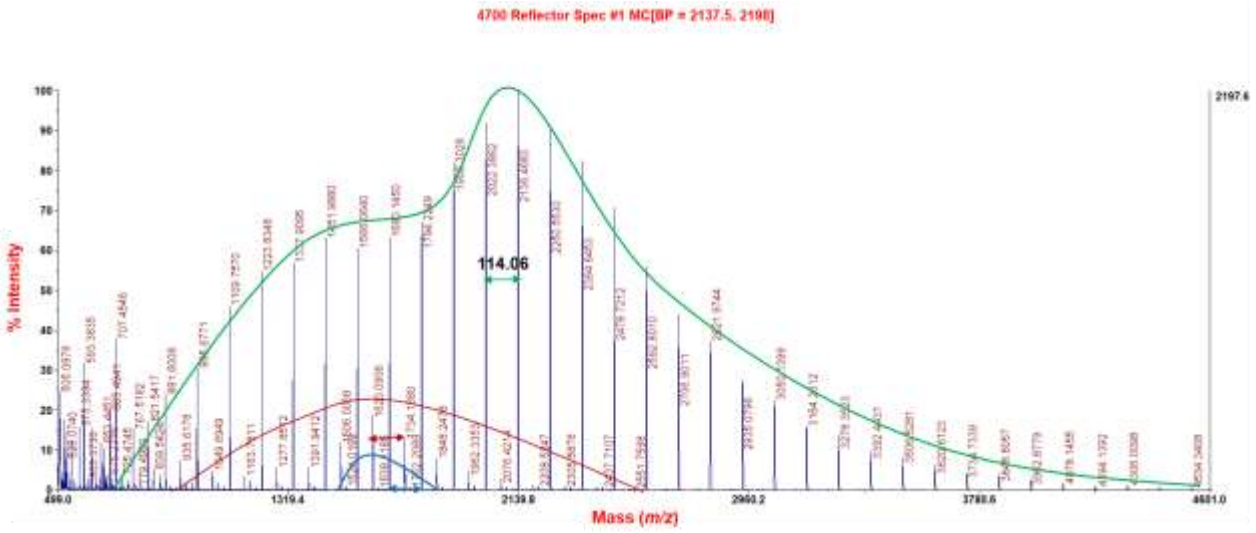

Figure 2-16 MALDI-TOF spectrum of poly-ε-caprolactone produced through *e*-ROP using 1-propanol as an initiator in flow. Green curve: chains initiated by the initiator (1-propanol) M = ($M_{monomer}$ × number of repetition) + $M_{propanol}$+ M $_{Na}^{+}$, Red curve: Macrocycles M = ($M_{monomer}$ × number of repetition) + M $_{Na}^{+}$, Blue curve: water end chain M = ($M_{monomer}$ × number of repetition) + M_{water}+ M $_{Na}^{+}$. The difference between the peaks is the molecular mass of ε-caprolactone = 114.06.

© 2020 Tous droits réservés.

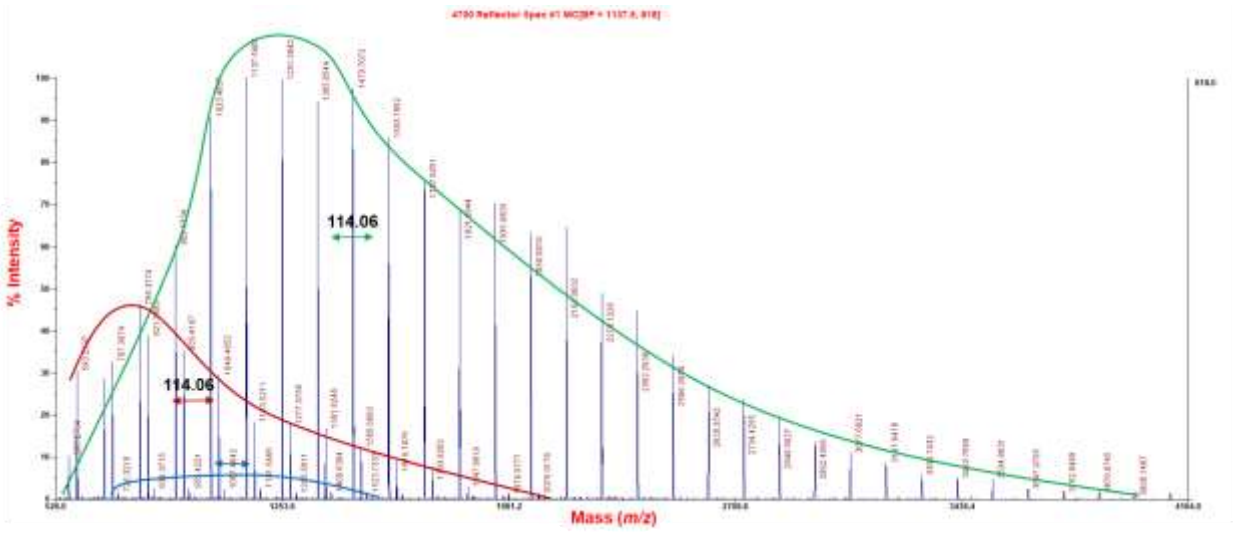

Figure 2-17 MALDI-TOF spectrum of poly-ε-caprolactone produced through *e*-ROP using 3-methyl-1-butanol as an initiator in flow. Green curve: chains initiated by the initiator (3-methyl-1-butanol) M = ($M_{monomer}$ × number of repetition) + $M_{methylbutanol}$+ M_{Na^+}, Red curve: Macrocycles M = ($M_{monomer}$ × number of repetition) + M_{Na^+}, Blue curve: water end chain M = ($M_{monomer}$ × number of repetition) + M_{water}+ M_{Na^+}. The difference between the peaks is the molecular mass of ε-caprolactone = 114.06.

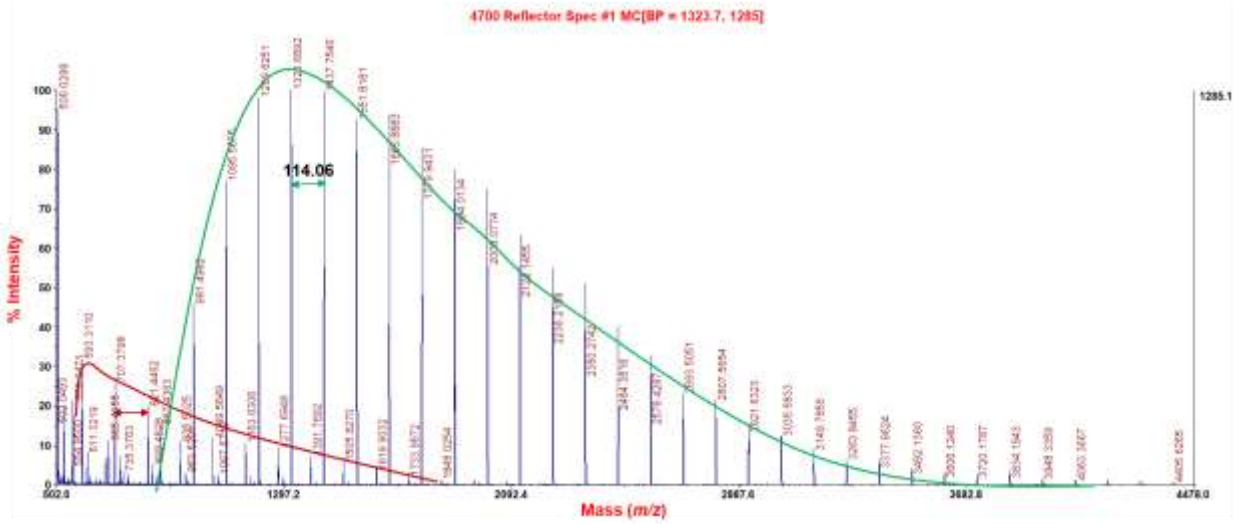

Figure 2-18 MALDI-TOF spectrum of poly-ε-caprolactone produced through *e*-ROP using pyrenebutanol as an initiator in flow. Green curve: chains initiated by the initiator (pyrenebutanol) M = ($M_{monomer}$ × number of repetition) + M pyrenebutanol + M_{Na^+}, Red curve: Macrocycles M = ($M_{monomer}$ × number of repetition) + M_{Na^+}, Blue curve: water end chain M = ($M_{monomer}$ × number of repetition) + M_{water}+ M_{Na^+}. The difference between the peaks is the molecular mass of ε-caprolactone = 114.06.

© 2020 Tous droits réservés.

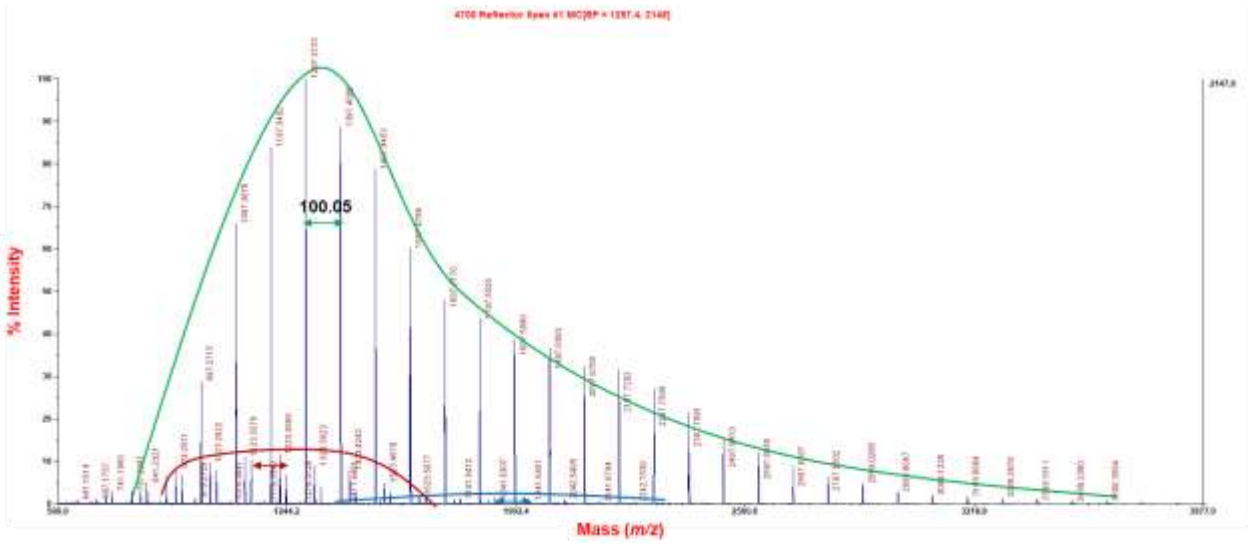

Figure 2-19 MALDI-TOF spectrum of poly-δ-valerolactone produced through *e*-ROP using pyrenebutanol as an initiator in flow. Green curve: chains initiated by the initiator (pyrenebutanol) M = ($M_{monomer}$ × number of repetition) + M pyrenebutanol + M_{Na^+}, Red curve: Macrocycles M = ($M_{monomer}$ × number of repetition) + M_{Na^+}, Blue curve: water end chain M = ($M_{monomer}$ × number of repetition) + M_{water}+ M_{Na^+}. The difference between the peaks is the molecular mass of ε-caprolactone = 100.05.

© 2020 Tous droits réservés.

e-ROP of lactones in flow

Then, we carried out the *e*-ROP of ε-CL at 70°C in the absence of initiator or enzyme. As shown in Table 2-6 , without initiator, we successfully polymerized ε-CL using 100 mg of N435® within 2 and 4 min of residence time (Runs 1 and 2) with 100% of conversion. Similar conversion was obtained after increasing the quantity of N435® to 200 mg (Run 3). With these previous polymerizations wide disperse polymers were obtained [$Đ$ = 1.99-2.68]. The increase of residence time from 2 min to 4 min contributed to an increase of $Đ$ from 1.99 to 2.68 (Runs 1 and 2). On the other hand, the increase of the enzyme quantity decreased $Đ$ values from 2.68 to 2.03 when remaining at 4 min as the residence time (Runs 2 and 3). The same experiment was done for the *e*-ROP of δ-VL in the absence of initiator. 100 % of conversion was obtained using 200 mg of N435® within 3.5 min of residence time at 60°C (Run 4). The MALDI-TOF spectra of these previous products indicate that the polymerization without initiator yielded just macrocycles (example of MALDI-TOF spectrum in Figure 2-20). The apparition of macrocycles is consequentially related to the enzyme action, that could explain the high $Đ$ values obtained due to the week control of this action. In addition, these four previous reactions result into polymers in form of cotton exactly like those obtained when using cholesterol as an initiator. So here, we can conclude that the cholesterol did not play its role to initiate the polymerization, and the action of N435® was way stronger. Moreover, when using the secondary alcohol 3-phenyl-2-butanol, the presence of high percentage of macrocycles with the chains ended by the alcohol component, can be explained now by the high competition between the secondary alcohol (initiator) and the enzyme action. In addition, 44% of ε-CL conversion was obtained within 4 min of residence time at RT without initiator (Run 5), thus even at RT the enzyme has an effect and can initiate by itself the polymerization. Finally, there is no polymerization in the absence of the enzyme N435® at RT nor at 70 °C (Runs 6 and 7), which proves that the polymerization is immediately quenched once the reaction media is recovered out of the enzyme.

© 2020 Tous droits réservés.

lilliad.univ-lille.fr

Table 2-6 Enzymatic ring opening polymerization of ε-caprolactone in flow in the absence of initiator (3-phenyl-1-propanol (PP)) or enzyme.

Run	Initiator	N435® (mg)	Residence time (min)	Temperature (°C)	$M_{n,GPC}$× 10^{-3} (g/mol)[a]	$M_{w,GPC}$× 10^{-3} (g/mol)[a]	$Đ$[a]	Conv[b] (%)
1	-	100	2.0	70	2.6	5.1	1.99	100
2	-	100	4.0	70	1.6	1.6	2.68	100
3	-	200	4.0	70	2.1	4.3	2.03	100
4[c]	-	200	3.5	60	-	-	-	100
5	-	100	4.0	RT	-	-	-	44
6	PP	-	4.0	RT	-	-	-	-
7	PP	-	4.0	70	-	-	-	-

[a] Determined by GPC
[b] Determined by ^{1}H NMR
[c] δ-valerolactone is used instead of ε-caprolactone as a monomer

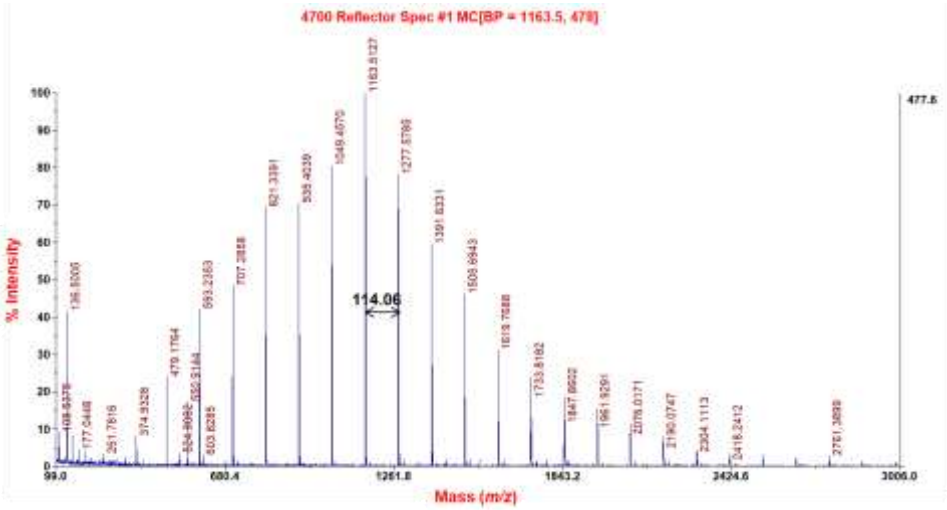

Figure 2-20 MALDI-TOF spectrum of polycaprolactone yielded without initiator using 100 mg of N435®, residence time = 4 min at 70 °C. Macrocycles M = (Mmonomer × number of repetition) + M_{Na}^+. The difference between the peaks is the molecular mass of ε-caprolactone = 114.06.

© 2020 Tous droits réservés.

As it mentioned in Figure 2-21, the mechanism steps of e-ROP of lactones, in principle, it's about a key step which is an acyl enzyme intermediate. It's well known that $–CH_2OH$ group of a serine-residue in the triad Ser-His-Asp is the active catalytic site of lipase. First, it is the reaction of lactone with lipase and the formation of enzyme-lactone complex (Figure 2-21, 1), followed by a ring opening of lactone giving the acyl-enzyme intermediate (enzyme-activated monomer, EM) (Figure 2-21, 2). Second, the initiation step which is an attack of a nucleophile (water, alcohol…) at the acyl carbon of the EM intermediate to produce the shortest propagating species containing an end hydroxyl function. Then, the propagation step continues by the action of the hydroxyl end group at the EM to elongate the number of the polymer units (Figure 2-21, 3-a).

On the other hand, without presence of initiator, the final step of the mechanism will be different. So the propagation takes place and the addition of monomers continues. But, the de-acylation will be done by an intramolecular attack which yields macrocycles (Figure 2-21, 3-a).

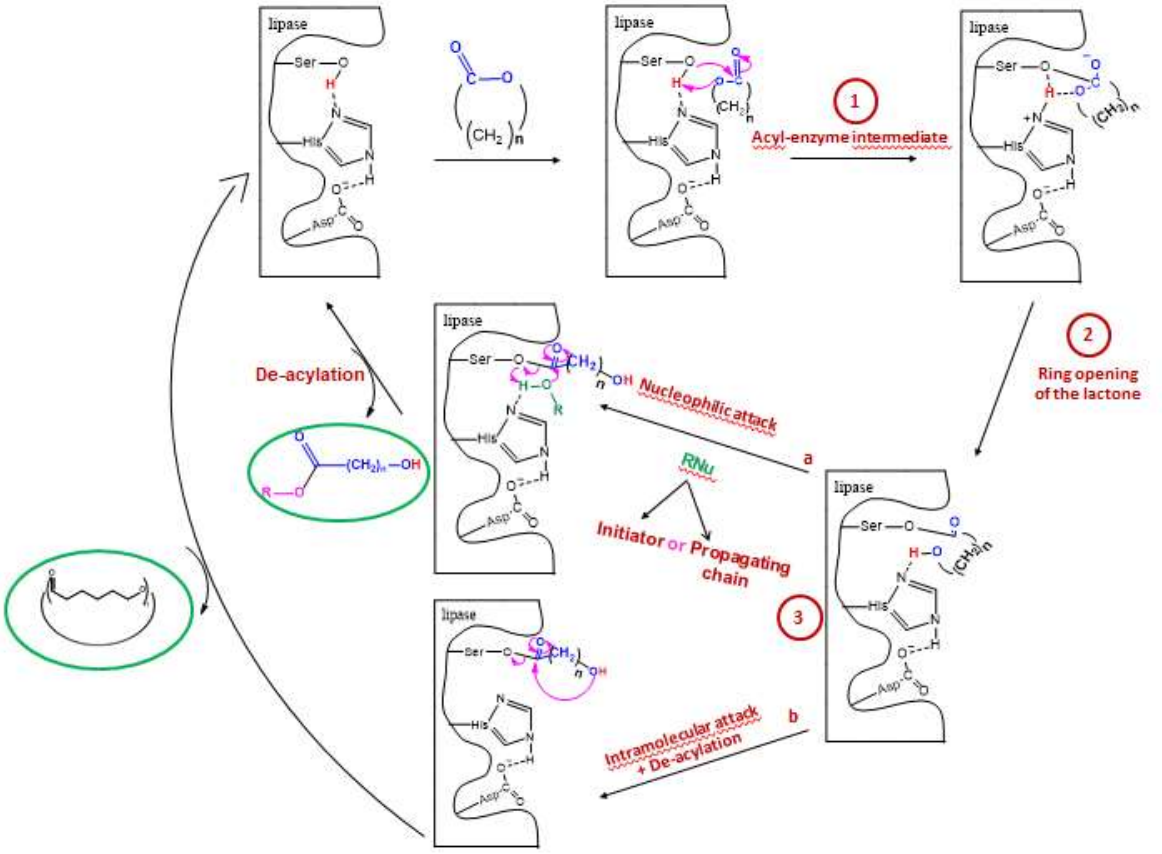

Figure 2-21 Suggested mechanism for the enzymatic ring opening polymerization of lactones. 1: first step of acylation, 2: second step of ring opening of lactones, 3, a: third step in presence of initiator, 3, b: third step without presence of initiator.

© 2020 Tous droits réservés.

2.5.4. Enzymatic ring opening copolymerization (*e*-ROCP) of lactones producing di-block copolymer in integrated microreator system by sequential addition

We present here four co-polymerizations of ε-CL and δ-VL by sequential addition of monomers (Figure 2-22), which are carried out under the same conditions with the difference of monomer's equivalents (Table 2-7). Based on the fact that δ-VL is a more difficult monomer to be polymerized compared to ε-CL, we can explain the least conversion of 88% obtained when using 20/40 equivalents respectively for ε-CL and δ-VL but which gives the best control ($Đ$ = 1.24) (Table 2-7, Run 1). So, in term of control, this result agrees the first ones obtained in section (II.1) [$Đ$ of PVL = 1.27 better than $Đ$ of PCL = 1.3] where δ-PVL is more controlled than ε-PCL. And when using the reverse 40/20 equivalents for CL and VL, the highest conversion was obtained 97% with losing a little of control ($Đ$ = 1.32) (Table 2-7, Run 2). Thus, the excess of ε-CL increases the conversion and the excess of δ-VL increases the control. Finally, using the same equivalents of the two monomers 20/20 or 40/40 almost the same conversion and $Đ$ were obtained respectively: conversion = 95% and 93%, $Đ$ = 1.27 and 1.26 (Table 2-7, Runs 3 and 4). In addition, the experimental molar masses were relatively close to the theoretical previewed ones. Hence, the copolymerization was successfully progressed using the first polymer (the ε-PCL) as a macro-initiator in order to initiate the copolymerization. This result proves the living aspect of the polymer produced in the first step and its efficiency as a macro-initiator.

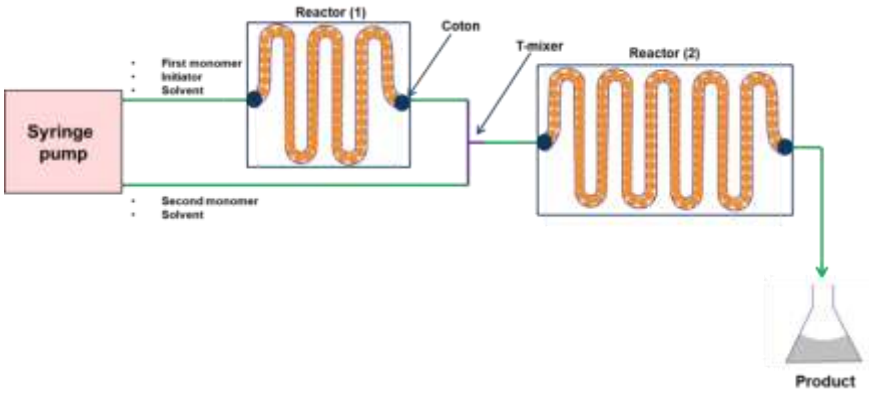

Figure 2-22 Immobilized enzymes in two FEP tubing for enzymatic ring opening copolymerization (e-ROCP) via sequential addition of monomers.

Ru	Monom	Monom	Equivalen	Residenc	Residenc	$M_{n,theo}$	$M_{n,NMR}$	$Đ^c$	Con

© 2020 Tous droits réservés.

lilliad.univ-lille.fr

n	er (1)	er (2)	ts	e time (1) (min)	e time (2) (min)	$\times 10^{-3}$ (g/mol)[a]	$\times 10^{-3}$ (g/mol)[b]		v (%)[a]
1	CL	VL	20/40/1	4	8	5.8	6.1	1.24	88
2	CL	VL	40/20/1	4	7.4	6.4	5.7	1.32	97
3	CL	VL	20/20/1	4	8	5.4	6.9	1.27	95
4	CL	VL	40/40/1	4	7.4	8.1	5.8	1.26	93

Table 2-7 Enzymatic ring opening copolymerization of ε-caprolactone (CL) and δ-valerolactone (VL) with different equivalents in a flow system.

[a] Calculated from (([M_1]+[M_2]/[I])×Conv).(M_W(CL)+ M_W(VL))+M_W(PP).
[b] Determined by ^{1}H NMR
[c] Determined by GPC

2.5.5. Degradation of poly-lactones by the action of N435®

We passed ε-PCL or δ-PVL (in toluene) over a tubular reactor (FEP) containing 300 mg of N435® with different residence times.

We analyzed the product at three stages: 1- the initial polylactone in its dried form; 2- the solution recovered after passing the initial polylactone through the tubular reactor filled of N435®, so before its purification; 3- the final product recovered after purification of the later solution (precipitation, filtration and drying). As shown in Table 2-8, we performed the degradation of δ-PVL by the action of N435®. First, we tested the injection of different initial masses of δ-PVL into the tubular reactor respecting the same residence times: 0.5 or 1 g of δ-PVL that passed through the reactor containing enzyme within 0.5 or 1 min. Second, we tested the degradation of 0.5 g of ε-PCL within residence times ranging from 0.5 to 4 min. After all these experiments cited above, we recovered around 30s percent of the initial masses of injected polymers. These results proved that polylactones are 70% degraded by the enzyme and they lost their molar mass to give smaller chains that are not able to be recovered. And this is a known action of enzyme towards polylactones, but here we can see that the

© 2020 Tous droits réservés.

lilliad.univ-lille.fr

degradation occurred in few minutes in flow instead of much hours needed with other reaction systems already reported.[94] The polymers are characterized by Matrix-assisted laser desorption/ionization Fourier transform ion cyclotron resonance mass spectrometry (MALDI-FTICR-MS) in each stage to detect the variation of their mass as well as their chains' structure. First at 60 °C, we saw the effect of the initial mass of δ-PVL injected on the degradation process with remaining at the same residence time of 1 min. So, after the injection of 1 g of δ-PVL, we recovered 30% of the polymer and 36% of it after injecting 0.5 g. Thus, the initial quantity doesn't greatly affect the enzyme degradation efficiency. MALDI-FTICR spectra presented in Figure 2-23, showed that the majority of the initial PVL peaks (red spectrum) ranges in 1200-2300 mass range. Otherwise, after degradation (spectra blue and green) the dominant peaks are shifted to smaller masses around 800. If we zoom the spectrum (Figure 2-23), we detect the presence of three species of polymer structure: 1- polymer chains with initiator extremity, which are the dominant structure in the initial PVL, 2- Macrocycles, which become at high intensity after degradation and finally 3- chains with H_2O extremity, which are at lower intensity before and after degradation. Same results were obtained, when fixing the injected mass to 0.5 g of PVL and applying different residence time of 0.5 and 1 min (Figure 2-24). Finally, we analyzed by MALDI-FTICR all δ-PVL obtained after their degradation and purification and we compared them with the initial δ-PVL spectrum (Figure 2-25). All spectra behave similarly, with the presence of the three species cited above, which proves that only non-degraded PVL are recovered at the end.

The same study was repeated with ε-PCL at 70 °C, this time, we injected 0.5 g of PCL and we changed the residence time in the range of 0.5-4 min. Same analyses of MALDI-FTICR were performed with the same interpretations (Figure 2-26 and Figure 2-27).

© 2020 Tous droits réservés.

lilliad.univ-lille.fr

Table 2-8 The degradation of poly(ε-caprolactone) and poly(δ-valerolactone) by the enzyme (N435) in a flow system.

Polylactones	Temperature (°C)	Initial mass introduced (g)	Residence time (min)	Mass of final product obtained (g)
PVL	60	0.5	0.5	0.18
			1.0	0.15
PVL	60	1.0	0.5	0.44
			1.0	0.36
PCL	70	0.5	0.5	0.16
			1.0	0.18
			2.0	0.15
			3.0	0.19
			4.0	0.17

© 2020 Tous droits réservés.

lilliad.univ-lille.fr

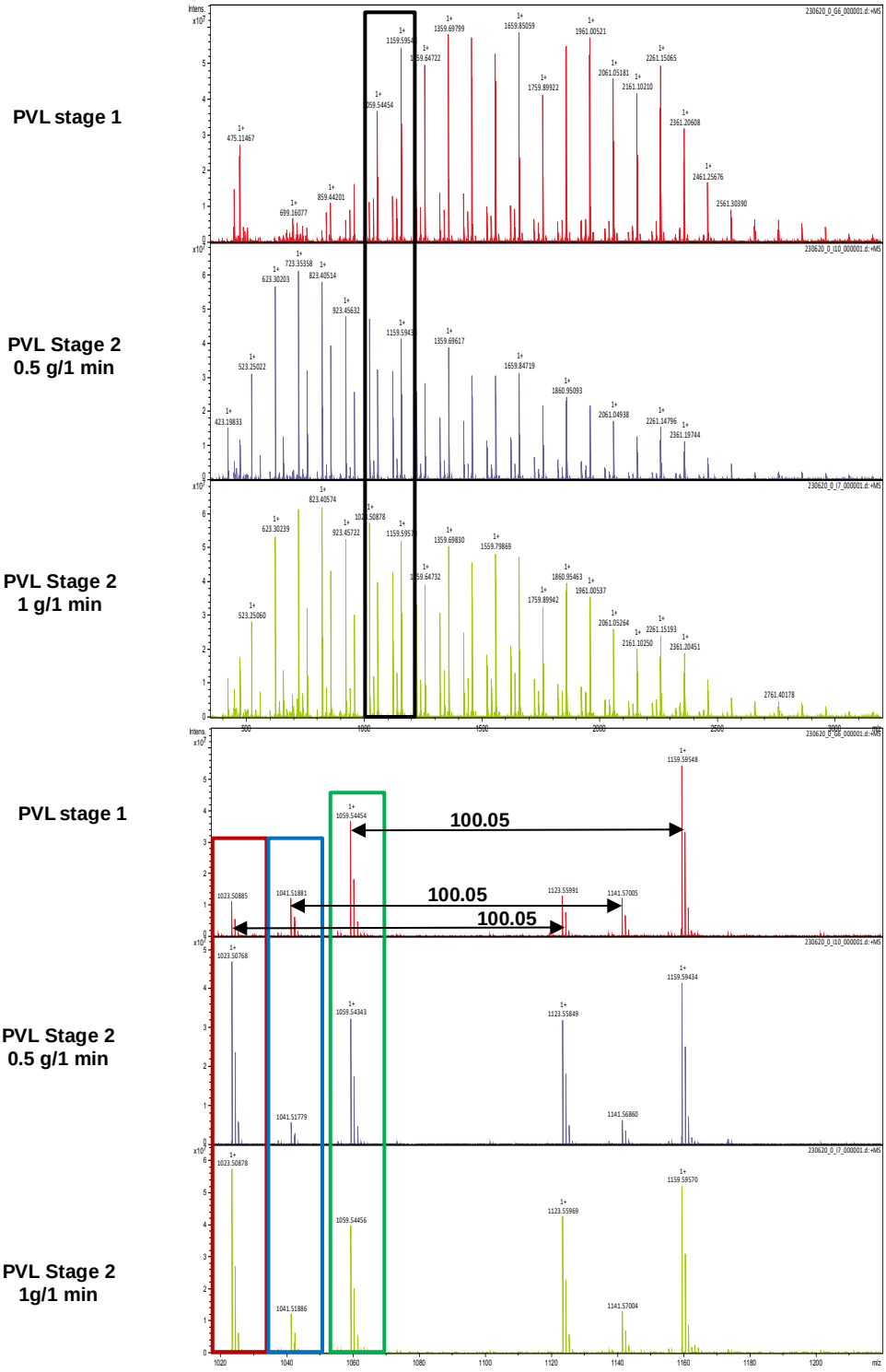

Figure 2-23 MALDI-FTICR spectra of poly-δ-valerolactone at 60 °C at stages 1 and 2 within 1 min of residence time. Stage 1: the initial PVL injected PVL_0; stage 2: PVL obtained after degradation and before purification. "x" g/ "y" min: the quantity of PVL injected/the residence time. Green frame: chains initiated by the initiator (phenylpropanol) M = ($M_{monomer}$ × number of repetition) + $M_{phenylpropanol}$ + N_{Na+}, Red frame: Macrocycles M = M = ($M_{monomer}$ × number of repetition) + N_{Na+}, Blue frame: water end chain M = ($M_{monomer}$ × number of repetition) + M_{water} + N_{Na+}. Black frame: Zoom. The difference between the peaks is the molecular mass of δ-VL = 100.05.

© 2020 Tous droits réservés.

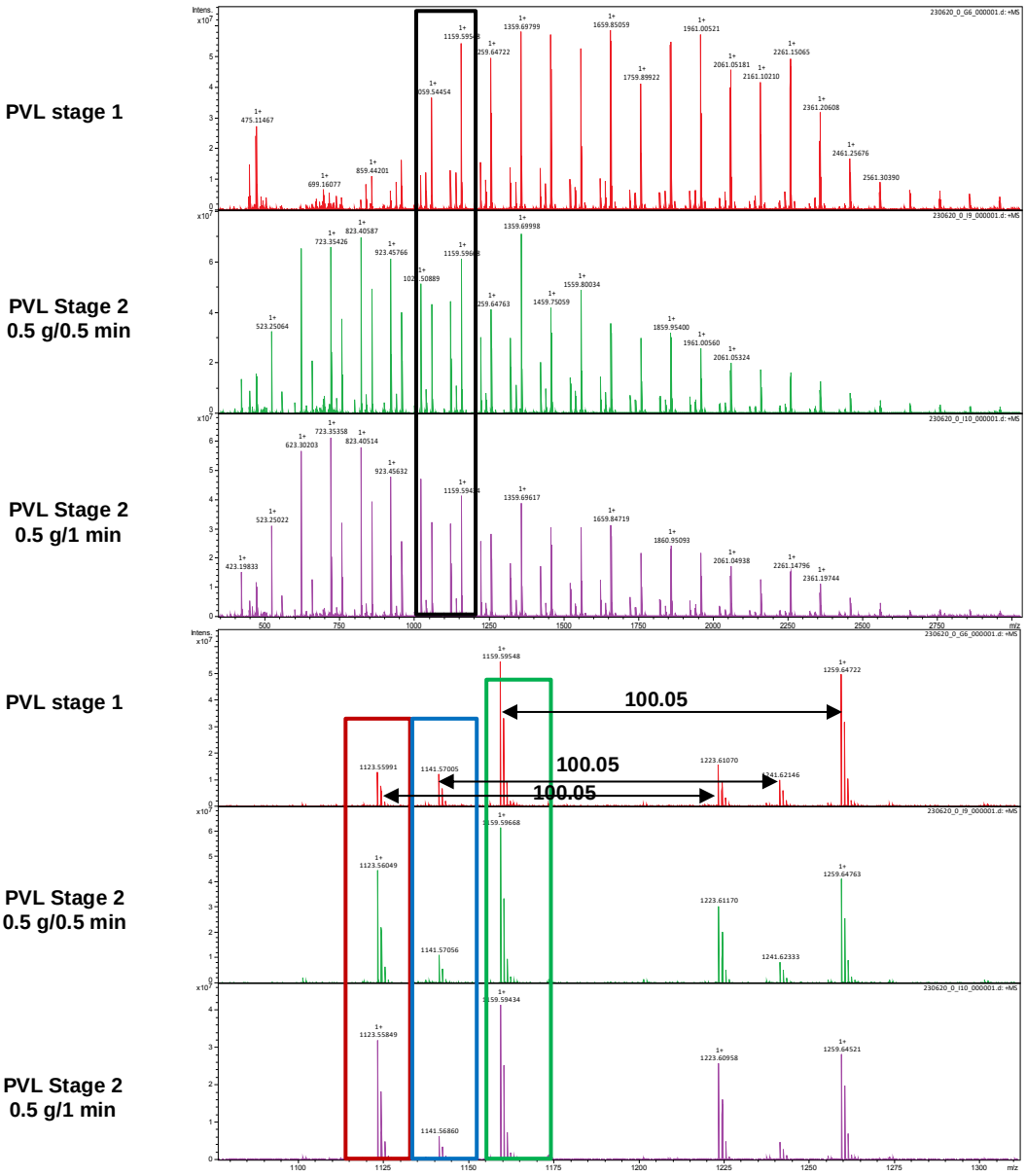

Figure 2-24 MALDI-FTICR spectra of poly-δ-valerolactone at 60 °C at stages 1 and 2 using 0.5 g of PVL. Stage 1: the initial PVL_0 injected; stage 2: PVL obtained after degradation and before purification. x g/ y min: the quantity of PVL injected/the residence time. Green frame: chains initiated by the initiator (phenylpropanol) M = ($M_{monomer}$ × number of repetition) + $M_{phenylpropanol}$ + M_{Na}^+, Red frame: Macrocycles M = ($M_{monomer}$ × number of repetition) + M_{Na}^+, Blue frame: water end chain M = ($M_{monomer}$ × number of repetition) + M_{water}+ M_{Na}^+. Black frame: Zoom. The difference between the peaks is the molecular mass of δ-VL = 100.05.

© 2020 Tous droits réservés.

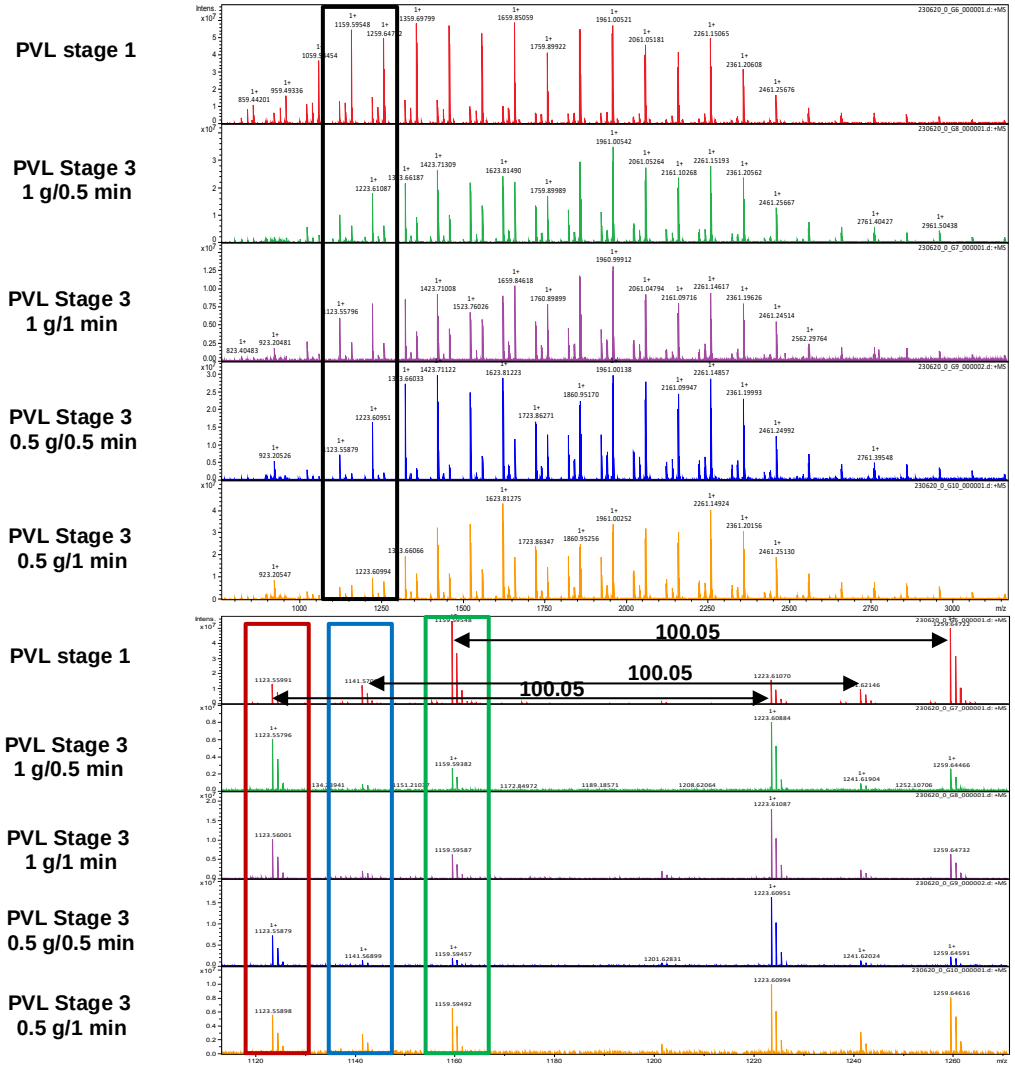

Figure 2-25 MALDI-FTICR spectra of poly-δ-valerolactone at 60 °C at stages 1 and 3. Stage 1: the initial PVL_0 injected; stage 3: PVL obtained after degradation and purification. x g/ y min: the quantity of PVL injected/the residence time. Green frame: chains initiated by the initiator (phenylpropanol) M = ($M_{monomer}$ × number of repetition) + $M_{phenylpropanol}$ + M_{Na}^+, Red frame: Macrocycles M = ($M_{monomer}$ × number of repetition) + M_{Na}^+, Blue frame: water end chain M = ($M_{monomer}$ × number of repetition) + M_{water}+ M_{Na}^+Black frame: Zoom. The difference between the peaks is the molecular mass of δ-VL = 100.05.

© 2020 Tous droits réservés.

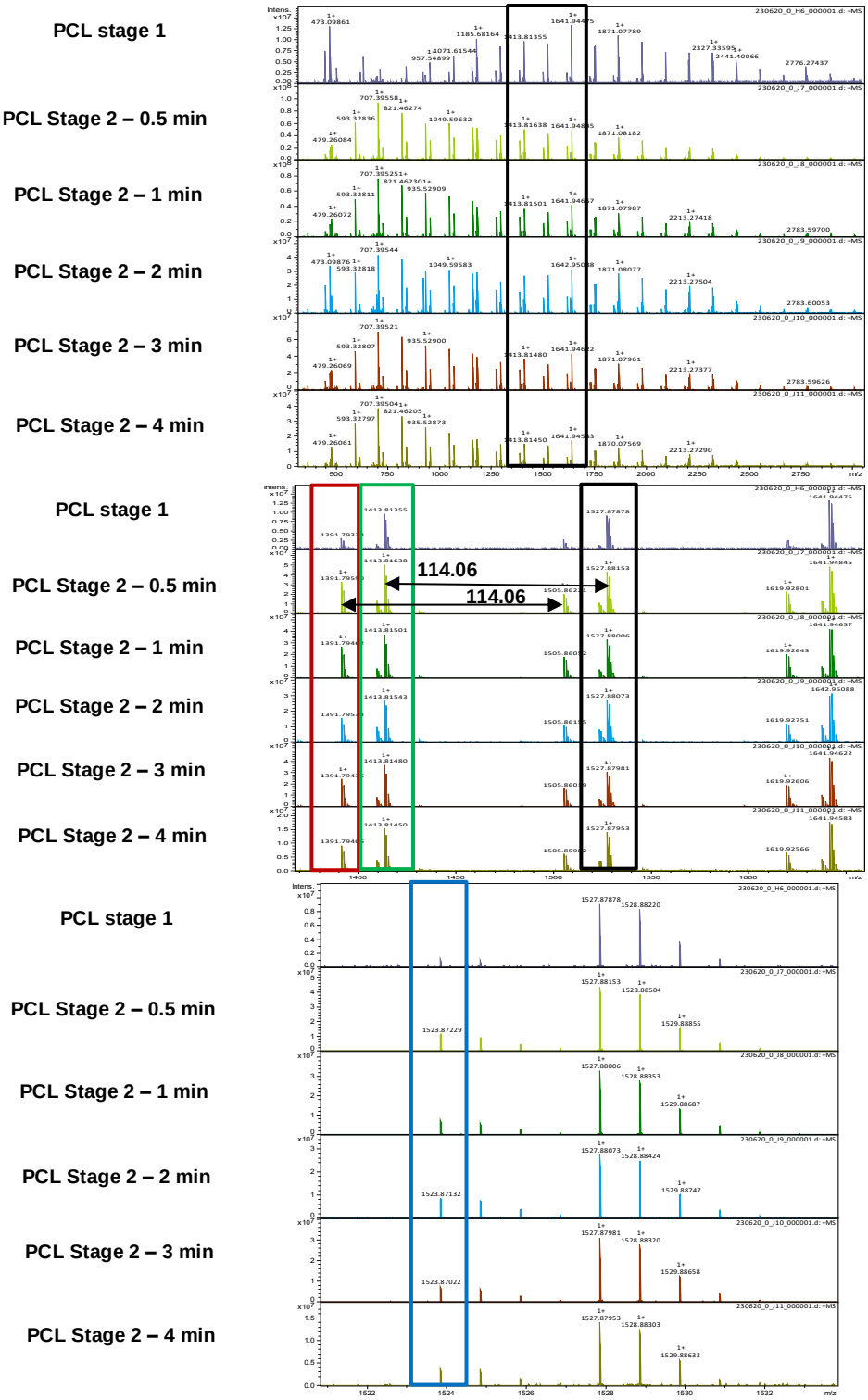

Figure 2-26 MALDI-FTICR spectra of poly-ε-caprolactone at 70 °C at stages 1 and 2. Stage 1: the initial PCL injected; stage 2: PCL obtained after degradation and before purification. x min: the residence time. Green frame: chains initiated by the initiator (phenylpropanol) M = ($M_{monomer}$ × number of repetition) + $M_{phenylpropanol}$ + M_{Na}^{+}, Red frame: Macrocycles M = ($M_{monomer}$ × number of repetition) + M_{Na}^{+}, Blue frame: water end chain M = ($M_{monomer}$ × number of repetition) + M_{water}+ M_{Na}^{+}. Black frame: Zoom. The difference between the peaks is the molecular mass of ε-CL = 114.06.

© 2020 Tous droits réservés.

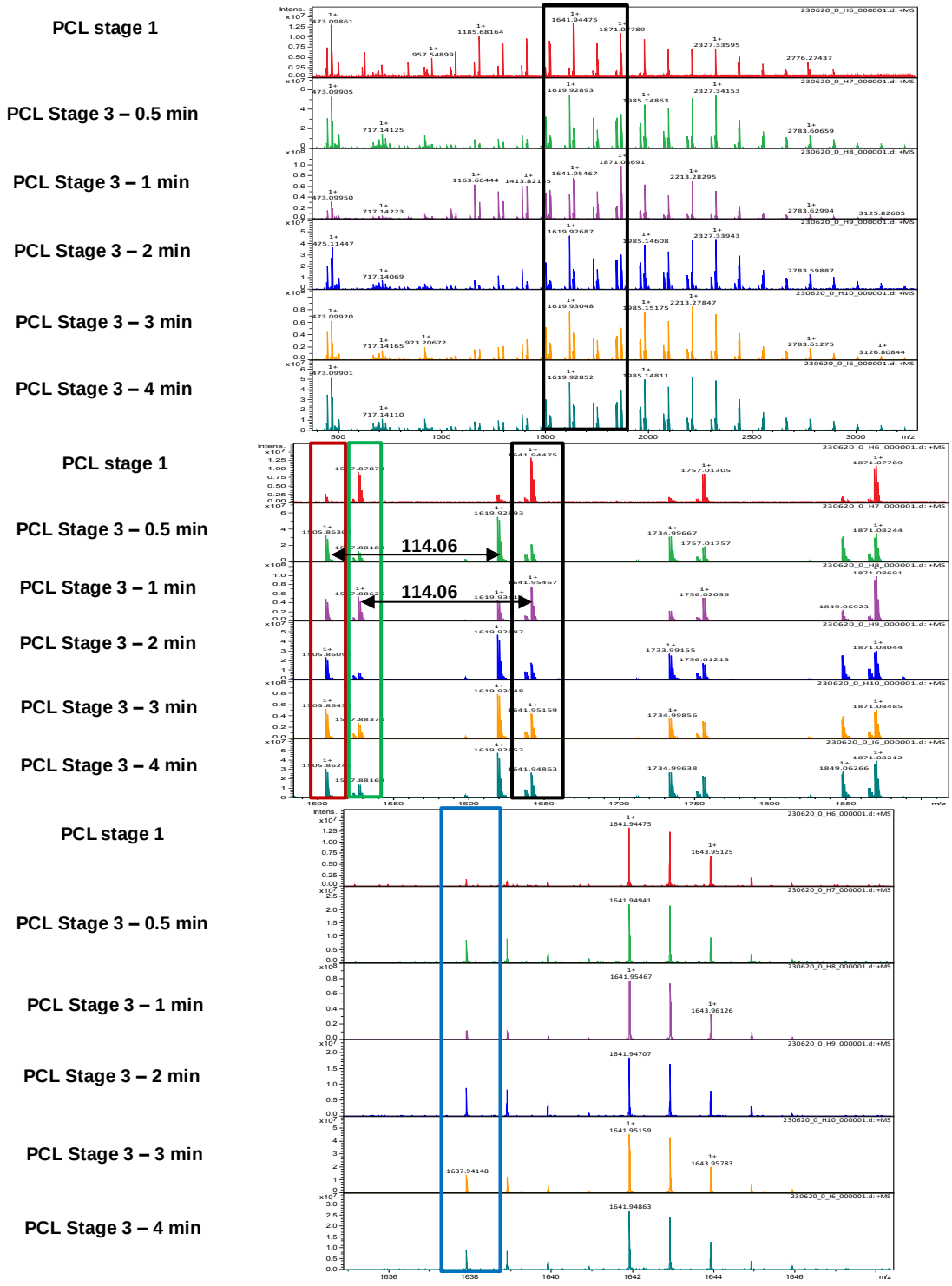

Figure 2-27 MALDI-FTICR spectra of poly-ε-caprolactone at 70 °C at stages 1 and 3. Stage 1: the initial PCL injected; stage 3: PCL obtained after degradation and purification. x min: the residence time. Green frame: chains initiated by the initiator (phenylpropanol) M = ($M_{monomer}$ × number of repetition) + $M_{phenylpropanol}$ + M_{Na}^{+}, Red frame: Macrocycles M = ($M_{monomer}$ × number of repetition) + M_{Na}^{+}, Blue frame: water end chain M = ($M_{monomer}$ × number of repetition) + M_{water}+ M_{Na}^{+}. Black frame: Zoom. The difference between the peaks is the molecular mass of ε-CL = 114.06.

© 2020 Tous droits réservés.

2.5.6. Recycling of N435®

As N435® was immobilized into the tubular reactor; it was reused many times in ring opening polymerization of ε-CL under identical conditions (residence time = 4 min and T = 70 °C). This study proved the efficiency of enzyme reusing in flow system without need for any extra step to recover the catalyst after each reaction. As Table 2-9 shows, until reaction number 8 the conversion was constantly upper than 96%. Practically after reaction 18 the conversion decreased below 90% and reached 77% on reaction number 21. So, the high conversion conserved during these reactions proves that N435® can be reused for at least eight times with conserving its very high efficiency. And we can greatly consider N435® as a green and an economic catalyst.

Table 2-9 The reuse of enzyme as a catalyst for ε-caprolactone polymerization in a flow mode[a]

Run	Conv (%)[b]
1	98
2	97
3	98
4	97
5	93
6	98
7	98
8	99
9	86
10	93
11	96
12	90
13	91
14	---
15	93
16	85
17	89
18	90
19	87
20	85
21	77

[a] Reaction temperature is 70 °C, in toluene, [M]/[I](mol) = 20, 100 mg of N435®, residence time = 4 min
[b] Determined by ^{1}H NMR

© 2020 Tous droits réservés.

2.6. Conclusions

In conclusion, we successfully produced ε-PCL [(at 70 °C, conversion = 100%, *Đ* = 1.3, residence time = 240 s), (at RT, conversion = 94%, residence time = 10 min, *Đ* = 1.34)] and δ-PVL [(at 60°C, conversion = 100%, *Đ* = 1.27, residence time = 214 s) (at RT, conversion = 100%, residence time = 10 min, *Đ* = 1.28)] via enzymatic ring opening polymerization in flow, so these polymerizations can be performed with energy save. As initiators, we found that primary alcohols are more efficient for the initiation than the secondary alcohols. A strong competition exists between the secondary alcohols and the enzyme, where the latter is responsible of the production of macrocycles and this is being proved by the polymerizations achieved without presence of initiator. Wide dispersed polymers were obtained by the single action of enzyme [*Đ* = 1.99-2.68], while the increase of residence time caused the increase of *Đ*, in contrast the increase of enzyme quantity had the opposite effect on *Đ*. In addition, no conversion was detected in the absence of N435® at RT nor at 70 °C**,** which proves that the polymerization is immediately quenched once the reaction media is recovered out of the enzyme. On the other hand, Successful co-polymerizations in flow were done via sequential addition yielded copolymers of *Đ* max = 1.27 and conversions of more than 88%. We proved also the enzyme capability to break down polylactones in flow mode at the same time with its effectiveness in polymerizing lactones. Finally, we proved the advantage of reusing N435® with a very good efficiency for more than ten times.

© 2020 Tous droits réservés.

3. CHAPTER THREE: PHOSPHAZENE BASES (PBs) CATALYZED THE RING OPENING POLYMERIZATION OF LACTONES IN FLOW SYSTEM

3.1. Phosphazene bases (PBs)

A new class of catalysts has been generated in order to develop controlled polymer materials.[296–298] The usual demands of catalysts for small molecule reactions like efficiency and selectivity are added to other requirements for polymerization reactions catalysts such as: tolerance to functional monomers, molecular weights control, polymers mass distributions, number and nature of chain end groups, macromolecules topologies, and the sequence of different monomers in the polymer chain.[299] It's well known that organometallic catalysts have gained a large interest in the field of polymerization catalysis with unlimited combinations of ligands and metals.[300–302] However, in response to environmental requirements for metal-free polymers as well as for biomedical[303] and microelectronic applications,[304] advances in organocatalyzed polymerizations were recorded during almost the past decade.[305]

Phosphazene bases (PBs) are quite strong, uncharged Brønsted bases that do not exhibit a nucleophilic character. In the beginning of 1970s, the first PB was synthesized that includes phosphorus atom P(V) bounded by one imine and three amine groups (Figure 3-1).[306–309] Until the late 1980s, few reports have appeared concerning this compound and its application when Schwesinger and co-workers restored the dynamic of this work.[12,13,310,311] They developed a general synthetic methodology by which a series of PBs have been generated (Figure 3-2).

© 2020 Tous droits réservés.
lilliad.univ-lille.fr

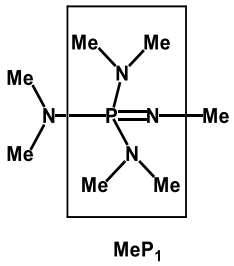

Figure 3-1 The first-reported phosphazene base, MeP_1.

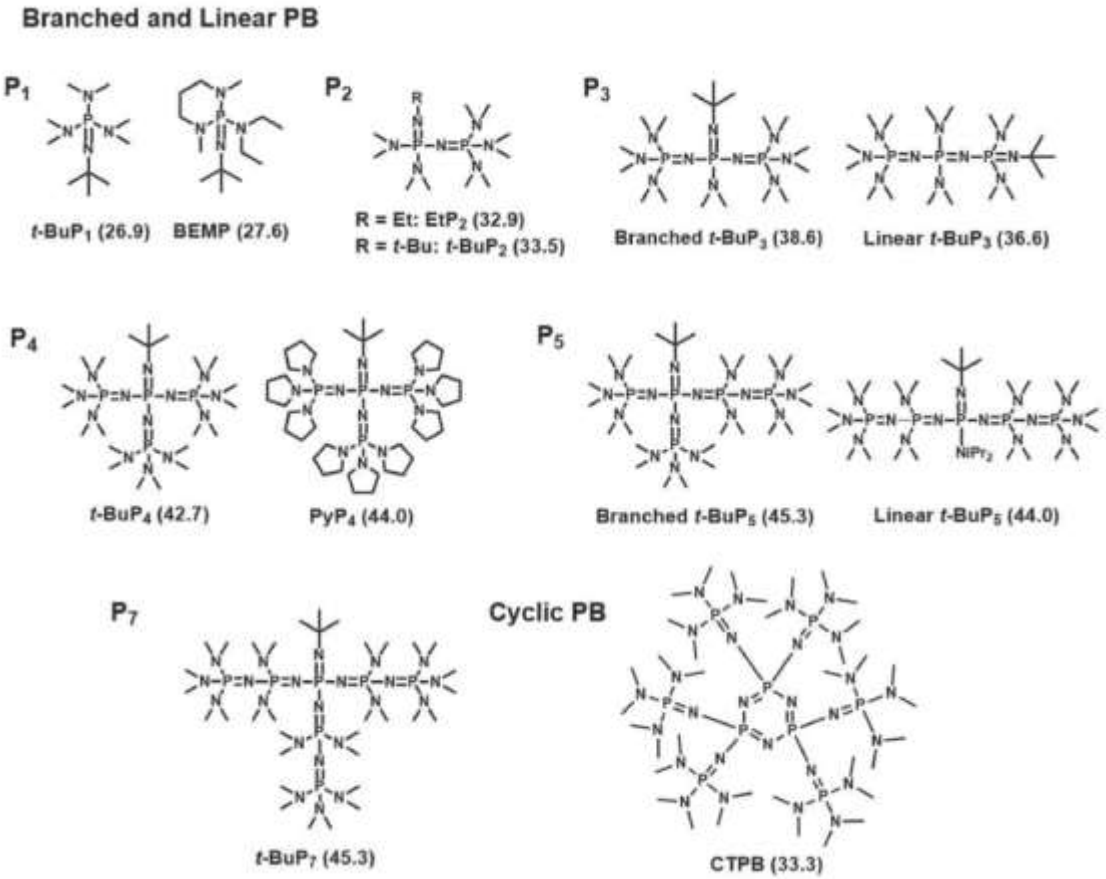

Figure 3-2 Branched, linear, and cyclic phosphazene bases used in polymer synthesis. pKa values measured in MeCN are shown in parenthesis.[310,312]

PBs are characterized by their quite basicity and non-nucleophilic nature. Thus, they are able to deprotonate or activate protic weak nucleophiles and turn them into nucleophilic initiating species that can further initiate rapid and controlled ROPs. The efficient protic initiators in the presence of PBs were found to be alcohols,[313] thiols[314] and amides,[315] among which alcohols are the most used due to their diversity and availability. An alternative way of initiator's activation was provided by using complexation/coordination of PB with lithium cation.[316]

© 2020 Tous droits réservés.

The molecular structure and the basicity of PBs affect highly their catalytic properties. It was found that high basicity can accelerate polymerization rates and lead to undesirable reactions, like chain transfer reactions and transesterifications, which make broader the M_w of the produced polymer chains.[312] Therefore, a correct choice of the PBs with the suitable basicity towards a specific monomer is important to perform a fast and controlled polymerization.[317]

3.2. Phosphazene bases features

3.2.1. Structural features of PBs

Based on Schwesinger's research, the $(R_2N)_2$-P = N part of the compound (Figure 3-1, the structure part in the frame) was taken as a standard part and considered as a "basicity battery cell".[310] So, by homologation, a series of neutral superbases were produced (Figure 3-2). The electronic and steric properties of the battery cells can be tuned by different dialkylated amino groups and the control of basicity and nucleophilicity of PBs can be greatly affected by the choice of =alkyl groups, and this is shown by the different pK_a values mentioned in Figure 3-2. Based on this concept, branched or linear phosphazene can be obtained and simply named as P_n, where n is the number of "battery cells". PBs presented in Figure 3-2 are of high importance for polymer synthesis.[305] Always based on "battery cell" concept, but this time using a cyclic starting material, hexachlorocyclotriphosphazene, Zhibo Li and co-workers have developed a new type of phosphazene base (CTPB).[312]

3.2.2. Basicity of PBs

Theoretically, the basicity of a wide range of PBs has been studied[318] and the values were experimentally measured in the gas phase[319] as well as in solution, such as THF,[320] MeCN[321] and DMSO.[310] The PBs shown in Figure 3-2 present p*K* values in the range of 27 to 45 pK_a units in MeCN. The pK_a values change similarly in the two solvents MeCN and DMSO. However, because of proton affinity difference between these two solvents, for a given PB, the pK_a value is larger in MeCN than that in DMSO. The structure of PBs is the main parameter that affects the basicity of them. First of all, it is related to the number of "battery cells", and an increase of it is recorded from p_1 to p_5 with the charge on the conjugated phosphazenium cation. However, a decrease of basicity is observed with larger system for each additional "battery cell", because of the resonance saturation of the cation. In fact, t-BuP_7 and t-BuP_5.have both the same basicity (pK_a = 45.3 in MeCN Figure 3-2).[310,311] In addition, the presence of different substituents on amino and imino groups is able also to

© 2020 Tous droits réservés.

affect the basicity. For example, the use of pyrrolidine groups instead of dimethylamino groups in the P_4 series contributes to basicity increase by 1.3 p*K* units (*t*-BuP_4 and PyP_4 in Figure 3-2). Finally, the topology tuned the basicity of PBs.In addition, the branched PBs present more basicity than the linear ones for those owning the same number of "battery cells" (examples: P_3 and P_5 in Figure 3-2). CTPB exhibits surprisingly a lower basicity compared to *t*-BuP_4 (33.3 and 44.0 respectively, Figure 3-2).[313]

3.2.3. Stability and solubility of PBs

PBs exhibit good thermal stability, in addition to the high stability towards oxygen and moisture.[310,311] They resist greatly to hydrolysis, even in highly basic solution. The most used PB which is *t*-BuP_4 remains stable in 1 M aqueous solution at 160 °C for 20 h.[13] On the other hand, these bases are strongly hydrophilic and lipophilic, and they are in a liquid form at room temperature, in the two air and hexane vapor. Even more, no smooth –or efficient enough- "physical" method was found in order to dry wet samples, and this task become more and more difficult with PBs beyond P_3 stage which are extremely basic. That is why; it is required to store PBs under dry nitrogen protection.

Another interesting feature of PBs is their good solubility in the most used organic solvents like: hexane, toluene, THF, MeCN and DMSO, which makes them easy to manipulate and a suitable choice for polymerization in solution. However, the high basicity of PBs could promote reactions between them and the solvent, like MeCN and DMSO. A self-condensation of acetonitrile resulting the quite acidic 4-amino-2,6-dimethylpyrimidine, can be catalyzed by the P_3, P_4 or even P_2 basic catalysts.[310] It was found that two isomers of commercial *t*-BuP_4 in hexane solution are detected by NMR, proving the possibility of decomposition/isomerization process of *t*-BuP_4 in solution to occur.[322] In the case of cyclic PBs, CTPB showed a good stability in hexane, toluene and THF over days, and no decomposition was observed. On the other hand, the two topologies of PBs branched and cyclic ones-including *t*-BuP_4 and CTPB- are instable in dichloromethane even at room temperature. *t*-BuP_4 in dichloromethane results directly in a brown solution.[323] Consequently, apolar or moderately solvents like hexane, toluene and THF are used commercially to prepare the PBs in solution under inert atmosphere

© 2020 Tous droits réservés.

3.3. General mechanism for ROP of cyclic esters by PBs

Related to the nature of ROP components which are: the catalyst, the initiator and the monomer; three types of mechanisms for organocatalyzed ROP are mentioned and known as: monomer activation mechanism, initiator/chain-end activation mechanism, and dual activation mechanism.[324] As superbases, PBs can initiate directly a polymerization reaction by simple abstraction of the monomer's relative acidic proton, without initiator interference. However, this route application was limited to polymerization of non-cyclic monomers, like methyl methacrylate (MMA), α-methylene-γ-butyrolactone, and their analogs, so without ring opening.[325,326] This way of initiation wasn't enough efficient for the polymerization of cyclic esters.[313,323] Therefore, conventionally, ROP of cyclic esters is catalyzed by PBs in combination with initiators following the initiator/chain-end activation catalytic mechanism (Scheme 3-1). Typically, the first step is the activation of the initiator or the polymer chain end by PBs through deprotonation or formation of hydrogen bond, resulting in the activation of initiating/chain propagating species under relative mild conditions compared to metal catalysts harder conditions requirements.[327–331] The activated species containing an alkoxide function (oxygen with negative charge) will make a nucleophilic attack on the electrophilic carbonyl group of the monomer, leading to the ring opening of the cyclic ester.

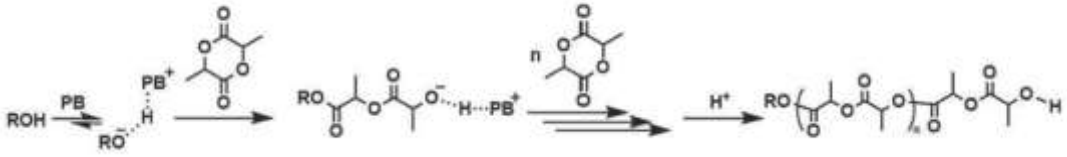

Scheme 3-1 ROP of lactide by PB in the presence of alcohol as the initiator with the initiator/chain-end activation mechanism.[305]

In addition, PBs can combine *H*-bond donors species to form a dual catalytic system which implies their cooperation to activate and promote the ROP under the dual activation mechanism (Scheme 3-2). In this mechanism, as strong bases, PBs activate the initiator/chain end by proton abstraction and the electrophiles presented by the H-bond donors activate the monomer.[332] Due to the amplified activity and selectivity of such dual catalytic systems, they have gained recently much interest.

© 2020 Tous droits réservés.

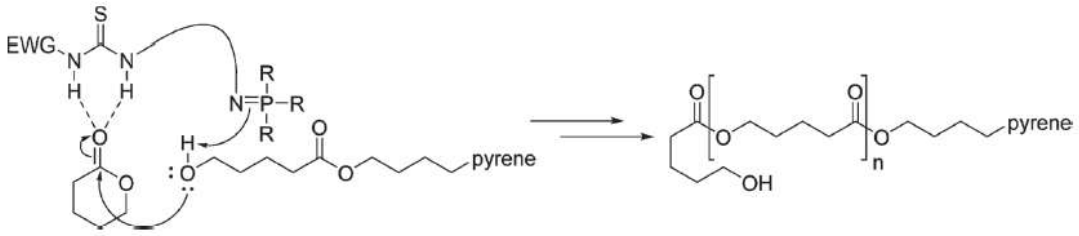

Scheme 3-2 Representation of dual activation of a monomer and growing polymer chain by a bifunctional iminophosphorane organocatalyst. R, aryl group; EWG, electron-withdrawing group. Reproduced with permission[332] Copyright 2014, American Chemical Society.

3.4. Phosphazene bases (PBs) catalysed the homo- and copolymerization of lactones.

BEMP, *t*-BuP_1 and *t*-BuP_2 are phosphazenes with relatively low basicity, and they successfully catalysed the ROP of cyclic esters like: L-lactide (L-LA), rac-latide (rac-LA), δ-VL and ε-CL.[333,334] Following this synthetic route, M_W of polymers produced can be predicted and they possess low dispersity indexes (PDIs) and high end-group fidelity. However, the rate of ROP catalyzed by these weak PBs is relatively low and it could take about hours or days to reach high conversions. On the other hand, with more strong PB such as *t*-BuP_4, an active ROP can be performed but with loss of reaction control manifested by a broad distributions of polymer chains, due to the apparition of transesterification side reactions.[312] Here appears the importance of the right choice of PB for a given monomer.

3.4.1. *O*-ROP of VL and CL

BEMP has been studied in ROP of VL promotion using either 1-pyrene butanol or benzyl alcohol as initiator, in bulk and at room temperature.[333] However, the same reaction but with LA monomer was done with faster polymerization rate under the same conditions. In addition, with CL, the less strained monomer, only 14% of conversion was reached after ten days at room temperature.[333] On the other hand, the catalytic system was improved by changing it to a dual catalytic system involving BEMP and triclocarban (TCC) as an *H*-bond donor, and full conversion of VL was reached after 3 min.[335]

Furthermore, *t*-BuP_2 was investigated to catalyze the ROP of ε-CL under different conditions such as: initiators, solvents, catalyst and monomer concentrations.[336] Overall, controlled ROP of ε-CL proceeded with expected M_W and good polydipersity index. The polymerization rates

© 2020 Tous droits réservés.

variate according to the solvent used in the following order: DCM > toluene > 1,4-dioxane > THF. The best solvent was the DCM in which 98% of conversion was reached within 1h, while in THF, only 39% was reached after 8 h. Although the highest conversion was obtained in DCM, a high degree of transesterification side reaction was recorded that contributed to broad polymer chains (PDI=1.42). The use of amide and macromolecular initiators were good for polymerization initiation but with lower rates.[336] The cyclic phosphazene (CTPB) was able to catalyze CL ROP and without presence of initiator, but with low efficiency. therefore, different alcohols were used as an initiator like: BnOH, diphenylmethanol, 3-phenyl-1-propanol (PP), and trimethylol propane, PCLs with different end groups and topologies were able to be prepared as shown in Scheme 3-3.[313]

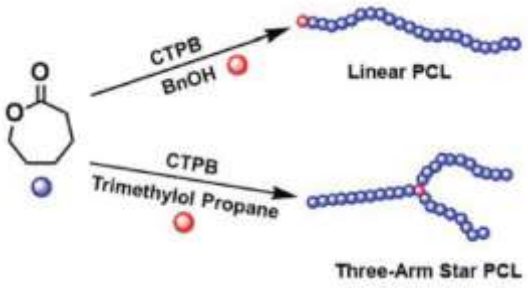

Scheme 3-3 Preparation of linear and three-arm star PCLs by CTPB with different initiators.[313]

In addition, the selectivity of phosphazene superbases towards lactone monomers was investigated.[337] Based on the ring sizes of lactones, they defined small lactones (SLs) (SLs ≤ 8 membered rings) and macrolactones (MLs) (ring size >8). The selectivity was showed to be as: t-BuP_4 for MLs and t-BuP2 for SLs. So, by switching these two catalysts, controlled copolymers of PMLs-b-PSLs can be obtained.

3.4.2. *O*-ROP of γ-Butyrolactone

γ-Butyrolactone (γ-BL) is a promisingrenewable monomer and biobased compound derived from succinic acid.[338] Normally this cyclic ester is considered as a "non-polymerizable" monomer due to the low strain energy of the five-membered ring.[275] However, it was polymerized by enzymatic catalysis but with extreme conditions and low M_W were obtained. Later, Chen and coworkers developed the ROP of γ-BL using earth metal complexes at -40°C.[281] And the same group continued their work and investigated the use of t-BuP_4 to polymerize γ-BL in the absence of initiator.[313] Besides, when adding the alcohol as an initiator to the system, a more efficient polymerization were performed with high conversion of 90% and M_n up to 36.7 KDa within 4 h. Moreover, a good investigation of t-BuP4 to

© 2020 Tous droits réservés.

catalyze the ROP of γ-BL was done with the presence of various electron-donation groups substituted (thio) ureas to form a dual organo-catalytic system. In a such system, the polymerization of γ-BL was conducted with high activity and selectivity to give linear PγBLs with high M_W.[339] Even more, the copolymerizations of γ-BL with CL or VL using t-BuP_4 as a catalyst were effective.[340]

© 2020 Tous droits réservés.

3.5. Results and discussion

3.5.1. Organo ring opening polymerization of ε-CL in microreator system catalyzed by phosphazene superbases in flow system.

In organo ring opening polymerization (*O*-ROP) we used as a catalyst four phosphazene bases (PBs), which are ordered from the strongest one to the weakest one as following: *t*-OctP_4, *t*-BuP_4, *t*-BuP_2, P_1-*t*-Bu-tris(tetramethylene) (BTPP) with $pKBH^+$ in MeCN respectively 42.7, 41.9, 33.5, 28.4 (Figure 3-3).

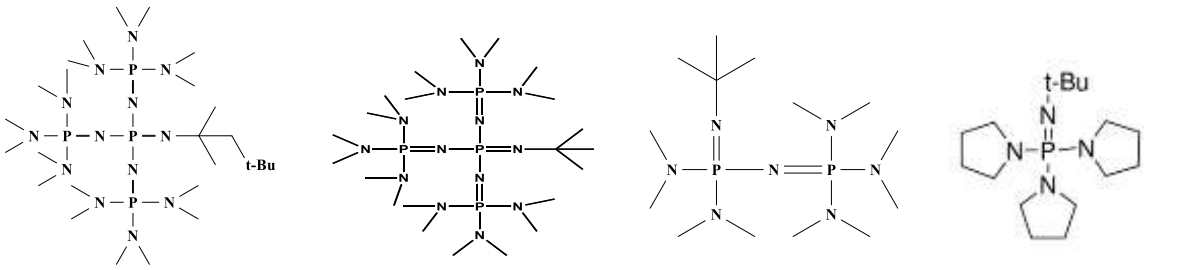

t-OctP_4 $^{MeCN}pKBH^+$42.7 | *t*-BuP_4 $^{MeCN}pKBH^+$41.9 | *t*-BuP_2 $^{MeCN}pKBH^+$33.5 | P_1-*t*-Bu-tris(tetramethylene) $^{MeCN}pKBH^+$28.4

Figure 3-3 Different phosphazene superbases.

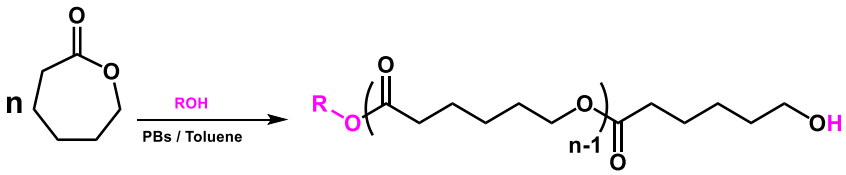

Figure 3-4 phosphazene superbases catalyzed rimg opening polymerization of ε- caprolactone.

Working on the ε-CL organo ring opening polymerization (Figure 3-4), we tried to find the best phosphazene superbase to use as a catalyst under the optimum conditions of temperature, residence time and reagents quantity (Table 3-1).

© 2020 Tous droits réservés.

Table 3-1 Organo ring opening polymerization of ε-caprolactone in microflow system with double entries using phozphazene superbases as catalysts in toluene. M/I/cat: Monomer/Initiotor/Catalyst

Run	M/I/Cat	Eq	Residence time (min)	T °C	Conv [a]	M_n [b] (theo)	M_n [a] (NMR)	M_n [c] (GPC)	$Đ$ [c]
1	ε-CL/PP/ *t*-OctP_4	50/1/1	30	5	100	5843	5100	7718	1.59
2	ε-CL/PP/ *t*-OctP_4	50/1/0.5	30	5	90	5272	5923	----	----
3	ε-CL/PP/ *t*-OctP_4	50/1/0.16	30	5	68	3240	3523	4250	1.32
4	ε-CL/PP/ *t*-OctP_4	50/1/1	20	5	92	5386	4800	8790	1.43
5	ε-CL/ BnOH/ *t*-BuP_4	100/1/1	60	50	95	11522	10950	9738	1.87
6	ε-CL/ BnOH/ *t*-BuP_4	100/2/1	60	50	96	5815	5586	9836	1.96
7	ε-CL/PP/ *t*-BuP_4	100/1/1	60	50	92	10637	4600	7649	1.64
8	ε-CL/PP/ *t*-BuP_4	100/2/1	60	50	95	5558	4700	8101	1.71
9	ε-CL/PP/ *t*-BuP_4	100/4/1	60	50	97	2904	3500	6435	1.50
10	ε-CL/PP/ *t*-BuP_4	100/1/1	60	23	96	11093	4360	11764	2.11
11	ε-CL/PP/ *t*-BuP_4	100/2/1	60	23	94	5500	4130	9779	2.09
12	ε-CL/Chol/ *t*-BuP_4	100/1/1	60	50	78	11800	----	8027	1.70
13	ε-CL/PP/ *t*-BuP_2	50/1/1	30	5	41	2476	----	3539	1.08
14	ε-CL/PP/ BTPP	40/1/1	60	70	0	----	----	----	----
15	ε-CL/PP/ BTPP	40/1/1	360	70	0	----	----	----	----
16	ε-CL/PP/ BTPP	100/1/1	360	70	0	----	----	----	----
17	ε-CL/PP/ BTPP	150/1/1	600	90	0	----	----	----	----

[a] Determined by ^{1}H NMR
[b] Calculated from (([M]/[I])×Conv) × M(monomer))+M_W(initiator).
[c] Determined by GPC

Using the strongest phosphazene *t*-OctP_4 as a catalyst with 50/1/1 of equivalents respectively for the monomer, initiator (PP) and the catalyst, 100% of conversion and $Đ$ of 1.59 were obtained at 5 °C within 30 min of residence time (Table 3-1, Run 1). Under the same conditions, but, with residence time of 20 min we obtained 92% of conversion and $Đ$ of 1.43

© 2020 Tous droits réservés.

(Table 3-1, Run 4). Compared to Run 1, the conversion decreased to 90% and 68% ($Đ$=1.3) with the decrease of the catalyst equivalent respectively to 0.5 and 0.16 (Table 3-1, Runs 2 and 3). So according to $Đ$ values, when increasing the yield, we lost a little bit of control. And in these three runs the molecular weights obtained were close to the theoretical ones predicted by ^{1}H NMR.

Second, we used *t*-BuP_4 as a catalyst to promote the *O*-ROP of ε-CL, wich is less basic than the *t*-OctP_4. First the initiation was done using BnOH as an initiator. We carried out the reaction with equimolar amounts of initiator and catalyst within 60 min at 50 °C (Table 3-1, Run 5). The polyesters result from 95% of monomers conversion. Interestingly, the theoretical M_n calculated by ^{1}H NMR is in accordance with the two experimental values obtained by ^{1}H NMR and GPC; however, the $Đ$ is of 1.87. When we increased the amount of the initiator to 2 equivalents (Table 3-1, Run 6), theoretical and experimental values of M_n calculated by ^{1}H NMR were correlated but with a difference with the one obtained by GPC and an increase of $Đ$ was recorded (1.96). Although the presence of three different species of polyesters in these two products, which is proved by MALDI-TOF spectra, these latter don't behave similarly in term of the abundance of each species. With equimolar conditions, chains initiated by BnOH are the most abundant with less presence of macrocycles and chains with H_2O extremity (Figure 3-5). However, when the initiator equivalent is doubled, the MALDI-TOF spectrum revealed a predominance of the macrocycles abundance over the two other species (Figure 3-6). And these results correspond to the increase of $Đ$ value so to a control loss.

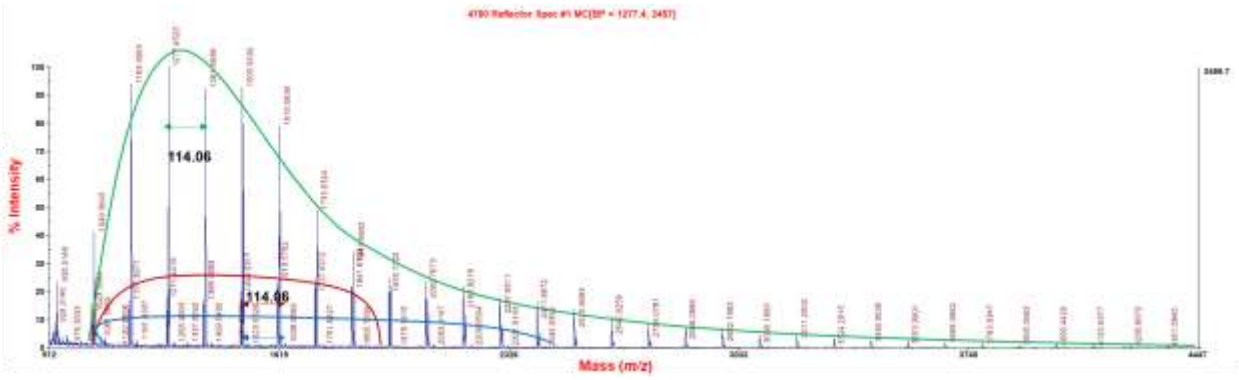

Figure 3-5 MALDI-TOF spectrum of poly-ε-caprolactone produced after 60 min of residence time via *O*-ROP initiated by BnOH in flow at 50 °C (Monomer/Initiator/Catalyst 100/1/1) (Table 3-1 Run 5). Green curve: chains initiated by the initiator (BnOH) M = ($M_{monomer}$ × number of repetition) + M_{BnOH} + M_{Na^+}, Red curve: Macrocycles M = ($M_{monomer}$ × number of repetition) + M_{Na^+}, Blue curve: water end chain M = ($M_{monomer}$ × number of repetition) + M_{water}+ M_{Na^+}. The difference between the peaks is the molecular mass of ε-caprolactone = 114.06.

© 2020 Tous droits réservés.

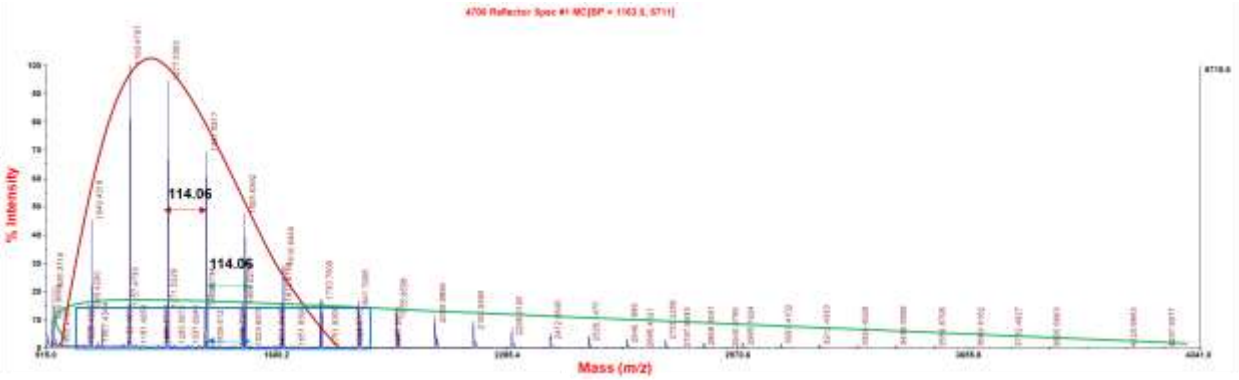

Figure 3-6 MALDI-TOF spectrum of poly-ε-caprolactone produced after 60 min of residence time via *O*-ROP initiated by BnOH in flow at 50 °C (Monomer/Initiator/catalyst 100/2/1) (Table 3-1 Run 6). Green curve: chains initiated by the initiator (BnOH) M = (Mmonomer × number of repetition) + M_{BnOH} + M_{Na}^+, Red curve: Macrocycles M = ($M_{monomer}$ × number of repetition) + M_{Na}^+, Blue frame: water end chain M = ($M_{monomer}$ × number of repetition) + M_{water}+ M_{Na}^+. The difference between the peaks is the molecular mass of ε-caprolactone = 114.06.

When changing the initiator to the PP and cholesterol, polymerizations yielded respectively 92% and 78% (Table 3-1, Runs 7 and 12). MALDI-TOF-MS spectra revealed the presence of linear and non-linear species in the polyester products. Besides the linear ε-PCL initiated by BnOH -the major species-, we observed the presence of macrocycles formed by the intramolecular transesterification reaction and linear ε-PCL with the H_2O group instead of BnOH (Figure 3-5). For the polyester initiated by PP, macrocycle species were more abundant (Figure 3-7). And finally, with cholesterol, the main species in the product was the macrocycles (Figure 3-8). In term of control, the PP gave the most controlled chains among the two other initiators (*Đ* = 1.64)

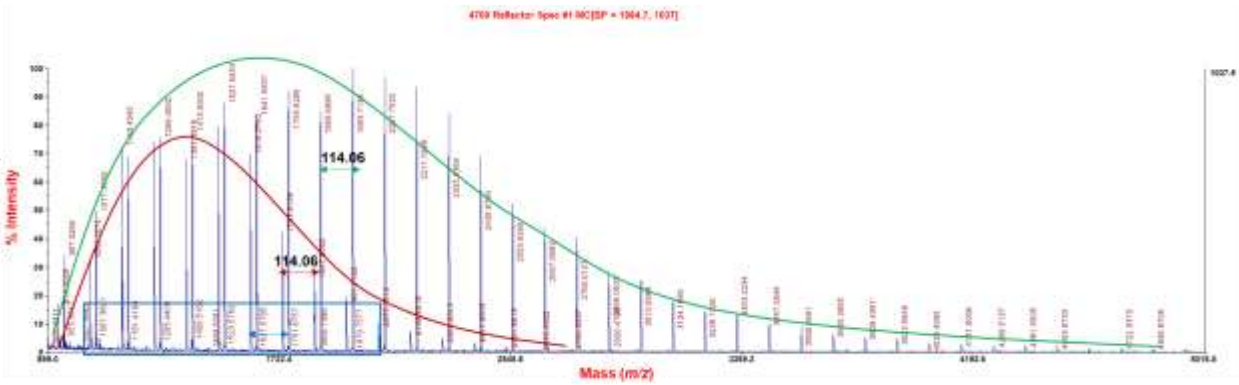

Figure 3-7 MALDI-TOF spectrum of poly-ε-caprolactone produced after 60 min of residence time via *O*-ROP initiated by PP in flow at 50 °C (Monomer/Initiator/Catalyst 100/1/1) (Table 3-1 Run 7). Green curve: chains initiated by the initiator (PP) M = ($M_{monomer}$ × number of repetition) + M_{PP} + M_{Na}^+, Red curve: Macrocycles M = ($M_{monomer}$ × number of repetition) + M_{Na}^+, Blue frame: water end chain M = ($M_{monomer}$ × number of repetition) + M_{water}+ M_{Na}^+. The difference between the peaks is the molecular mass of ε-caprolactone = 114.06.

© 2020 Tous droits réservés.

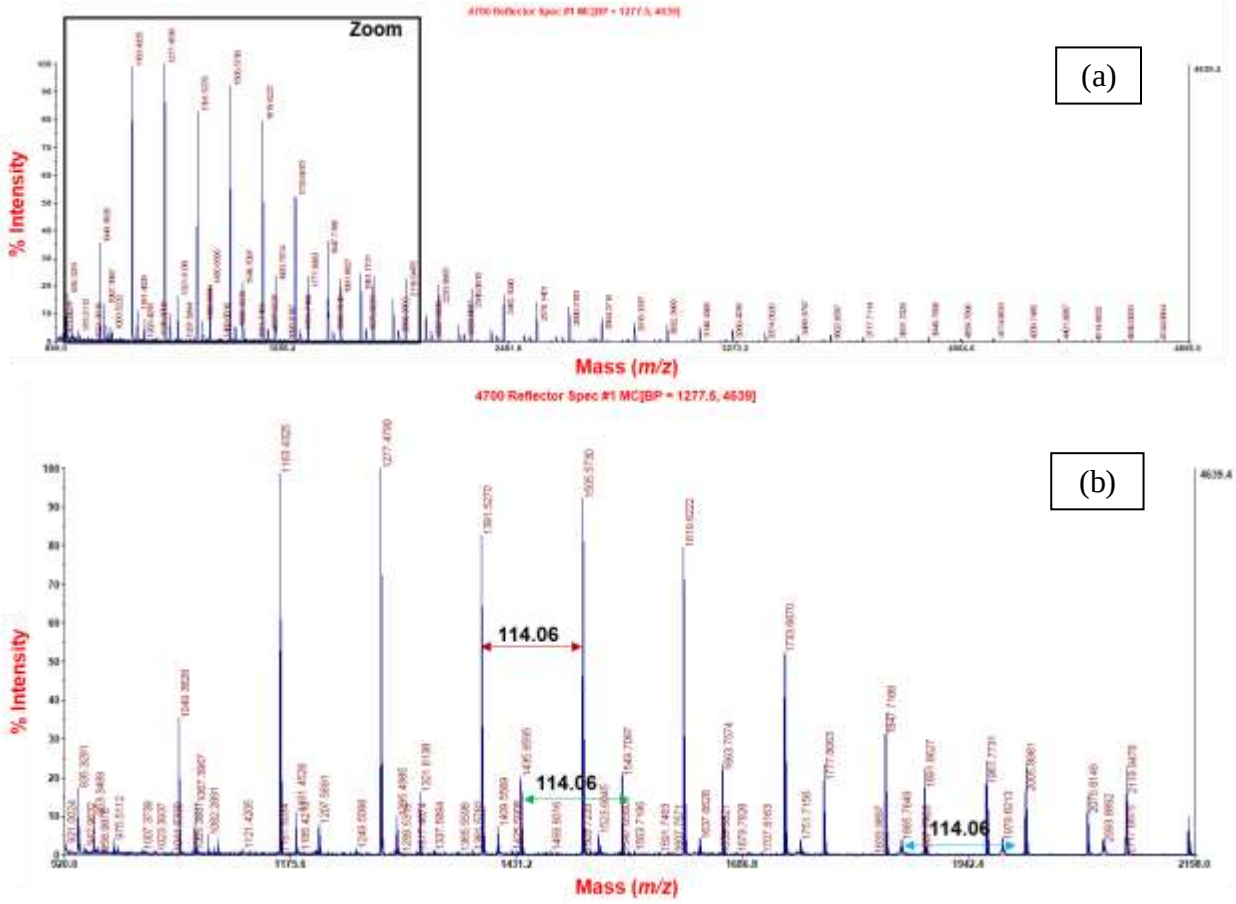

Figure 3-8 (a) MALDI-TOF spectrum of poly-ε-caprolactone produced after 60 min of residence time via *O*-ROP initiated by cholesterol in flow at 50 °C (Monomer/Initiator/Catalyst 100/1/1) (Table 3-1 Run 12). (b) a zoom of the black framed part, Green arrow: chains initiated by the initiator (Cholesterol) M = ($M_{monomer}$ × number of repetition) + $M_{phenylpropanol}$ + M_H^+, Red arrow: Macrocycles M = ($M_{monomer}$ × number of repetition) + M_{Na}^+, Blue arrow: water end chain M = ($M_{monomer}$ × number of repetition) + M_{water}+ M_{Na}^+. The difference between the peaks is the molecular mass of ε-caprolactone = 114.06.

We widened the study of the ε-CL *O*-ROP catalyzed by *t*-BuP_4 and initiated by PP. We were interested to change the amount of this latter from 1, 2 to 4 equivalents to reveal its effect on resulting polyesters within 60 min at 50 °C. For these three attempts, the conversion exceeded 90% (Table 3-1, Runs 7, 8 and 9). In term of control, the highest *Đ* was recorded when using two equivalents of PP (*Đ* = 1.71) and the corresponding MALDI-TOF-MS spectrum showed the abundance of macrocycle species (Figure 3-9), and the lowest *Đ* was obtained with four equivalents of PP (*Đ* = 1.5) for which MALDI-TOF-MS spectrum clarified that polyesters with PP extremity are the major species among the others that we detect frequently (macrocycles and chains with H_2O extremity) (Figure 3-10).

© 2020 Tous droits réservés.

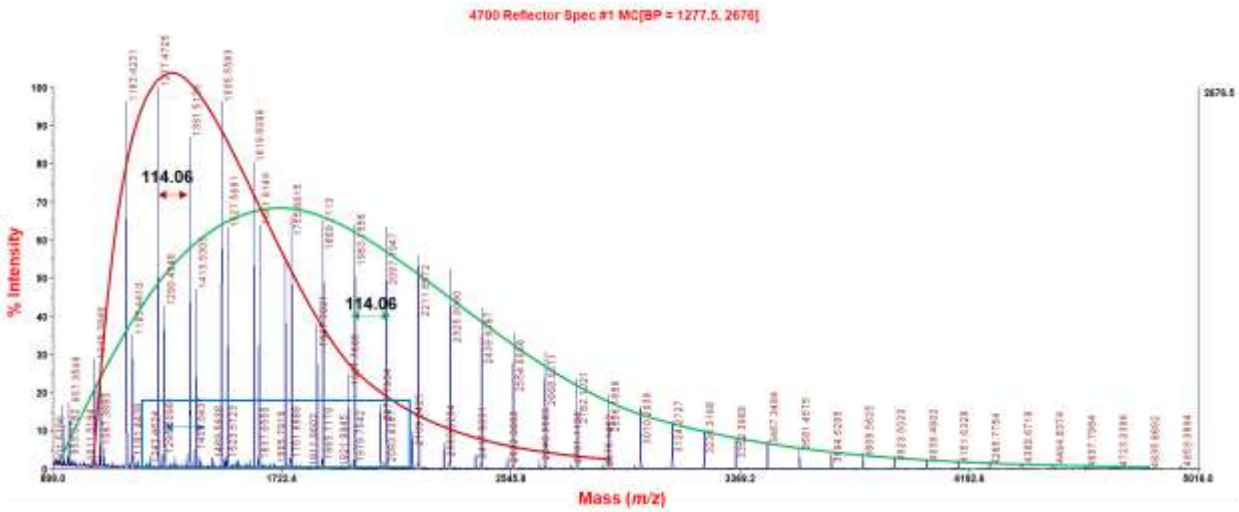

Figure 3-9 MALDI-TOF spectrum of poly-ε-caprolactone produced after 60 min of residence time via *O*-ROP initiated by PP in flow at 50 °C (Monomer/Initiator/Catalyst 100/2/1) (Table 3-1 Run 8). Green curve: chains initiated by the initiator (PP) M = ($M_{monomer}$ × number of repetition) + M_{PP} + M_{Na}^+, Red curve: Macrocycles M = ($M_{monomer}$ × number of repetition) + M_{Na}^+, Blue frame: water end chain M = ($M_{monomer}$ × number of repetition) + M_{water}+ M_{Na}^+. The difference between the peaks is the molecular mass of ε-caprolactone = 114.06.

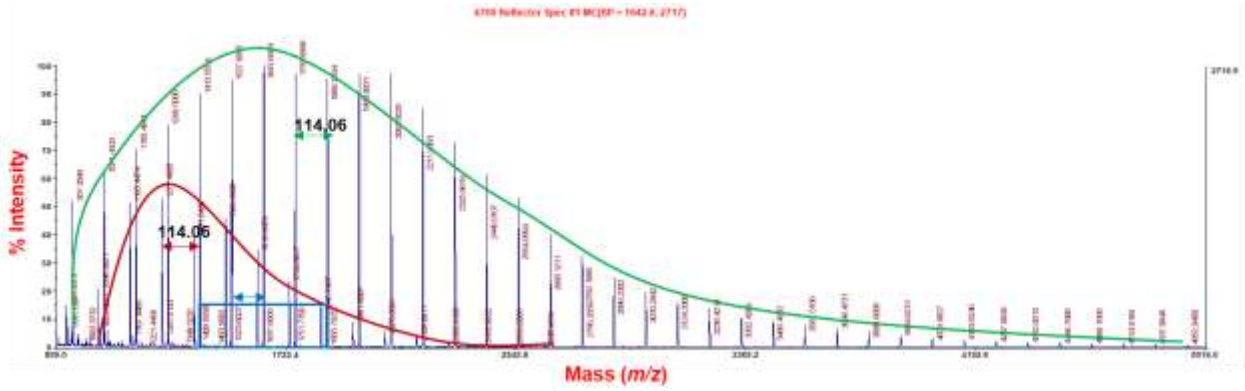

Figure 3-10 MALDI-TOF spectrum of poly-ε-caprolactone produced after 60 min of residence time via *O*-ROP initiated by PP in flow at 50 °C (Monomer/Initiator/Catalyst 100/4/1) (Table 3-1 Run 9). Green curve: chains initiated by the initiator (PP) M = ($M_{monomer}$ × number of repetition) + M_{PP} + M_{Na}^+, Red curve: Macrocycles M = ($M_{monomer}$ × number of repetition) + M_{Na}^+, Blue frame: water end chain M = ($M_{monomer}$ × number of repetition) + M_{water}+ M_{Na}^+. The difference between the peaks is the molecular mass of ε-caprolactone = 114.06.

Furthermore, we did again the same study but at room temperature (23 °C). As results for using one and two equivalents of PP, we obtained conversions exceeding 90% but with broad polyesters ($Đ$ > 2) (Table 3-1, Runs 10 and 11). This can be explained by the corresponding MALDI-TOF-MS spectra that showed the dominance of macrocycles in the produced polyesters (Figure 3-11and Figure 3-12).

© 2020 Tous droits réservés.

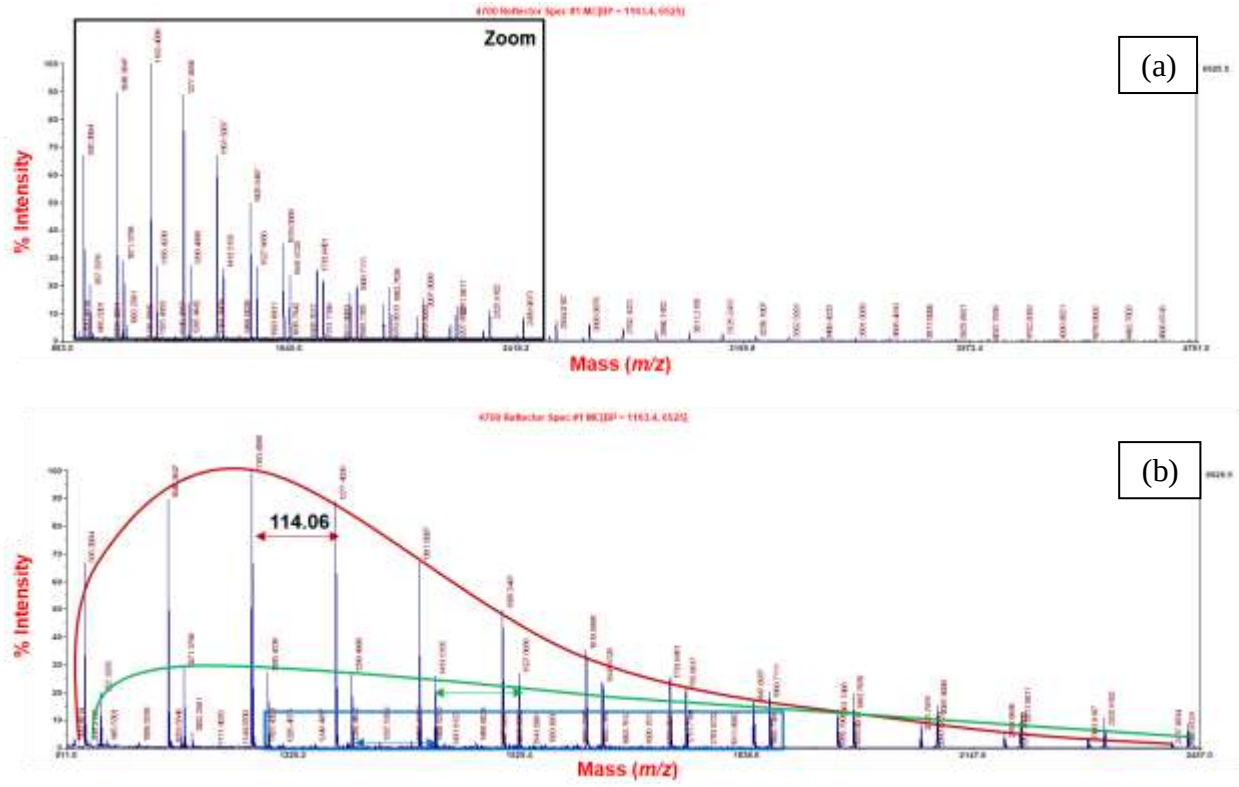

Figure 3-11 (a) MALDI-TOF spectrum of poly-ε-caprolactone produced after 60 min of residence time via *O*-ROP initiated by PP in flow at 23 °C (Monomer/Initiator/Catalyst 100/1/1) (Table 3-1 Run 10). (b) a zoom of the black framed part Green curve: chains initiated by the initiator (PP) M = ($M_{monomer}$ × number of repetition) + M_{PP} + M_{Na}^+, Red curve: Macrocycles M = ($M_{monomer}$ × number of repetition) + M_{Na}^+, Blue frame: water end chain M = ($M_{monomer}$ × number of repetition) + M_{water}+ M_{Na}^+. The difference between the peaks is the molecular mass of ε-caprolactone = 114.06.

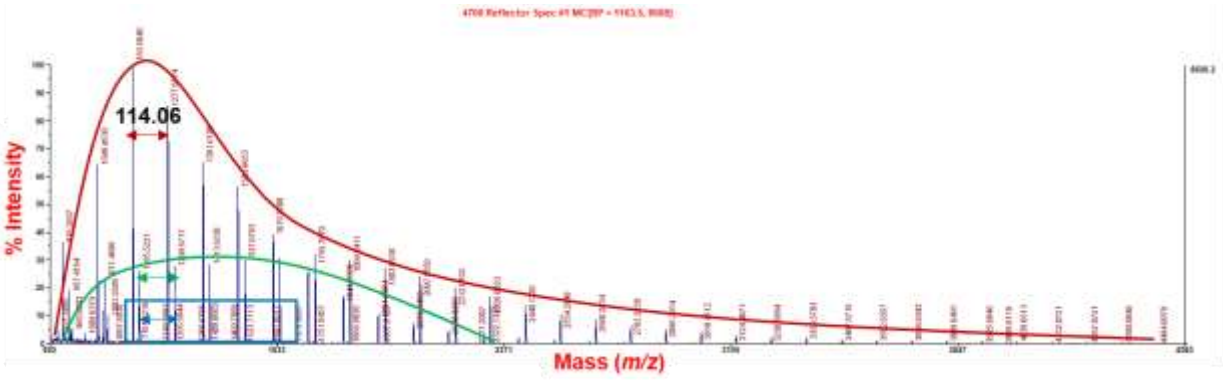

Figure 3-12 MALDI-TOF spectrum of poly-ε-caprolactone produced after 60 min of residence time via *O*-ROP initiated by PP in flow at 23 °C (Monomer/Initiator/Catalyst 100/2/1) (Table 3-1 Run 11). Green curve: chains initiated by the initiator (PP) M = ($M_{monomer}$ × number of repetition) + M_{PP} + M_{Na}^+, Red curve: Macrocycles M = ($M_{monomer}$ × number of repetition) + M_{Na}^+, Blue frame: water end chain M = ($M_{monomer}$ × number of repetition) + M_{water}+ M_{Na}^+. The difference between the peaks is the molecular mass of ε-caprolactone = 114.06.

By comparing runs 1 and 13, which are two reactions carried out under the same conditions but with different phosphazene bases, we can detect that the strongest base gave the excellent yield with $Đ$=1.59 (run 1) and the less basic one (*t*-BuP_2) gave a well-controlled

© 2020 Tous droits réservés.

polymerization with $Đ$ = 1.08 but with low conversion (41%) (run 13). So, the high basicity of the catalyst contributes to an increase of monomers conversion but a control loss and vice versa.

Finally, no conversions were recorded when using P_1-*t*-Bu-tris(tetramethylene) (BTPP) as a catalyst (Table 10, Runs 11, 12 and 13), which is the weakest phosphazene base, so we suppose that its basicity wasn't sufficient to initiate the ROP. Note that in the case of *O*-ROP initiated by benzyl alcohol and cholesterol, we can't calculate the molecular weight by ^{1}H NMR due to the fact that the initiator proton peaks were not clear.

3.5.2. Organo ring opening polymerization of ε-VL catalyzed by phosphazene superbases in flow system.

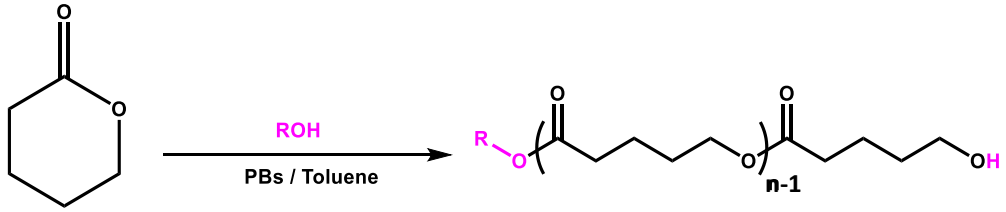

Figure 3-13 phosphazene superbases catalyzed rimg opening polymerization of δ-valerolactone.

Table 3-2 Organo ring opening polymerization of δ-valerolactone in microflow system with double entries using phosphazene superbases as a catalysts in toluene. M/I/cat: Monomer/Initiotor/Catalyst.

Run	M/I/Cat	Eq	Residence time (min)	T (°C)	Conv[a]	M_n[b] (theo)	M_n[a] (NMR)	M_n[c] (GPC)	$Đ$[c]
1	δ-VL/PP/ *t*-BuP_4	40/1/1	60	23	83	4140	2140	5503	1.58
2	δ-VL/PP/ *t*-BuP_4	40/1/1	120	23	93	4140	2140	6053	1.55
3	δ-VL/PP/ *t*-BuP_4	40/1/0.5	120	23	49	4140	2390	5400	1.42
4	δ-VL/PP/ *t*-BuP_4	40/1/1	60	50	86	3580	2640	4399	1.31
5	δ-VL/PP/ BTPP	40/1/1	120	23	0	-----	-----	-----	-----

[a] Determined by ^{1}H NMR
[b] Calculated from (([M]/[I])×Conv) × M(monomer))+M_W(initiator).
[c] Determined by GPC

© 2020 Tous droits réservés.
lilliad.univ-lille.fr

In this section, we worked on the *O*-ROP of δ-valerolactone (Figure 3-13), for which we used *t*-BuP_4 as a catalyst. 83% of conversion was obtained within 60 min of residence time at RT (23 °C) and using 40/1/1 equivalents respectively for the monomer, the initiator (PP) and the catalyst (Table 3-2, Run 1). After increasing the residence time to 120 min, the conversion increased as well to 93% (Table 3-2, Run 2). In addition, a decrease of the conversion to 49% was recorded after decreasing the catalyst amount to the half (Table 3-2, Run 3), so we lost almost the half of the conversion compared to Run 2. In addition, *Đ* values of these three polyesters are ranged between 1.42 and 1.58. MALDI-TOF-MS spectra revealed the presence of linear and non-linear species in the polyester products. Besides the linear δ-PVL initiated by PP showed the presence of macrocycles formed by the intramolecular transesterification reaction and δ-PVL with H_2O extremity (Figure 3-14, Figure 3-15 and Figure 3-16). By increasing the temperature to 60 °C (Table 3-2, Run 4), the *Đ* decreased to 1.31 but always the important presence of macrocycles is detected (Figure 3-17). Finally, no conversions were recorded when using P_1-*t*-Bu-tris(tetramethylene) (BTPP) as a catalyst (Table 3-2, Run 4).

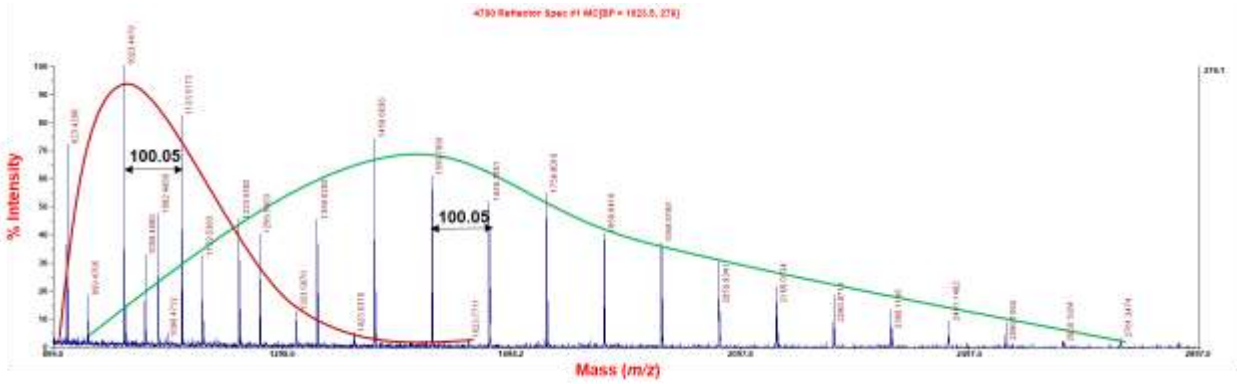

Figure 3-14 MALDI-TOF spectrum of poly-δ-valerolactone produced after 60 min of residence time via *O*-ROP initiated by PP in flow at 23 °C (Table 3-1 Run 1). Green curve: chains initiated by the initiator (phenylpropanol) M = ($M_{monomer}$ × number of repetition) + M_{PP} + M_{Na}^+, Red curve: Macrocycles M = ($M_{monomer}$ × number of repetition) + M_{Na}^+, Blue curve: water end chain M = ($M_{monomer}$ × number of repetition) + M_{water}+ M_{Na}^+. The difference between the peaks is the molecular mass of δ-valerolactone = 100.05.

© 2020 Tous droits réservés.

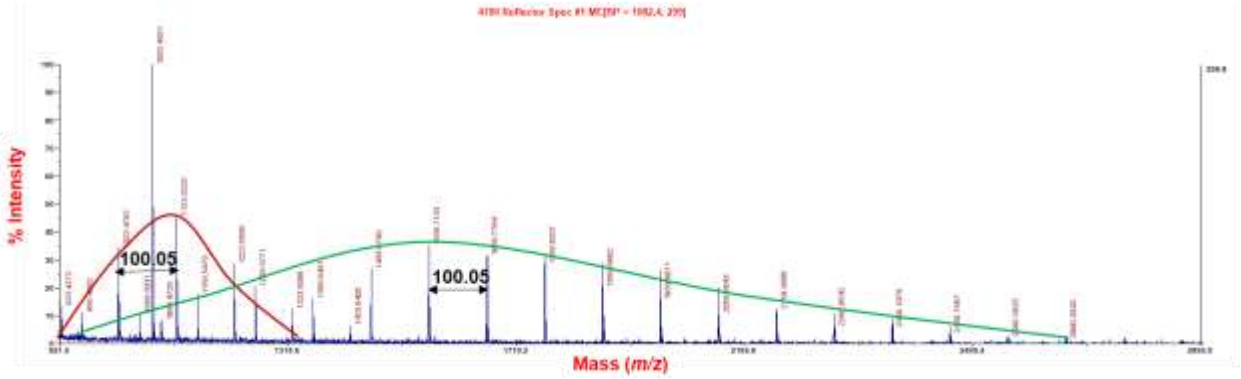

Figure 3-15 MALDI-TOF spectrum of poly-δ-valerolactone produced after 120 min of residence time via *O*-ROP initiated by PP in flow at 23 °C Table 3-2 Run 2). Green curve: chains initiated by the initiator (phenylpropanol) M = ($M_{monomer}$ × number of repetition) + M_{PP} + M_{Na}^+, Red curve: Macrocycles M = ($M_{monomer}$ × number of repetition) + M_{Na}^+, Blue curve: water end chain M = ($M_{monomer}$ × number of repetition) + M_{water}+ M_{Na}^+. The difference between the peaks is the molecular mass of δ-valerolactone = 100.05.

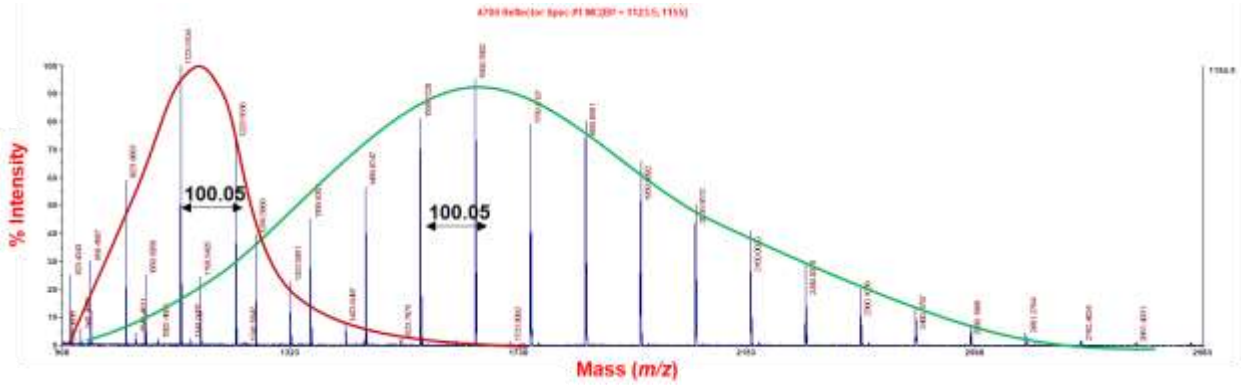

Figure 3-16 MALDI-TOF spectrum of poly-δ-valerolactone produced after 120 min of residence time via *O*-ROP initiated by PP in flow at 23 °C (Table 3-2 Run 3). Green curve: chains initiated by the initiator (phenylpropanol) M = ($M_{monomer}$ × number of repetition) + M_{PP} + M_{Na}^+, Red curve: Macrocycles M = ($M_{monomer}$ × number of repetition) + M_{Na}^+, Blue curve: water end chain M = ($M_{monomer}$ × number of repetition) + M_{water}+ M_{Na}^+. The difference between the peaks is the molecular mass of δ-valerolactone = 100.05.

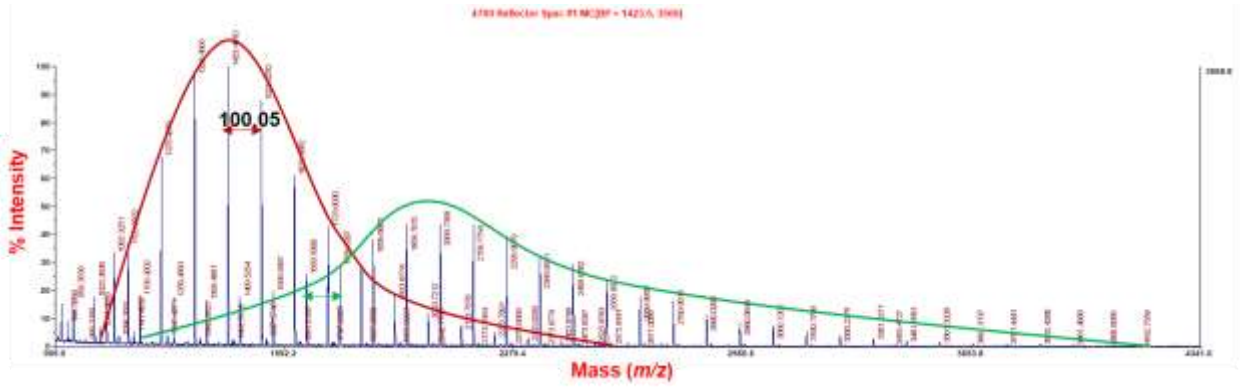

Figure 3-17 MALDI-TOF spectrum of poly-δ-valerolactone produced after 60 min of residence time via *O*-ROP initiated by PP in flow at 50 °C (Table 3-2 Run 4). Green curve: chains initiated by the initiator (phenylpropanol) M = ($M_{monomer}$ × number of repetition) + M_{PP} + M_{Na}^+, Red curve: Macrocycles M = ($M_{monomer}$ × number of repetition) + M_{Na}^+, Blue curve: water end chain M = ($M_{monomer}$ × number of repetition) + M_{water}+ M_{Na}^+. The difference between the peaks is the molecular mass of δ-valerolactone = 100.05.

© 2020 Tous droits réservés.

3.5.3. Organo ring opening polymerization of ε-CL and δ-VL catalyzed by *t*-BuP_4 in the absence of initiator

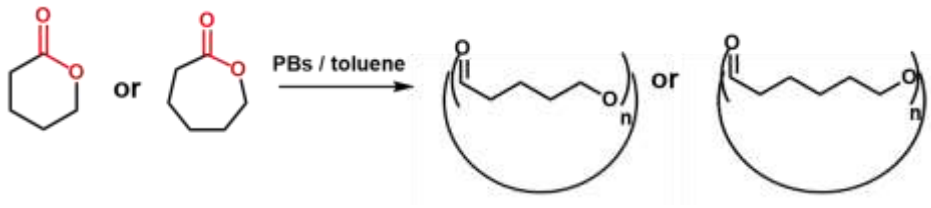

Figure 3-18 *O*-ROP of ε-CL and δ-VL in flow in the absence of initiator at room temperature

The *O*-ROP of ε-CL in the absence of initiator (Figure 3-22) contributes instantly to the formation of gel (Figure 3-19) directly when the catalyst was added to the solvent and monomer's mixture, which indicates a sharp decrease of polymer mass proved by GPC (Table 3-3, run 1) . This gel might be the product formed by the interaction of the monomer and the catalyst which yielded only macrocycles as the MALDI-TOF-MS spectrum shows (Figure 3-20). With δ-VL, no gel was obtained, but instantly the reaction medium became very viscous after the addition of the catalyst, and yielded -like with ε-CL- only macrocycles (MALDI-TOF-MS spectrum, Figure 3-21). High M_n values and broad polymers distributions ($Đ$ > 2) were recorded by GPC analysis. Note that ε-CL gave polyesters of higher $Đ$ value (3.15 vs 2.12), which can be related to its higher reactivity compared to δ-VL

Table 3-3 Organo ring opening polymerization of ε-CL and δ-VL in flow catalyzed by *t*-BuP_4 in the absence of initiator at room temperature. M/I/cat: Monomer/Initiotor/Catalyst in toluene

Run	M/I/Cat	Eq	Residence time (min)	T (°C)	Conv[a]	M_n[b] (GPC)	$Đ$[b]
1	ε-CL/ *t*-BuP_4	100/1	instantly	RT	95%	16843	3.15
2	δ-VL/ *t*-BuP_4	40/1	instantly	RT	89%	7539	2.12

[a] Determined by ^{1}H NMR
[b] Determined by GPC

© 2020 Tous droits réservés.

Figure 3-19 PCL obtained instantly after the addition of the monomer to the reaction media in presence of the catalyst *t*-BuP_4 **and the absence of initiator**

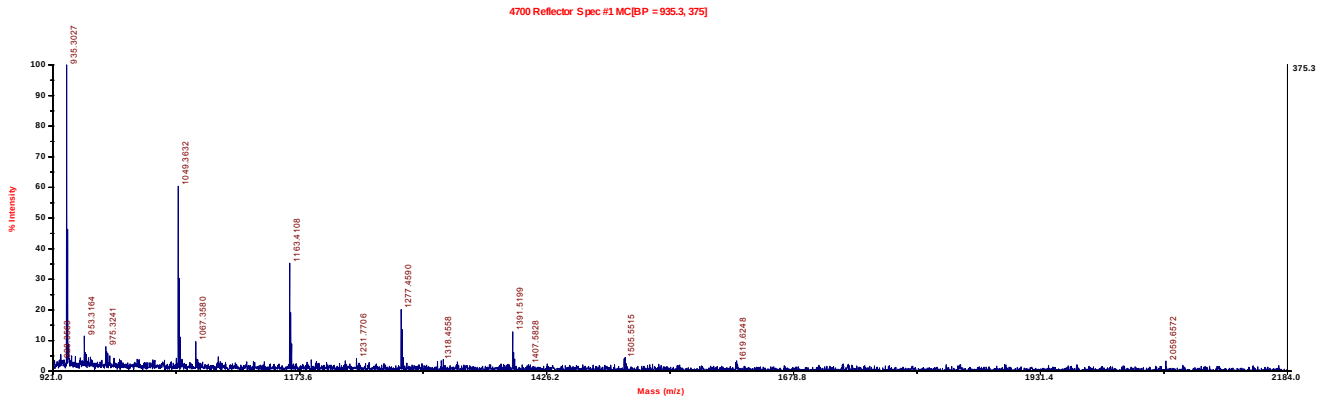

Figure 3-20 MALDI-TOF spectrum of PCL obtained by *O*-ROP instantly in the absence of initiator. The mass of each peak = number of motif × M_{CL} + M_{Na}±0.1 = number of motif × 114.06 + 22.9±0.1. The difference between the peaks is the molecular mass of ε-caprolactone = 114.06.

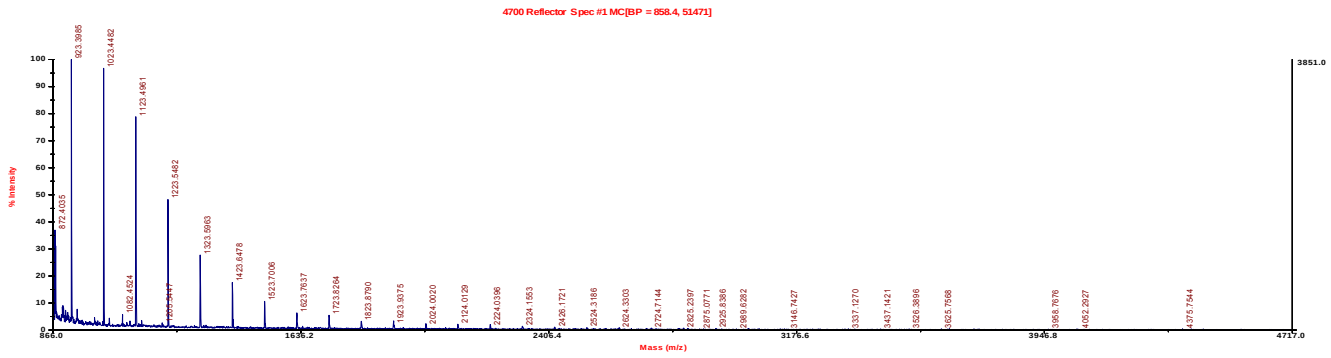

Figure 3-21 MALDI-TOF spectrum of PVL obtained by *O*-ROP instantly in the absence of initiator. The mass of each peak = number of motif × M_{VL} +M_{Na}±0.1 = numberis of motif × 100.052 + 22.9±0.1. The difference between the peaks is the molecular mass of δ-valerolactone = 100.05.

3.5.4. Organo ring opening polymerization of γ-BL and γ-VL catalyzed by phosphazene superbases in flow system.

γ-valerolactone and γ-butyrolactone are two five membered cyclic esters and are so difficult to be polymerized. We tried to polymerize these two monomers using *t*-BuP_4 and *t*-BuP_2 as

© 2020 Tous droits réservés.

catalysts under different residence times and reaction systems: in flow (one and double entries) and batch systems (Figure 3-22). But till now we didn't succeed to have any conversion (Table 3-4).

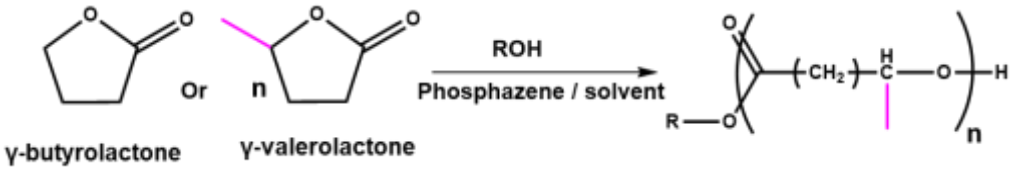

Figure 3-22 Organo ring opening polymerization of γ-valerolactone and γ-butyrolactone

Table 3-4 Organo ring opening polymerization of γ-valerolactone and γ-butyrolactone in microflow system with double entries using phosphazene superbases as catalysts. M/I/cat: Monomer/Initiotor/Catalyst in THF

Run	M/I/Cat	Eq	Residence time (min)	T (°C)	Conv[d]
1[a, b]	γ-VL/BnOH/ *t*-BuP$_2$	100/1/1	60	-40	0
2[b]	γ-VL/BnOH/ *t*-BuP$_2$	100/1/1	390	-40	0
3	γ-VL/BnOH/ *t*-BuP$_2$	100/1/1	390	-40	0
5	γ-VL/Prop/ *t*-BuP$_2$	100/1.5/1	240	-40	0
6	γ-VL/PP/ *t*-BuP$_4$	40/1/1	120	23	0
7	γ-BL/PP/ *t*-BuP$_4$	40/1/1	360	-40	0
8	γ-BL/BnOH/ *t*-BuP$_4$	100/1/1	120	-40	0
4[c]	γ-BL/BnOH/ *t*-BuP$_4$	100/1/1	300	-40	0

[a] Toluene was used as solvent instead of THF
[b] Microreactor used with one entrance
[c] Reaction carried out in batch system
[d] Determined by ^{1}H NMR

Concerning the underlying mechanism (Figure 3-23), it's already cited in the literature. First, the base catalyst reacts with the initiator to give an alkoxide. The latter will make a nucleophilic attack to the carbonyl group followed by the ring opening of the cycle ester. Then, the addition of the rest of monomers will continue on the polymer chain in progress,

© 2020 Tous droits réservés.

which presents an alkoxide group. Finally, the reaction will be quenched by a benzoic acid solution in chloroform.

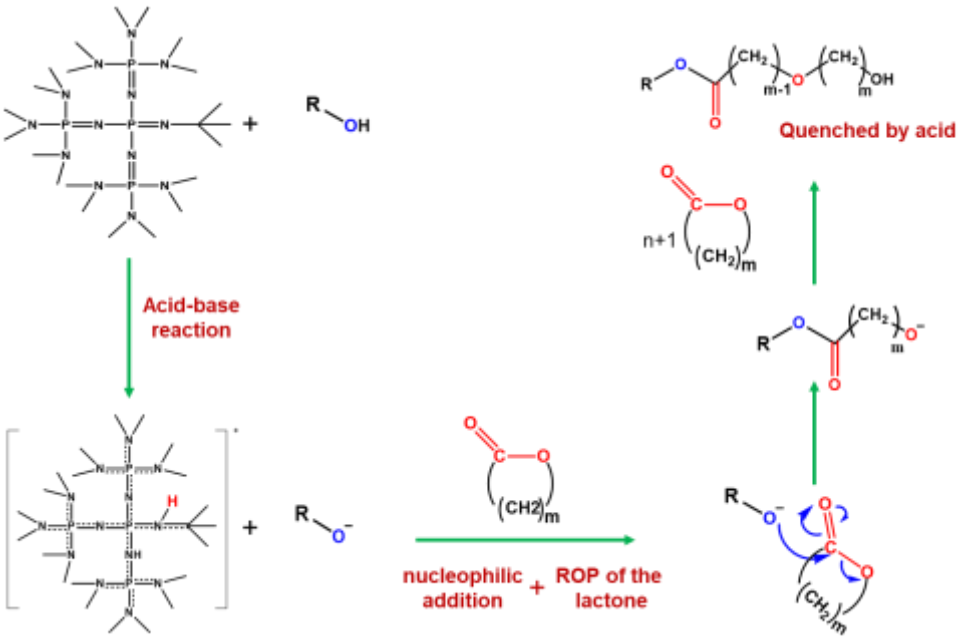

Figure 3-23 Mechanism of organo ring opening polymerisation

Conclusions

We successfully polymerized ε-CL by *O*-ROP in microflow system. First with using *t*-OctP_4 as a catalyst, a conversion of 100% and $Đ$ = 1.59 were obtained within 30 min of residence time at 5 °C. Second, with *t*-BuP_4, a conversion of 92% was obtained within 60 min of residence time at 50 °C and gave a polyester with $Đ$ = 1.64. With *t*-BuP_2 lower conversion was recorded (45%) but more controlled polymers were obtained with $Đ$ =1.08. So, the decrease of the catalyst basicity contributes to a loss in conversion but with a better control. Finally, no conversions were observed using P_1-*t*-Bu-tris(tetramethylene) (BTPP) as a catalyst. Primary alcohols were more efficient for the initiation of the *O*-ROP of ε-CL like in the *e*-ROP discussed in 1. In addition, we successfully polymerized δ-VL (93%, $Đ$ = 1.55) using *t*-BuP_4 as a catalyst within 120 min of residence time at 23 °C. Finally, we didn't succeed to polymerize γ-VL and γ-BL even with applying different reaction conditions, so that various attempts were carried out at room temperature or -40 °C within residence time in range of [1-6.5] hours. In perspective, we are interested to continue the study of ROP of CL

© 2020 Tous droits réservés.

using *t*-BuP_2 as a catalyst which allowed the obtainment of the beast control, and try to find the optimum conditions permitting to increase the conversion.

© 2020 Tous droits réservés.

4. CHAPTER FOUR: SYNTHESIS OF POLYESTERS BY POLYCONDENSATION IN BATCH

Polycondensation reactions have been widely investigated, by means of which a wide range of polymers were produced like: polyesters (PEs), polyamides (PAs), polyurethanes, polyureas, polysiloxanes, poly-sulfides and polyethers. These polymers promote the sustainability of a relevant production due to their biodegradability and/or their biobased sources.[341] In the following, we will develop the evolution of polycondensation reactions: feed stocks, catalysts, etc.[342]

4.1. Synthesis of aliphatic polyesters through polycondensation

Typically, polyesters are synthesized by the condensation of the AB type monomers like hydroxyl acid, or from those of AA and BB difunctional monomers type.[343,344] The polycondensation reactions of difunctional monomers cover the esterification of diacid and diols, diacid chlorides and diols, or the ester exchange reaction of diesters and diols (Figure 4-1). The use of monomers with functionalities more than two give access to a network polyester.[342]

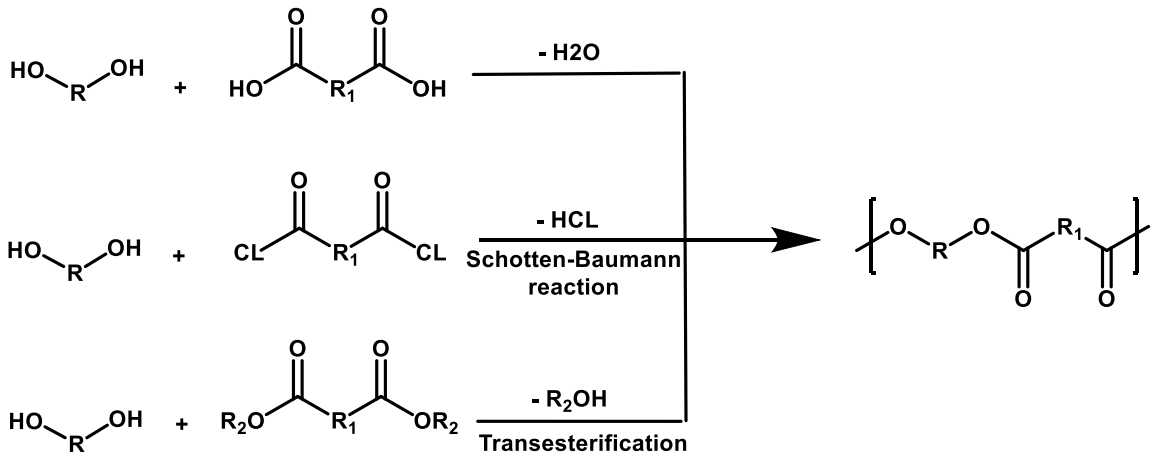

Figure 4-1 Preparation of polyesters by stepwise polycondensation.[342]

© 2020 Tous droits réservés.

Carothers was the first researcher who studied polycondensation reaction to produce polyester and polyanhydride in 1930.[55,343,344] His work engendered the Carothers equation relating the degree of polymerization to the extent of reaction (conversion) (Equation 4-1).

$$\overline{X}_n = \frac{1}{(1-p)}$$

Equation 4-1 Carothers equation, where ($\overline{X}_n$) is the degree of polymerization and (p) is the conversion

Basically, it's difficult to produce polymers with high molecular weight through polycondensation, since very high conversions (>98-99%) are required. In order to reach these conversion values, an exact stoichiometric balance of monomers must be respected and applied. This is readily established for AB monomers type but it is still complicated for AA and BB monomers (like diacids and diols), where a little practical error in reagents quantity can affect the conversion. In this case, the Carothers equation becomes (Equation 4-2):

$$\overline{X}_n = \frac{1+r}{(1+r-2rp)}$$

Equation 4-2

In Equation 4-2, "r" is the stoichiometric ratio of reactants; conventionally, the excess reactant is the denominator so that r < 1. If neither monomer is in excess, then r = 1 and the equation returns to its initial form (Equation 4-1).

And as it is well known, an equilibrium characterizes the formation of ester molecule, and a production of by-product accompanies the synthesis of desired polymer, like water, that should be extracted from the reaction media in order to drive the reaction toward a higher conversion. In order to facilitate high conversion, long reaction times at high temperatures are required too.

When using multi-functional monomers (up to two functions), more complicated topologies of polyesters can be produced like: hyperbranched, dendritic, star, and network polyesters that are widely used in so many areas, among which we cite: pharmaceuticals, cosmetics, lubricants and adhesives.[342,345,346]

Biodegradable aliphatic polyesters are produced from the polycondensation of simple diols and diacids like ethylene glycol or 1,4-butanediol (BDO), and succinic acid, or adipic acid (AAc) or similar monomers.[347–351]

© 2020 Tous droits réservés.

The classic polymerization methods to produce aliphatic polyesters require metal based catalysts and hard reaction temperature above 150 °C. The most catalysts used are: ZnAc, Sb_2O_3, $Ti(OBu)_4$, $Ti(OiPr)_4$, $Ti(OEt)_4$, $Zr(OBu)_4$, $Bi(OTf)_3$ and $Nb(OEt)_5$.[352–356] For example, a series of PE has been prepared in bulk with three reaction stages. The first occurred at 180 °C for 3 h catalyzed by 0.05 mol% $Ti(OBu)_4$ under atmospheric pressure. In the second stage a gradual increase of temperature to 210 °C is applied with a reduction of pressure to 0.02 mmHg.[357] finally, polycondensation was carried out for additional 4 h at 210 °C under 0.2-0.02 mmHg. Also in the work of Jovanovic *et al.*, they used $Ti(OBu)_4$ as a catalyst to produce PE through bulk polymerization for 6 h at 220 °C.[358] And this catalyst was an important investigated one .[359–362] Furthermore, the efficiency of other organometal- (Ti, Zr, Sn, Hf, and Bi) and metal oxide- (Ge and Sb) based catalysts has been studied and their efficiency was ordered as following: Ti >> Zr ~ Sn > Hf > Sb > Bi.[363] In addition, p-toluenesulfonic acid, $SnCl_4$ and zinc acetylacetonate were used as catalysts to produce HO-terminated polyesters through polycondensation between succinic acid and excess of BDO.[364]

Furthermore, enzymatic polyesterification has been extensively investigated.[58] And actually, enzymes gain a high interest aiming to catalyze the polyesterification of diacid monomers.[365]

4.2. Organo catalysts promote esterification reactions

The esterification (transesterification) is the direct condensation of carboxylic acids (diesters) with alcohols in the presence of small amounts of catalyst. In general, acid-catalyzed dehydration reaction of carboxylic acids and alcohols is the way to produce esters molecules in the presence of dehydrating reagents.[366] Traditional acidic acid like H_2SO_4 and HCl…etc were adopted to catalyze the esterification reaction in the presence of a dehydrating reagent to push forward the reaction to higher conversions. However, these catalysts are greatly contaminative and corrosive, which result in low selectivity, high energy demand and critical environmental pollution.[367–370] Moreover, the following treatment steps including the separation of the dehydrating reagent and catalyst from the product require significant time and energy. Therefore, “green” approaches for esters syntheses have gained much of interest. Regardless the achievements that have been exploited in the past decade, the development of environmentally helpful and cost-effective methods is still a powerful demand.[366,371–376]

Free-metal organocatalysts are good alternatives in organic synthesis, due to non-toxicity, high efficiency and eco-friendly features that they exhibit.[377,378] Chemists started to use

© 2020 Tous droits réservés.

organo-catalysts aiming to promote esterification such as diphenylammonium triflate (DPAT Figure 4-2), pentafluorophenylammonium triflate (PFPAT Figure 4-3) and 2,2,6,6-tetramethylpiperidinium triflate (TMPT) (Figure 4-4).[14,15,379] These catalysts offer many advantages like the self-separation feature from the reaction mixture, mild reaction conditions and the allowed use of equimolar reagents amount. And due to the catalyst structure containing hydrophobic parts, the reaction can progress without needing to remove the hydrophilic by-product produced, which makes the reaction system less complicated. Even more, an important advantage to mention is the easy way to synthesize these catalysts *in vitro* with no long reaction time and very high yield (up to 90%).

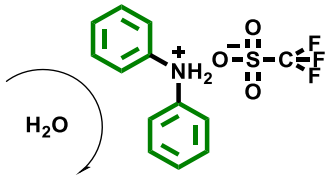

Figure 4-2 Diphenylammonium triflate (DPAT)

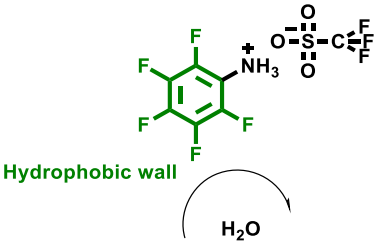

Figure 4-3 Pentafluorophenylammonium triflate (PFPAT)

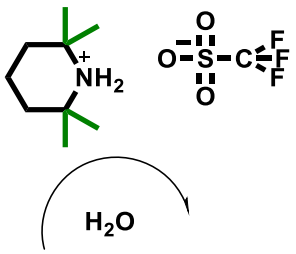

Figure 4-4 Tetramethylpiperidinium triflate (TMPT)

In 2000, Tanabe *et al* introduced the synthesis of esters series catalyzed by DPAT (Scheme 4-1). DPAT was synthesized *in vitro* by a simple reaction between trifluoromethanesulfonic acid (CF_3SO_3H) and diphenylamine (Ph_2NH) in toluene at 20-25°C for 15 min and yielded 97% of the product. They developed the esterification of equimolar amounts of acids and alcohols in the presence of 1-10% of DPAT at 80 °C for different

© 2020 Tous droits réservés.

reaction times according to the used reagents. In addition, for the transesterification reaction, an additional quantity of catalyst was required to range between 10-20%.[14] However, DPAT is relatively a strong acid salt which affects the selectivity towards acid-sensitive alcohols.[380]

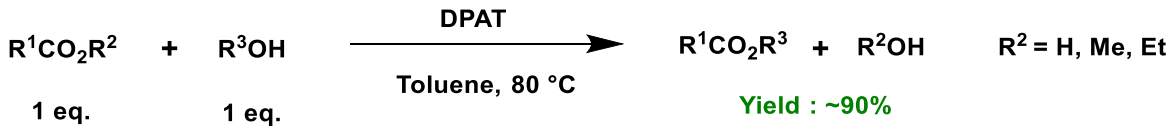

Scheme 4-1 Esterification or transesterification catalyzed by DPAT (adapted)[14]

Ishihara and Sakakura's group developed more efficient catalysts than DPAT which are bulky diarylammonium arenesulfonates that present remarkable catalytic esterification activity due to their hydrophobic effect related to the bulky ammonium triflates.[380,381] And based on these results, Tanabe *et al* worked on the synthesis of pentafluorophenylammonium triflate ($C_6F_5N^+H_3.OTf^-$; PFPAT), and they proved its efficiency as a catalyst for esterification and transesterification reactions (Scheme 4-2).[15]

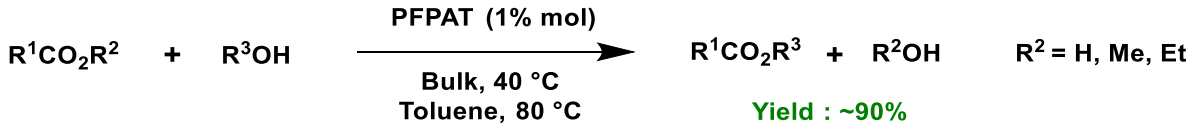

Scheme 4-2 Esterification or transesterification catalyzed by PFPAT (adapted)[15]

PFPAT is also simple to synthesize *in vitro* by the reaction between trifluoromethanesulfonic acid (CF_3SO_3H) and 2,3,4,5,6-pentafluoroaniline in toluene for 30 min at 0-5 °C and 95% of PFPAT was yielded. Beyond several ammonium triflates designed, PFPAT was the best one. Its catalytic efficiency was compared to those of four other metal-free catalysts which are: CSA (camphorsulfonic acid; $C_{10}H_{16}O_4S$), PTS (p-toluenesulfonic acid; $C_7H_8O_3S$) and DPAT. The standard reaction was carried out with a 1 : 1 mixture of Me_3CCO_2H and 1-octanol at 80 °C in toluene, without need to any dehydration technique. In this study, PFPAT has shown the best results in term of activity (> 95% of conversion) compared to other studied catalysts including DPAT. The outperformance of PFPAT is ascribed to the lower basicity of $C_6F_5NH_2$ amine group compared to Ph_2NH of DPAT. In addition, they assumed that the removal of water is not required, due to the functionality in the organic phase: even in the presence of small amount of water, pentafluorophenyl moiety creates a hydrophobic wall that helpfully repels water molecules produced as a by-product.[15]

© 2020 Tous droits réservés.

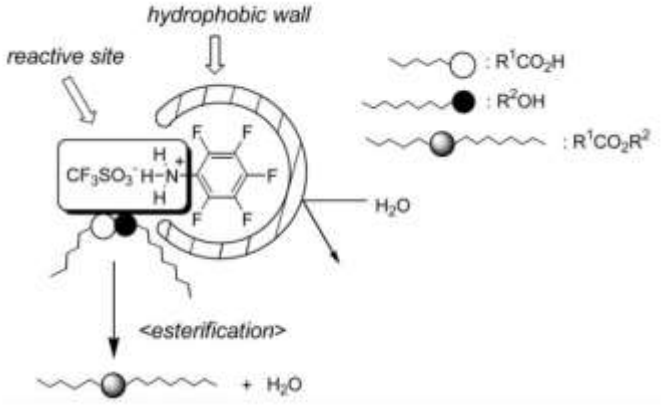

Figure 4-5 Schematic representation of esterification process[15]

Based on the contributions of Ishihara and Tanabe, Huang and co-workers developed a new free-metal catalyst for the esterification in 2016 which is the 2,2,6,6-Tetramethylpiperidinium triflate (TMPT) (Scheme 4-3).[379] This catalyst showed high selectivity and an impulsive self-separation process in esterification. Due to the bulky groups surrounding the active site, TMPT owns a hypothetical "hydrophobic wall" that could greatly prevent the approach of generated water to the reactive site and thus water will be unable to affect the catalyst activity (Scheme 4-4).

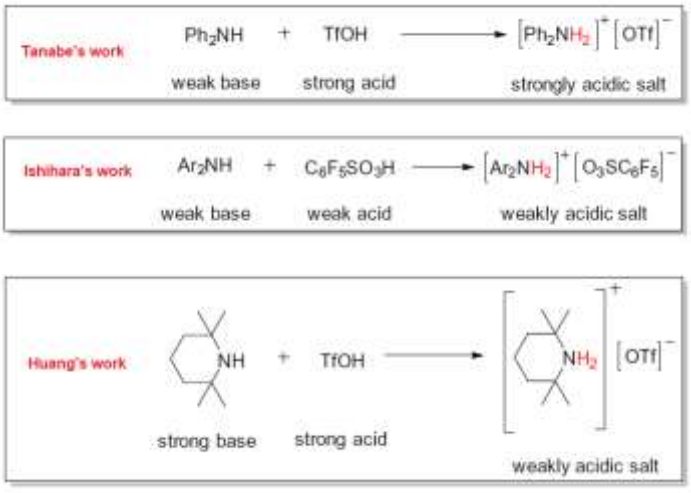

Scheme 4-3 Strategy to prepare a practical and selective catalyst based on Tanabe's method (adapted).[379]

© 2020 Tous droits réservés.

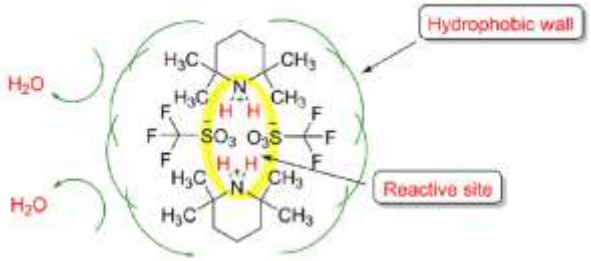

Scheme 4-4 Schematic diagram of the 'hydrophobic wall' (green) and reactive site (yellow) (adapted).[379]

The self-separating feature of TMPT from ester products is attributed to its excellent solubility in polar alcohols and the opposite feature towards apolar esters.

Actually, the investigation of this kind of catalysts covered the syntheses of small ester molecules, and to the best of our knowledge, just one group studied the use of DPAT as a catalyst for polycondensations of diacids and diols followed by a kinetic study that have been reported.[382,383] Otherwise, the investigation of these catalysts to produce polyesters at the polymer level didn't take place strongly.

And as we mentioned in the first part of our work, ROP reactions were studied to overcome the difficulties of polycondensation pathways. Here, a second way suggested to overcome these difficulties consists of the organocatalytic pathway use to promote polyesterification or polytransesterifcation reactions.

So as a second aim, organo-catalysts such as diphenylammonium triflate (DPAT) pentafluorophenylammonium triflate (PFPAT) and 2,2,6,6-tetramethylpiperidinium triflate (TMPT) will be used to promote polyesterification (polycondensation) between diols and diacids (or their diesters).

© 2020 Tous droits réservés.

4.3. Results and discussion

4.3.1. Polycondensation in Batch using Diphenylammonium triflate (DPAT) as a catalyst.

4.3.1.1. DPAT promotes Polyesterification between diacids and diols in Batch system

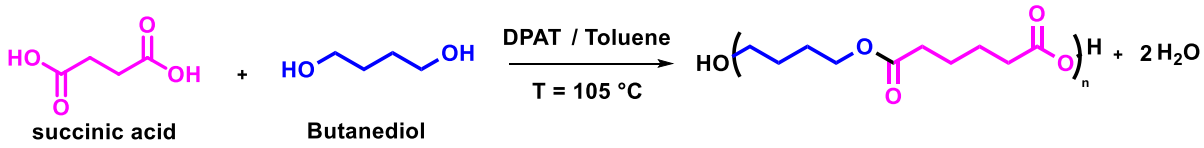

Figure 4-6 polyesterification between succinic acid and butanediol using PDAT as a catalyst at 105 °C.

Based on Carothers equation mentioned in section 4.1, we tried to find the ideal reagents composition in order to reach the high yield with PEs of high molecular weight. In batch system, we carried out the polyesterification between succinic acid and butanediol (BDO) (

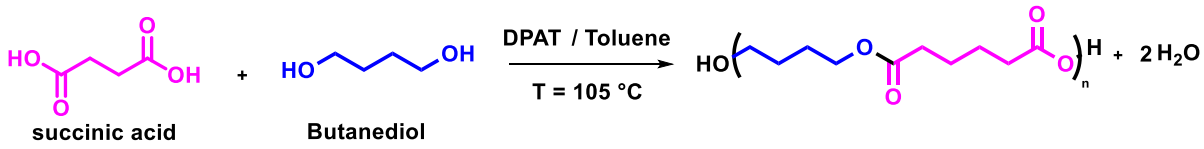

Figure 4-6 polyesterification between succinic acid and butanediol using PDAT as a catalyst at 105 °C.

) catalyzed by DPAT within 6 hours. The highest yield of 78% was obtained at 105 °C using 1/1/0.5 of equivalents respectively for the diacid, the diol and the catalyst. Almost the same results were obtained using the commercial catalyst and the one that we synthesized *in vitro* (Table 4-1, Runs 1 and 2). So equivalent amounts of diol and diacid was quite good to overpass the 50% of yield, which proves the good efficiency of DPAT to catalyze this polyesterification. When performing the reaction at 95 °C, the yield decreased to 61% (Table 4-1, Run 4). After changing the equivalent of diol to 1.05, the yield decreased to 54% at 105 °C (Table 4-1, Run 3), and to 51% at 95 °C (Table 4-1, Run 5).

© 2020 Tous droits réservés.

Table 4-1 Polyesterification between succinic acid and butanediol using DPAT as a catalyst in batch system at 105 °C.

Run	Diacid/Diol/cat	Equivalents	Reaction time (h)	Yield[c] (%)
1[a]	succ ac/BDO/DPAT	1/1/0.5	06	78
2	succ ac/ BDO /DPAT	1/1/0.5	06	76
3	succ ac/ BDO /DPAT	1/1.05/0.5	06	54
4[b]	succ ac/ BDO /DPAT	1/1/0.5	06	61
5[b]	succ ac/ BDO /DPAT	1/1.05/0.5	06	51

[a] Commercial DPAT was used
[b] T = 95 °C
[c] Gravimetric conversion = $m_{experimental}/m_{theoretical} \times 100$

4.3.1.2. DPAT promotes Polytransesterification between diesters and diols in Batch system

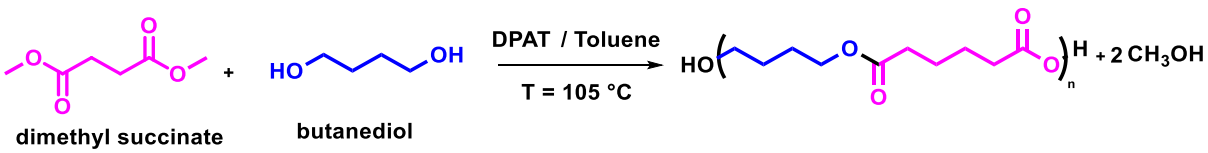

Figure 4-7 Polytransesterification between dimethyl succinate and butanediol using PDAT as a catalyst at 105 °C.

© 2020 Tous droits réservés.

Table 4-2 Polytransesterification between dimethyl succinate and butanediol using DPAT as a catalyst in batch system at 105 °C.

[a] Room temperature

Run	Diacid/Diol/cat	Equivalents	Reaction time (h)	Yield[c] (%)
1[a]	dim succ/propanediol/DPAT	1/1.5/0.1	17	0
2	dim succ/ BDO /DPAT	1/1.5/2.5	17	0
3	dim succ/ BDO /DPAT	1/1.5/5	17	10
4	dim succ/ BDO /DPAT	1/1.25/10	17	5
5	dim succ/ BDO /DPAT	1/1.25/1	17	12
6	dim succ/ BDO /DPAT	1/1.25/2	24	2
7	dim succ/ BDO /DPAT	1/1.25/2.5	3	29
8	dim succ/ BDO /DPAT	1/1.25/1	3	19
9	dim succ/ BDO /DPAT	1/1.25/5	3	26
10	dim succ/ BDO /DPAT	1/1.25/10	3	18
11	dim succ/ BDO /DPAT	1/1.05/0.5	6	23
12	dim succ/ BDO /DPAT	1/1.11/0.5	6	23
13	dim succ/ BDO /DPAT	1/1.5/0.5	6	26
14	dim succ/ BDO /DPAT	1/1.25/1	6	9
15	dim succ/ BDO /DPAT	1/1.25/2	6	18
16	dim succ/ BDO /DPAT	1/1.25/2.5	6	27
17	dim succ/ BDO /DPAT	1/1.5/3.5	6	38
18[b]	dim succ/ BDO /DPAT	1/1.5/3.5	6	8
19	dim succ/ BDO /DPAT	1/1.25/10	6	19

[b] T = 120 °C

[c] Gravimetric conversion = $m_{experimental}/m_{theoretical} \times 100$

© 2020 Tous droits réservés.

Second, we studied the polytransesterification between dimethyl succinate and butanediol (Figure 4-8), which is -as well- catalyzed by DPAT. Table 4-2 shows our attempts to find the optimal reaction conditions: in term of reaction time and reactants equivalents, with a particular interest to the catalyst amount, in order to reach the good yield with high molecular weight of PEs

We didn't reach more than 12% of yield within 17 hours (runs 1. 2, 3, 4 and 5) when applying different stoichiometric ratio of reactants (r = 0.66 or 0.8) and varying the percentage of catalyst from 1 to 10%. And almost there is no conversion within 24 hours (run 6). On the other hand, within 3 hours, when we used diol/diacid with r = 0.8 in addition to 2 or 5% of catalyst, we reached 29% and 26% of yield respectively (runs 7 and 9). However, with the same reaction time when changing the catalyst quantity (1 or 10 %), the conversion decreased to 19% and 18 % respectively (runs 8 and 10). So the maximum yield within 3 h reaction didn't exceed 29%.

Finally, within 6 hours of reaction time (runs 11 to 19) using different quantity of catalyst (from 0.5 to 10 %) and BDO excess (r = 0.66, 0.8, 0.9 or 0.95), the highest conversion attained-for the moment- was 38% with 1/1.5/3.5 equivalents respectively for dimethyl succinate, butanediol and catalyst. While increasing the temperature to 120 °C the conversion decreased from 38% to 8% (run 14).

4.3.2. Polycondensation in Batch system using pentafluorophenylammonium triflate (PFPAT) as a catalyst.

4.3.2.1. PFPAT promotes Polyesterification between diacids and diols in Batch system

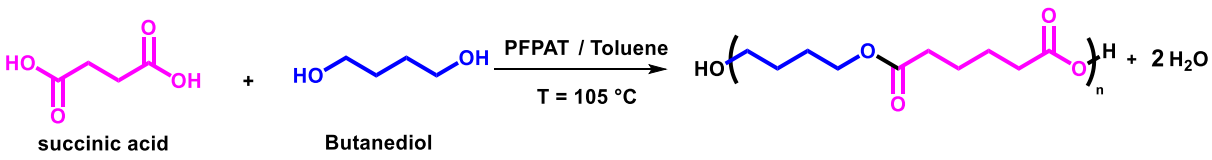

Figure 4-8 polyesterification between succinic acid and butanediol using PFPAT as a catalyst at 105 °C.

© 2020 Tous droits réservés.

Table 4-3 Polyesterification between succinic acid and butanediol using PFPAT as a catalyst in batch system at 105 °C.

Run	Diacid/Diol/cat	Equivalents	Reaction time (h)	Yield[a] (%)
1	ad ac/ BDO /PFPAT	1/1/0.5	06	39
2	succ ac/ BDO /PFPAT	1/1.05/0.5	06	42
3	succ ac/ BDO /PFPAT	1/1.05/0.5	07	57
4	succ ac/ BDO /PFPAT	1/1.11/0.5	06	60
5	succ ac/ BDO /PFPAT	1/1.11/1	06	61
6	succ ac/ BDO /PFPAT	1/1.11/1	05	67
7	succ ac/ BDO /PFPAT	1/1.11/1	03	54

[a] Gravimetric conversion = $m_{experimental}/m_{theoretical} \times 100$

The second catalyst used to promote the polyesterification between succinic acid and butanediol is PFPAT (Figure 4-8). Following the same equivalents of the two reagents and 0.5% of catalyst (1/1/0.5), 39% of conversion was obtained at 105 °C within 6 hours (Table 4-3, run 1). When we add an excess for 1.05 of BDO, the conversion increased to 42 % (Table 4-3, run 2) and to 57% within 7 hours (Table 4-3, run 3). When we added a more excess of BDO (1.11), we reached 60% of yield (Table 4-3, run4).

Respecting the same excess of BDO for 1.11, we increased the amount of catalyst to 1%. No significant changes were recorded within 6 hours (Table 4-3, run 5). But within 5 hours a 67% of conversion was recorded, which is the highest one obtained using PFPAT as a catalyst (Table 4-3, run 6). In addition, the decrease of reaction time to 3 hours resulted into lower yield percentage of 54% (Table 4-3, run7).

© 2020 Tous droits réservés.

4.3.2.2. PFPAT promotes Polytransesterification between diacids and diols in batch system

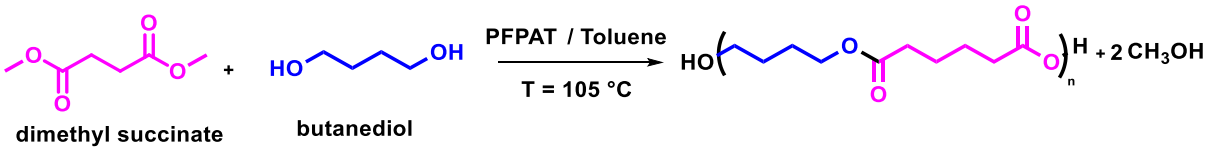

Figure 4-9 polytransesterification between dimethyl succinate and butanediol using PFPAT as a catalyst at 105 °C.

For this study, we used PFPAT as a catalyst to promote polytransesterification reaction between dimethyl succinate and BDO (Figure 4-9). Table 4-4 shows our attempts to find the best reagents equivalents to apply within 6 hours of reaction time, since it was the best reaction time using DPAT as a catalyst.

Overall, we applied 1.05 (runs 1 and 3) and 1.11 (runs 2 and 4) of BDO excess, while varying the quantity of catalyst and the temperature (run 3): we didn't reach more than 21% of conversion with 1/1.05/0.5 equivalents respectively for dimethyl succinate, butanediol, and the catalyst.

© 2020 Tous droits réservés.

Table 4-4 Polytransesterification between dimethyl succinate and butanediol using PFPAT as a catalyst in batch system at 105 °C.

Run	Diacid/Diol/cat	Equivalents	Reaction time (h)	Yield[b](%)
1	dim succ/ BDO /PFPAT	1/1.05/0.5	6	21
2	dim succ/ BDO /PFPAT	1/1.11/1.5	6	17
3[a]	dim succ/ BDO /PFPAT	1/1.05/1.5	6	18
4	dim succ/ BDO /PFPAT	1/1.11/3	6	15

[a] T = 95 °C
[b] Gravimetric conversion = $m_{experimental}/m_{theoretical} \times 100$

4.3.3. Comparison of polycondensations catalyzed by DAPT and PFPAT

Table 4-5 Polycondensation between succinic acid or dimethyl succinate and butanediol using DPAT or PFPAT as a catalyst in batch system at 105 °C within 6 hours in toluene.

Run	Reagents Diacid or diester/diol/catalyst	Equivalents	$M_n \times 10^{-3}$ (g/mol)[a]	$M_w \times 10^{-3}$ (g/mol)[a]	Conversion[b]	$Đ$[a]
1	succ ac/ BDO /DPAT	1/1/0.5	2.6	3.4	76	1.31
2[c]	succ ac / BDO /PFPAT	1/1.11/1	4.5	5.9	67	1.31
3	dim succ/ BDO /DPAT	1/1.5/3.5	3.2	3.6	38	1.12
4	dim succ/ BDO /PFPAT	1/1.05/0.5	2.9	3.1	21	1.07
5[d]	succ ac/ BDO /DPAT	1/1/0.5	2.3	3.0	61	1.30
6[e]	succ ac / BDO /PFPAT	1/1.11/1	2.5	3.4	54	1.36

[a] Determined by GPC
[b] Gravimetric conversion = $m_{experimental}/m_{theoretical} \times 100$
[c] Reaction time = 5 hours
[d] T = 95 °C
[e] Reaction time = 3 hours

© 2020 Tous droits réservés.

In this section, we present GPC and MALDI-TOF results for polyesters produced with the highest conversions from polycondensation reactions already discussed in sections 4.3.1 and 4.3.2. GPC traces revealed the presence of several peaks and we present in Table 4-5 the values of the major peak compared to the others that are negligible. In term of molecular mass, the values indicate that we reached more than oligomers (polymer, more than ten repetitive motifs) under 105 °C which is a mild temperature for polyesterification reaction compared to the literature, where the reaction temperature reaches the 200 °C and above.[342] So that working under this temperature and obtaining a polyester can be considered as a good improvement.

In fact, the structure of PEs is detected from MALDI-MS spectra and their masses are detected from GPC analysis. MALDI-TOF spectra showed the presence of different species in the polymer product. For those obtained from polyesterification (Figure 4-10 and Figure 4-11), we detected the presence of seven species of polyester with different chain extremities which are: succinic acid ($C_4H_6O_4$), dimethyl succinate with loss of CH_2 ($C_5H_8O_4$), water (H_2O), methanol (CH_3OH), dimethyl succinate ($C_6H_{10}O_4$) or butanediol ($C_4H_{10}O_2$) in addition to the macrocycles (Figure 4-12). For those obtained by polytransesterification, their MALDI-TOF (Figure 4-13 and Figure 4-14) spectra revealed the presence of three species of polyesters with different extremities which are: dimethyl succinate, dimethyl succinate with loss of CH_2 or methanol (Figure 4-15). These different extremities of chains apparently don't have the same reactivity, which means that the propagation of the reaction is not at the same rate in the reaction medium. This statement can explain the minority masses detected by GPC.

© 2020 Tous droits réservés.

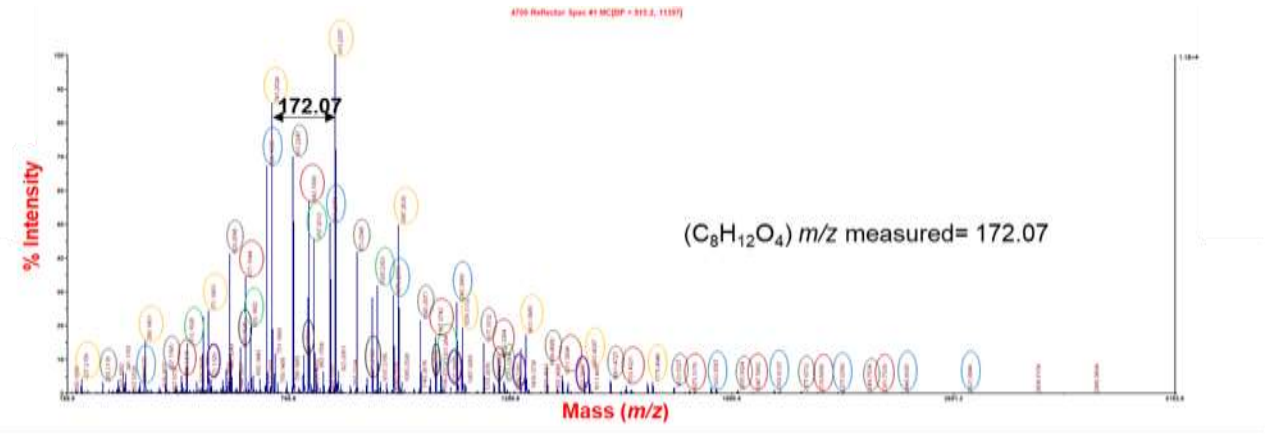

Figure 4-10 MALDI-TOF spectrum of polyester obtained by polyesterification of succinic acid and butanediol and catalyzed by DPAT respecting the conditions of Table 4-5, run 1. $C_8H_{12}O_4$ is the repetitive motif of the polyester chain and the difference between the peaks is equivalent to its mass (*m/z* = 172.07). Circles with different colors present each species of polyester with the correspondent end chain. Yellow: methanol (CH_3OH), gray: butanediol ($C_4H_{10}O_2$), blue: water (H_2O), red: dimethyl succinate with loss of CH_2 ($C_5H_8O_4$), green: dimethyl succinate ($C_6H_{10}O_4$) and black: succinic acid ($C_4H_6O_4$); M = (M_{motif} × number of repetition) + $M_{(extremity\ molecule)}$ + M_{Na}^+. Purple: Macrocycles; M = (M_{motif} × number of repetition) + M_{Na}^+.

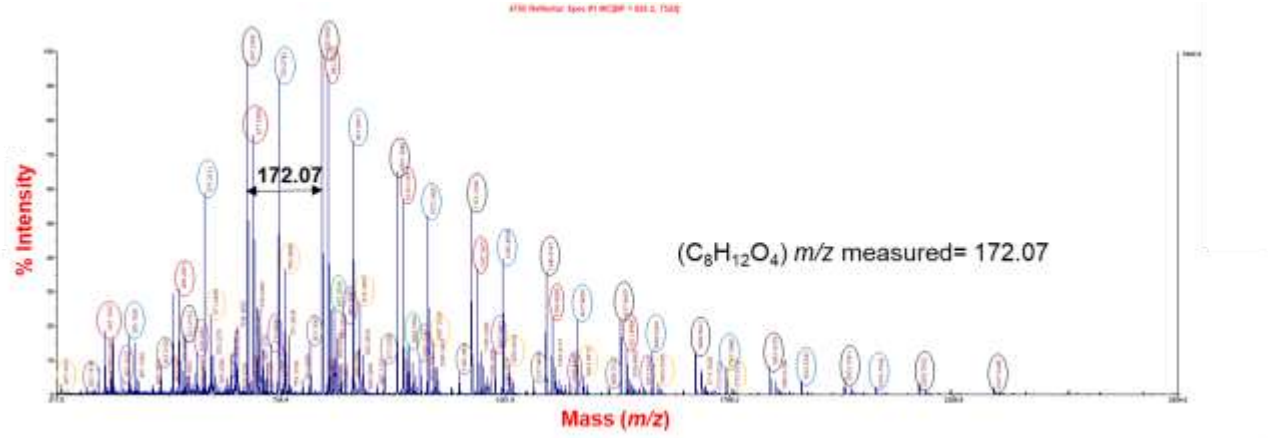

Figure 4-11 MALDI-TOF spectrum of polyester obtained by polyesterification of succinic acid and butanediol and catalyzed by PFPAT respecting the conditions of Table 4-5, run 2. $C_8H_{12}O_4$ is the repetitive motif of the polyester chain and the difference between the peaks is equivalent to its mass (*m/z* = 172.07). Circles with different colors present each species of polyester with the correspondent end chain. Yellow: methanol (CH_3OH), gray: butanediol ($C_4H_{10}O_2$), blue: water (H_2O), red: dimethyl succinate with loss of CH_2 ($C_5H_8O_4$), green: dimethyl succinate ($C_6H_{10}O_4$) and black: succinic acid ($C_4H_6O_4$); M = (M_{motif} × number of repetition) + $M_{(extremity\ molecule)}$ + M_{Na}^+. Purple: Macrocycles; M = (M_{motif} × number of repetition) + M_{Na}^+.

© 2020 Tous droits réservés.

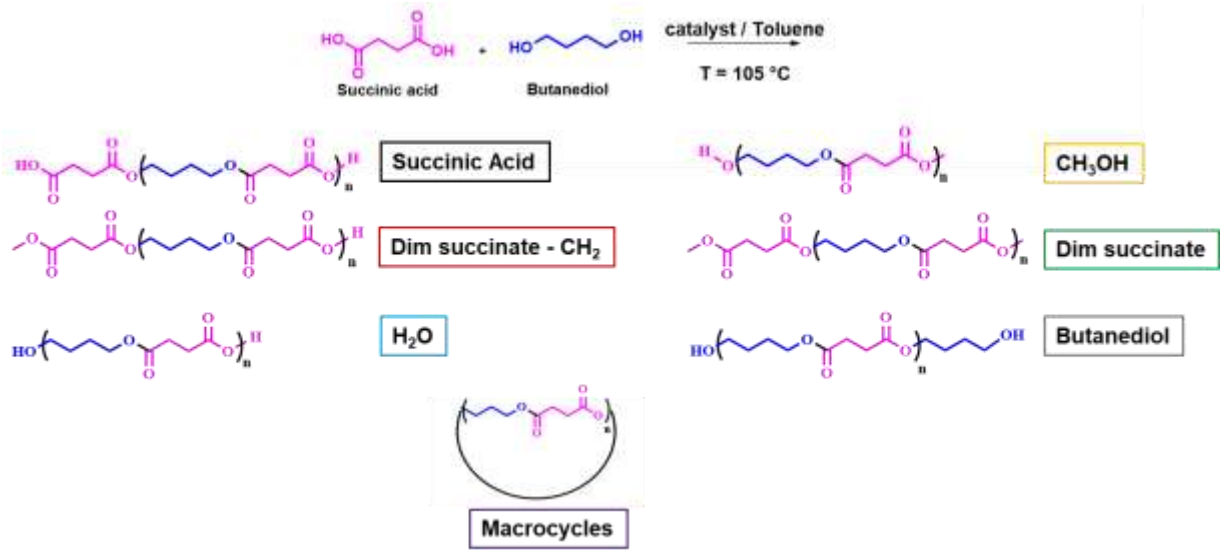

Figure 4-12 Different species of polyester obtained by polyesterification of succinic acid and butanediol and catalyzed by DPAT or PFPAT. They differ by their chain extremity that can be: succinic acid ($C_4H_6O_4$), dimethyl succinate with loss of CH_2 ($C_5H_8O_4$), water (H_2O), methanol (CH_3OH), dimethyl succinate ($C_6H_{10}O_4$) or butanediol ($C_4H_{10}O_2$) in addition to the macrocycles.

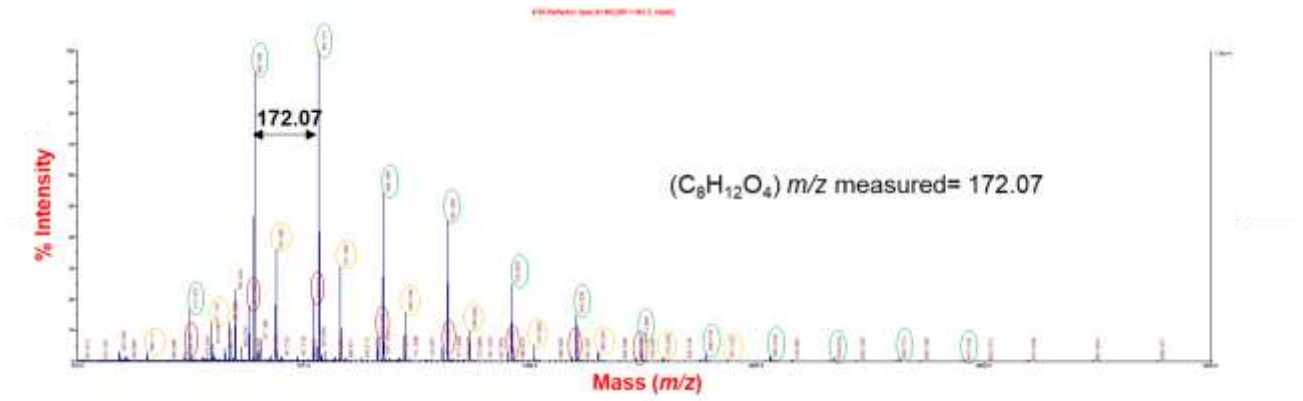

Figure 4-13 MALDI-TOF spectrum of polyester obtained by polytransesterification of dimethyl succinate and butanediol and catalyzed by DPAT respecting the conditions of Table 4-5, run 3. $C_8H_{12}O_4$ is the repetitive motif of the polyester chain and the difference between the peaks is equivalent to its mass (m/z = 172.07). Circles with different colors present each species of polyester with the correspondent end chain. Yellow: methanol (CH_3OH), red: dimethyl succinate with loss of CH_2 ($C_5H_8O_4$) and green: dimethyl succinate ($C_6H_{10}O_4$); M = (M_{motif} × number of repetition) + $M_{(extremity\ molecule)}$ + M_{Na^+}.

© 2020 Tous droits réservés.

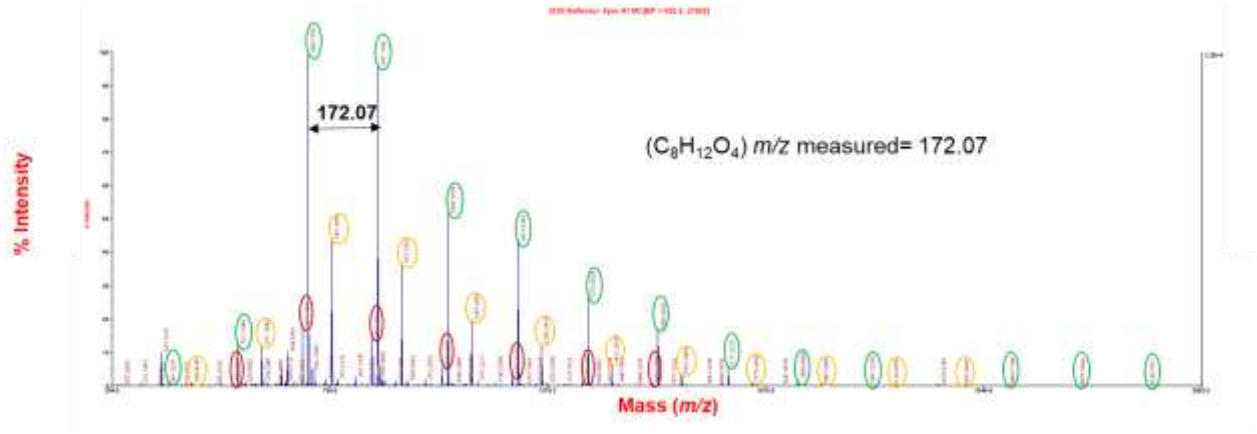

Figure 4-14 MALDI-TOF spectrum of polyester obtained by polytransesterification of dimethyl succinate and butanediol and catalyzed by PFPAT respecting the conditions of Table 4-5, run 4. $C_8H_{12}O_4$ is the repetitive motif of the polyester chain and the difference between the peaks is equivalent to its mass (*m/z* = 172.07). Circles with different colors present each species of polyester with the correspondent end chain. Yellow: methanol (CH_3OH), red: dimethyl succinate with loss of CH_2 ($C_5H_8O_4$) and green: dimethyl succinate ($C_6H_{10}O_4$); M = (M_{motif} × number of repetition) + $M_{(extremity\ molecule)}$ + M_{Na^+}.

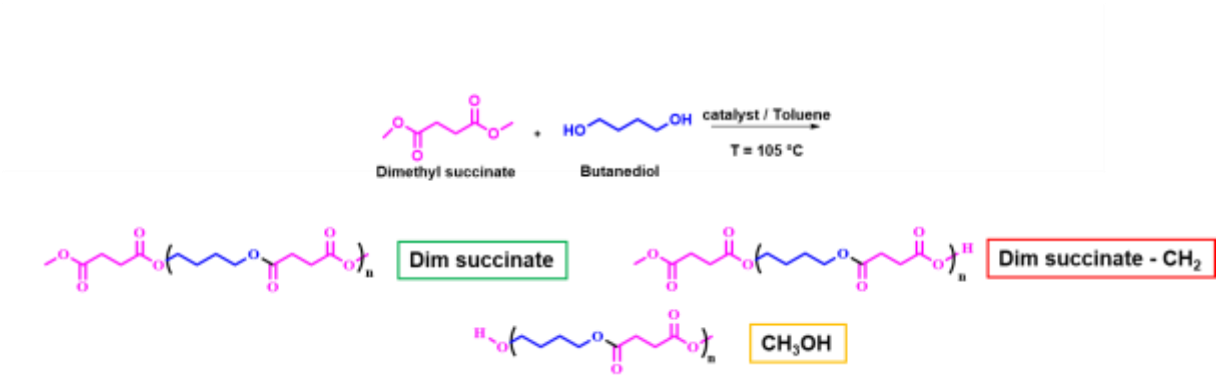

Figure 4-15 Different species of polyester obtained by poly-trans-esterification of dimethyl succinate and butanediol and catalyzed by DPAT or PFPAT. They differ by their chain extremity that can be: dimethyl succinate ($C_6H_{10}O_4$), dimethyl succinate with loss of CH_2 ($C_5H_8O_4$) or methanol (CH_3OH).

In term of control, the best *Đ* were recorded for polyesters yielded from polytransesterification reaction; *Đ* = 1.07 for the one catalyzed by PFPAT (Table 4-5, Run 4) and *Đ* = 1.12 for the one catalyzed by DPAT (Table 4-5, Run 3) but with low conversions (21% and 38% respectively). On the other hand, the polyesterification catalyzed by DPAT or PFPAT behaved similarly with *Đ* = 1.31 (Table 4-5, Runs 1 and 2). When we decreased the temperature to 95 °C for the polyesterification catalyzed by DPAT, the *Đ* and the molar mass have not been affected that much, however, we lost some of the conversion (Table 4-5, run 5 compared to run 1). In addition, when we decreased the reaction time of the polyesterification catalyzed by PFPAT, we lost almost the half of the molar mass of the polyester: M_n = 2500 *vs* 4500 and M_w = 3400 *vs* 5900 respectively for runs 3 and 6 of Table 4-5. This similar decrease

© 2020 Tous droits réservés.

of M_n and M_w resulted into maintaining almost the same $Đ$ value (1.36 *vs* 1.31). So, the optimal temperature to apply is 105 °C for a reaction time of 6 hours, constituting the parameters for which we obtained the highest conversion and molar mass with the best control.

4.3.4. Polycondensation in flow system

In flow mode, we aimed to carry out the polytransesterification reaction, by which we have a homogenous mixture at RT. This is a key feature that should be insured in order to transfer the reaction medium into the syringe and pump it into the tubular reactor. So it is important to have this homogenous mixture to prevent any clogging of the tubular reactor like the one illustrated in (Figure 4-16). However, diacids are not soluble at RT in any solvent (to our knowledge). So we worked on using the diesters in polytransesterification in flow system.

The problem here is to find a kind of tubular reactor that shouldn't have any interaction with the reagents or the solvent. In addition, it should be permeable to methanol (the by-product) in order to drive forward the reaction equilibrium.

Figure 4-16 unsuccessful polyesterification of succinic acid and propanediol in flow mode using FEP tubing (i.d. = 1.55 mm), where the tube is clugged.

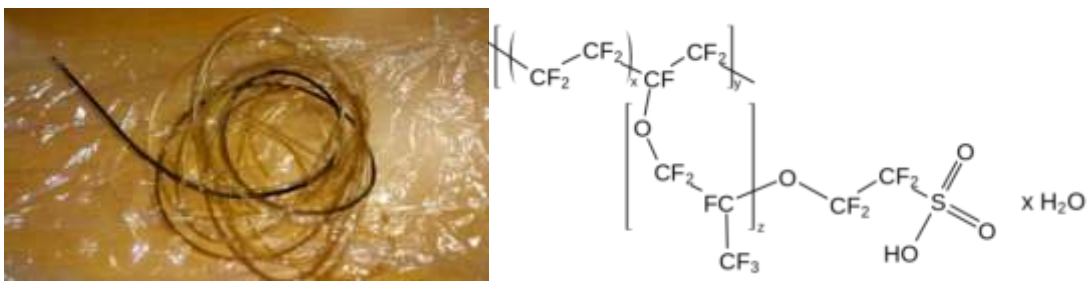

Figure 4-17 NafionTM tube and its chemical structure

© 2020 Tous droits réservés.

First, we used Nafion^{TM} tube (Figure 4-17), for the polytransesterification, but no polymerization was recorded. And when we analyzed the recovered solution by ^{1}H NMR, we missed alcohol peaks. That's why we predicted that there is an interaction between the diol and Nafion^{TM} tube and we supposed that the diol is grafted onto the wall tube because the latter became more rigid. The ^{1}H NMR spectra of propanediol before and after being injected into the tube are presented in Figure 4-18 and Figure 4-19respectively.

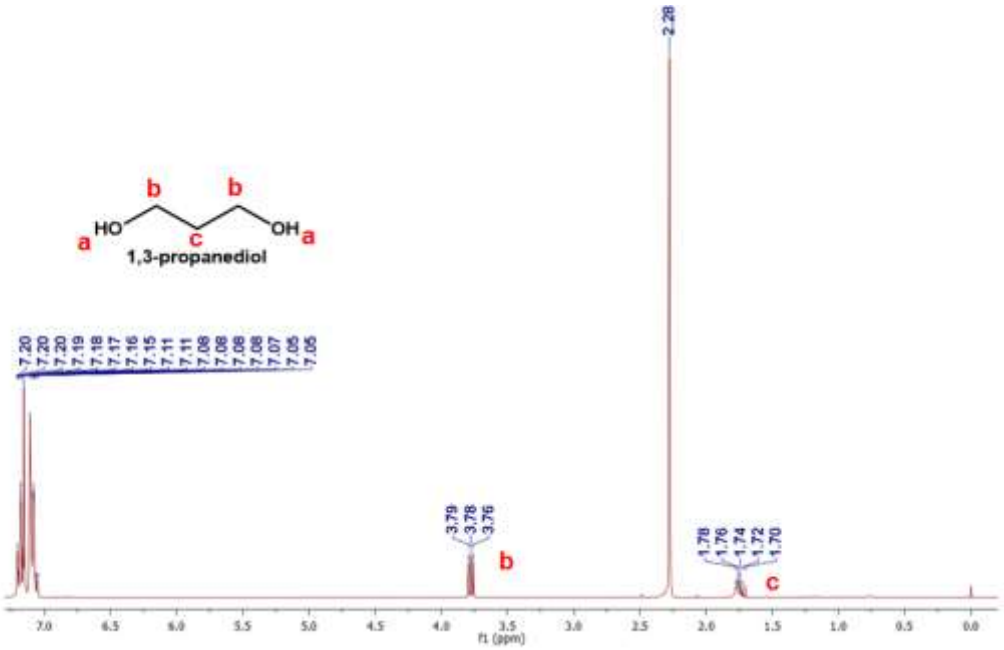

Figure 4-18 ^{1}H NMR spectrum of propanediol in toluene before being injected into Nafion^{TM} tube

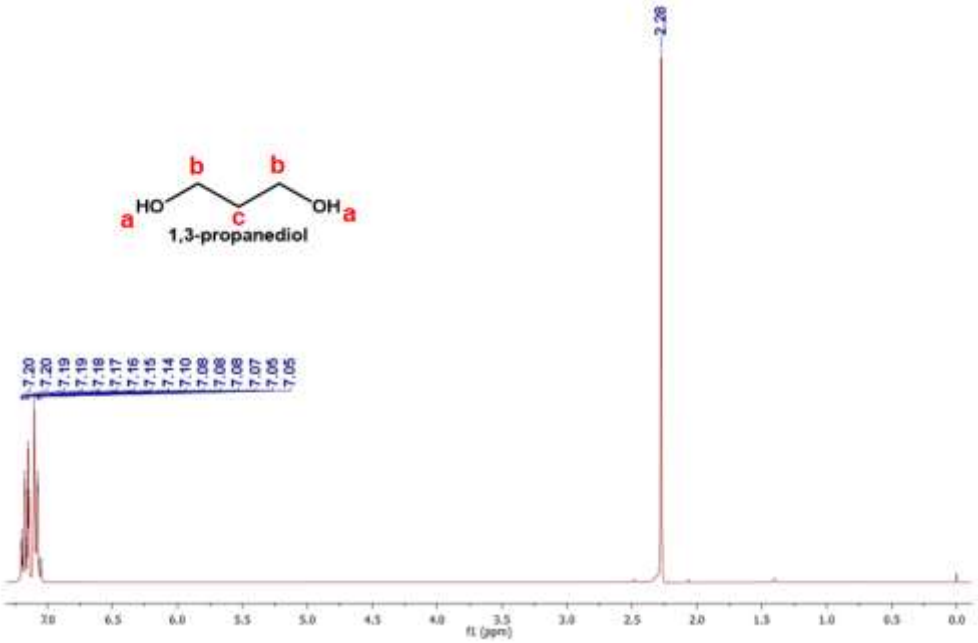

© 2020 Tous droits réservés.

Figure 4-19 ^{1}H NMR spectrum of propanediol in toluene after being injected into the Nafion™ tube

Then, we tested two other tubular reactors, which are: the PureWeld XL-a thermoplastic elastomer tube- and Silicone (Figure 4-20). We started by pumping the solvent alone into the tubes to make a test. Our solvent consisted of toluene and it didn't remain in these two tubes. Even the silicone based one was degraded by toluene.

So that's why for the moment, we didn't succeed to proceed the polytransesterification in flow mode.

Figure 4-20 Silicone (left) and PureWeld XL (right) tubes.

4.4. Conclusions

In batch system, we successfully carried out the polycondensation between succinic acid and butanediol using DPAT as a catalyst (76% of conversion, $Đ$ = 1.31) within 6 hours at 105 °C. And we reached 67% of conversion with $Đ$ = 1.31 using PFPAT as a catalyst within 5 hours at 105 °C. Unfortunately, we couldn't attain more than 38% of conversion for the polytransesterifcation catalyzed by DPAT within 6 hours at 105 °C ($Đ$ = 1.12). So in perspective, we will continue experiments aiming to find a solution for the polytransesterification reaction, by which we can be able to reach high polymer molecular weight with a high yield. Finally, till now, we didn't find a compatible tubular reactor to carry out the polytransesterification in flow mode. So in perspective, we suggest to keep the FEP tubing that we have already used in our work, but this time we shall add an anhydrous gas in the reaction medium. And this gas is supposed to absorb the by-product and drive the reaction equilibrium forward.

© 2020 Tous droits réservés.

5. CHAPTER FIVE: METAL-FREE CONTROLLED POLYMERIZATION IN FLOW: PHOTO-INDUCED ATRP USING EOSIN Y

5.1. Introduction

Conventional radical polymerization (RP) is employed to produce annually ca. 100 million tons of polymers, with thousands of different compositions. However, the production of advanced materials with controlled molecular architecture is so limited using RP. Therefore, the advantage of living/controlled radical polymerization has opened up the capability of such production.[35]

A living polymerization is obtained when polymer chains are initiated at the same time with no unwanted side reactions occurence.[34] the polymer chains formed are characterized by their living aspect. Indeed, they can be active for successive polymerizations as long as they are supplied with the monomer. The ideal case for living polymers is to have a polydispersity index (*Đ*) of 1.0 as all the polymers are initiated and undergo the propagation step at the same time and with the same rate. However, this perfect case is still in theoretical. Note that the smallest *Đ* reported has been 1.05, presenting a continuous progress in this field.[35,36]

Depending on the active species nature, living polymerizations can be classified as “ionic” and “radical” polymerizations.

The first discovery of living polymerization was done by Michael Szwarc, who worked on living anionic polymerization.[384] It remained the only example of a living process for more than ten years. Since that time, other living techniques have been discovered.[43]

Nowadays, controlled/living radical polymerization (CLRP) techniques are very attractive due to their ability to produce vinyl polymers with interesting characteristics: predetermined molecular weight, narrow molecular weight distribution, various architectures, and useful end-functionalities.[36] The most important are: atom transfer radical polymerization (ATRP),[47,385] reversible addition–fragmentation chain transfer polymerization (RAFT),[52] and nitroxide-mediated radical polymerization (NMRP).[49] Among these different types of controlled/living radical polymerization techniques, ATRP , the topic of our work, is

© 2020 Tous droits réservés.

applicable to a wide range of monomer formulations and initiators, making it most adopted approach.[35,47]

Photo-induced controlled radical polymerization was observed while carrying out a Cu mediated living radical polymerization of methyl acrylate (MA) in a flow system, whereby this experiment, a slow but effective polymerization, was obtained.[16] To precise the optimal wavelength to use, many light sources were tested covering the UV-VIS spectrum. The best results were recorded under a UV lamp with $\lambda_{max} \approx 360$ nm.[17]

In fact, metal contamination was a drawback when using ATRP.[18,19] To overcome this contamination, a significant focus has been directed toward lowering catalyst loading,[20] and/or working on nullifying residual metals present in the mixture.[21] Although the presence of these methods aims to minimize the quantity of metal, they are still not practical and ambitious enough. So, a much more viable solution was suggested: the development of a metal-free catalyst system for atom transfer radical polymerization.[23]

Like any photo-induced reaction, photo-polymerization is affected by the intensity of light, and it was proved that chain growth is conditioned by the presence of light while maintaining control over molecular weight and dispersity (*Đ*).[386] As a consequence of Beer-Lambert's law, achieving a uniform and complete penetration of light into the reaction medium is considered the most important obstacle for large-scale polymerization.[387,388] Furthermore, increasing the distance from a light source leads to an exponential decrease of degree of polymerization. In addition, the range of polymerization rates is affected by unevenly absorbed light through the depth of the reactor. The presence of different rates of growing chains which depend on their location in the reactor could give rise to wider dispersions for the resulting polymer. Continuous flow microreators are particularly advantageous responding to the drawbacks of light-mediated reactions.[330,389]

The aim of our work is to carry out photo-induced atom transfer radical polymerizations (ATRP) in a flow system, using an organic-based photo-redox catalyst in a lab designed tubular microreator (L = 3.37 m; i.e. = 800 µm) which is placed in direct contact with the green LEDs (530 nm). We will also evince the advantages of combining the continuous flow and the metal-free catalysis. All syntheses will be based on safe, easily removable and cheap resources. The produced polymers will be analyzed with solvent and time saving analytical techniques which are proton Nuclear Magnetic Resonance (^{1}H NMR) for determining the percentage of conversion and Gel Permeation Chromatography (GPC) for determining the

© 2020 Tous droits réservés.
lilliad.univ-lille.fr

molecular weight average and the Polydispersity index. Practically, we will focus on the synthesis of poly-methylmethacrylate (PMMA) using EosinY as a metal-free catalyst that absorbs in the green region. The advantages of such a photocatalyst are: its simple removal by washing with water, the relative low toxicity compared to the typical metal-based catalyst and its cost-effectiveness (13 euros/g eosin Y, *vs.* 1160 euros/g iridium catalyst). In addition, we use the visible light instead of UV irradiation where the former is cheaper and easier to apply. Traditionally, the polymerization reaction takes around 10 hours to get a high conversion. In order to accelerate this reaction, we intend to switch it to the continuous flow technology, which provides higher photon flux to reaction mixture and consequently increases the reaction rate. We are also interested to characterize the polymers formed by such a system and determine whether such an assembly succeeds to support the well-controlled feature of ATRP or not. The livingness of PMMA will be proved by using it as a macro-initiator in further copolymerization in order to produce linear di-block copolymer. In our case, we will use separately buthylacrylate, buthylmethacrylate and styrene as a second monomer. Finally, we will test the scale up of these reactions using a tubular microreactor of 5 m length.

© 2020 Tous droits réservés.

5.2. Photo-initiated ATRP

There are many ways that can be used as controlling stimuli including: temperature,[47] light,[390] applied voltage,[391] and mechanical force.[392] From these different options, light triggered reactions emerged to be the most advantageous, and this is due to its low cost, simple experimental setup, mild reaction conditions by activating the dormant species at low temperature and minimal side reactions, in addition to the tunable and accessible light sources, and the possibility of spatial and temporal control.[393]

Generating initiating radical species is not the only purpose that photo-irradiation is used for. Many other goals are expected: activation of catalysis, generation of controlling agents, and increasing the polymer-end structure which can be initiated over several cycles.[46]

The innovation of photo-CRP will lead to new applications in different fields such as coatings, microelectronics, printing, adhesives, nanoparticles functionalization, drug delivery and gel production.[17]

Most of the widely used photo-polymerization reactions are neither completely switchable with light nor living.[17] Using dithiocarbonate, Otsu and co-workers developed the first successful photo-induced CRP, in which polymers whose molar masses increased linearly with the monomer conversion were produced.[394]

Similar to the strategies of conventional thermal CRP methods including NMP, RAFT and ATRP, efficient process of photo-controlled living radical polymerization was reported. What is remarkable is the rapid growth and development of this field despite its novelty.[17,47,395–398]

The mechanism of photo-induced ATRP is similar to the previous one presented in section 2.6. In such a system, Cu (I)/L (activator) and X-Cu(II)/L (deactivator) complexes are the typical used catalysts.[46]

In contrast to conventional thermal ATRP, there are photo-induced ATRP systems based on directly using a high oxidation state transition-metal in order to control the activator oxidation.[399,400] Unfortunately, applying these systems involves a high concentration of the metal catalyst in order to maintain the control of polymerization reaction. To overcome this requirement of catalyst high quantity, regeneration ways of the activator can be achieved *in situ* by reducing the deactivator, which leads to the decrease of catalyst loading to 100 ppm level.[19,399,401] This reduction pathway can be ensured by adding organic reducing agents,

© 2020 Tous droits réservés.

introducing an external radical initiator, applying a cathodic current or via irradiation with light.[402,403]

We can classify the pho-induced ATRP referring to the primary photochemical process into photo-initiated and photo-redox ATRP. During the first one, the photo-initiator undergoes an homolytic cleavage, whereas during the second one, an electron transfer reaction is ensured, which either generates the activator or establishes the ATRP equilibrium.[17]

5.2.1. Metals mediated photo-redox catalysis

The key step of photo-redox mediated ATRP is the single electron transfer (SET). The excited photocatalyst (PC) after irradiation undergoes oxidative or reductive quenching. This is engendered from SET to the alkyl halide followed by generating an alkyl radical. Propagation step takes place in the presence of monomer in the reaction mixture. Depending on the catalytic system, the exact mechanism of photo-redox ATRP and the regeneration of the photo-catalyst at its initial state can be predicted.[404]

A key advantage of photo-redox processes is that the initiator and polymer chains do not necessarily need to have any absorbing group. This is explained by the fact that only the PC is responsible of light absorption and it is not incorporated into the polymer chain. To ensure an efficient SET, a PC with long lived exited state is required, like: $Ir(ppy)_3$, τ = 1900 ns, $Ru(bipy)_3^{2+}$, τ = 900 ns.[17] This system is light switchable: no polymerization occurs in the dark where dormant species are formed, whereas the regeneration of radicals (active species) is applied by simple light re-exposure.

Guan and Smart reported in 2000 the synthesis of MMA using photo-enhanced ATRP by visible light irradiation.[405] A better result was obtained under visible light irradiation compared to the dark conditions. A conversion of 41% was obtained after 16 h at 80 °C in the dark, whereas 100% of conversion was reached with M_W close to the theoretical value and a narrow $Đ$. The two experiments were conducted in the same conditions ([MMA]/[RCl]/[CuCl]/[bipy]:100/0.1/0.3/1 ratio).[406]

Fors and Hawker reported successful MMA polymerization via photo-redox catalyzed ATRP using fac-$Ir(ppy)_3$ as a catalyst and ethyl 2-bromo-2-phenylacetate as an initiator 0.0125/1 ratio. Well-controlled polymerization with low $Đ$ was obtained (M_w/M_n < 1.25).[23] Alkyl halides can be activated by Ruthenium(II)polypyridine complexes (*e.g.*, $RuII(bpy)_3$) under visible light irradiation. In addition, organo-cobalt porphyrins give an organic radical and a

© 2020 Tous droits réservés.
lilliad.univ-lille.fr

cobalt(II) porphyrin metal-central radical for chain propagation after a photo-cleavage of the Co–C bond. A good control over the molecular weight and polydispersity was recorded.[406]

5.2.2. Metal-free photo-redox catalysis.

As mentioned before, metal contamination and expensive catalysts remain as drawbacks for both traditional and photo-induced ATRP processes. Wide range of organic-photocatalysts were exploited as photocatalysts for various radical-mediated organic reactions and that is referred to its easy availability, low cost and toxicity.[393]

To overcome these challenges, Hawker, Fors and co-workers successfully worked on developing a photo-controlled ATRP process mediated by light and catalyzed by an organic catalyst.[23] 10-phenylphenothiazine (PTH) (Figure 5-1) having a highly reducing excited state which surpassed that of $Ir(ppy)_3$ was found to be a great candidate for these polymerizations. Under irradiation of 380 nm, they used 0.1 mol % of PTH as a new organic catalyst to efficiently polymerize MMA. Interestingly, PMMA samples with narrow dispersity values were produced. This polymerization was the first example of a free-metal ATRP system.

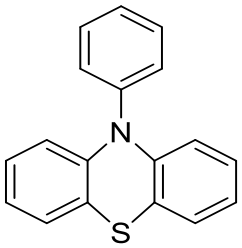

Figure 5-1 Structure of PTH

Later, Hawker managed to realize the polymerization of 2-(dimethylamino)ethyl methacrylate (DMAEMA) where polymers with broad $Đ$ values and poor control over M_n were obtained using $Ir(ppy)_3$, in contrast with the use of PTH, where good control and narrow $Đ$ values were obtained.[407]

Furthermore, another efficient ATRP process catalyzed by PTH was developed by Matyjaszewski and co-workers for the polymerization of acrylonitriles.[408]

Concurrently with these different reports, Miyake and Theriot used perylene as another organic catalyst in ATRP for the polymerization of (meth)acrylates and styrene.[153]

Fluorescein (FL) (Figure 5-2) has been successfully evaluated as an efficient catalyst for photo-induced *O*–ATRP of MMA under visible light irradiation.[393]

© 2020 Tous droits réservés.

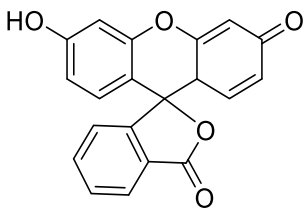

Figure 5-2 Structure of Fluorescein

In this work we used Eosin Y as an organic catalyst to polymerize MMA and for further co-polymerizations.

Eosin Y (Figure 5-3) is the 2',4',5',7'-tetrabromo-derivative of fluorescein. It is a classic dye that has been known for a long time and widely used in various applications like: cell staining,[409] lip stick,[410] as a pH indicator[411] and as an indicator in the analytical field for the determination of halide.[412]

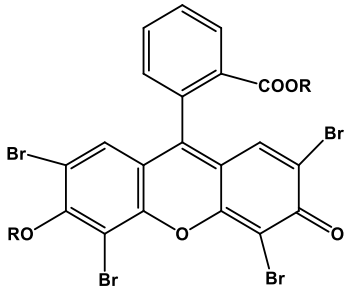

Figure 5-3 structure of Eosin Y

Under visible light irradiation, Eosin Y will be excited to its singlet excited state. This excited component will undergo a rapid intersystem crossing to the lowest energy triplet state. This state is characterized by a long life time of 24 μs[413,414] which makes from it a good candidate as a photo-catalyst for photo-redox reactions. Eosin Y absorbs light ideally at 539 nm with molar extinction coefficient ε = 60 800 $M^{-1}.cm^{-1}$. Following Eosin Y excitation, it becomes more reducing and more oxidizing than the ground state Eosin Y (Figure 5-4).

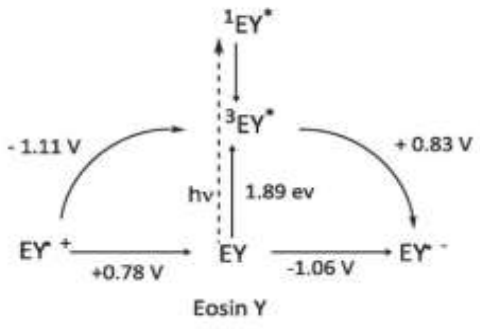

© 2020 Tous droits réservés.

Figure 5-4 Estimated redox potentials of Eosin Y in ground and excited states.[415]

Eosin Y was widely used in several organic syntheses like: reduction, oxidation, and generation of aryl radicals.[415]

In addition, Eosin Y has been utilized by Bowman,[416] Perez-Luna,[417] and others,[418] to mediate free radical polymerization under photochemical conditions. The Boyer group carried out a series of photo-CRP using Eosin Y as a photo-redox catalyst and different functional monomers of GMA, HEMA, OEGMA, DMAEMA, PFPMA, MAA, and HPMA which led to the production of corresponding polymers with narrow molar mass distributions .[307] Various solvents were compatible with this method like MeCN, water, DMSO, and DMF. Working under an aerobic atmosphere was enabled due to the addition of trimethylamine, which ensures oxygen reduction.[17]

5.3. Flow system

The irradiation of the photo-catalyst species plays an important role in the efficiency of its photo-excitation, as well as relative concentrations of PC species used in polymerization reaction, which affects directly the control over the polymerization. In order to enhance irradiation efficiency and facilitate the synthesis of well-defined polymers, an *O*-ATRP in continuous flow was developed.[113]

Photo-mediated continuous flow reactors were successfully used as an alternative to traditional batch reactors in both small molecule[388,419] and macromolecular[228,420] syntheses to enhance efficient and uniform irradiation conditions.

According to the Beer-Lambert law, in a photo-mediated batch reaction, photons cannot travel the reaction medium easily with increasing path length, conducting to non-uniform irradiation and limiting the reaction efficiency.[387,388] As a particularity of photo-induced CRP reactions, poor irradiation leads to broad molecular weight distributions, slower reaction times, and limited scalability.[421,422] Unlike to batch reactors, continuous flow is characterized by a high surface-area-to-volume ratio of reactor to solution, which allows uniform irradiation, fast reaction times, efficient heat and mass transfer, reduction of batch-to-batch variations, and facile scalability.[421–423]

© 2020 Tous droits réservés.

The use of continuous flow reactors was reported for various CRP systems: nitroxide-mediated polymerization (NMP),[424,425] reversible addition-fragmentation chain transfer (RAFT)[236,426] and metal-catalyzed ATRP. Furthermore, this method has been successfully used in photo-induced RAFT, and photo-induced metal-catalyzed ATRP.[386,427] Recently, methylmethacrylate and diverse groups of methacrylate monomers using photo-induced *O*-ATRP in continuous flow were investigated. As a result, a robust and efficient method of polymerization was proved.[113]

© 2020 Tous droits réservés.

5.4. Results and discussion

5.4.1. Eosin Y catalyzed the ATRP of MMA

Entry	Catalyst	Initiator/additive	Polymerization conditions[a]	LEDs	Conv. (%)[b]	Time (min)	*Mn* theo[c]	*Mn*[d]	*Đ*[d]
1	$Ru(bpy)_3Cl_2$	EBiB/*i*-Pr_2NEt	200:1:0.01:10	Blue	86	430	17,200	20,600	1.96
2[e]	Eosin Y	EBiB/*i*-Pr_2NEt	200:1:0.01:10	Green	54	360	11,000	24,300	1.64
3	Eosin Y	EBiB/*i*-Pr_2NEt	200:1:0.01:10	Green	70	216	14,000	25,000	1.58
4	Eosin Y	EBiB/*i*-Pr_2NEt	200:1:0.05:10	Green	43	216	8,600	18,000	1.86
5	Eosin Y	EBiB/*i*-Pr_2NEt	200:1:0.003:10	Green	50	216	10,000	17,600	1.85
6	Eosin Y	EBPA/*i*-Pr_2NEt	200:1:0.01:10	Green	91	180	18,000	18,000	1.42

Table 5-1 ATRP polymerization of MMA in DMF in a flow microreactor using LEDs irradiation[a].

[a]Polymerization conditions: [MMA]: [initiator]: [catalyst]:[additive] = 200:1:x:y in DMF at RT in a microreactor illuminated with LEDs.
[b]Determined by 1H NMR.
[c]Mn theo = ([MMA]/[Initiator] × conv. × MMMA) + MInitiator .
[d]Determined by GPC.
[e]Performed in batch.

Table 5-2 Eosin Y catalysed ATRP of MMA using EB*i*B as an initiator in flow[a].

Entry	Time	% Conv.[b]	*Mn* theo[c]	*Mn* by GPC	*Đ*[d]
1[e]	180	0	---	---	---
2	36	25	5200	13110	1.42
3	72	39	8000	18250	1.41
4	90	45	6210	19380	1.60
5	180	58	11810	20670	1.51
6	240	68	13810	24870	1.58
7[f]	360	56	11400	24260	2.09

[a] Polymerization conditions: [MMA]: [EB*i*B]: [Eosin Y]: [*i*-Pr_2NEt] = 200:1:0.02:10 in DMF at RT in microreactor illuminated with green LEDs.
[b] Determined by 1H NMR.
[c] *Mn* theo= ([MMA]/[EB*i*B] × conversion × MMMA) + MEBiB; where [MMA] and [EBiB] are the concentrations of the monomer and the initiator respectively and MMMA and MEB*i*B are their corresponding molar masses.

© 2020 Tous droits réservés.

[d] Determined by GPC.
[e] Control experiments missing Eosin Y, EB*i*B or light. [f] Performed in batch.

Note that this work is recently published,[241] in which we performed the metallic visible-light photoredox catalysis using the $Ru(bpy)_3Cl_2$, *i*-Pr_2NEt system in DMF irradiated by blue LEDs in flow. The modest dispersity (Table 5-1, entry 1; $Đ \approx 2$) obtained is in agreement with the results obtained in batch.[428] We then decided to check the activity of Eosin Y to perform the polymerization of MMA under flow conditions. Eosin Y has its maximum absorption at 539 nm in the visible region of the spectrum and with a high absorption coefficient (ε = 60 800 $M^{-1}.cm^{-1}$) (Figure 5-4). The irradiation was afforded by green LEDs with a power of 20 $mW \cdot cm^{-2}$. We originally performed polymerization of MMA in DMF using ethyl α-bromoisobutyrate (EB*i*B) as initiator and Eosin Y as photocatalyst in both batch (Table 5-1, entry 2) and flow (Table 5-1, entry 3). Interestingly, the change from batch to flow system was enough to improve remarkably both the rate of the reaction and its control. Although 360 min was required in batch to reach a 50% conversion, only 216 min was needed in flow for 70% conversion. Moreover, the dispersity decreased from1.64 in batch to 1.58 in flow. The results obtained herein in flow are also better than those reported in batch by Yagci's group where 120 min of green LED irradiation of the reaction mixture gave 28% conversion but with a dispersity of 1.85.[429] Following these results, blank experiments were performed where one of the components (catalyst, initiator, *i*-Pr_2NEt, and light) was removed (Table 5-2, entry 1). In all of these cases, no PMMA was detected showing that all of these components are essential for the polymerization process. Moreover, since Eosin Y has a high extinction coefficient, a large amount of the catalyst in flow (Table 5-1, entry 4) will lead to a similar situation to that in batch where the light will only illuminate a small portion of the reactor (Table 5-3, Figure 5-5), leading to a decrease in the conversion to 43%. Similarly, decreasing the quantity of Eosin Y will lead to a decrease in the conversion to 50% despite having a better light penetration in the system as the quantity of the catalyst is not efficient to activate the initiators (Table 5-1, entry 5).

© 2020 Tous droits réservés.

Table 5-3 Light transmittance for a 0.25 mM solution of Eosin Y in acetone in batch and flow systems.

Conventional glassware			Microreactor		
Optical length (cm)	Absorbance	Transmission	Optical length(mm)	Absorbance	Transmission
0.00	0.00	100.00	0.00	0.00	100.00
0.10	1.37	4.32	0.10	0.14	73.03
0.20	2.73	0.19	0.20	0.27	53.33
0.30	4.10	8.04E-03	0.30	0.41	38.95
0.40	5.46	3.47E-04	0.40	0.55	28.44
0.50	6.83	1.50E-05	0.50	0.68	20.77
0.60	8.19	6.46E-07	0.60	0.82	15.17
0.70	9.56	2.79E-08	0.70	0.96	11.08
0.80	10.92	1.20E-09	0.80	1.09	8.09
0.90	12.29	5.19E-11	0.90	1.23	5.91
1.00	13.65	2.24E-12	1.00	1.37	4.32
1.10	15.02	9.66E-14	1.10	1.50	3.15
1.20	16.38	4.17E-15	1.20	1.64	2.30
1.30	17.75	1.80E-16	1.30	1.77	1.68
1.40	19.11	7.76E-18	1.40	1.91	1.23
1.50	20.48	3.35E-19	1.50	2.05	0.90
1.60	21.84	1.45E-20	1.60	2.18	0.65
1.70	23.21	6.24E-22	1.70	2.32	0.48
1.80	24.57	2.69E-23	1.80	2.46	0.35
1.90	25.94	1.16E-24	1.90	2.59	0.25
2.00	27.30	5.01E-26	2.00	2.73	0.19

A tube of 800 micron has a mean optical path of $\frac{\pi}{4} \times d = 628$ micron. The transmission is around 14%.

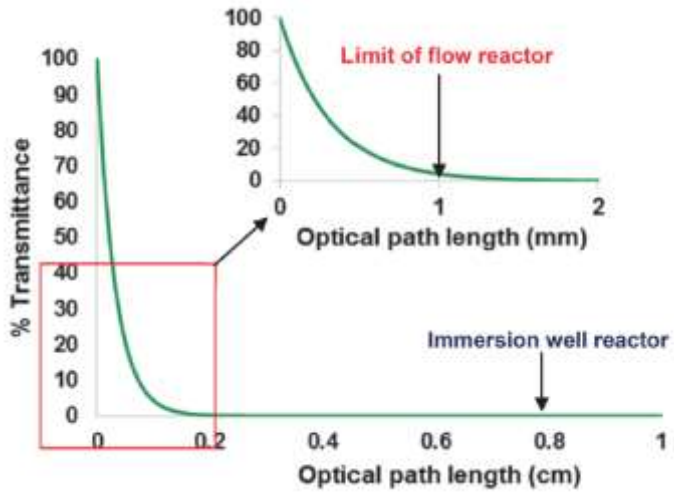

Figure 5-5 Light transmittance for a 0.25 mM solution of Eosin Y in acetone in batch and flow systems

Using ethyl α-bromophenylacetate (EBPA) as initiator, which has been previously reported to have a higher activation rate k_{act} compared to EB*i*B due to the radical stability enforced by a phenyl group,[43] the rate of the polymerization increased remarkably leading to more than 90% of conversion after only 180 min of irradiation (Table 5-1, entry 6). The polydispersity

© 2020 Tous droits réservés.

was also improved to 1.42, and the M_n values of the polymers formed were closer to the theoretical ones compared to those obtained using EB*i*B (Table 5-2, Figure 5-6 and Figure 5-7).

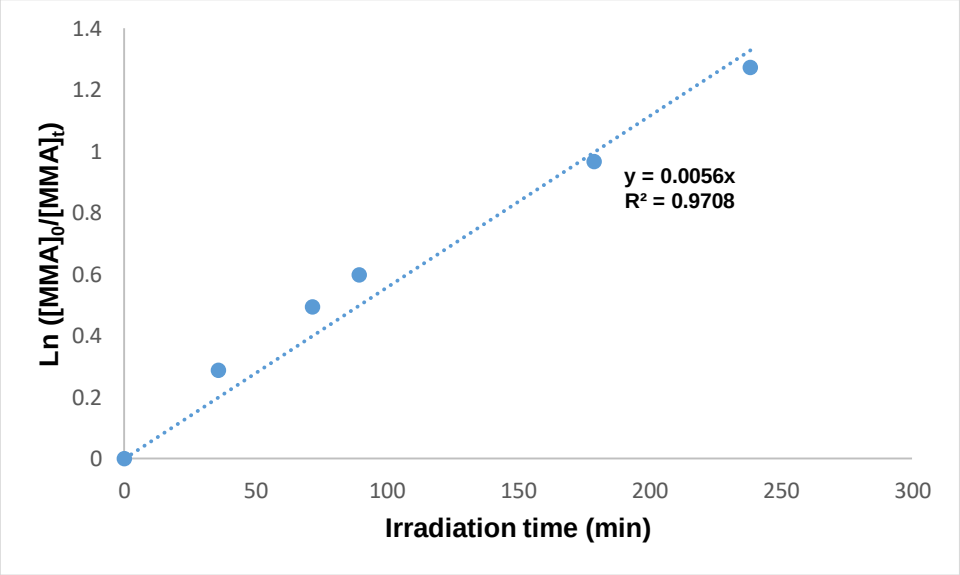

Figure 5-6 A plot of ln([MMA]$_0$/[MMA]$_t$) *vs* irradiation time for polymerization using EB*i*B as an initiator.

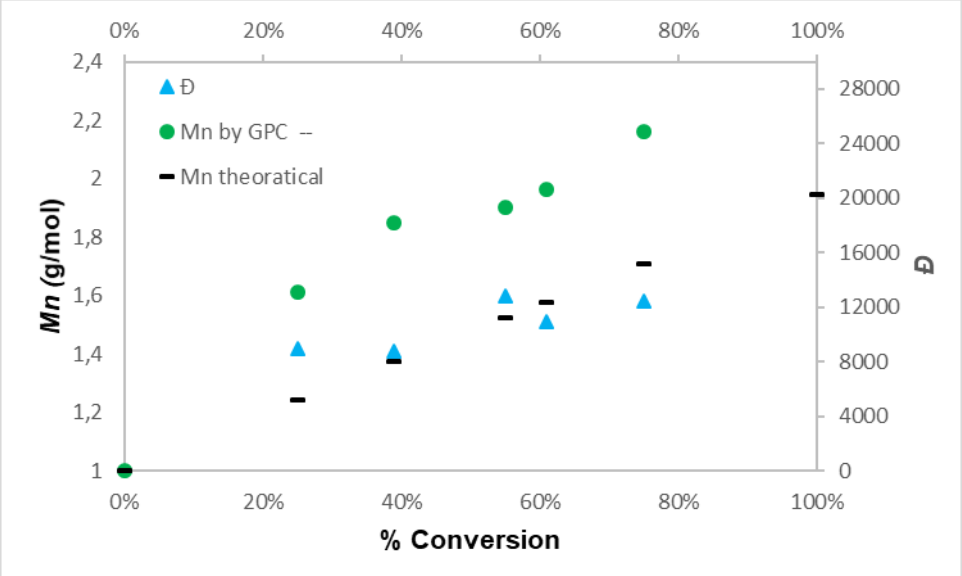

Figure 5-7 M_n (green) & $Đ$ (blue) of PMMA as a function of monomer conversion using EB*i*B as an initiator. M_n & $Đ$ values were determined by GPC relative to PMMA standards. Conversions were determined by ^{1}H NMR analysis. Black dashes represent M_n theo= ([MMA]/[EB*i*B] × conversion × M_{MMA}) + M_{EBiB}; where [MMA] and [EBiB] are the concentrations of the monomer and the initiator respectively and M_{MMA} and M_{EBiB} are their corresponding molar masses

© 2020 Tous droits réservés.

To further stabilize the intermediate radical in order to increase the polymerization rate, we used (p-OMe)EBPA as initiator; however, the results were quite disappointing (Table 5-4, entry 9). The best conditions obtained for the ATRP initiated by EBPA (Table 5-1, entry 6) were further investigated in details (Table 5-4, entries 1–6). The polymerization follows a first-order kinetics during the whole course of the reaction with an equation of y = 0.0121x for $\ln([MMA]_0/[MMA]_t)$ vs. irradiation time (min). The rate constant is 0.0121 min^{-1} (Figure 5-8), suggesting that the concentration of the propagating radicals is almost constant throughout the polymerization. Molecular weights measured by GPC follow the theoretical values starting from 37% and up to 90% of conversion suggesting a complete initiation (Figure 5-9; Table 5-4, entries 1–6). Figure 5-10, which includes the GPC traces of the polymers of Table 5-4, entries 1–6, shows how the increase in the irradiation time leads to the increase in the size of the polymers (GPC traces shifting to lower retention volumes). Moderate values of *Đ* (1.36–1.49) indicate relatively slow deactivation though still in the range of controlled polymerization (<1.5).

Table 5-4 Eosin Y catalyzed ATRP of MMA using EBPA as an initiator in flow[a].

Entry	Time (min)	% Conv.[b]	*Mn* theo[c]	*Mn* by GPC	*Đ*[d]
1	36	20	4,280	10,400	1.46
2	45	37	7,650	9,040	1.49
3	60	52	10,650	12,050	1.44
4	90	63	12,860	13,050	1.36
5	120	79	16,060	16,350	1.43
6	180	89	18,060	18,250	1.41
7[e]	60	53	10,650	13,000	1.42
8[f]	360	54	11,100	24280	1.64
9[g]	180	70	14,290	19,500	1.46

[a]Polymerization conditions: [MMA]: [EBPA]: [Eosin Y]: [*i*-Pr_2NEt] = 200:1:0.02:10 in DMF at RT in microreactor illuminated with green LEDs.
[b]Determined by 1H NMR.
[c]Mn theo = ([MMA]/[EBPA] × conversion × MMMA) + MEBPA; where [MMA] and [EBPA] are the concentrations of the monomer and the initiator, respectively and MMMA and MEBPA are their corresponding molar masses.
[d]Determined by GPC.
[e]Used for copolymerization with styrene.

© 2020 Tous droits réservés.

[f]Performed in batch.
[g]Using p(OMe)-EBPA synthesized according to the procedure listed by Sharma and Tepe.[430]

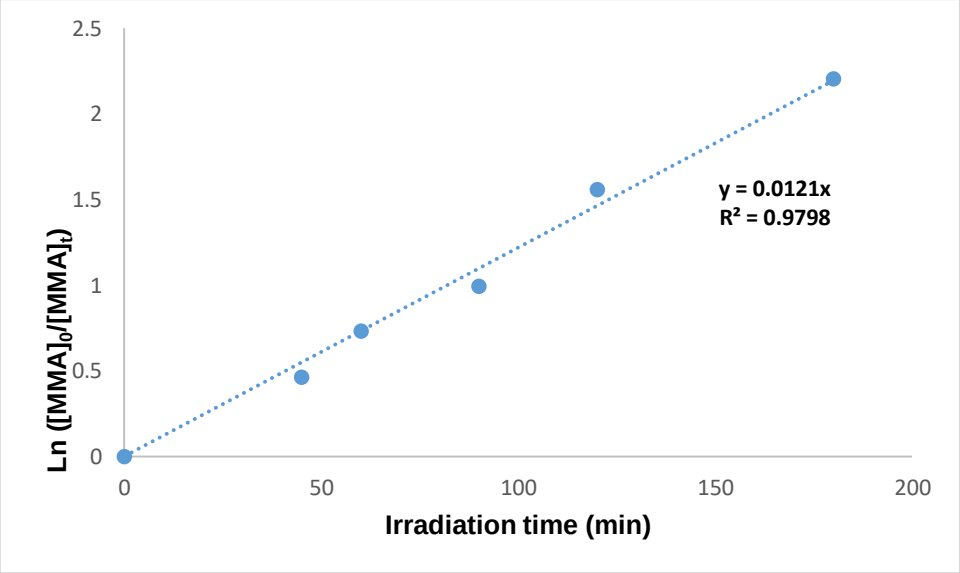

Figure 5-8 A plot of ln([MMA]$_0$/[MMA]$_t$) *vs* irradiation time for polymerization using EBPA as an initiator.

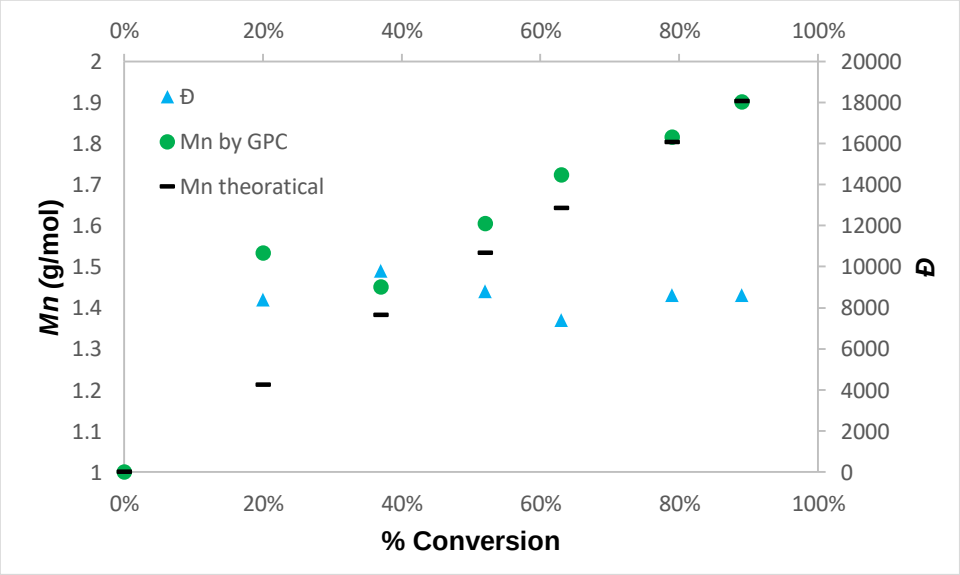

Figure 5-9 MMA polymerization catalyzed by Eosin Y using EBPA as initiator. PMMA *Mn* measured by GPC (left scale) and dispersity (right scale)

© 2020 Tous droits réservés.

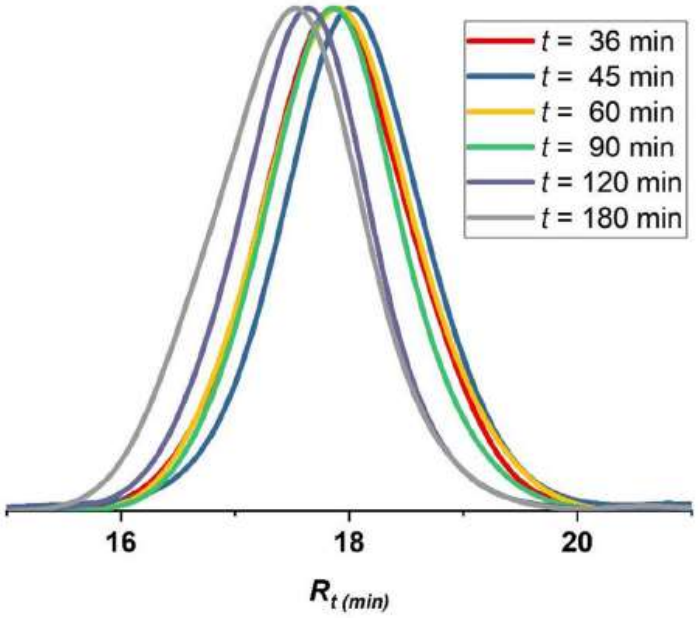

Figure 5-10 GPC traces of polymers formed following MMA polymerization catalyzed by Eosin Y usinf EBPA as initiator (Table 5-4, entries 1-6). Red trace (*t* = 36 min), blue trace (*t* = 45 min), yellow trace (*t* = 60 min), green trace (*t* = 90 min), violet trace (*t* = 120 min), gray trace (*t* = 180 min).

Moreover, polymerization in flow gave better conversion and *Đ* values compared to batch, which highlights the importance of flow settings for photocatalytic ATRP reactions (Table 5-4, entry 6 vs. Table 5-4 entry 9). However, note that the first point (Table 5-4, entry 1; Figure 5-10**,** red GPC trace) does not follow the theoretical M_n so that it deviates upward in Figure 5-9. This can be attributed to that Eosin Y undergoes an induction period before it can enter the catalytic cycle.[431] As a result, this point was excluded from the kinetic analysis (Figure 5-8).

© 2020 Tous droits réservés.

5.4.2. Livingness of PMMA–Br by Copolymerization

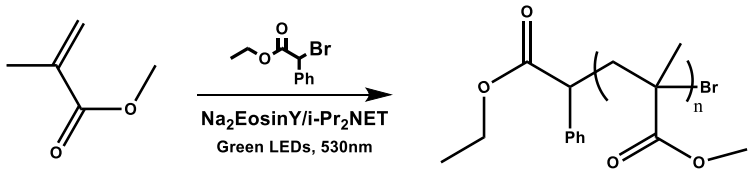

Figure 5-11 PMMA macro-initiator synthesis in flow conditions catalyzed by Eosin Y

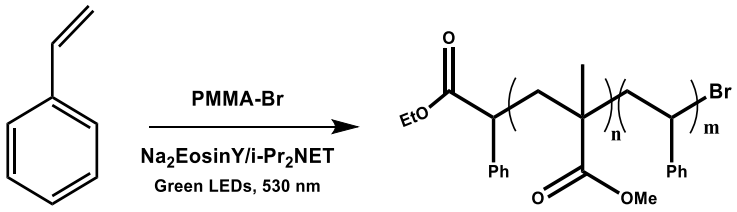

Figure 5-12 PMMA–Br copolymerization with styrene using Eosin Y in flow.

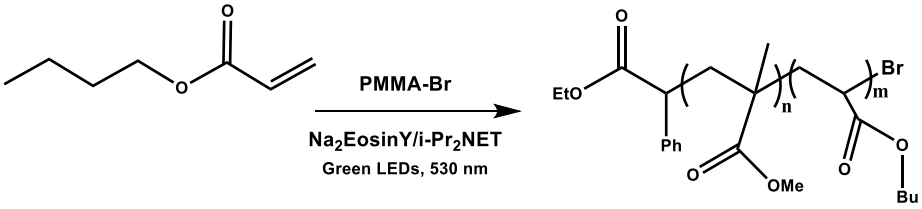

Figure 5-13 Eosin Y mediated ATRP of Buth ylacrylate using PMMA as a macroinitiator

The "livingness" of the Eosin Y photoinduced ATRP and the termination of the formed polymers by an active bromide ion were demonstrated by a copolymerization reaction of styrene with a PMMA–Br macroinitiator. The PMMA–Br macroinitiator was firstly synthesized by photoinduced ATRP in flow to get PMMA–Br (Figure 5-11, Table 5-4, entry 7, M_n = 13, 000, $Đ$ = 1.42) and then used as a macroinitiator for Eosin Y-catalyzed ATRP of styrene (St) (Figure 5-12) and butyl acrylate (BA) (Figure 5-13). The GPC traces of the macroinitiator and the corresponding copolymers are displayed in Figure 5-14**,** and the NMR spectrum of PMMA-co-PSt is represented in Figure 5-15. The results of PMMA-co-PBA (Figure 5-14**,** red trace) were not very convenient as the $Đ$ value was 2.1, which signifies a loss in control which can be attributed with the high reactivity of butylacrylate that requires strictly anhydrous and oxygen-free conditions.[432] However, the clear shift of M_n of PMMA-co-PSt to a higher molecular weight while still having a good $Đ$ (Figure 5-14, blue trace) and the presence of peaks that correspond to PSt and PMMA in the NMR spectrum indicate an

© 2020 Tous droits réservés.

effective copolymerization by reinitiation. These results of PSt copolymerization are in accordance with the literature where clear shifts to lower retention volumes were also reported by performing PMMA chain extension and copolymerization with PSt using the same condition but in batch.[429,433]

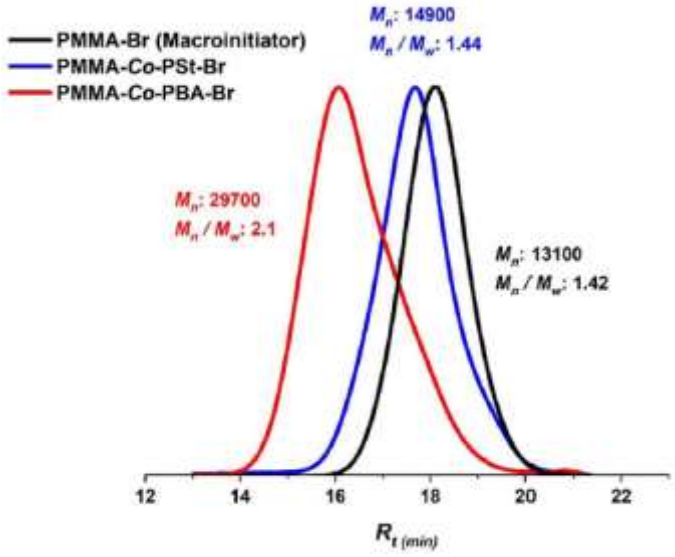

Figure 5-14 Block polymer synthesis. GPC traces of PMMA (black), PMMA-co-PSt (blue), and PMMA-co-PBA (red) block polymers.

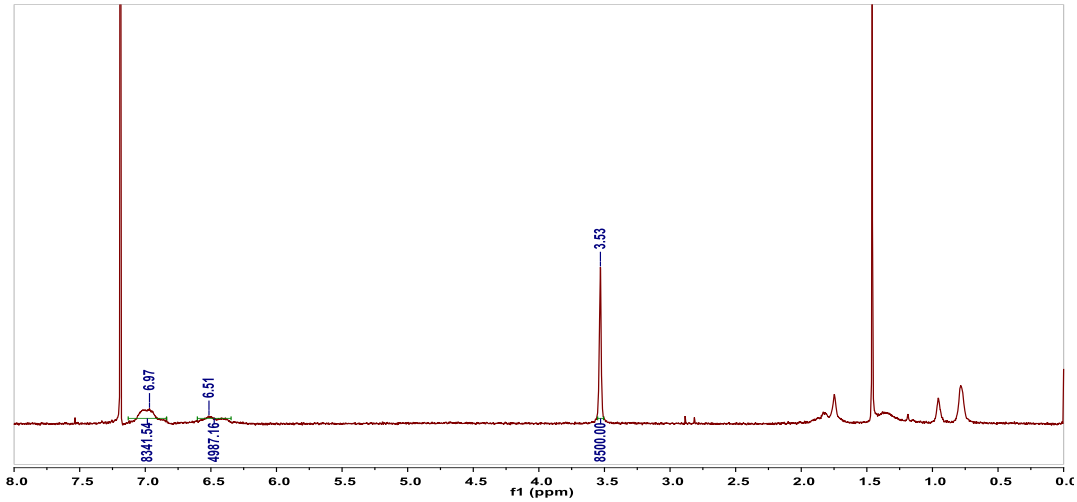

Figure 5-15 1H NMR trace of PMMA-b-PSt showing the presence of the PSt ^{1}H peaks (6.97-6.5 ppm) (3.53 ppm) after styrene addition to PMMA-Br that is catalyzed by Eosin Y in continuous

© 2020 Tous droits réservés.

5.4.3. Mechanism

The suggested mechanism of the Eosin Y-photoinduced electron transfer (PET)-ATRP is represented in Figure 5-16.[241] Upon irradiation with green LEDs, Eosin Y affords the excited state EY* which has a high oxidation potential (E^0(EY/EY*) = 1.89V). In the activation step, the electron donor, *i*-Pr_2NEt, reductively quenches EY* by a single electron transfer to form a radical anion EY•- and an amine radical cation *i*-$Pr_2N^{\bullet}$+Et intermediate (E°(*i*-Pr_2NEt/*i*-$Pr_2N^{\bullet}$+Et) ≈ 1.0V). The latter rearranges almost at a diffusion rate to the C-centered radical *i*-PrEtNC•$(CH_3)_2$ or *i*-Pr_2NCH•CH_3. The radical anion EY•−(E^0(EY•−/EY) = −1.06V), or the reductive C-centered radical (E_0(C-centered radical/iminium) = −1.12V), then transfers an electron to the alkyl bromide EB*i*B or EBPA (E^0(RX/R•+Br^-) = −0.42V and −0.20V, respectively). The EB*i*B or EBPA radical anion cleaves generating an alkyl radical that adds to the monomer-inducing propagation. In the reductive propagation step, the excited Eosin Y recaptures an electron by oxidizing either the bromide ion Br^- into bromine radical Br• (E^0(Br^-/Br•) = 1.75V), or the complex propagating radical-bromide ion by a concerted electron transfer. The bromine radical Br• deactivates propagation and forms the dormant polymer. The formed radical anion EY•− is reduced to back to EY by providing an electron to the dormant polymer, which has the same structure as a tertiary a-bromoester that reacts with the monomer. The consumption of the sacrificial amine is to compensate the irreversible terminations of the propagating cycle. In this mechanism, the very unlikely oxidation of Br^- by the radical cation *i*-$Pr_2N^{\bullet}$+Et or the chain radical oxidation to a cation is avoided; only a catalytic amount of the sacrificial amine is required to initiate the reaction. Furthermore, all of the steps have favorable redox potentials. This mechanism shows that Eosin Y has well-established activation deactivation processes that result in the control of the molecular weights and dispersities of the formed polymers.

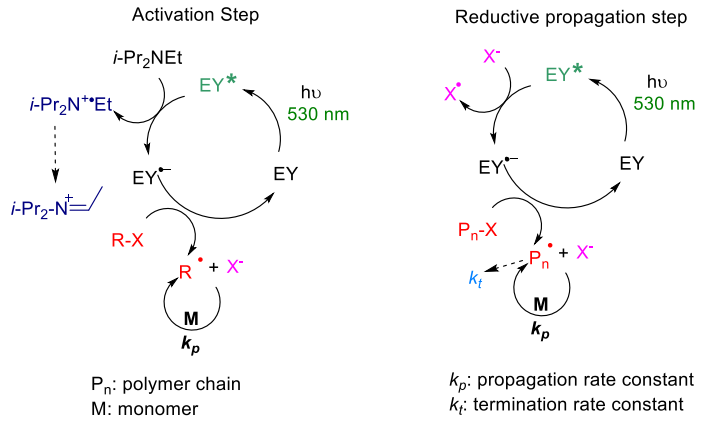

© 2020 Tous droits réservés.

Figure 5-16 Suggested photoinduced electron transfer ATRP mechanism by the Eosin Y/*i*-Pr_2NEt catalyst.

5.5. Conclusion

In conclusion, we have demonstrated that ATRP of MMA using Eosin Y as a photocatalyst in a flow reactor illuminated by green LEDs is very efficient, affording 91% of conversion in 3 h. Perfect first-order kinetics, full-initiation or dormant polymer activation, moderate dispersity, and masses in agreement with the theoretical values were obtained showing the great mechanistic and synthetic potentials of our conditions. The livingness of polymers produced via ATRP is well proved by using it as a macro-initiator in further copolymerization, which confirms their termination by Br group. The main reason for this improvement is the homogeneous illumination in flow mode.

© 2020 Tous droits réservés.

CHAPTER SIX: CONCLUSIONS

The work presented herein addressed the exploration of polymerization reactions using the microflow technology.

Chapter 1 introduced the different ways of polymerizations and the principle of microflow technology. In addition, the components of ring opening polymerization system and polycondensation were introduced. Moreover, the different catalytic systems that can be used were presented, and we ended the introduction by citing examples of the ROP and the ATRP performed in flow system.

Chapter 2 developed the *e*-ROP of lactones in flow mode. According to the outline, the immobilized lipase (N435®) on acrylic resins was shown to be an efficient catalyst for the ROP of lactones. Successful productions of ε-PCL and δ-PVL were performed using FEP tubing of *i.d.* = 1.55 mm. High conversions -up to 90%- were obtained at high and at room temperatures with narrow dispersities ($Đ_{max}$ = 1.34). As initiators, we found that primary alcohols are more efficient for the initiation than the secondary ones. The enzyme is responsible of the apparition of macrocycles in the product, so it is important to find the optimum conditions to prevent their production if possible. In addition, no reaction took place in the absence of enzyme. On the other hand, Successful co-polymerizations in flow were done via sequential addition that yielded copolymers of $Đ_{max}$ = 1.27 and conversions above 88%. Finally, in flow mode, the degradation action of the enzyme regarding poly-lactones has been improved. At the end, N 435® is well proved as a green and economic catalyst to use in polyester synthesis integrated with flow chemistry.

Chapter 3 is an extension of the previous chapter 2. But here, we investigated the ROP in flow through another catalytic pathway. In this section, PBs have been used to catalyze the ROP of lactones. The PBs differ by their basicity, from the strongest one to the weakest one: *t*-OctP_4, *t*-BuP_4, *t*-BuP_2 and BTPP. The high basicity of the catalyst contributes to high conversions and low control of the reaction, and the decrease of its basicity results in loss of conversions and better control. The best choice of catalyst was the *t*-BuP_4that gave the best compromise between the good conversion and the good control. *t*-BuP_4 catalyzed the ROP of ε-CL and generated PCL of $Đ$ = 1.64 and conversion of 95% during 60 min of residence time at 50 °C. This work can be extended to investigate the copolymerization of different lactones

© 2020 Tous droits réservés.
lilliad.univ-lille.fr

in flow mode using PBs as catalyst, considering the selectivity of phosphazene towards the different ring sizes of lactones.

Chapter 4 investigated the synthesis of polyesters by polycondensation reactions that include polyesterification and polytransesterification of diesters/diols in batch system. These reactions were catalyzed by two novel organo-based catalysts that have been studied in the literature to promote simple esterification reactions, and they are DPAT and PFPAT. We tried to find the best conditions of reaction time, temperature and reagents quantity. We successfully carried out the polycondensation between succinic acid and butanediol using DPAT as a catalyst (76% of conversion, $Đ$= 1.31) within 6 hours at 105 °C which is a mild temperature for polyesterification reaction. And we managed to reach 67% of conversion using PFPAT as catalyst within 5 hours at 105 °C ($Đ$ = 1.31). For polytransesterification reactions, the best conversion was obtained for the reaction catalyzed by DPAT which gave polyester with $Đ$ of 1.12 and 38% of monomers conversion within 6 hours at 105 °C. Thus, the study of this reaction is not ended yet, and it is still ongoing to find the conditions that permit the obtainment of high conversions and high polymer masses. Since we are interested to perform the polymerizations in flow mode due to its inherent advantages, we tried to find the suitable tubular reactor for this polymerization system that can be permeable to water. Unfortunately, the available tubular reactors offering this character are not chemically compatible with the reagents, which contribute their degradation or their modification. In perspective, we aim to test the FEP tubing but with applying the segmented mixture between anhydrous gas (like nitrogen) and the reaction media. In this way, we suggest that the anhydrous gas should absorb the water or alcohol produced as co-product and drive the reaction equilibrium forward.

Chapter 5 envisaged a good combination of the continuous flow mode and photo-induced ATRP catalyzed by metal-free catalysts to produce polymers of well-controlled masses and narrow dispersity. We focused on the investigation of Eosin Y as a metal free photo-initiator - which is a derivative of Fluorescein- for ATRP of MMA. In such a system we used EBPA and EB*i*B as an efficient initiator and the reaction started under green LEDs irradiation. As a result, we successfully produced PMMA with $Đ$ = 1.41 and conversion of 89% using EBPA as an initiator. On the other hand, PMMA with Conversion of 91% and $Đ$ = 1.42 was obtained using EB*i*B as an initiator. The livingness of polymers produced via ATRP is well proved by using it as a macro-initiator in further copolymerization, which confirms their termination by Br group. The work under flow conditions was a key step to ensure the control

© 2020 Tous droits réservés.
lilliad.univ-lille.fr

of the polymerization, where the strong illumination ensures a rapid initiation which is important to guarantee the uniform growth of polymer chains thus obtaining a low polydispersity.

So this work has confirmed the exceptional advantages of flow mode on polymer chemistry concerning the obtainment of well-controlled polymerizations and polymers with estimated masses and narrow dispersities.

© 2020 Tous droits réservés.

7. CHAPTER SEVEN: EXPERIMENTAL PART

7.1. Flow system principle

For all sections, when working with flow microreactors, we must distinguish between the residence time and the reaction time. The residence time is defined as the time spent by every molecule of the reaction mixture when remaining in the microreactor. This parameter depends on two factors, the microreactor volume and the flow rate of reaction mixture (Equation 7-1). The change of this contact time can be established easily (remaining in the same tubular reactor) by changing the flow rate of reaction mixture: smaller flow rates for longer residence times and vice versa.

$$t = v_{(reactor)}/q$$

Equation 7-1 t represents the residence time, v the reactor volume and q the flow rate

In contrary, the reaction time depends on the volume of reaction mixture to be purged within the microreactor and the flow rate (Equation 7-2). This factor can be modified by changing both the volume injected and the flow rate. For a given flow rate, and when the reactor's volume is lower than the volume of reaction mixture, the reaction time will be greater than the residence time. Generally, this is the case when working in micro-scale reactors, and this can be considered as a drawback in flow chemistry.

$$t = v_{(reaction\ mixture)}/q$$

Equation 7-2 t represents the reaction time, v the volume of reaction mixture and q the flow rate

7.2. ^{1}H NMR analysis

Proton magnetic resonance spectra (^{1}H NMR) was recorded on a Bruker AVANCE 300 spectrometer (300 MHz) using tetramethylsilane (TMS) as the internal standard. We used deuterated chloroform $CDCl_3$ as a solvent. Note that the peak of deuterated chloroform resonates at 7.23 ppm. The experiments were carried out at 293 K. Chemical shifts, δ, are given in ppm and coupling constants, J, in Hz. 1H NMR data are reported as follows: chemical shift, multiplicity (s = singlet, d =doublet, t = triplet, q = quadruplet, dd = doublet of doublets, ddd = doublet of doublet of doublets, dt = doublet of triplets, td = triplet of doublets, dp = doublet of pentuplet ddt = doublet of doublet of triplet, dtd = doublet of triplet of doublet, m = multiplet, br = broad singlet), coupling constants and integration.

© 2020 Tous droits réservés.

^{1}H NMR was used to determine the percentage of conversion. In this case, before any treatment of the crude, ^{1}NMR analysis should be done. In the presence of polymer and monomer in the crude, the % conversion will be determined by the integration of a peak corresponding to the same protons of the monomer and the polymer (Equation 7-3). For example, if we choose one of the monomer's (-CH_2) proton peaks (lactones), the same (-CH_2) proton peak should be chosen in the polymer. The distinction between the two peaks is easy to reach due to the polymer's broad peak in contrast of that of the monomer.

$$\%\ conversion = \frac{I\ polymer}{I\ monomer + I\ polymer} \times 100$$

Equation 7-3

Note that the number of protons should be the same for both the monomer and the polymer using this equation or further calculation will be necessarily required (Equation 7-4). This method is more precise because of the exclusion of polymers during precipitation and filtration.

$$\%\ conversion = \frac{\frac{I\ polymer}{nH\ polymer}}{\frac{I\ monomer}{nH\ monomer} + \frac{I\ polymer}{nH\ polymer}} \times 100$$

Equation 7-4

After the treatment of the product (precipitation, filtration and drying), the molar mass of the formed polymer can be determined by ^{1}H NMR. After the integration of the (O-CH_2) of the initiator at 3.58 ppm for 2 protons, we apply this Equation 7-5:

$$M = \left[\frac{I(CH2)\ of\ the\ polymer}{I(CH2)\ of\ the\ monomer} \times M(Lactone)\right] + M(initiator)$$

Equation 7-5

© 2020 Tous droits réservés.

7.3. NMR values of reagents and products

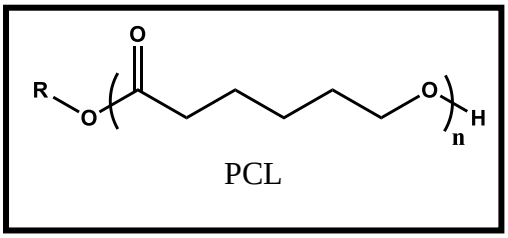

PCL

^{1}H NMR (300 MHz, $CDCl_3$) δ 3.99 (t, *J* = 6.7 Hz, 2H), 2.24 (t, *J* = 7.5 Hz, 2H), 1.64 – 1.51 (m, 4H), 1.38 – 1.25 (m, 2H).

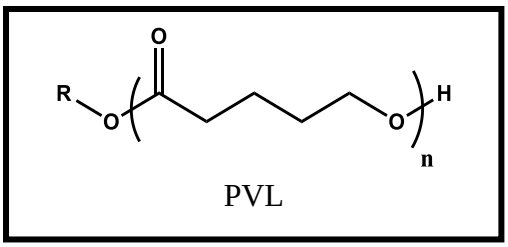

PVL

^{1}H NMR (300 MHz, $CDCl_3$) δ 4.01 (t, *J* = 5.8 Hz, 2H), 2.27 (t, *J* = 7.1 Hz, 2H), 1.62 (dd, *J* = 6.3, 3.2 Hz, 4H).

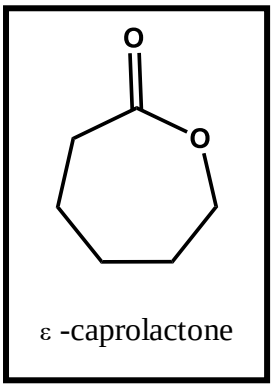

ε -caprolactone

^{1}H NMR (300 MHz, $CDCl_3$) δ 4.19 – 4.14 (m, 1H), 2.58 (dd, *J* = 9.1, 2.9 Hz, 1H), 1.84 – 1.75 (m, 1H), 1.70 (td, *J* = 4.3, 1.8 Hz, 2H)

© 2020 Tous droits réservés.

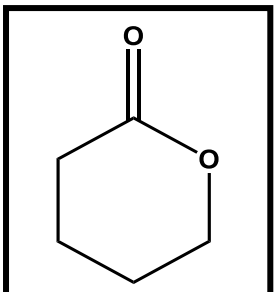

δ-valerolactone

^{1}H NMR (300 MHz, $CDCl_3$) δ 4.28 (ddd, *J* = 6.1, 5.1, 0.7 Hz, 1H), 2.49 (t, *J* = 7.1 Hz, 1H), 1.92 – 1.72 (m, 2H)

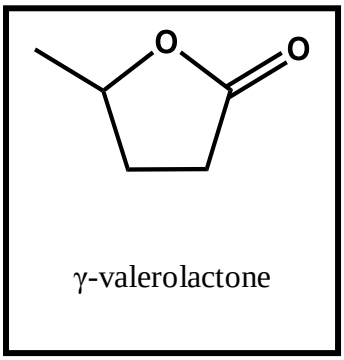

γ-valerolactone

^{1}H NMR (300 MHz, $CDCl_3$) δ 4.57 (dp, *J* = 7.8, 6.3 Hz, 1H), 2.48 (ddd, *J* = 9.2, 6.9, 1.5 Hz, 2H), 2.29 (ddt, *J* = 12.7, 7.5, 6.3 Hz, 1H), 1.76 (dtd, *J* = 12.7, 9.3, 7.8 Hz, 1H), 1.35 (d, *J* = 6.2 Hz, 3H).

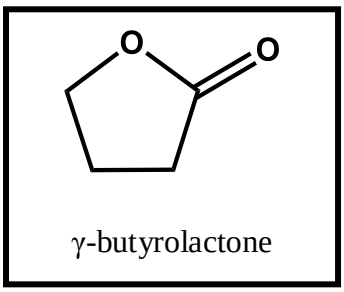

γ-butyrolactone

^{1}H NMR (300 MHz, $CDCl_3$) δ 4.28 (t, *J* = 7.0 Hz, 1H), 2.47 – 2.39 (m, 1H), 2.20 (qd, *J* = 7.2, 0.9 Hz, 1H).

© 2020 Tous droits réservés.

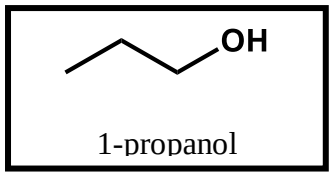

1-propanol

^{1}H NMR (300 MHz, $CDCl_3$) δ 3.54 (t, *J* = 6.7 Hz, 2H), 1.59 – 1.46 (m, 2H), 1.40 (s, 1H), 0.87 (t, *J* = 7.4 Hz, 3H).

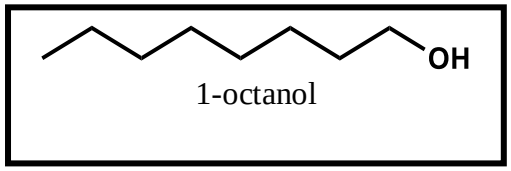

1-octanol

^{1}H NMR (300 MHz, $CDCl_3$) δ 3.57 (td, *J* = 6.6, 1.5 Hz, 2H), 1.49 (dd, *J* = 13.9, 7.1 Hz, 2H), 1.37 (s, 1H), 1.31 – 1.16 (m, 10H), 0.81 (t, *J* = 6.7 Hz, 3H).

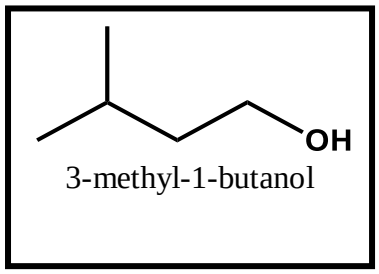

3-methyl-1-butanol

^{1}H NMR (300 MHz, $CDCl_3$) δ 3.61 (t, *J* = 6.8 Hz, 2H), 1.65 (dp, *J* = 13.4, 6.7 Hz, 1H), 1.40 (q, *J* = 6.9 Hz, 2H), 1.25 (s, 1H), 0.85 (d, *J* = 6.6 Hz, 6H).

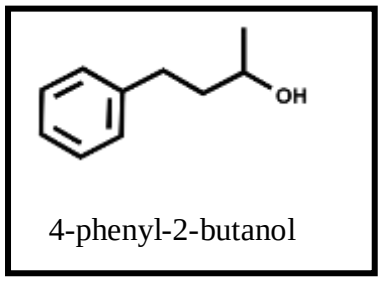

4-phenyl-2-butanol

^{1}H NMR (300 MHz, $CDCl_3$) δ 7.25 – 7.17 (m, 2H), 7.16 – 7.08 (m, 3H), 3.81 – 3.70 (m, 1H), 2.75 – 2.54 (m, 2H), 1.75 – 1.65 (m, 2H), 1.35 (s, 1H), 1.16 (d, *J* = 6.2 Hz, 3H).

© 2020 Tous droits réservés.

lilliad.univ-lille.fr

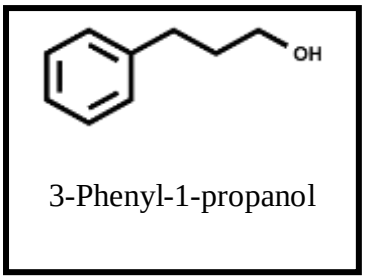

3-Phenyl-1-propanol

^{1}H NMR (300 MHz, $CDCl_3$) δ 7.24 – 7.15 (m, 2H), 7.10 (dd, *J* = 9.5, 5.0 Hz, 3H), 3.58 (t, *J* = 6.5 Hz, 2H), 2.66 – 2.58 (m, 2H), 1.86 – 1.75 (m, 2H), 1.61 (s, 1H).

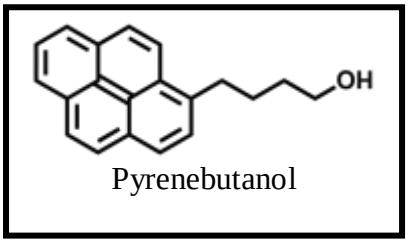

Pyrenebutanol

^{1}H NMR (300 MHz, $CDCl_3$) δ 8.22 – 7.98 (m, 66H), 3.75 (t, *J* = 6.5 Hz, 19H), 3.45 – 3.37 (m, 19H), 2.05 – 1.92 (m, 20H), 1.78 (dt, *J* = 13.0, 6.8 Hz, 20H).

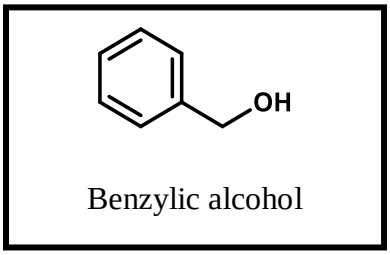

Benzylic alcohol

^{1}H NMR (300 MHz, $CDCl_3$) δ 7.30 – 7.16 (m, 5H), 4.58 (s, 2H), 1.86 (s, 1H).

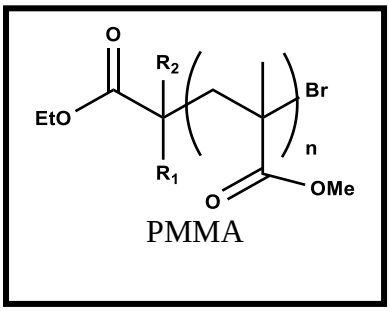

PMMA

^{1}H NMR (300 MHz, $CDCl_3$):3.72 (broad s, 3H), 1.94-2.04 (m, 2H), 1.00 (t, J = 7.2 Hz, 3H).

© 2020 Tous droits réservés.

7.4. Enzymatic ring opening polymerization in flow

7.4.1. Chemicals

The initiators: cholesterol, 3-phenyl-1-propanol (PPA), 3-methyl,1-butanol and 4-phenyl,2-butanol, propanol and octanol, the solvent: toluene and the ionization agent for MALDI-MS analyses sodium iodide (NaI) as well as the matrix Dithranol were purchased from Sigma-Aldrich®. δ-valerolactone (δ-VL) and ε-caprolactone (ε-CL) were purchased from TCI. Novozyme 435® was purchased from STREM chemicals. All products were used as received.

7.4.2. Analytical methods

Matrix assisted laser desorption ionization-time of flight mass spectra (MALDI-TOF-MS) were recorded at 20 kV on Applied Biosystems Voyager-DE™ STR mass spectrometer. Samples and NaI were dissolved in THF at 5 mg/mL and the matrix Dithranol was dissolved in THF at 15 mg/mL. These three prepared solutions were mixed in a volume ratio of 1:1:1. Then, 1 μL of the final solution was spotted on the target plate.

Mass spectrometry data acquisition was done on a SolariX XR FTICR instrument with a 9.4 T actively shielded superconducting magnet and a dynamically harmonized cell (Bruker Daltonics, Bremen, Germany). This instrument is equipped with both laser desorption ionization source (smartbeam II, Nd:YAG×3 laser at 355 nm, Bruker) and an electrospray source. Matrix-assisted laser desorption/ionization Fourier transform ion cyclotron resonance (MALDI-FT-ICR) mass spectra were acquired in positive ion mode. The mass range was adjusted to *m/z* 200–5000. The applied laser power was for 20% and 500 laser shots were accumulated for each scan. Samples and NaI were dissolved in ACN at 5 mg/mL and the matrix (Dithranol) was dissolved in THF (15 mg/mL). These three prepared solutions were mixed in a volume ratio of 1:1:1. Then, 1 μL of the final solution was spotted on the target plate.

At Mader group (Haute Borne- Villeneuve d'Ascq), the size exclusion chromatography (SEC) used was a Shimadzu Prominence fitted with a Refractive Index (RI) detector (RID-20A) and an UV detector (SPD-20A). The columns (KF-802 and KF-803L from Shodex) were eluted with tetrahydrofuran (THF) at a flow rate of 1 mL/min at 30 °C. The samples were previously prepared by dissolving 10 mg of sample in 1 mL THF. The solution was then filtered through a PTFE filter with a pore diameter of 0.45 μm. A volume of 20 μL was injected into the size exclusion chromatography to carry out the analysis. The SEC has been

© 2020 Tous droits réservés.

calibrated with poly(styrene) standards. The number average molecular weight was determined from the UV detector absorbance.

7.4.3. Enzymatic ROP of lactones in the microreator

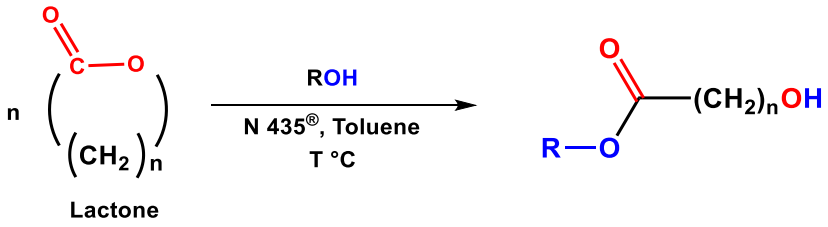

The tubular reactor with immobilized enzyme was assembled (Figure 7-1), containing one 8 mL stainless steel syringe, one syringe pump and one fluorinated ethylene propylene (FEP) tube (diameter 1.55 mm). The tube was filled with CALB and the outlet was loaded by cotton to hold the enzyme beads. The residence volume of tubular reactor was estimated by flowing toluene through the reactor. The stock solution lactone and initiator in dried toluene was prepared by using Schlenk technique under nitrogen. It was transferred into the 8 mL stainless steel syringe under nitrogen atmosphere. The enzyme pack tubular reactor was flushed with dried toluene to remove the moisture and air. The stock solution was pumped into the tubular reactor with desired flow rate, and the reactor was placed into water bath at specific temperature. The residence time was calculated respecting the flow rate and the residence volume of the tubular reactor filled by CALB. The products were collected after precipitation in the cold methanol, filtration, and drying.

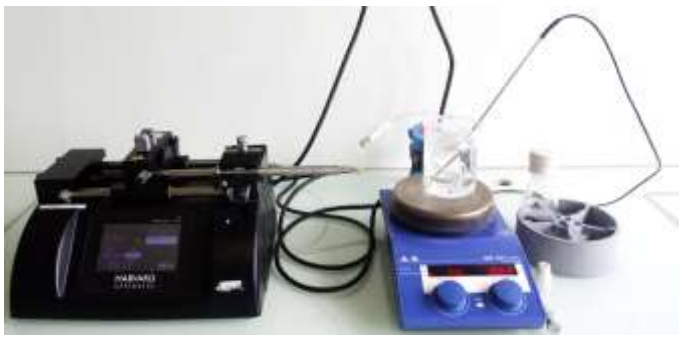

Figure 7-1 The flow system (left: the syringe pump)

© 2020 Tous droits réservés.

7.4.4. Enzymatic ROP of lactones, block copolymers in the integrated microreator system by sequential addition.

The integrated enzyme immobilized tubular reactor system was assembled, containing two 8 mL stainless steel syringes, one syringe pump, one T-type mixer, and two FEP tubes (diameter = 1.55 mm, length = 25 and 50 cm). The tubes were filled with CALB and the outlets were loaded by cotton to hold CALB beads. The residence volumes of each tubular reactor were estimated to be 0.12 and 0.2 mL, respectively by flowing toluene through the reactor. The stock solution (A) contains the first monomer (ε-caprolactone), the initiator and toluene as solvent and the stock solution (B) contains the second monomer (δ-valerolactone) and toluene as solvent. These two solutions were prepared by using Schlenk technique under nitrogen and were transferred into two 8 mL stainless steel syringes under nitrogen atmosphere. The tubular reactors were flushed with dried toluene to remove the moisture and air. The stock solutions A and B were pumped into the tubular reactor with the same flow rate. The reactors were placed into water bath at 70 °C. The residence time in the first and second reactor was calculated to be 4 and 8 min, respectively. The products were collected after precipitation in the cold methanol, filtration, and drying.

7.4.5. Degradation of polylactones

In order to verify the degradation of polylactones by the action of the enzyme, we prepared poly-caprolactone and pol-δ-valerolactone with a specific molar mass. Then, we passed 1g (in toluene) of each polymer over a tubular reactor (FEP) containing 300 mg of N435® with a residence time of 4 min at 70°C.

© 2020 Tous droits réservés.

7.5. Organo-ring opening polymerization in flow system

7.5.1. Chemicals

The catalysts phosphazene superbases : *t*-BuP_4: 0.8 M in hexane / *t*-BuP_2 2M in THF / *t*-OctP_4 1 M in hexane), the initiators: benzyl alcohol (BnOH), 3-phenyl 1-propanol (PPA), 1-propanol and cholesterol, sodium trifluoroacetate (TFA), the solvents : toluene and tetrahydrofurane (THF) were purchased from Sigma-Aldrich®. γ-valerolactone (γ-VL) and benzoic acid were purchased from Alfa Aeser. δ-valerolactone (δ-VL) and ε-caprolactone (ε-CL) were purchased from TCI.

7.5.2. Analytical methods

Matrix assisted laser desorption ionization-time of flight mass spectra (MALDI-TOF) were recorded at 20 kV on Applied Biosystems Voyager-DE^{TM} STR mass spectrometer. Samples and TFA were dissolved in THF at 5 mg/mL and the matrix Dithranol was dissolved in THF (15 mg/mL). These three prepared solutions were mixed in a volume ratio of 1:1:1. Then, 1 µL of the final solution was spotted on the target plate.

At University of Montpellier (Institut des Biomolécules Max Mousseron IBMM), Average molecular weights (*M*) and dispersities (*Đ*) were determined using size exclusion chromatography (SEC) on a Shimadzu Prominence system (*Shimadzu* Corp, Kyoto, Japan). This system is equipped with a PLgel MIXED-C guard column (Agilent, 5 µm, 50 x 7.5 mm), two mixed medium columns PLgel MIXED-C (5 µm, 300 x 7.8 mm) and a Shimadzu RI detector 20-A. The mobile phase was THF with a flow of 1 mL.min^{-1} at 35 °C. Polystyrene standards were used for calibration and polymers characteristics obtained expressed according to those standards.

7.5.3. Organo ROP of lactones in the microreator system with single entry

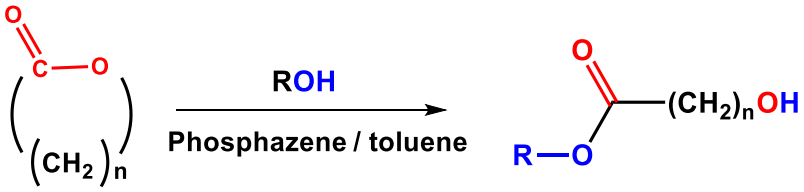

The tubular reactor was assembled (Figure 7-2, a), composed of one 8 mL stainless steel syringe, one syringe pump and one fluorinated ethylene propylene (FEP) tube (diameter = 0.8

© 2020 Tous droits réservés.

mm). The residence volume of tubular reactor was estimated by flowing toluene through the reactor. The stock solution: lactone, initiator and catalyst in dried toluene was prepared by using Schlenk technique under nitrogen. It was transferred into the 8 mL stainless steel syringe under nitrogen atmosphere. The tubular reactor was flushed with dried toluene to remove the moisture and air. The stock solution was pumped into the tubular reactor with desired flow rate, and the reactor was placed into water bath at specific temperature. The residence time was calculated respecting the flow rate and the residence volume of the tubular reactor. The reaction medium was recovered into 3 ml of benzoic acid solution in chloroform (10 mg/ml). The products were collected after precipitation in the cold methanol, filtration, and drying.

7.5.4. Organo ROP of lactones in the integrated microreator system with double entries

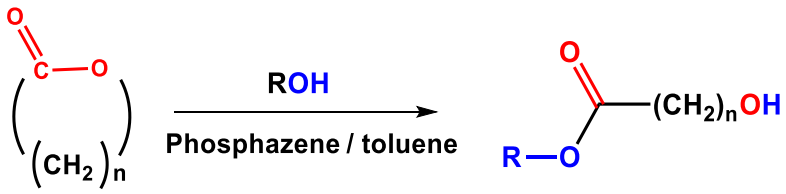

The integrated tubular reactor system was assembled (Figure 7-2, b), comprising two 8 mL stainless steel syringes, one syringe pump, and two FEP tubes of 0.8 mm internal diameter with the same length -two entries for reagents- related by one T-type mixer to the third principle tubular reactor where the reaction takes place. The residence volume of the tubular reactor was estimated by flowing toluene through the reactor where the volume of the entrance tube was eliminated. The residence time was calculated respecting the flow rate and the residence volume of the tubular reactor. The stock solution (A) contains the initiator, the catalyst and toluene as a solvent and the stock solution (B) contains the second monomer and toluene as a solvent. These two solutions were prepared by using Schlenk technique under nitrogen and were transferred into two 8 mL stainless steel syringes under nitrogen atmosphere. The tubular reactors were flushed with dried toluene to remove the moisture and air. The stock solutions A and B were pumped into the tubular reactor with the same flow rate. The reactors were placed into water bath at specific temperature. The reaction media was recovered into 3 ml of benzoic acid solution in chloroform (10 mg/ml). The products were collected after precipitation in the cold methanol, filtration, and drying.

© 2020 Tous droits réservés.

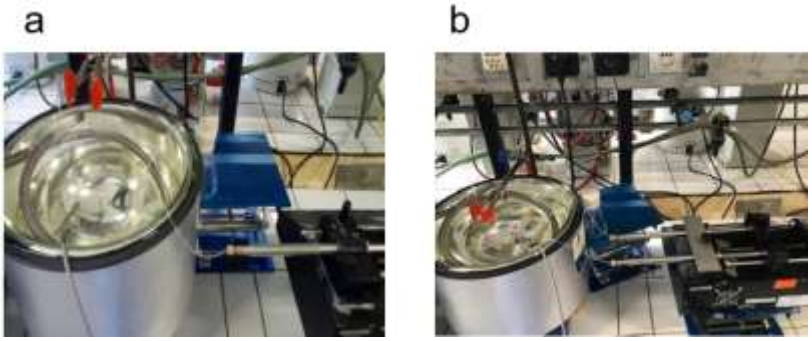

Figure 7-2 a) flow microreactor system with single entry b) flow microreactor system with double entries

7.5.5. Organo ring opening polymerization in batch

Using a shlenk tube, we prepare the mixture of initiator, catalyst and solvent under nitrogen atmosphere (Figure 7-3, a). This mixture was stirred for 10 min at room temperature. After, we put the shlenk tube in acetone bath at the desired temperature using a cryogenic system to adjust the temperature (Figure 7-3, b), and we add the monomer to the mixture.

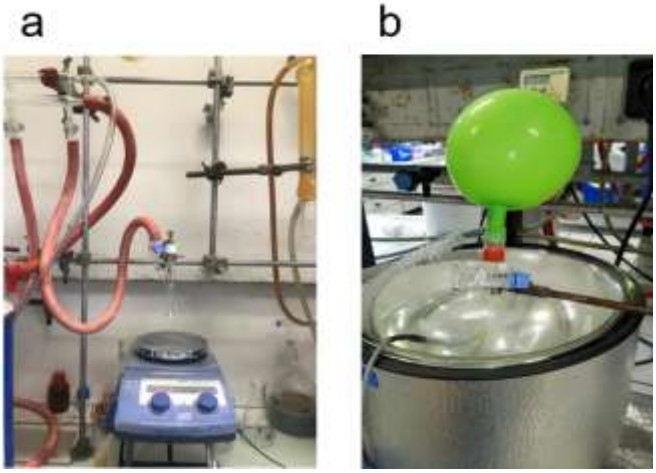

Figure 7-3 a- preparation of the mixture composed of the initiator, the catalyst and the solvent in a shlenk tube under nitrogen atmosphere b- the organo ring opening polymerization in batch under nitrogen.

© 2020 Tous droits réservés.

7.6. Polycondensation in batch and attempts in flow system.

7.6.1. Chemicals

The catalysts Diphenylammonium triflate (DPAT) and pentafluorophenylammonium triflate (PFPAT) were synthesized according to the literature,[14,15]. Succinic acid, adipic acid and DPAT were purchased from Sigma-Aldrich®. Dimethyl succinate and butanediol were purchased from TCI. All products are used as received.

7.6.2. Analytical methods

Matrix assisted laser desorption ionization-time of flight (MALDI-TOF) mass spectra were recorded at 20 kV Applied Biosystems Voyager-DE^{TM} STR mass spectrometer. Samples were dissolved in ACN and chloroform 30/70 at 10 mg/mL. NaI and the matrix DHB were dissolved in ACN/MeOH 90/10 respectively at 5 and 20 mg/mL. These three prepared solutions were mixed in a volume ratio of 1:1:1. Then, 1 µL of the final solution was spotted on the target plate.

At University of Lille (Unité Matériaux et Transformations (UMET)), size exclusion chromatography (SEC) was performed at 25°C using Agilent 1260 series pump, degasser and autosampler system equipped with Shodex K-802.5, 803 et 804 (500-400.000 g/mol) columns fitted with a Wyatt Optilab differential refractometer detector. Chloroform was used as solvent with a flow rate of 1 mL·min^{-1}. The samples were previously prepared by dissolving 4 mg of sample in 1 mL chloroform. The solution was then filtered through a PTFE filter with a pore diameter of 0.45 µm. All molecular weights (*M*) and molecular weight distributions (dispersity, Mw/Mn, D) were determined by calibration to known standard Polystyrene.

7.6.3. Polycondensation in batch system

Into a round bottom flask, the polyesters were synthesized from different equivalent moles of corresponding dicarboxylic acid or diester and diol in the presence of catalyst at 105 °C for a specific reaction time. Toluene was used as solvent. The by-product (water or methanol) was removed from the flask by azeotropic distillation of toluene with water or methanol and then fractionated by the Dean–Stark trap. The recovered mixture can be diluted if needed by chloroform. The products were collected after precipitation in the cold methanol, filtration, and drying.

© 2020 Tous droits réservés.

7.6.4. Polycondensation in Flow

The tubular reactor was assembled, which contained one 8 mL stainless steel syringe, one syringe pump and the tubular reactor. The residence volume of tubular reactor was estimated by flowing toluene through the reactor. The stock solution: diacid or diester, diol and catalyst in toluene was prepared in a round bottom flask. It was transferred into the 8 mL stainless steel syringe. The stock solution was pumped into the tubular reactor with the desired flow rate, and the reactor was placed into GC oven at specific temperature. The residence time was calculated respecting the flow rate and the residence volume of the tubular reactor. The products were collected after precipitation in the cold methanol, filtration, and drying.

7.7. Metal-free controlled polymerization in flow: Photo-Induced ATRP using EOSIN Y

7.7.1. Chemicals

Tris(2,2′-bipyridyl)ruthenium(II) chloride hexahydrate ($Ru(bpy)_3Cl_2 \cdot 6H_2O$, 99.95%) was purchased from Strem Chemicals Inc. (Newbury Port, MA, USA); Eosin Y was purchased fromAlfa Aesar (Haverhill,MA, USA); and all other reagents were purchased from Sigma-Aldrich (St. Louis, MO, USA). All solvents were purchased dry from Sigma-Aldrich (St. Louis, MO, USA) and used as received unless otherwise stated. Anhydrous N, N diisopropylethylamine (*i*-Pr_2NEt, ≥99%) was further distilled over KOH and stored in the dark under argon before usage. Methyl methacrylate (99%) was passed over alumina to remove the hydroquinone stabilizer immediately prior to use.

7.7.2. Analytical methods

At University of Montpellier (Institut des Biomolécules Max Mousseron IBMM), size exclusion chromatography (SEC) was performed at room temperature using a Viscotek GPC max system equipped with a Viscotek guard column (10 × 4.6mm) and two Viscotek columns LT 5000-L mixed medium (300 × 7.8mm) fitted with a Viscotek VE 3580 refractometric detector and a Viscotek VE 3210 UV/Vis detector. THF was used as solvent with a flow rate of 1 $mL \cdot min^{-1}$. All molecular weights (M_n) and molecular weight distributions (dispersity, M_w/M_n, D) were determined by calibration to known, standard poly(methyl methacrylate) samples purchased from Polymer Laboratories (Church Stretton, United Kingdom).

© 2020 Tous droits réservés.

7.7.3. Flow system

We used a lab designed microreactors composed of FEP tubing. The first has the following dimensions (L=3.37 m; *i.d.*= 800 µm) fitted on a metallic support which is in direct contact with the green LEDs (530 nm) (Figure 7-4).

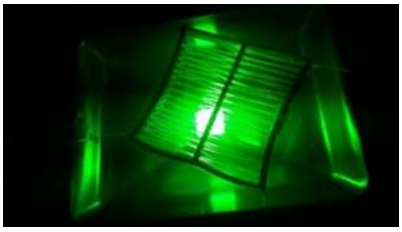

Figure 7-4 - Tubular microreactors: a *l* = 3.37m; *i.d.* = 800 µm.

7.7.4. Syringe pump

The different flow rates of performed reactions were regulated using a Harvard Apparatus (Holliston, MA, USA) PHD ULTRA CP syringe pump (Figure 7-5).

Figure 7-5 syringe pump

7.7.5. LED system

Green (λ= 530 nm) high power spots (50 W electrical power, 4500 lumen, 0.02 $W.cm^{-2}$) LED from Bridgelux (Liver-more, CA, USA) were used in photo-induced ATRP.

7.7.6. General procedure of ATRP

A Schlenk flask was charged with monomer, initiator, photo-catalyst, *i*-Pr_2NET as an electron donor species and dimethylformamide (DMF) as a solvent. The flask was sealed with rubber septum and was degassed by three freeze–vacuum–thaw cycles to remove the oxygen (Figure 7-6). Note that during freezing step the flask was purged with nitrogen gas and immersed in a bath of liquid nitrogen. The reaction mixture obtained was injected within the

© 2020 Tous droits réservés.
lilliad.univ-lille.fr

lab designed microfluidic reactor (FEP tubing, *i.d.* = 800 µm; L =3.37 m or 5m) that was placed in direct contact with the green LEDs. Depending on irradiation time, the flow rate was adjusted by the syringe pump. Note that working under oxygen free conditions was insured, even during the transfer of the reaction mixture from the Schlenk tube to the syringe (Figure 7-7). The produced polymers were precipitated, filtered, dried under vacuum and analyzed by ^{1}H NMR. A solution of 10 mg/ml in THF was prepared from the precipitated and dried polymers for further GPC analysis.

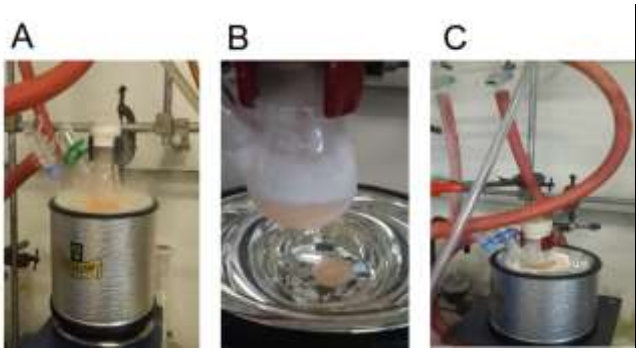

Figure 7-6 Freeze (A), Vacuum (B), Thaw (C) cycle

Figure 7-7 insuring the oxygen free condition

© 2020 Tous droits réservés.

7.7.7. Preparation of PMMA macro-initiator

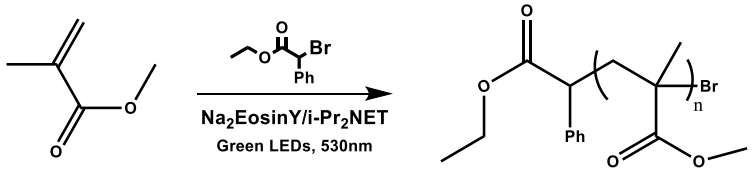

Figure 7-8 PMMA macro-initiator synthesis

EBPA (40 µL, 0.2 mmol), *i*-Pr_2NEt (371 µL, 2 mmol) and Na2Eosin Y (3 mg, 4 µmol) using the composition 200:1:0.02:10, were added to a solution of MMA (42 mmol) in DMF (8 mL, 1:1 v/v) placed in a Schlenk tube (Figure 20). The solution was degassed by three Freeze-Vacuum-Thaw cycles then transferred into the syringe that was connected to the lab designed reactor (FEP tubing, *i.d.* = 800µm.). The solution was pumped into the flow system, irradiated by green LEDs (50 W, 4500 Lumens), at a flow rate of 68 µl.min^{-1} (irradiation time = 25 min). The polymer was purified by precipitation in methanol to which some drops of water were added for catalyst elimination. The resulting macro-initiator was dried under vacuum, then analyzed by GPC to give a macro-initiator of M_n = 8723, and M_w/M_n = 1.5.

7.7.8. Chain Extension of PMMA macro-initiator with Styrene

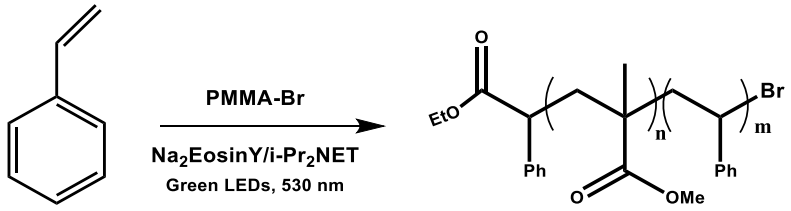

Figure 7-9 PMMA-b-PSty synthesis

PMMA macro-initiator, *i*-Pr_2NET and Na_2EosinY were combined to a solution of styrene in DMF (Figure 7-9). The solution was degassed by three Freeze-Pump-Thaw cycles then transferred into the syringe that was connected to the lab designed reactor (FEP tubing, *i.d.* = 800µm). The solution was pumped into the flow system, irradiated by green LEDs (50 W, 4500 Lumens) at a flow rate of 34 µl.min^{-1} (irradiation time = 50 min). The polymer was purified by precipitation in methanol to which are added some drops of water for catalyst

© 2020 Tous droits réservés.
lilliad.univ-lille.fr

elimination. The resulting copolymer was dried under vacuum, then analyzed by GPC to give a copolymer of M_n = 14900, and M_w/M_n = 1.44.

7.7.9. Chain Extension of PMMA macro-initiator with Buthylacrylate

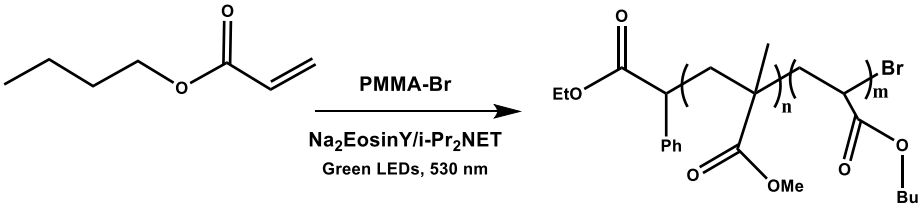

Figure 7-10 PMMA-b-PBA synthesis

PMMA macro-initiator, *i*-Pr_2NEt and Na_2EosinY were combined to a solution of buthylacrylate in DMF (Figure 7-10). The solution was degassed by three Freeze-Pump-Thaw cycles then transferred into the syringe that was connected to the lab designed reactor (FEP tubing, *i.d.* = 800µm.). The solution was pumped into the flow system, irradiated by green LEDs (50 W, 4500 Lumens) at a flow rate of 34 µl.min^{-1} (irradiation time = 50 min). The polymer was purified by precipitation in methanol to which are added some drops of water for catalyst elimination. The resulting copolymer was dried under vacuum, then analyzed by GPC to give a copolymer of M_n = 29700, and M_w/M_n = 2.1.

© 2020 Tous droits réservés.

BIBLIOGRAPHY

(1) Kobayashi, S. Lipase-Catalyzed Polyester Synthesis–a Green Polymer Chemistry. *Proc. Jpn. Acad. Ser. B* **2010**, *86* (4), 338–365.

(2) Dechy-Cabaret, O.; Martin-Vaca, B.; Bourissou, D. Controlled Ring-Opening Polymerization of Lactide and Glycolide. *Chem. Rev.* **2004**, *104* (12), 6147–6176.

(3) Zhu, N.; Gong, H.; Han, W.; Zeng, W.-B.; Wang, H.-X.; Fang, Z.; Li, X.; Zhang, K.; Li, Z.-J.; Guo, K. Synthesis and Characterization of Star-Branched Polyamide 6 via Anionic Ring-Opening Polymerization with N, N′, N ″-Trimesoyltricaprolactam as a Multifunctional Activator. *Chin. Chem. Lett.* **2015**, *26* (11), 1389–1392.

(4) Saini, R. D. Biodegradable Polymers. *Int. J. Appl. Chem.* **2017**, *13* (2), 179–196.

(5) Horváth, I. T.; Anastas, P. T. *Innovations and Green Chemistry*; ACS Publications, 2007.

(6) Casajus, H.; Saba, S.; Vlach, M.; Vène, E.; Ribault, C.; Tranchimand, S.; Nugier-Chauvin, C.; Dubreucq, E.; Loyer, P.; Cammas-Marion, S. Cell Uptake and Biocompatibility of Nanoparticles Prepared from Poly (Benzyl Malate)(Co) Polymers Obtained through Chemical and Enzymatic Polymerization in Human HepaRG Cells and Primary Macrophages. *Polymers* **2018**, *10* (11), 1244.

(7) Kobayashi, S. Enzymatic Ring-Opening Polymerization and Polycondensation for the Green Synthesis of Polyesters. *Polym. Adv. Technol.* **2015**, *26* (7), 677–686. https://doi.org/10.1002/pat.3564.

(8) Kobayashi, S.; Shoda, S.-I.; Wen, X.; Okamoto, E.; Kiyosada, T. Choroselective Enzymatic Polymerization for Synthesis of Natural Polysaccharides. *J. Macromol. Sci. Part Pure Appl. Chem.* **1997**, *34* (10), 2135–2142.

(9) Shoda, S.; Uyama, H.; Kadokawa, J.; Kimura, S.; Kobayashi, S. Enzymes as Green Catalysts for Precision Macromolecular Synthesis. *Chem. Rev.* **2016**, *116* (4), 2307–2413. https://doi.org/10.1021/acs.chemrev.5b00472.

(10) Veneral, J. G.; de Oliveira, D.; Ferreira, S. R.; Oliveira, J. V. Continuous Enzymatic Synthesis of Polycaprolactone in Packed Bed Reactor Using Pressurized Fluids. *Chem. Eng. Sci.* **2018**, *175*, 139–147.

(11) Hu, S.; Zhao, J.; Zhang, G.; Schlaad, H. Macromolecular Architectures through Organocatalysis. *Prog. Polym. Sci.* **2017**, *74*, 34–77. https://doi.org/10.1016/j.progpolymsci.2017.07.002.

(12) Schwesinger, R.; Hasenfratz, C.; Schlemper, H.; Walz, L.; Peters, E.-M.; Peters, K.; Schnering, H. G. von. How Strong and How Hindered Can Uncharged Phosphazene Bases Be? *Angew. Chem. Int. Ed. Engl.* **1993**, *32* (9), 1361–1363. https://doi.org/10.1002/anie.199313611.

(13) Schwesinger, R.; Schlemper, H. Peralkylated Polyaminophosphazenes— Extremely Strong, Neutral Nitrogen Bases. *Angew. Chem. Int. Ed. Engl.* **1987**, *26* (11), 1167–1169. https://doi.org/10.1002/anie.198711671.

(14) Wakasugi, K.; Misaki, T.; Yamada, K.; Tanabe, Y. Diphenylammonium Triflate (DPAT): Efficient Catalyst for Esterification of Carboxylic Acids and for Transesterification of Carboxylic Esters with Nearly Equimolar Amounts of Alcohols. *Tetrahedron Lett.* **2000**, *41* (27), 5249–5252. https://doi.org/10.1016/S0040-4039(00)00821-2.

(15) Funatomi, T.; Wakasugi, K.; Misaki, T.; Tanabe, Y. Pentafluorophenylammonium Triflate (PFPAT): An Efficient, Practical, and Cost-Effective Catalyst for Esterification, Thioesterification, Transesterification, and Macrolactone Formation. *Green Chem.* **2006**, *8* (12), 1022–1027. https://doi.org/10.1039/B609181B.

© 2020 Tous droits réservés.

lilliad.univ-lille.fr

(16) Burns, J. A.; Houben, C.; Anastasaki, A.; Waldron, C.; Lapkin, A. A.; Haddleton, D. M. Poly(Acrylates) via SET-LRP in a Continuous Tubular Reactor. *Polym. Chem.* **2013**, *4* (17), 4809–4813. https://doi.org/10.1039/C3PY00833A.

(17) Chen, M.; Zhong, M.; Johnson, J. A. Light-Controlled Radical Polymerization: Mechanisms, Methods, and Applications. *Chem. Rev.* **2016**, *116* (17), 10167–10211. https://doi.org/10.1021/acs.chemrev.5b00671.

(18) Cheng, C.; Khoshdel, E.; Wooley, K. L. Facile One-Pot Synthesis of Brush Polymers through Tandem Catalysis Using Grubbs' Catalyst for Both Ring-Opening Metathesis and Atom Transfer Radical Polymerizations. *Nano Lett.* **2006**, *6* (8), 1741–1746. https://doi.org/10.1021/nl0611900.

(19) Matyjaszewski, K.; Tsarevsky, N. V. Macromolecular Engineering by Atom Transfer Radical Polymerization. *J. Am. Chem. Soc.* **2014**, *136* (18), 6513–6533. https://doi.org/10.1021/ja408069v.

(20) Kwak, Y.; Magenau, A. J. D.; Matyjaszewski, K. ARGET ATRP of Methyl Acrylate with Inexpensive Ligands and Ppm Concentrations of Catalyst. *Macromolecules* **2011**, *44* (4), 811–819. https://doi.org/10.1021/ma102665c.

(21) Matyjaszewski, K.; Pintauer, T.; Gaynor, S. Removal of Copper-Based Catalyst in Atom Transfer Radical Polymerization Using Ion Exchange Resins. *Macromolecules* **2000**, *33* (4), 1476–1478. https://doi.org/10.1021/ma9911445.

(22) Shen, Y.; Zhu, S. Atom Transfer Radical Polymerization of Methyl Methacrylate Mediated by Copper Bromide−Tetraethyldiethylenetriamine Grafted on Soluble and Recoverable Poly(Ethylene-b-Ethylene Glycol) Supports. *Macromolecules* **2001**, *34* (25), 8603–8609. https://doi.org/10.1021/ma010996d.

(23) Treat, N. J.; Sprafke, H.; Kramer, J. W.; Clark, P. G.; Barton, B. E.; Read de Alaniz, J.; Fors, B. P.; Hawker, C. J. Metal-Free Atom Transfer Radical Polymerization. *J. Am. Chem. Soc.* **2014**, *136* (45), 16096–16101. https://doi.org/10.1021/ja510389m.

(24) Hessel, V.; Kralisch, D.; Kockmann, N.; Noël, T.; Wang, Q. Novel Process Windows for Enabling, Accelerating, and Uplifting Flow Chemistry. *ChemSusChem* **2013**, *6* (5), 746–789.

(25) Newman, S. G.; Jensen, K. F. The Role of Flow in Green Chemistry and Engineering. *Green Chem.* **2013**, *15* (6), 1456–1472.

(26) Protasova, L. N.; Bulut, M.; Ormerod, D.; Buekenhoudt, A.; Berton, J.; Stevens, C. V. Latest Highlights in Liquid-Phase Reactions for Organic Synthesis in Microreactors. *Org. Process Res. Dev.* **2013**, *17* (5), 760–791. https://doi.org/10.1021/op4000169.

(27) Wirth, T. *Microreactors in Organic Chemistry and Catalysis*; John Wiley & Sons, 2013.

(28) Kundu, S.; Bhangale, A. S.; Wallace, W. E.; Flynn, K. M.; Guttman, C. M.; Gross, R. A.; Beers, K. L. Continuous Flow Enzyme-Catalyzed Polymerization in a Microreactor. *J. Am. Chem. Soc.* **2011**, *133* (15), 6006–6011.

(29) Bhangale, A. S.; Beers, K. L.; Gross, R. A. Enzyme-Catalyzed Polymerization of End-Functionalized Polymers in a Microreactor. *Macromolecules* **2012**, *45* (17), 7000–7008.

(30) Hu, X.; Zhu, N.; Fang, Z.; Guo, K. Continuous Flow Ring-Opening Polymerizations. *React. Chem. Eng.* **2017**, *2* (1), 20–26.

(31) Huang, W.; Zhu, N.; Liu, Y.; Wang, J.; Zhong, J.; Sun, Q.; Sun, T.; Hu, X.; Fang, Z.; Guo, K. A Novel Microfluidic Enzyme-Organocatalysis Combination Strategy for Ring-Opening Copolymerizations of Lactone, Lactide and Cyclic Carbonate. *Chem. Eng. J.* **2019**, *356*, 592–597. https://doi.org/10.1016/j.cej.2018.09.033.

© 2020 Tous droits réservés.

lilliad.univ-lille.fr

(32) Zhu, N.; Huang, W.; Hu, X.; Liu, Y.; Fang, Z.; Guo, K. Chemoselective Polymerization Platform for Flow Synthesis of Functional Polymers and Nanoparticles. *Chem. Eng. J.* **2018**, *333*, 43–48.

(33) Zhu, N.; Huang, W.; Hu, X.; Liu, Y.; Fang, Z.; Guo, K. Enzymatic Continuous Flow Synthesis of Thiol-Terminated Poly (δ-Valerolactone) and Block Copolymers. *Macromol. Rapid Commun.* **2018**, *39* (8), 1700807.

(34) Darling, T. R.; Davis, T. P.; Fryd, M.; Gridnev, A. A.; Haddleton, D. M.; Ittel, S. D.; Matheson, R. R.; Moad, G.; Rizzardo, E. Living Polymerization: Rationale for Uniform Terminology. *J. Polym. Sci. Part Polym. Chem.* **2000**, *38* (10), 1706–1708. https://doi.org/10.1002/(SICI)1099-0518(20000515)38:10<1706::AID-POLA20>3.0.CO;2-5.

(35) Matyjaszewski, K. Atom Transfer Radical Polymerization (ATRP): Current Status and Future Perspectives. *Macromolecules* **2012**, *45* (10), 4015–4039. https://doi.org/10.1021/ma3001719.

(36) Szwarc, M. Living Polymers. Their Discovery, Characterization, and Properties. *J. Polym. Sci. Part Polym. Chem.* **1998**, *36* (1), IX–XV. https://doi.org/10.1002/(SICI)1099-0518(19980115)36:13.0.CO;2-9.

(37) Hansen, N. M. L. Synthesis of Amphiphilic Copolymwers by Atom Transfer Radical Polymerization. **2007**.

(38) Szwarc, M.; Levy, M.; Milkovich, R. POLYMERIZATION INITIATED BY ELECTRON TRANSFER TO MONOMER. A NEW METHOD OF FORMATION OF BLOCK POLYMERS1. *J. Am. Chem. Soc.* **1956**, *78* (11), 2656–2657. https://doi.org/10.1021/ja01592a101.

(39) Van Beylen, M.; Bywater, S.; Smets, G.; Szwarc, M.; Worsfold, D. J. Developments in Anionic Polymerization — A Critical Review. In *Polysiloxane Copolymers/Anionic Polymerization*; Advances in Polymer Science; Springer: Berlin, Heidelberg, 1988; pp 87–143. https://doi.org/10.1007/BFb0025275.

(40) Hadjichristidis, N.; Iatrou, H.; Pispas, S.; Pitsikalis, M. Anionic Polymerization: High Vacuum Techniques. *J. Polym. Sci. Part Polym. Chem.* **2000**, *38* (18), 3211–3234. https://doi.org/10.1002/1099-0518(20000915)38:18<3211::AID-POLA10>3.0.CO;2-L.

(41) Miyamoto, M.; Sawamoto, M.; Higashimura, T. Living Polymerization of Isobutyl Vinyl Ether with Hydrogen Iodide/Iodine Initiating System. *Macromolecules* **1984**, *17* (3), 265–268. https://doi.org/10.1021/ma00133a001.

(42) Aoshima, S.; Kanaoka, S. A Renaissance in Living Cationic Polymerization. *Chem. Rev.* **2009**, *109* (11), 5245–5287. https://doi.org/10.1021/cr900225g.

(43) Braunecker, W. A.; Matyjaszewski, K. Controlled/Living Radical Polymerization: Features, Developments, and Perspectives. *Prog. Polym. Sci.* **2007**, *32* (1), 93–146. https://doi.org/10.1016/j.progpolymsci.2006.11.002.

(44) Matyjaszewski, K. *General Concepts and History of Living Radical Polymerization*; Wiley Online Library, 2002.

(45) Chatgilialoglu, C.; Studer, A. *Encyclopedia of Radicals in Chemistry, Biology, and Materials*; John Wiley & Sons Chichester, UK:, 2012; Vol. 2.

(46) Yamago, S.; Nakamura, Y. Recent Progress in the Use of Photoirradiation in Living Radical Polymerization. *Polymer* **2013**, *54* (3), 981–994. https://doi.org/10.1016/j.polymer.2012.11.046.

(47) Matyjaszewski, K.; Xia, J. Atom Transfer Radical Polymerization. *Chem. Rev.* **2001**, *101* (9), 2921–2990. https://doi.org/10.1021/cr940534g.

© 2020 Tous droits réservés.

(48) Georges, M. K.; Veregin, R. P. N.; Kazmaier, P. M.; Hamer, G. K. Narrow Molecular Weight Resins by a Free-Radical Polymerization Process. *Macromolecules* **1993**, *26* (11), 2987–2988. https://doi.org/10.1021/ma00063a054.
(49) Hawker, C. J.; Bosman, A. W.; Harth, E. New Polymer Synthesis by Nitroxide Mediated Living Radical Polymerizations. *Chem. Rev.* **2001**, *101* (12), 3661–3688. https://doi.org/10.1021/cr990119u.
(50) Gaynor, S. G.; Wang, J.-S.; Matyjaszewski, K. Controlled Radical Polymerization by Degenerative Transfer: Effect of the Structure of the Transfer Agent. *Macromolecules* **1995**, *28* (24), 8051–8056. https://doi.org/10.1021/ma00128a012.
(51) Kato, M.; Kamigaito, M.; Sawamoto, M.; Higashimura, T. Polymerization of Methyl Methacrylate with the Carbon Tetrachloride/Dichlorotris-(Triphenylphosphine)Ruthenium(II)/Methylaluminum Bis(2,6-Di-Tert-Butylphenoxide) Initiating System: Possibility of Living Radical Polymerization. *Macromolecules* **1995**, *28* (5), 1721–1723. https://doi.org/10.1021/ma00109a056.
(52) Chiefari, J.; Chong, Y. K.; Ercole, F.; Krstina, J.; Jeffery, J.; Le, T. P.; Mayadunne, R. T.; Meijs, G. F.; Moad, C. L.; Moad, G. Living Free-Radical Polymerization by Reversible Addition- Fragmentation Chain Transfer: The RAFT Process. *Macromolecules* **1998**, *31* (16), 5559–5562.
(53) Lowe, A. B.; McCormick, C. L. Reversible Addition–Fragmentation Chain Transfer (RAFT) Radical Polymerization and the Synthesis of Water-Soluble (Co)Polymers under Homogeneous Conditions in Organic and Aqueous Media. *Prog. Polym. Sci.* **2007**, *32* (3), 283–351. https://doi.org/10.1016/j.progpolymsci.2006.11.003.
(54) Moad, G.; Mayadunne, R. T. A.; Rizzardo, E.; Skidmore, M.; Thang, S. H. Synthesis of Novel Architectures by Radical Polymerization with Reversible Addition Fragmentation Chain Transfer (RAFT Polymerization). *Macromol. Symp.* **2003**, *192* (1), 1–12. https://doi.org/10.1002/masy.200390029.
(55) Carothers, W. H.; Natta, F. V. Studies on Polymerization and Ring Formation. III. Glycol Esters of Carbonic Acid. *J. Am. Chem. Soc.* **1930**, *52* (1), 314–326.
(56) Anastas, P. T.; Warner, J. C. Green Chemistry: Theory and Practice. *Oxf. Univ. Press Oxf.* **1998**.
(57) Kobayashi, S. Enzymatic Polymerization. *Encycl. Polym. Sci. Technol.* **2002**.
(58) Kobayashi, S. Enzymatic Polymerization: A New Method of Polymer Synthesis. *J. Polym. Sci. Part Polym. Chem.* **1999**, *37* (16), 3041–3056. https://doi.org/10.1002/(SICI)1099-0518(19990815)37:16<3041::AID-POLA1>3.0.CO;2-V.
(59) Kobayashi, S.; Ritter, H.; Kaplan, D. *Enzyme-Catalyzed Synthesis of Polymers*; Springer Science & Business Media, 2006.
(60) Kobayashi, S.; Uyama, H.; Ohmae, M. Enzymatic Polymerization for Precision Polymer Synthesis. *Bull. Chem. Soc. Jpn.* **2001**, *74* (4), 613–635. https://doi.org/10.1246/bcsj.74.613.
(61) Kobayashi, S.; Shoda, S.; Uyama, H. Enzymatic Polymerization and Oligomerization. In *Polymer Synthesis/Polymer Engineering*; Advances in Polymer Science; Springer: Berlin, Heidelberg, 1995; pp 1–30.
(62) Kobayashi, S.; 1941-. *Catalysis in Precision Polymerization*; John Wiley, 1997.
(63) Kobayashi, S.; Makino, A. Enzymatic Polymer Synthesis: An Opportunity for Green Polymer Chemistry. *Chem. Rev.* **2009**, *109* (11), 5288–5353. https://doi.org/10.1021/cr900165z.
(64) Kobayashi, S.; Ohmae, M. Polymer Synthesis and Modification by Enzymatic Catalysis. *Macromol. Eng. Precise Synth. Mater. Prop. Appl.* **2007**, 401–477.

© 2020 Tous droits réservés.
lilliad.univ-lille.fr

(65) Payen, A.; Persoz, J. F. Memoir on Diastase, the Principal Products of Its Reactions, and Their Applications to the Industrial Arts. *Ann Chim Phys* **1833**, *53*, 73–92.
(66) Webb, E. C. *Enzyme Nomenclature 1992. Recommendations of the Nomenclature Committee of the International Union of Biochemistry and Molecular Biology on the Nomenclature and Classification of Enzymes.*; Academic Press, 1992.
(67) Fischer, E. Einfluss Der Configuration Auf Die Wirkung Der Enzyme. Ber Dtsch Chem Ges 27: 2985–2993. *Trans Holmstedt B Liljestrand G Eds Read. Pharmacol. 1963* **1894**, *251*.
(68) Kollman, P. A.; Kuhn, B.; Donini, O.; Perakyla, M.; Stanton, R.; Bakowies, D. Elucidating the Nature of Enzyme Catalysis Utilizing a New Twist on an Old Methodology: Quantum Mechanical- Free Energy Calculations on Chemical Reactions in Enzymes and in Aqueous Solution. *Acc. Chem. Res.* **2001**, *34* (1), 72–79.
(69) Pauling, L. Molecular Architecture and Biological Reactions. *Chem. Eng. News* **1946**, *24* (10), 1375–1377.
(70) Borman, S. Much Ado about Enzyme Mechanisms. *Chem. Eng. News* **2004**, *82* (8), 35–35.
(71) Kobayashi, S. Recent Developments in Lipase-Catalyzed Synthesis of Polyesters. *Macromol. Rapid Commun.* **2009**, *30* (4–5), 237–266.
(72) Kobayashi, S. Green Polymer Chemistry: Recent Developments. In *Hierarchical Macromolecular Structures: 60 Years after the Staudinger Nobel Prize II*; Springer, 2013; pp 141–166.
(73) Anderson, E. M.; Larsson, K. M.; Kirk, O. One Biocatalyst–Many Applications: The Use of Candida Antarctica B-Lipase in Organic Synthesis. *Biocatal. Biotransformation* **1998**, *16* (3), 181–204.
(74) Uppenberg, J.; Hansen, M. T.; Patkar, S.; Jones, T. A. The Sequence, Crystal Structure Determination and Refinement of Two Crystal Forms of Lipase B from Candida Antarctica. *Structure* **1994**, *2* (4), 293–308.
(75) Namekawa, S.; Suda, S.; Uyama, H.; Kobayashi, S. Lipase-Catalyzed Ring-Opening Polymerization of Lactones to Polyesters and Its Mechanistic Aspects. *Int. J. Biol. Macromol.* **1999**, *25* (1–3), 145–151.
(76) Uyama, H.; Namekawa, S.; Kobayash, S. Mechanistic Studies on the Lipase-Catalyzed Ring-Opening Polymerization of Lactones. *Polym. J.* **1997**, *29* (3), 299–301. https://doi.org/10.1295/polymj.29.299.
(77) Duda, A.; Kowalski, A.; Penczek, S.; Uyama, H.; Kobayashi, S. Kinetics of the Ring-Opening Polymerization of 6-, 7-, 9-, 12-, 13-, 16-, and 17-Membered Lactones. Comparison of Chemical and Enzymatic Polymerizations. *Macromolecules* **2002**, *35* (11), 4266–4270.
(78) Kikuchi, H.; Uyama, H.; Kobayashi, S. Lipase-Catalyzed Enantioselective Copolymerization of Substituted Lactones to Optically Active Polyesters. *Macromolecules* **2000**, *33* (24), 8971–8975.
(79) Kobayashi, S. Enzymatic Ring-Opening Polymerization of Lactones by Lipase Catalyst: Mechanistic Aspects. *Macromol. Symp.* **2006**, *240* (1), 178–185. https://doi.org/10.1002/masy.200650822.
(80) Kobayashi, S.; Uyama, H.; Namekawa, S. In Vitro Biosynthesis of Polyesters with Isolated Enzymes in Aqueous Systems and Organic Solvents. *Polym. Degrad. Stab.* **1998**, *59* (1), 195–201. https://doi.org/10.1016/S0141-3910(97)00178-X.
(81) Kobayashi, S.; Uyama, H. Enantioselective and Regioselective Polymerization with Lipase Catalysis to Polyesters; ACS Publications, 2003.

© 2020 Tous droits réservés.
lilliad.univ-lille.fr

(82) Uyama, H.; Kikuchi, H.; Takeya, K.; Kabayashi, S. Lipase-Catalyzed Ring-Opening Polymerization and Copolymerization of 15-Pentadecanolide. *Acta Polym.* **1996**, *47* (8), 357–360. https://doi.org/10.1002/actp.1996.010470807.

(83) van der Mee, L.; Helmich, F.; de Bruijn, R.; Vekemans, J. A. J. M.; Palmans, A. R. A.; Meijer, E. W. Investigation of Lipase-Catalyzed Ring-Opening Polymerizations of Lactones with Various Ring Sizes: Kinetic Evaluation. *Macromolecules* **2006**, *39* (15), 5021–5027. https://doi.org/10.1021/ma060668j.

(84) Uyama, H.; Suda, S.; Kobayashi, S. Enzymatic Synthesis of Terminal-Functionalized Polyesters by Initiator Method. *Acta Polym.* **1998**, *49* (12), 700–703.

(85) Uyama, H.; Kobayashi, S.; Morita, M.; Habaue, S.; Okamoto, Y. Chemoselective Ring-Opening Polymerization of a Lactone Having e Xo-Methylene Group with Lipase Catalysis. *Macromolecules* **2001**, *34* (19), 6554–6556.

(86) Uyama, H.; Kikuchi, H.; Kobayashi, S. Single-Step Acylation of Polyester Terminals by Enzymatic Ring-Opening Polymerization of 12-Dodecanolide in the Presence of Acyclic Vinyl Esters. *Bull. Chem. Soc. Jpn.* **1997**, *70* (7), 1691–1695.

(87) Uyama, H.; Kikuchi, H.; Kobayashi, S. One-Shot Synthesis of Polyester Macromonomer by Enzymatic Ring-Opening Polymerization of Lactone in the Presence of Vinyl Ester. *Chem. Lett.* **1995**, *24* (11), 1047–1048.

(88) Habaue, S.; Asai, M.; Morita, M.; Okamoto, Y.; Uyama, H.; Kobayashi, S. Chemospecific Ring-Opening Polymerization of α-Methylenemacrolides. *Polymer* **2003**, *44* (18), 5195–5200.

(89) Puskas, J. E.; Sen, M. Y.; Seo, K. S. Green Polymer Chemistry Using Nature's Catalysts, Enzymes. *J. Polym. Sci. Part Polym. Chem.* **2009**, *47* (12), 2959–2976.

(90) Kobayashi, S.; Uyama, H.; Takamoto, T. Lipase-Catalyzed Degradation of Polyesters in Organic Solvents. A New Methodology of Polymer Recycling Using Enzyme as Catalyst. *Biomacromolecules* **2000**, *1* (1), 3–5.

(91) Matsumura, S.; Ebata, H.; Toshima, K. A New Strategy for Sustainable Polymer Recycling Using an Enzyme: Poly(ε-Caprolactone). *Macromol. Rapid Commun.* **2000**, *21* (12), 860–863. https://doi.org/10.1002/1521-3927(20000801)21:12<860::AID-MARC860>3.0.CO;2-U.

(92) Soeda, Y.; Toshima, K.; Matsumura, S. Synthesis and Chemical Recycling of Novel Poly (Ester-Urethane) s Using an Enzyme. *Macromol. Biosci.* **2005**, *5* (4), 277–288.

(93) Eubeler, J. P.; Bernhard, M.; Knepper, T. P. Environmental Biodegradation of Synthetic Polymers II. Biodegradation of Different Polymer Groups. *TrAC Trends Anal. Chem.* **2010**, *29* (1), 84–100. https://doi.org/10.1016/j.trac.2009.09.005.

(94) Kundys, A.; Bia\lecka-Florjańczyk, E.; Fabiszewska, A.; Ma\lajowicz, J. Candida Antarctica Lipase B as Catalyst for Cyclic Esters Synthesis, Their Polymerization and Degradation of Aliphatic Polyesters. *J. Polym. Environ.* **2018**, *26* (1), 396–407.

(95) Lucas, N.; Bienaime, C.; Belloy, C.; Queneudec, M.; Silvestre, F.; Nava-Saucedo, J.-E. Polymer Biodegradation: Mechanisms and Estimation Techniques – A Review. *Chemosphere* **2008**, *73* (4), 429–442. https://doi.org/10.1016/j.chemosphere.2008.06.064.

(96) Takahashi, Y.; Okajima, S.; Toshima, K.; Matsumura, S. Lipase-Catalyzed Transformation of Poly(Lactic Acid) into Cyclic Oligomers. *Macromol. Biosci.* **2004**, *4* (3), 346–353. https://doi.org/10.1002/mabi.200300094.

(97) Okajima, S.; Kondo, R.; Toshima, K.; Matsumura, S. Lipase-Catalyzed Transformation of Poly(Butylene Adipate) and Poly(Butylene Succinate) into Repolymerizable Cyclic Oligomers. *Biomacromolecules* **2003**, *4* (6), 1514–1519. https://doi.org/10.1021/bm034043u.

© 2020 Tous droits réservés.

lilliad.univ-lille.fr

(98) Osanai, Y.; Toshima, K.; Matsumura, S. Transformation of Biodegradable Polyesters into Cyclic Oligomers under Continuous Flow Using an Enzyme-Packed Column. *Macromol. Biosci.* **2004**, *4* (10), 936–942. https://doi.org/10.1002/mabi.200400046.

(99) Osanai, Y.; Toshima, K.; Yoshie, N.; Inoue, Y.; Matsumura, S. Lipase-Catalyzed Transformation of Unnatural-Type Poly(3-Hydroxybutanoate) into Reactive Cyclic Oligomer. *Macromol. Biosci.* **2002**, *2* (2), 88–94. https://doi.org/10.1002/1616-5195(20020201)2:2<88::AID-MABI88>3.0.CO;2-5.

(100) Shimokawa, K.; Kato, M.; Matsumura, S. Enzymatic Synthesis and Chemical Recycling of Polythiocaprolactone. *Macromol. Chem. Phys.* **2011**, *212* (2), 150–158. https://doi.org/10.1002/macp.201000488.

(101) Osanai, Y.; Toshima, K.; Matsumura, S. Enzymatic Degradation of Poly(R,S-3-Hydroxybutanoate) to Cyclic Oligomers under Continuous Flow. *Green Chem.* **2003**, *5* (5), 567–570. https://doi.org/10.1039/B304640K.

(102) Matsumura, S.; Harai, S.; Toshima, K. Lipase-Catalyzed Transformation of Poly(Trimethylene Carbonate) into Cyclic Monomer, Trimethylene Carbonate: A New Strategy for Sustainable Polymer Recycling Using an Enzyme. *Macromol. Rapid Commun.* **2001**, *22* (3), 215–218. https://doi.org/10.1002/1521-3927(200102)22:3<215::AID-MARC215>3.0.CO;2-#.

(103) Liu, F.; Yang, J.; Fan, Z.; Li, S.; Kasperczyk, J.; Dobrzynski, P. Enzyme-Catalyzed Degradation of Biodegradable Polymers Derived from Trimethylene Carbonate and Glycolide by Lipases from Candida Antarctica and Hog Pancreas. *J. Biomater. Sci. Polym. Ed.* **2012**, *23* (10), 1355–1368. https://doi.org/10.1163/092050611X581525.

(104) Ganesh, M.; Dave, R. N.; L'Amoreaux, W.; Gross, R. A. Embedded Enzymatic Biomaterial Degradation. *Macromolecules* **2009**, *42* (18), 6836–6839. https://doi.org/10.1021/ma901481h.

(105) Ganesh, M.; Gross, R. A. Embedded Enzymatic Biomaterial Degradation: Flow Conditions & Relative Humidity. *Polymer* **2012**, *53* (16), 3454–3461. https://doi.org/10.1016/j.polymer.2012.06.017.

(106) Orozco-Castellanos, L. M.; Marcos-Fernández, A.; Martínez-Richa, A. Hydrolytic Degradation of Poly(ε-Caprolactone) with Different End Groups and Poly(ε-Caprolactone-Co-γ-Butyrolactone): Characterization and Kinetics of Hydrocortisone Delivery. *Polym. Adv. Technol.* **2011**, *22* (4), 430–436. https://doi.org/10.1002/pat.1531.

(107) Gunatillake, P.; Mayadunne, R.; Adhikari, R. Recent Developments in Biodegradable Synthetic Polymers. In *Biotechnology Annual Review*; El-Gewely, M. R., Ed.; Elsevier, 2006; Vol. 12, pp 301–347. https://doi.org/10.1016/S1387-2656(06)12009-8.

(108) Moad, G.; Rizzardo, E.; Solomon, D. H. Selectivity of the Reaction of Free Radicals with Styrene. *Macromolecules* **1982**, *15* (3), 909–914.

(109) Mougnier, S.-J.; Brochon, C.; Cloutet, E.; Magnet, S.; Navarro, C.; Hadziioannou, G. Facile and Versatile Synthesis of Rod-Coil Poly(3-Hexylthiophene)-Based Block Copolymers by Nitroxide-Mediated Radical Polymerization. *J. Polym. Sci. Part Polym. Chem.* **2012**, *50* (12), 2463–2470. https://doi.org/10.1002/pola.26023.

(110) Delduc, P.; Tailhan, C.; Zard, S. Z. A Convenient Source of Alkyl and Acyl Radicals. *J. Chem. Soc. Chem. Commun.* **1988**, No. 4, 308–310. https://doi.org/10.1039/C39880000308.

(111) Destarac, M.; Bzducha, W.; Taton, D.; Gauthier-Gillaizeau, I.; Zard, S. Z. Xanthates as Chain-Transfer Agents in Controlled Radical Polymerization (MADIX): Structural Effect of the O-Alkyl Group. *Macromol. Rapid Commun.* **2002**, *23* (17), 1049–1054. https://doi.org/10.1002/marc.200290002.

© 2020 Tous droits réservés.

lilliad.univ-lille.fr

(112) Perrier, S.; Takolpuckdee, P. Macromolecular Design via Reversible Addition–Fragmentation Chain Transfer (RAFT)/Xanthates (MADIX) Polymerization. *J. Polym. Sci. Part Polym. Chem.* **2005**, *43* (22), 5347–5393. https://doi.org/10.1002/pola.20986.

(113) Ramsey, B. L.; Pearson, R. M.; Beck, L. R.; Miyake, G. M. Photoinduced Organocatalyzed Atom Transfer Radical Polymerization Using Continuous Flow. *Macromolecules* **2017**, *50* (7), 2668–2674. https://doi.org/10.1021/acs.macromol.6b02791.

(114) Hansen, N. M. L.; Haddleton, D. M.; Hvilsted, S. Fluorinated Bio-Acceptable Polymers via an ATRP Macroinitiator Approach. *J. Polym. Sci. Part Polym. Chem.* **2007**, *45* (24), 5770–5780. https://doi.org/10.1002/pola.22326.

(115) Bednarek, M.; Jankova, K.; Hvilsted, S. Novel Polymers Based on Atom Transfer Radical Polymerization of 2-Methoxyethyl Acrylate. *J. Polym. Sci. Part Polym. Chem.* **2007**, *45* (3), 333–340. https://doi.org/10.1002/pola.21784.

(116) Kabachii, Y. A.; Kochev, S. Y.; Bronstein, L. M.; Blagodatskikh, I. B.; Valetsky, P. M. Atom Transfer Radical Polymerization with Ti(III) Halides and Alkoxides. *Polym. Bull.* **2003**, *50* (4), 271–278. https://doi.org/10.1007/s00289-003-0157-9.

(117) Le Grognec, E.; Claverie, J.; Poli, R. Radical Polymerization of Styrene Controlled by Half-Sandwich Mo(III)/Mo(IV) Couples: All Basic Mechanisms Are Possible. *J. Am. Chem. Soc.* **2001**, *123* (39), 9513–9524. https://doi.org/10.1021/ja010998d.

(118) Maria, S.; Stoffelbach, F.; Mata, J.; Daran, J.-C.; Richard, P.; Poli, R. The Radical Trap in Atom Transfer Radical Polymerization Need Not Be Thermodynamically Stable. A Study of the MoX3(PMe3)3 Catalysts. *J. Am. Chem. Soc.* **2005**, *127* (16), 5946–5956. https://doi.org/10.1021/ja043078e.

(119) Kotani, Y.; Kamigaito, M.; Sawamoto, M. Re(V)-Mediated Living Radical Polymerization of Styrene: ReO2I(PPh3)2/R−I Initiating Systems. *Macromolecules* **1999**, *32* (8), 2420–2424. https://doi.org/10.1021/ma981614f.

(120) Matyjaszewski, K.; Wei, M.; Xia, J.; McDermott, N. E. Controlled/"Living" Radical Polymerization of Styrene and Methyl Methacrylate Catalyzed by Iron Complexes. *Macromolecules* **1997**, *30* (26), 8161–8164. https://doi.org/10.1021/ma971010w.

(121) Teodorescu, M.; Gaynor, S. G.; Matyjaszewski, K. Halide Anions as Ligands in Iron-Mediated Atom Transfer Radical Polymerization. *Macromolecules* **2000**, *33* (7), 2335–2339. https://doi.org/10.1021/ma991652e.

(122) Simal, F.; Demonceau, A.; Noels, A. F. Highly Efficient Ruthenium-Based Catalytic Systems for the Controlled Free-Radical Polymerization of Vinyl Monomers. *Angew. Chem. Int. Ed.* **1999**, *38* (4), 538–540. https://doi.org/10.1002/(SICI)1521-3773(19990215)38:4<538::AID-ANIE538>3.0.CO;2-W.

(123) Braunecker, W. A.; Itami, Y.; Matyjaszewski, K. Osmium-Mediated Radical Polymerization. *Macromolecules* **2005**, *38* (23), 9402–9404. https://doi.org/10.1021/ma051877r.

(124) Percec, V.; Barboiu, B.; Neumann, A.; Ronda, J. C.; Zhao, M. Metal-Catalyzed "Living" Radical Polymerization of Styrene Initiated with Arenesulfonyl Chlorides. From Heterogeneous to Homogeneous Catalysis. *Macromolecules* **1996**, *29* (10), 3665–3668. https://doi.org/10.1021/ma960061a.

(125) Wang, B.; Zhuang, Y.; Luo, X.; Xu, S.; Zhou, X. Controlled/"Living" Radical Polymerization of MMA Catalyzed by Cobaltocene. *Macromolecules* **2003**, *36* (26), 9684–9686. https://doi.org/10.1021/ma035334y.

(126) Granel, C.; Dubois, Ph.; Jérôme, R.; Teyssié, Ph. Controlled Radical Polymerization of Methacrylic Monomers in the Presence of a Bis(Ortho-Chelated) Arylnickel(II)

© 2020 Tous droits réservés.

lilliad.univ-lille.fr

Complex and Different Activated Alkyl Halides. *Macromolecules* **1996**, *29* (27), 8576–8582. https://doi.org/10.1021/ma9608380.

(127) Uegaki, H.; Kotani, Y.; Kamigaito, M.; Sawamoto, M. NiBr2(Pn-Bu3)2-Mediated Living Radical Polymerization of Methacrylates and Acrylates and Their Block or Random Copolymerizations. *Macromolecules* **1998**, *31* (20), 6756–6761. https://doi.org/10.1021/ma9805957.

(128) Lecomte, Ph.; Drapier, I.; Dubois, Ph.; Teyssié, Ph.; Jérôme, R. Controlled Radical Polymerization of Methyl Methacrylate in the Presence of Palladium Acetate, Triphenylphosphine, and Carbon Tetrachloride. *Macromolecules* **1997**, *30* (24), 7631–7633. https://doi.org/10.1021/ma970890b.

(129) Wang, J.-S.; Matyjaszewski, K. Controlled/" Living" Radical Polymerization. Atom Transfer Radical Polymerization in the Presence of Transition-Metal Complexes. *J. Am. Chem. Soc.* **1995**, *117* (20), 5614–5615.

(130) Matyjaszewski, K. Controlled Radical Polymerization: State-of-the-Art in 2014. In *Controlled Radical Polymerization: Mechanisms*; ACS Symposium Series; American Chemical Society, 2015; Vol. 1187, pp 1–17. https://doi.org/10.1021/bk-2015-1187.ch001.

(131) Davis, K.; OMalley, J.; Paik, H. J.; Matyjaszewski, K. Effect of the Counteranion in Atom Transfer Radical Polymerization Using Alkyl (Pseudo) Halide Initiators. In *ABSTRACTS OF PAPERS OF THE AMERICAN CHEMICAL SOCIETY*; AMER CHEMICAL SOC 1155 16TH ST, NW, WASHINGTON, DC 20036, 1997; Vol. 213, pp 320–POLY.

(132) Kotani, Y.; Kamigaito, M.; Sawamoto, M. Living Radical Polymerization of Para-Substituted Styrenes and Synthesis of Styrene-Based Copolymers with Rhenium and Iron Complex Catalysts. *Macromolecules* **2000**, *33* (18), 6746–6751. https://doi.org/10.1021/ma000624p.

(133) Tang, W.; Matyjaszewski, K. Effects of Initiator Structure on Activation Rate Constants in ATRP. *Macromolecules* **2007**, *40* (6), 1858–1863. https://doi.org/10.1021/ma062897b.

(134) Golas, P. L.; Tsarevsky, N. V.; Sumerlin, B. S.; Matyjaszewski, K. Catalyst Performance in “Click” Coupling Reactions of Polymers Prepared by ATRP: Ligand and Metal Effects. *Macromolecules* **2006**, *39* (19), 6451–6457. https://doi.org/10.1021/ma061592u.

(135) Xia, J.; Zhang, X.; Matyjaszewski, K. The Effect of Ligands on Copper-Mediated Atom Transfer Radical Polymerization. In *Transition Metal Catalysis in Macromolecular Design*; ACS Symposium Series; American Chemical Society, 2000; Vol. 760, pp 207–223. https://doi.org/10.1021/bk-2000-0760.ch013.

(136) Evchuk, I. Y.; Musii, R. I.; Makitra, R. G.; Pristanskii, R. E. Solubility of Polymethyl Methacrylate in Organic Solvents. *Russ. J. Appl. Chem.* **2005**, *78* (10), 1576–1580.

(137) Wang, J. S.; Greszta, D.; Matyjaszewski, K. Atom-Transfer Radical Polymerization (Atrp)-a New Approach Towards Well-Defined (Co) Polymers. In *ABSTRACTS OF PAPERS OF THE AMERICAN CHEMICAL SOCIETY*; AMER CHEMICAL SOC PO BOX 57136, WASHINGTON, DC 20037-0136, 1995; Vol. 210, pp 227–PMSE.

(138) Fernández-García, M.; Fuente, J. L. D. L.; Fernández-Sanz, M.; Madruga, E. L. Synthesis and Characterization of PMMA-b-PBMA Block Copolymers by Atom Transfer Radical Polymerization. *J. Appl. Polym. Sci.* **2002**, *84* (14), 2683–2691. https://doi.org/10.1002/app.10471.

(139) Shipp, D. A.; Wang, J.-L.; Matyjaszewski, K. Synthesis of Acrylate and Methacrylate Block Copolymers Using Atom Transfer Radical Polymerization. *Macromolecules* **1998**, *31* (23), 8005–8008. https://doi.org/10.1021/ma981033q.

© 2020 Tous droits réservés.

lilliad.univ-lille.fr

(140) Zhang, Z.-B.; Ying, S.-K.; Shi, Z.-Q. Synthesis of Fluorine-Containing Block Copolymers via ATRP 2. Synthesis and Characterization of Semifluorinated Di- and Triblock Copolymers. *Polymer* **1999**, *40* (19), 5439–5444. https://doi.org/10.1016/S0032-3861(99)00029-4.

(141) Matyjaszewski, K.; Shipp, D. A.; McMurtry, G. P.; Gaynor, S. G.; Pakula, T. Simple and Effective One-Pot Synthesis of (Meth)Acrylic Block Copolymers through Atom Transfer Radical Polymerization. *J. Polym. Sci. Part Polym. Chem.* **2000**, *38* (11), 2023–2031. https://doi.org/10.1002/(SICI)1099-0518(20000601)38:11<2023::AID-POLA110>3.0.CO;2-L.

(142) Tong, J. D.; Moineau, G.; Leclère, Ph.; Brédas; Lazzaroni, R.; Jérôme, R. Synthesis, Morphology, and Mechanical Properties of Poly(Methyl Methacrylate)-b-Poly(n-Butyl Acrylate)-b-Poly(Methyl Methacrylate) Triblocks. Ligated Anionic Polymerization vs Atom Transfer Radical Polymerization. *Macromolecules* **2000**, *33* (2), 470–479. https://doi.org/10.1021/ma990886v.

(143) Ashford, E. J.; Naldi, V.; O'Dell, R.; Billingham, N. C.; Armes, S. P. First Example of the Atom Transfer Radical Polymerisation of an Acidic Monomer: Direct Synthesis of Methacrylic Acid Copolymers in Aqueous Media. *Chem. Commun.* **1999**, *0* (14), 1285–1286. https://doi.org/10.1039/A903773J.

(144) Becer, C. R.; Hoogenboom, R.; Schubert, U. S. Click Chemistry beyond Metal-Catalyzed Cycloaddition. *Angew. Chem. Int. Ed.* **2009**, *48* (27), 4900–4908. https://doi.org/10.1002/anie.200900755.

(145) Lutz, J.-F. Copper-Free Azide–Alkyne Cycloadditions: New Insights and Perspectives. *Angew. Chem. Int. Ed.* **2008**, *47* (12), 2182–2184. https://doi.org/10.1002/anie.200705365.

(146) Konkolewicz, D.; Schröder, K.; Buback, J.; Bernhard, S.; Matyjaszewski, K. Visible Light and Sunlight Photoinduced ATRP with Ppm of Cu Catalyst. *ACS Macro Lett.* **2012**, *1* (10), 1219–1223. https://doi.org/10.1021/mz300457e.

(147) Zhou, Y.-N.; Luo, Z.-H. An Old Kinetic Method for a New Polymerization Mechanism: Toward Photochemically Mediated ATRP. *AIChE J.* **2015**, *61* (6), 1947–1958. https://doi.org/10.1002/aic.14792.

(148) Faucher, S.; Okrutny, P.; Zhu, S. Facile and Effective Purification of Polymers Produced by Atom Transfer Radical Polymerization via Simple Catalyst Precipitation and Microfiltration. *Macromolecules* **2006**, *39* (1), 3–5. https://doi.org/10.1021/ma051920a.

(149) Haddleton, D. M.; Kukulj, D.; Radigue, A. P. Atom Transfer Polymerisation of Methyl Methacrylate Mediated by Solid Supported Copper Catalysts. *Chem. Commun.* **1999**, No. 1, 99–100. https://doi.org/10.1039/A808308H.

(150) Kickelbick, G.; Paik, H.; Matyjaszewski, K. Immobilization of the Copper Catalyst in Atom Transfer Radical Polymerization. *Macromolecules* **1999**, *32* (9), 2941–2947. https://doi.org/10.1021/ma9818432.

(151) Shen, Y.; Tang, H.; Ding, S. Catalyst Separation in Atom Transfer Radical Polymerization. *Prog. Polym. Sci.* **2004**, *29* (10), 1053–1078. https://doi.org/10.1016/j.progpolymsci.2004.08.002.

(152) Huang, Z.; Gu, Y.; Liu, X.; Zhang, L.; Cheng, Z.; Zhu, X. Metal-Free Atom Transfer Radical Polymerization of Methyl Methacrylate with Ppm Level of Organic Photocatalyst. *Macromol. Rapid Commun.* **2017**, *38* (10), 1600461. https://doi.org/10.1002/marc.201600461.

(153) Miyake, G. M.; Theriot, J. C. Perylene as an Organic Photocatalyst for the Radical Polymerization of Functionalized Vinyl Monomers through Oxidative Quenching

© 2020 Tous droits réservés.

with Alkyl Bromides and Visible Light. *Macromolecules* **2014**, *47* (23), 8255–8261. https://doi.org/10.1021/ma502044f.

(154) Fetters, L. J.; Lohse, D. J.; Richter, D.; Witten, T. A.; Zirkel, A. Connection between Polymer Molecular Weight, Density, Chain Dimensions, and Melt Viscoelastic Properties. *Macromolecules* **1994**, *27* (17), 4639–4647.

(155) Fried, J. R. *Polymer Science and Technology*; Pearson Education, 2014.

(156) Stevens, M. P. *Entitled "Polymer Chemistry, An Introduction" Third Edition, 1999*; Oxford University Press, New York.

(157) Sibilia, J. P. *A Guide to Materials Characterization and Chemical Analysis*; John Wiley & Sons, 1988.

(158) Chen, A.; Wu, D.; Johnson Jr, C. S. Determination of Molecular Weight Distributions for Polymers by Diffusion-Ordered NMR. *J. Am. Chem. Soc.* **1995**, *117* (30), 7965–7970.

(159) Izunobi, J. U.; Higginbotham, C. L. Polymer Molecular Weight Analysis by 1H NMR Spectroscopy. *J. Chem. Educ.* **2011**, *88* (8), 1098–1104. https://doi.org/10.1021/ed100461v.

(160) Baxendale, I. R.; Ley, S. V.; Mansfield, A. C.; Smith, C. D. Multistep Synthesis Using Modular Flow Reactors: Bestmann–Ohira Reagent for the Formation of Alkynes and Triazoles. *Angew. Chem.* **2009**, *121* (22), 4077–4081. https://doi.org/10.1002/ange.200900970.

(161) R. Baxendale, I.; Deeley, J.; M. Griffiths-Jones, C.; V. Ley, S.; Saaby, S.; K. Tranmer, G. A Flow Process for the Multi-Step Synthesis of the Alkaloid Natural Product Oxomaritidine : A New Paradigm for Molecular Assembly. *Chem. Commun.* **2006**, *0* (24), 2566–2568. https://doi.org/10.1039/B600382F.

(162) Mason, B. P.; Price, K. E.; Steinbacher, J. L.; Bogdan, A. R.; McQuade, D. T. Greener Approaches to Organic Synthesis Using Microreactor Technology. *Chem. Rev.* **2007**, *107* (6), 2300–2318. https://doi.org/10.1021/cr050944c.

(163) Exchangers, M. H. *Microreactors: New Technology for Modern Chemistry*; Weinheim: Wiley/VCH, 2000.

(164) Cambié, D.; Bottecchia, C.; Straathof, N. J.; Hessel, V.; Noel, T. Applications of Continuous-Flow Photochemistry in Organic Synthesis, Material Science, and Water Treatment. *Chem. Rev.* **2016**, *116* (17), 10276–10341.

(165) El Achi, N. Photochemical and Photoredox Reactions in Continuous Microreactors : Application to Cycloaddition, Controlled Polymerization and Radical Chemistry. These de doctorat, Lille 1, 2016.

(166) Strike, D. J.; Thiébaud, P.; Van der Sluis, A. C.; Koudelka-Hep, M.; de Rooij, N. F. Glucose Measurement Using a Micromachined Open Tubular Heterogeneous Enzyme Reactor (MOTHER). *Microsyst. Technol.* **1994**, *1* (1), 48–50.

(167) Laurino, P. Photochemical Transformations in Continuous Flow Devices. PhD Thesis, ETH Zurich, 2011.

(168) Jovanović, J.; Rebrov, E. V.; Nijhuis, T. A. (Xander); Kreutzer, M. T.; Hessel, V.; Schouten, J. C. Liquid–Liquid Flow in a Capillary Microreactor: Hydrodynamic Flow Patterns and Extraction Performance. *Ind. Eng. Chem. Res.* **2012**, *51* (2), 1015–1026. https://doi.org/10.1021/ie200715m.

(169) Woitalka, A.; Kuhn, S.; Jensen, K. F. Scalability of Mass Transfer in Liquid–Liquid Flow. *Chem. Eng. Sci.* **2014**, *116*, 1–8. https://doi.org/10.1016/j.ces.2014.04.036.

(170) Wang, C.-W.; Bains, A.; Sinton, D.; Moffitt, M. G. Flow-Directed Loading of Block Copolymer Micelles with Hydrophobic Probes in a Gas–Liquid Microreactor. *Langmuir* **2013**, *29* (26), 8385–8394. https://doi.org/10.1021/la400011n.

© 2020 Tous droits réservés.

lilliad.univ-lille.fr

(171) Gambhire, S.; Patel, N.; Gambhire, G.; Kale, S. A Review on Different Micromixers and Its Micromixing within Microchannel. *Int. J. Curr. Eng. Technol.* **2016**, *4* (4), 409–413.
(172) Ober, T. J.; Foresti, D.; Lewis, J. A. Active Mixing of Complex Fluids at the Microscale. *Proc. Natl. Acad. Sci.* **2015**, *112* (40), 12293–12298. https://doi.org/10.1073/pnas.1509224112.
(173) Ward, K.; Fan, Z. H. Mixing in Microfluidic Devices and Enhancement Methods. *J. Micromechanics Microengineering* **2015**, *25* (9), 094001. https://doi.org/10.1088/0960-1317/25/9/094001.
(174) Farshchian, B.; Amirsadeghi, A.; Choi, J.; Park, D. S.; Kim, N.; Park, S. 3D Nanomolding and Fluid Mixing in Micromixers with Micro-Patterned Microchannel Walls. *Nano Converg.* **2017**, *4* (1), 4. https://doi.org/10.1186/s40580-017-0098-x.
(175) Yue, J.; H. Falke, F.; C. Schouten, J.; Alexander Nijhuis, T. Microreactors with Integrated UV/Vis Spectroscopic Detection for Online Process Analysis under Segmented Flow. *Lab. Chip* **2013**, *13* (24), 4855–4863. https://doi.org/10.1039/C3LC50876E.
(176) Yu, X.-Y. *Advances in Microfluidics: New Applications in Biology, Energy, and Materials Sciences*; BoD – Books on Demand, 2016.
(177) Kumar, C. S. S. R.; Li, Y.; Katla, S. Lab-on-a-Chip Synthesis of Inorganic Nanomaterials and Quantum Dots for Biomedical Applications. *Adv Drug Rev 65*. https://doi.org/10.1016/j.addr.2013.05.006.
(178) W. Phillips, T.; G. Lignos, I.; M. Maceiczyk, R.; J. deMello, A.; C. deMello, J. Nanocrystal Synthesis in Microfluidic Reactors: Where Next? *Lab. Chip* **2014**, *14* (17), 3172–3180. https://doi.org/10.1039/C4LC00429A.
(179) Yen, B. K. H.; Stott, N. E.; Jensen, K. F.; Bawendi, M. G. A Continuous-Flow Microcapillary Reactor for the Preparation of a Size Series of CdSe Nanocrystals. *Adv. Mater.* **2003**, *15* (21), 1858–1862. https://doi.org/10.1002/adma.200305162.
(180) Kralj, J. G.; Sahoo, H. R.; Jensen, K. F. Integrated Continuous Microfluidic Liquid–Liquid Extraction. *Lab. Chip* **2007**, *7* (2), 256–263. https://doi.org/10.1039/B610888A.
(181) Jolliffe, H. G.; Gerogiorgis, D. I. Process Modelling and Simulation for Continuous Pharmaceutical Manufacturing of Ibuprofen. *Chem. Eng. Res. Des.* **2015**, *97*, 175–191. https://doi.org/10.1016/j.cherd.2014.12.005.
(182) Rossetti, I.; Compagnoni, M. Chemical Reaction Engineering, Process Design and Scale-up Issues at the Frontier of Synthesis: Flow Chemistry. *Chem. Eng. J.* **2016**, *296*, 56–70. https://doi.org/10.1016/j.cej.2016.02.119.
(183) E. Fitzpatrick, D.; V. Ley, S. Engineering Chemistry: Integrating Batch and Flow Reactions on a Single, Automated Reactor Platform. *React. Chem. Eng.* **2016**, *1* (6), 629–635. https://doi.org/10.1039/C6RE00160B.
(184) F. Jensen, K.; J. Reizman, B.; G. Newman, S. Tools for Chemical Synthesis in Microsystems. *Lab. Chip* **2014**, *14* (17), 3206–3212. https://doi.org/10.1039/C4LC00330F.
(185) Dong, C.; Wang, K.; Zhang, J. S.; Luo, G. S. Reaction Kinetics of Cyclohexanone Ammoximation over TS-1 Catalyst in a Microreactor. *Chem. Eng. Sci.* **2015**, *126*, 633–640. https://doi.org/10.1016/j.ces.2015.01.006.
(186) Jensen, K. F. Flow Chemistry—Microreaction Technology Comes of Age. *AIChE J.* **2017**, *63* (3), 858–869. https://doi.org/10.1002/aic.15642.
(187) Martínez-Cisneros, C. S.; Pedro, S. G.; Puyol, M.; García-García, J.; Alonso-Chamarro, J. Design, Fabrication and Characterization of Microreactors for High

© 2020 Tous droits réservés.
lilliad.univ-lille.fr

Temperature Syntheses. *Chem. Eng. J.* **2012**, *211–212*, 432–441. https://doi.org/10.1016/j.cej.2012.09.101.

(188) Ren, W.; Perumal, J.; Wang, J.; Wang, H.; Sharma, S.; Kim, D.-P. Whole Ceramic-like Microreactors from Inorganic Polymers for High Temperature or/and High Pressure Chemical Syntheses. *Lab. Chip* **2014**, *14* (4), 779–786. https://doi.org/10.1039/C3LC51191J.

(189) Shang, M.; Noël, T.; Su, Y.; Hessel, V. Kinetic Study of Hydrogen Peroxide Decomposition at High Temperatures and Concentrations in Two Capillary Microreactors. *AIChE J.* **2017**, *63* (2), 689–697. https://doi.org/10.1002/aic.15385.

(190) Floyd, T. M.; Losey, M. W.; Firebaugh, S. L.; Jensen, K. F.; Schmidt, M. A. Novel Liquid Phase Microreactors for Safe Production of Hazardous Specialty Chemicals. In *Microreaction Technology: Industrial Prospects*; Ehrfeld, W., Ed.; Springer: Berlin, Heidelberg, 2000; pp 171–180. https://doi.org/10.1007/978-3-642-59738-1_16.

(191) Saksena, P.; Tadigadapa, S.; Yetter, R. A. Design, Fabrication and Analysis of Stagnation Flow Microreactors Used to Study Hypergolic Reactions. *Lab. Chip* **2015**, *15* (10), 2248–2257. https://doi.org/10.1039/C5LC00306G.

(192) Srinivasan, R.; Hsing, I.-M.; Berger, P. E.; Jensen, K. F.; Firebaugh, S. L.; Schmidt, M. A.; Harold, M. P.; Lerou, J. J.; Ryley, J. F. Micromachined Reactors for Catalytic Partial Oxidation Reactions. *AIChE J.* **1997**, *43* (11), 3059–3069. https://doi.org/10.1002/aic.690431117.

(193) Azouz, A. B.; Murphy, S.; Karazi, S.; Vázquez, M.; Brabazon, D. Fast Fabrication Process of Microfluidic Devices Based on Cyclic Olefin Copolymer. *Mater. Manuf. Process.* **2014**, *29* (2), 93–99. https://doi.org/10.1080/10426914.2013.811739.

(194) Fouillet, Y.; Parent, C.; Gropplero, G.; Davoust, L.; Achard, J. L.; Revol-Cavalier, F.; Verplanck, N. Stretchable Material for Microfluidic Applications. *Proceedings* **2017**, *1* (4), 501. https://doi.org/10.3390/proceedings1040501.

(195) Halldorsson, S.; Lucumi, E.; Gómez-Sjöberg, R.; Fleming, R. M. T. Advantages and Challenges of Microfluidic Cell Culture in Polydimethylsiloxane Devices. *Biosens. Bioelectron.* **2015**, *63*, 218–231. https://doi.org/10.1016/j.bios.2014.07.029.

(196) Kucuk, I.; Edirisinghe, M. Microfluidic Preparation of Polymer Nanospheres. *J. Nanoparticle Res.* **2014**, *16* (12), 2626. https://doi.org/10.1007/s11051-014-2626-5.

(197) Zilio, C.; Sola, L.; Damin, F.; Faggioni, L.; Chiari, M. Universal Hydrophilic Coating of Thermoplastic Polymers Currently Used in Microfluidics. *Biomed. Microdevices* **2014**, *16* (1), 107–114. https://doi.org/10.1007/s10544-013-9810-8.

(198) Suryawanshi, P. L.; Gumfekar, S. P.; Bhanvase, B. A.; Sonawane, S. H.; Pimplapure, M. S. A Review on Microreactors: Reactor Fabrication, Design, and Cutting-Edge Applications. *Chem. Eng. Sci.* **2018**, *189*, 431–448. https://doi.org/10.1016/j.ces.2018.03.026.

(199) Su, Y.; Straathof, N. J.; Hessel, V.; Noël, T. Photochemical Transformations Accelerated in Continuous-Flow Reactors: Basic Concepts and Applications. *Chem. Eur. J.* **2014**, *20* (34), 10562–10589.

(200) Albini, A.; Fagnoni, M. *Handbook of Synthetic Photochemistry*; John Wiley & Sons, 2009.

(201) Fukuyama, T.; Rahman, M. T.; Sato, M.; Ryu, I. Adventures in Inner Space: Microflow Systems for Practical Organic Synthesis. *Synlett* **2008**, *2008* (02), 151–163. https://doi.org/10.1055/s-2007-1000884.

(202) Ciana, C.-L.; Bochet, C. G. Clean and Easy Photochemistry. *Chim. Int. J. Chem.* **2007**, *61* (10), 650–654. https://doi.org/10.2533/chimia.2007.650.

© 2020 Tous droits réservés.

lilliad.univ-lille.fr

(203) Coyle, E. E.; Oelgemöller, M. Micro-Photochemistry: Photochemistry in Microstructured Reactors. The New Photochemistry of the Future? *Photochem. Photobiol. Sci.* **2008**, *7* (11), 1313–1322. https://doi.org/10.1039/B808778D.
(204) Shvydkiv, O.; Yavorskyy, A.; Tan, S. B.; Nolan, K.; Hoffmann, N.; Youssef, A.; Oelgemöller, M. Microphotochemistry: A Reactor Comparison Study Using the Photosensitized Addition of Isopropanol to Furanones as a Model Reaction. *Photochem. Photobiol. Sci.* **2011**, *10* (9), 1399–1404. https://doi.org/10.1039/C1PP05024A.
(205) Shvydkiv, O.; Gallagher, S.; Nolan, K.; Oelgemöller, M. From Conventional to Microphotochemistry: Photodecarboxylation Reactions Involving Phthalimides. *Org. Lett.* **2010**, *12* (22), 5170–5173. https://doi.org/10.1021/ol102184u.
(206) Shvydkiv, O.; Yavorskyy, A.; Nolan, K.; Youssef, A.; Riguet, E.; Hoffmann, N.; Oelgemöller, M. Photosensitized Addition of Isopropanol to Furanones in a 365 Nm UV-LED Microchip. *Photochem. Photobiol. Sci.* **2010**, *9* (12), 1601–1603. https://doi.org/10.1039/C0PP00223B.
(207) Wiles, C.; Watts, P. Continuous Flow Reactors: A Perspective. *Green Chem.* **2012**, *14* (1), 38–54. https://doi.org/10.1039/C1GC16022B.
(208) Ley, S. V. On Being Green: Can Flow Chemistry Help? *Chem. Rec.* **2012**, *12* (4), 378–390. https://doi.org/10.1002/tcr.201100041.
(209) Jones, E.; McClean, K.; Housden, S.; Gasparini, G.; Archer, I. Biocatalytic Oxidase: Batch to Continuous. *Chem. Eng. Res. Des.* **2012**, *90* (6), 726–731. https://doi.org/10.1016/j.cherd.2012.01.018.
(210) Tamborini, L.; Fernandes, P.; Paradisi, F.; Molinari, F. Flow Bioreactors as Complementary Tools for Biocatalytic Process Intensification. *Trends Biotechnol.* **2018**, *36* (1), 73–88. https://doi.org/10.1016/j.tibtech.2017.09.005.
(211) Junior, I. I.; Flores, M. C.; Sutili, F. K.; Leite, S. G. F.; de M. Miranda, L. S.; Leal, I. C. R.; de Souza, R. O. M. A. Lipase-Catalyzed Monostearin Synthesis under Continuous Flow Conditions. *Org. Process Res. Dev.* **2012**, *16* (5), 1098–1101. https://doi.org/10.1021/op200132y.
(212) Bolivar, J. M.; Nidetzky, B. Smart Enzyme Immobilization in Microstructured Reactors. *Chim Oggi* **2013**, *31* (3), 50–4.
(213) Wohlgemuth, R.; Plazl, I.; Žnidaršič-Plazl, P.; Gernaey, K. V.; Woodley, J. M. Microscale Technology and Biocatalytic Processes: Opportunities and Challenges for Synthesis. *Trends Biotechnol.* **2015**, *33* (5), 302–314. https://doi.org/10.1016/j.tibtech.2015.02.010.
(214) Hajba, L.; Guttman, A. Continuous-Flow Biochemical Reactors: Biocatalysis, Bioconversion, and Bioanalytical Applications Utilizing Immobilized Microfluidic Enzyme Reactors. *J. Flow Chem.* **2016**, *6* (1), 8–12. https://doi.org/10.1556/1846.2015.00028.
(215) Laurenti, E.; dos Santos Vianna Jr, A. Enzymatic Microreactors in Biocatalysis: History, Features, and Future Perspectives. *Biocatalysis* **2016**, *1* (1), 148–165.
(216) Ardao, I.; Hwang, E. T.; Zeng, A.-P. In Vitro Multienzymatic Reaction Systems for Biosynthesis. In *Fundamentals and Application of New Bioproduction Systems*; Zeng, A.-P., Ed.; Advances in Biochemical Engineering/Biotechnology; Springer: Berlin, Heidelberg, 2013; pp 153–184. https://doi.org/10.1007/10_2013_232.
(217) Styring, P.; Parracho, A. I. R. From Discovery to Production: Scale-out of Continuous Flow Meso Reactors. *Beilstein J. Org. Chem.* **2009**, *5* (1), 29. https://doi.org/10.3762/bjoc.5.29.

© 2020 Tous droits réservés.

(218) Wheeler, R. C.; Benali, O.; Deal, M.; Farrant, E.; MacDonald, S. J. F.; Warrington, B. H. Mesoscale Flow Chemistry: A Plug-Flow Approach to Reaction Optimisation. *Org. Process Res. Dev.* **2007**, *11* (4), 704–710. https://doi.org/10.1021/op7000707.
(219) Baumann, M.; Baxendale, I. R.; Ley, S. V.; Smith, C. D.; Tranmer, G. K. Fully Automated Continuous Flow Synthesis of 4,5-Disubstituted Oxazoles. *Org. Lett.* **2006**, *8* (23), 5231–5234. https://doi.org/10.1021/ol061975c.
(220) Hartman, R. L.; Sahoo, H. R.; Yen, B. C.; Jensen, K. F. Distillation in Microchemical Systems Using Capillary Forces and Segmented Flow. *Lab. Chip* **2009**, *9* (13), 1843–1849. https://doi.org/10.1039/B901790A.
(221) Hartman, R. L.; Naber, J. R.; Buchwald, S. L.; Jensen, K. F. Multistep Microchemical Synthesis Enabled by Microfluidic Distillation. *Angew. Chem. Int. Ed.* **2010**, *49* (5), 899–903. https://doi.org/10.1002/anie.200904634.
(222) Losey, M. W.; Schmidt, M. A.; Jensen, K. F. Microfabricated Multiphase Packed-Bed Reactors: Characterization of Mass Transfer and Reactions. *Ind. Eng. Chem. Res.* **2001**, *40* (12), 2555–2562. https://doi.org/10.1021/ie000523f.
(223) Aillet, T.; Loubiere, K.; Dechy-Cabaret, O.; Prat, L. Accurate Measurement of the Photon Flux Received Inside Two Continuous Flow Microphotoreactors by Actinometry. *Int. J. Chem. React. Eng.* **2014**, *1* (open-issue). https://doi.org/10.1515/ijcre-2013-0121.
(224) Jamali, A.; Vanraes, R.; Hanselaer, P.; Van Gerven, T. A Batch LED Reactor for the Photocatalytic Degradation of Phenol. *Chem. Eng. Process. Process Intensif.* **2013**, *71*, 43–50. https://doi.org/10.1016/j.cep.2013.03.010.
(225) Su, Y.; Hessel, V.; Noël, T. A Compact Photomicroreactor Design for Kinetic Studies of Gas-Liquid Photocatalytic Transformations. *AIChE J.* **2015**, *61* (7), 2215–2227. https://doi.org/10.1002/aic.14813.
(226) Reis, M. H.; Leibfarth, F. A.; Pitet, L. M. Polymerizations in Continuous Flow: Recent Advances in the Synthesis of Diverse Polymeric Materials. *ACS Macro Lett.* **2020**, *9* (1), 123–133. https://doi.org/10.1021/acsmacrolett.9b00933.
(227) Tonhauser, C.; Natalello, A.; Löwe, H.; Frey, H. Microflow Technology in Polymer Synthesis. *Macromolecules* **2012**, *45* (24), 9551–9570. https://doi.org/10.1021/ma301671x.
(228) Diehl, C.; Laurino, P.; Azzouz, N.; Seeberger, P. H. Accelerated Continuous Flow RAFT Polymerization. *Macromolecules* **2010**, *43* (24), 10311–10314. https://doi.org/10.1021/ma1025253.
(229) Hornung, C. H.; Guerrero-Sanchez, C.; Brasholz, M.; Saubern, S.; Chiefari, J.; Moad, G.; Rizzardo, E.; Thang, S. H. Controlled RAFT Polymerization in a Continuous Flow Microreactor. *Org. Process Res. Dev.* **2011**, *15* (3), 593–601. https://doi.org/10.1021/op1003314.
(230) Chuang, Y.-M.; Wenn, B.; Gielen, S.; Ethirajan, A.; Junkers, T. Ligand Switch in Photoinduced Copper-Mediated Polymerization: Synthesis of Methacrylate–Acrylate Block Copolymers. *Polym. Chem.* **2015**, *6* (36), 6488–6497. https://doi.org/10.1039/C5PY00592B.
(231) Lauterbach, F.; Rubens, M.; Abetz, V.; Junkers, T. Ultrafast PhotoRAFT Block Copolymerization of Isoprene and Styrene Facilitated through Continuous-Flow Operation. *Angew. Chem. Int. Ed.* **2018**, *57* (43), 14260–14264. https://doi.org/10.1002/anie.201809759.
(232) Li, Z.; Chen, W.; Zhang, L.; Cheng, Z.; Zhu, X. Fast RAFT Aqueous Polymerization in a Continuous Tubular Reactor: Consecutive Synthesis of a Double Hydrophilic Block Copolymer. *Polym. Chem.* **2015**, *6* (28), 5030–5035. https://doi.org/10.1039/C5PY00847F.

© 2020 Tous droits réservés.
lilliad.univ-lille.fr

(233) Baeten, E.; Haven, J. J.; Junkers, T. RAFT Multiblock Reactor Telescoping: From Monomers to Tetrablock Copolymers in a Continuous Multistage Reactor Cascade. *Polym. Chem.* **2017**, *8* (25), 3815–3824. https://doi.org/10.1039/C7PY00585G.

(234) Rubens, M.; Latsrisaeng, P.; Junkers, T. Visible Light-Induced Iniferter Polymerization of Methacrylates Enhanced by Continuous Flow. *Polym. Chem.* **2017**, *8* (42), 6496–6505. https://doi.org/10.1039/C7PY01157A.

(235) Gardiner, J.; Hornung, C. H.; Tsanaktsidis, J.; Guthrie, D. Continuous Flow Photo-Initiated RAFT Polymerisation Using a Tubular Photochemical Reactor. *Eur. Polym. J.* **2016**, *80*, 200–207. https://doi.org/10.1016/j.eurpolymj.2016.01.033.

(236) Corrigan, N.; Rosli, D.; Jones, J. W. J.; Xu, J.; Boyer, C. Oxygen Tolerance in Living Radical Polymerization: Investigation of Mechanism and Implementation. *Macromolecules* **2016**, *49* (18), 6779–6789. https://doi.org/10.1021/acs.macromol.6b01306.

(237) Rosenfeld, C.; Serra, C.; Brochon, C.; Hessel, V.; Hadziioannou, G. Use of Micromixers to Control the Molecular Weight Distribution in Continuous Two-Stage Nitroxide-Mediated Copolymerizations. *Chem. Eng. J.* **2008**, *135*, S242–S246. https://doi.org/10.1016/j.cej.2007.07.038.

(238) Wu, T.; Mei, Y.; Cabral, J. T.; Xu, C.; Beers, K. L. A New Synthetic Method for Controlled Polymerization Using a Microfluidic System. *J. Am. Chem. Soc.* **2004**, *126* (32), 9880–9881. https://doi.org/10.1021/ja048432n.

(239) Gong, H.; Zhao, Y.; Shen, X.; Lin, J.; Chen, M. Organocatalyzed Photocontrolled Radical Polymerization of Semifluorinated (Meth)Acrylates Driven by Visible Light. *Angew. Chem. Int. Ed.* **2018**, *57* (1), 333–337. https://doi.org/10.1002/anie.201711053.

(240) Noda, T.; Grice, A. J.; Levere, M. E.; Haddleton, D. M. Continuous Process for ATRP: Synthesis of Homo and Block Copolymers. *Eur. Polym. J.* **2007**, *43* (6), 2321–2330. https://doi.org/10.1016/j.eurpolymj.2007.03.010.

(241) El Achi, N.; Bakkour, Y.; Adhami, W.; Molina, J.; Penhoat, M.; Azaroual, N.; Chausset-Boissarie, L.; Rolando, C. Metal-Free ATRP Catalyzed by Visible Light in Continuous Flow. *Front. Chem.* **2020**, *8*. https://doi.org/10.3389/fchem.2020.00740.

(242) Zhu, N.; Liu, Y.; Feng, W.; Huang, W.; Zhang, Z.; Hu, X.; Fang, Z.; Li, Z.; Guo, K. Continuous Flow Protecting-Group-Free Synthetic Approach to Thiol-Terminated Poly (ε-Caprolactone). *Eur. Polym. J.* **2016**, *80*, 234–239.

(243) Zhu, N.; Zhang, Z.; Feng, W.; Zeng, Y.; Li, Z.; Fang, Z.; Zhang, K.; Li, Z.; Guo, K. Sn (OTf) 2 Catalyzed Continuous Flow Ring-Opening Polymerization of ε-Caprolactone. *RSC Adv.* **2015**, *5* (40), 31554–31557.

(244) Zhu, N.; Feng, W.; Hu, X.; Zhang, Z.; Fang, Z.; Zhang, K.; Li, Z.; Guo, K. Organocatalyzed Continuous Flow Ring-Opening Polymerizations to Homo- and Block-Polylactones. *Polymer* **2016**, *84*, 391–397. https://doi.org/10.1016/j.polymer.2016.01.019.

(245) Lu, S.; Wang, K. Kinetic Study of TBD Catalyzed δ-Valerolactone Polymerization Using a Gas-Driven Droplet Flow Reactor. *React. Chem. Eng.* **2019**, *4* (7), 1189–1194. https://doi.org/10.1039/C9RE00046A.

(246) Morsbach, J.; Müller, A. H. E.; Berger-Nicoletti, E.; Frey, H. Living Polymer Chains with Predictable Molecular Weight and Dispersity via Carbanionic Polymerization in Continuous Flow: Mixing Rate as a Key Parameter. *Macromolecules* **2016**, *49* (14), 5043–5050. https://doi.org/10.1021/acs.macromol.6b00975.

(247) Corrigan, N.; Zhernakov, L.; Hashim, M. H.; Xu, J.; Boyer, C. Flow Mediated Metal-Free PET-RAFT Polymerisation for Upscaled and Consistent Polymer Production. *React. Chem. Eng.* **2019**, *4* (7), 1216–1228. https://doi.org/10.1039/C9RE00014C.

© 2020 Tous droits réservés.

lilliad.univ-lille.fr

(248) Reis, M. H.; Varner, T. P.; Leibfarth, F. A. The Influence of Residence Time Distribution on Continuous-Flow Polymerization. *Macromolecules* **2019**, *52* (9), 3551–3557. https://doi.org/10.1021/acs.macromol.9b00454.

(249) Numata, K.; Srivastava, R. K.; Finne-Wistrand, A.; Albertsson, A.-C.; Doi, Y.; Abe, H. Branched Poly(Lactide) Synthesized by Enzymatic Polymerization: Effects of Molecular Branches and Stereochemistry on Enzymatic Degradation and Alkaline Hydrolysis. *Biomacromolecules* **2007**, *8* (10), 3115–3125. https://doi.org/10.1021/bm700537x.

(250) Duchiron, S. W.; Pollet, E.; Givry, S.; Avérous, L. Mixed Systems to Assist Enzymatic Ring Opening Polymerization of Lactide Stereoisomers. *RSC Adv.* **2015**, *5* (103), 84627–84635. https://doi.org/10.1039/C5RA18954C.

(251) Målberg, S.; Finne-Wistrand, A.; Albertsson, A.-C. The Environmental Influence in Enzymatic Polymerization of Aliphatic Polyesters in Bulk and Aqueous Mini-Emulsion. *Polymer* **2010**, *51* (23), 5318–5322. https://doi.org/10.1016/j.polymer.2010.09.016.

(252) Barrera-Rivera, K. A.; Flores-Carreón, A.; Martínez-Richa, A. Enzymatic Ring-Opening Polymerization of ε-Caprolactone by a New Lipase from Yarrowia Lipolytica. *J. Appl. Polym. Sci.* **2008**, *109* (2), 708–719. https://doi.org/10.1002/app.28116.

(253) Henderson, L. A.; Svirkin, Y. Y.; Gross, R. A.; Kaplan, D. L.; Swift, G. Enzyme-Catalyzed Polymerizations of ε-Caprolactone: Effects of Initiator on Product Structure, Propagation Kinetics, and Mechanism. *Macromolecules* **1996**, *29* (24), 7759–7766. https://doi.org/10.1021/ma960821h.

(254) Cao, H.; Han, H.; Li, G.; Yang, J.; Zhang, L.; Yang, Y.; Fang, X.; Li, Q. Biocatalytic Synthesis of Poly(δ-Valerolactone) Using a Thermophilic Esterase from Archaeoglobus Fulgidus as Catalyst. *Int. J. Mol. Sci.* **2012**, *13* (10), 12232–12241. https://doi.org/10.3390/ijms131012232.

(255) Ma, J.; Li, Q.; Song, B.; Liu, D.; Zheng, B.; Zhang, Z.; Feng, Y. Ring-Opening Polymerization of ε-Caprolactone Catalyzed by a Novel Thermophilic Esterase from the Archaeon Archaeoglobus Fulgidus. *J. Mol. Catal. B Enzym.* **2009**, *56* (2), 151–157. https://doi.org/10.1016/j.molcatb.2008.03.012.

(256) Uppenberg, J.; Oehrner, N.; Norin, M.; Hult, K.; Kleywegt, G. J.; Patkar, S.; Waagen, V.; Anthonsen, T.; Jones, T. A. Crystallographic and Molecular-Modeling Studies of Lipase B from Candida Antarctica Reveal a Stereospecificity Pocket for Secondary Alcohols. *Biochemistry* **1995**, *34* (51), 16838–16851.

(257) Stauch, B.; Fisher, S. J.; Cianci, M. Open and Closed States of Candida Antarctica Lipase B: Protonation and the Mechanism of Interfacial Activation. *J. Lipid Res.* **2015**, *56* (12), 2348–2358.

(258) Zisis, T.; Freddolino, P. L.; Turunen, P.; van Teeseling, M. C.; Rowan, A. E.; Blank, K. G. Interfacial Activation of Candida Antarctica Lipase B: Combined Evidence from Experiment and Simulation. *Biochemistry* **2015**, *54* (38), 5969–5979.

(259) Arana-Peña, S.; Lokha, Y.; Fernández-Lafuente, R. Immobilization of Eversa Lipase on Octyl Agarose Beads and Preliminary Characterization of Stability and Activity Features. *Catalysts* **2018**, *8* (11), 511. https://doi.org/10.3390/catal8110511.

(260) Arana-Peña, S.; Lokha, Y.; Fernández-Lafuente, R. Immobilization on Octyl-Agarose Beads and Some Catalytic Features of Commercial Preparations of Lipase a from Candida Antarctica (Novocor ADL): Comparison with Immobilized Lipase B from Candida Antarctica. *Biotechnol. Prog.* **2019**, *35* (1), e2735. https://doi.org/10.1002/btpr.2735.

© 2020 Tous droits réservés.

(261) Gotor-Fernández, V.; Busto, E.; Gotor, V. Candida Antarctica Lipase B: An Ideal Biocatalyst for the Preparation of Nitrogenated Organic Compounds. *Adv. Synth. Catal.* **2006**, *348* (7–8), 797–812. https://doi.org/10.1002/adsc.200606057.

(262) Kirk, O.; Christensen, M. W. Lipases from Candida Antarctica: Unique Biocatalysts from a Unique Origin. *Org. Process Res. Dev.* **2002**, *6* (4), 446–451. https://doi.org/10.1021/op0200165.

(263) Ortiz, C.; Luján Ferreira, M.; Barbosa, O.; Santos, J. C. S. dos; C. Rodrigues, R.; Berenguer-Murcia, Á.; E. Briand, L.; Fernandez-Lafuente, R. Novozym 435: The "Perfect" Lipase Immobilized Biocatalyst? *Catal. Sci. Technol.* **2019**, *9* (10), 2380–2420. https://doi.org/10.1039/C9CY00415G.

(264) Mokhtar, N. F.; Abd. Rahman, R. N. Z. R.; Muhd Noor, N. D.; Mohd Shariff, F.; Mohamad Ali, M. S. The Immobilization of Lipases on Porous Support by Adsorption and Hydrophobic Interaction Method. *Catalysts* **2020**, *10* (7), 744. https://doi.org/10.3390/catal10070744.

(265) Okumura, S.; Iwai, M.; Tominaga, Y. Synthesis of Ester Oligomer by Aspergillus Niger Lipase. *Agric. Biol. Chem.* **1984**, *48* (11), 2805–2808. https://doi.org/10.1080/00021369.1984.10866573.

(266) Knani, D.; Gutman, A. L.; Kohn, D. H. Enzymatic Polyesterification in Organic Media. Enzyme-Catalyzed Synthesis of Linear Polyesters. I. Condensation Polymerization of Linear Hydroxyesters. II. Ring-Opening Polymerization of ϵ-Caprolactone. *J. Polym. Sci. Part Polym. Chem.* **1993**, *31* (5), 1221–1232. https://doi.org/10.1002/pola.1993.080310518.

(267) Uyama, H.; Takeya, K.; Kobayashi, S. Synthesis of Polyesters by Enzymatic Ring-Opening Copolymerization Using Lipase Catalyst. *Proc. Jpn. Acad. Ser. B* **1993**, *69* (8), 203–207. https://doi.org/10.2183/pjab.69.203.

(268) Uyama, H.; Kobayashi, S. Enzymatic Ring-Opening Polymerization of Lactones Catalyzed by Lipase. *Chem. Lett.* **1993**, *22* (7), 1149–1150. https://doi.org/10.1246/cl.1993.1149.

(269) Kobayashi, S.; Uyama, H.; Kadokawa, J. *Enzymatic Polymerization towards Green Polymer Chemistry*; Springer, 2019.

(270) Kobayashi, S.; Uyama, H. In Vitro Polyester Synthesis via Enzymatic Polymerization. *Curr. Org. Chem.* **2002**, *6* (2), 209–222.

(271) Kobayashi, S.; Uyama, H. In Vitro Biosynthesis of Polyesters. In *Biopolyesters*; Babel, W., Steinbüchel, A., Eds.; Advances in Biochemical Engineering/Biotechnology; Springer: Berlin, Heidelberg, 2001; pp 241–262.

(272) Kobayashi, S.; Uyama, H. Precision Enzymatic Polymerization to Polyesters with Lipase Catalysts. *Macromol. Symp.* **1999**, *144* (1), 237–246. https://doi.org/10.1002/masy.19991440121.

(273) Namekawa, S.; Uyama, H.; Kobayashi, S. Lipase-Catalyzed Ring-Opening Polymerization and Copolymerization of β-Propiolactone. *Polym. J.* **1996**, *28* (8), 730–731. https://doi.org/10.1295/polymj.28.730.

(274) Brown, J. M.; Conn, A. D.; Pilcher, G.; Leitão, M. L. P.; Meng-Yan, Y. On the Strain Energy of 5-Ring and 6-Ring Lactones. *J. Chem. Soc. Chem. Commun.* **1989**, No. 23, 1817–1819. https://doi.org/10.1039/C39890001817.

(275) Houk, K. N.; Jabbari, A.; Hall, H. K.; Alemán, C. Why δ-Valerolactone Polymerizes and γ-Butyrolactone Does Not. *J. Org. Chem.* **2008**, *73* (7), 2674–2678. https://doi.org/10.1021/jo702567v.

(276) Saiyasombat, W.; Molloy, R.; Nicholson, T. M.; Johnson, A. F.; Ward, I. M.; Poshyachinda, S. Ring Strain and Polymerizability of Cyclic Esters. *Polymer* **1998**, *39* (23), 5581–5585. https://doi.org/10.1016/S0032-3861(97)10370-6.

© 2020 Tous droits réservés.

lilliad.univ-lille.fr

(277) Witt, T.; Häußler, M.; Mecking, S. No Strain, No Gain? Enzymatic Ring-Opening Polymerization of Strainless Aliphatic Macrolactones. *Macromol. Rapid Commun.* **2017**, *38* (4), 1600638. https://doi.org/10.1002/marc.201600638.

(278) Küllmer, K.; Kikuchi, H.; Uyama, H.; Kobayashi, S. Lipase-Catalyzed Ring-Opening Polymerization of α-Methyl-δ-Valerolactone and α-Methyl-ε-Caprolactone. *Macromol. Rapid Commun.* **1998**, *19* (2), 127–130. https://doi.org/10.1002/(SICI)1521-3927(19980201)19:2<127::AID-MARC127>3.0.CO;2-3.

(279) Duda, A.; Penczek, S.; Dubois, P.; Mecerreyes, D.; Jérôme, R. Oligomerization and Copolymerization of γ-Butyrolactone — a Monomer Known as Unable to Homopolymerize, 1. Copolymerization with ε-Caprolactone. *Macromol. Chem. Phys.* **1996**, *197* (4), 1273–1283. https://doi.org/10.1002/macp.1996.021970408.

(280) Gagliardi, M.; Bifone, A. Ring-Opening Copolymerization Thermodynamics and Kinetics of γ-Valerolactone/ϵ-Caprolactone. *PLOS ONE* **2018**, *13* (6), e0199231. https://doi.org/10.1371/journal.pone.0199231.

(281) Hong, M.; Chen, E. Y.-X. Completely Recyclable Biopolymers with Linear and Cyclic Topologies via Ring-Opening Polymerization of γ-Butyrolactone. *Nat. Chem.* **2016**, *8* (1), 42.

(282) Chalid, M.; Heeres, H. J.; Broekhuis, A. A. Ring-Opening of γ-Valerolactone with Amino Compounds. *J. Appl. Polym. Sci.* **2012**, *123* (6), 3556–3564. https://doi.org/10.1002/app.34842.

(283) MacDonald, R. T.; Pulapura, S. K.; Svirkin, Y. Y.; Gross, R. A.; Kaplan, D. L.; Akkara, J.; Swift, G.; Wolk, S. Enzyme-Catalyzed .Epsilon.-Caprolactone Ring-Opening Polymerization. *Macromolecules* **1995**, *28* (1), 73–78. https://doi.org/10.1021/ma00105a008.

(284) Kikuchi, H.; Uyama, H.; Kobayashi, S. Lipase-Catalyzed Ring-Opening Polymerization of Substituted Lactones. *Polym. J.* **2002**, *34* (11), 835–840. https://doi.org/10.1295/polymj.34.835.

(285) Kobayashi, S.; Takeya, K.; Suda, S.; Uyama, H. Lipase-Catalyzed Ring-Opening Polymerization of Medium-Size Lactones to Polyesters. *Macromol. Chem. Phys.* **1998**, *199* (8), 1729–1736. https://doi.org/10.1002/(SICI)1521-3935(19980801)199:8<1729::AID-MACP1729>3.0.CO;2-V.

(286) Uyama, H.; Suda, S.; Kikuchi, H.; Kobayashi, S. Extremely Efficient Catalysis of Immobilized Lipase in Ring-Opening Polymerization of Lactones. *Chem. Lett.* **1997**, *26* (11), 1109–1110. https://doi.org/10.1246/cl.1997.1109.

(287) Uyama, H.; Takeya, K.; Kobayashi, S. Enzymatic Ring-Opening Polymerization of Lactones to Polyesters by Lipase Catalyst: Unusually High Reactivity of Macrolides. *Bull. Chem. Soc. Jpn.* **1995**, *68* (1), 56–61. https://doi.org/10.1246/bcsj.68.56.

(288) Kobayashi, S.; Uyama, H.; Namekawa, S.; Hayakawa, H. Enzymatic Ring-Opening Polymerization and Copolymerization of 8-Octanolide by Lipase Catalyst. *Macromolecules* **1998**, *31* (17), 5655–5659. https://doi.org/10.1021/ma980396n.

(289) Namekawa, S.; Uyama, H.; Kobayashi, S. Lipase-Catalyzed Ring-Opening Polymerization of 16-Hexadecanolide. *Proc. Jpn. Acad. Ser. B* **1998**, *74* (4), 65–68. https://doi.org/10.2183/pjab.74.65.

(290) Uyama, H.; Kikuchi, H.; Takeya, K.; Hoshi, N.; Kobayashi, S. Immobilized Lipase Showing High Catalytic Activity toward Enzymatic Ring-Opening Polymerization of Macrolides. *Chem. Lett.* **1996**, *25* (2), 107–108. https://doi.org/10.1246/cl.1996.107.

(291) Uyama, H.; Takeya, K.; Hoshi, N.; Kobayashi, S. Lipase-Catalyzed Ring-Opening Polymerization of 12-Dodecanolide. *Macromolecules* **1995**, *28* (21), 7046–7050. https://doi.org/10.1021/ma00125a002.

© 2020 Tous droits réservés.

(292) Bisht, K. S.; Henderson, L. A.; Gross, R. A.; Kaplan, D. L.; Swift, G. Enzyme-Catalyzed Ring-Opening Polymerization of ω-Pentadecalactone. *Macromolecules* **1997**, *30* (9), 2705–2711. https://doi.org/10.1021/ma961869y.

(293) Müller, S.; Uyama, H.; Kobayashi, S. Lipase-Catalyzed Ring-Opening Polymerization of Cyclic Diesters. *Chem. Lett.* **1999**, *28* (12), 1317–1318. https://doi.org/10.1246/cl.1999.1317.

(294) Kaluzynski, K.; Lewinski, P.; Pretula, J.; Szymanski, R.; Penczek, S. ε-Caprolactone Polymerization Catalyzed by Heteropolyacid. Derivation of the Kinetic Equation for Activated Monomer Propagation and Determination of the Rate Constants of Propagation. *Macromolecules* **2019**, *52* (17), 6405–6415. https://doi.org/10.1021/acs.macromol.9b00672.

(295) Zhu, N.; Huang, W.; Hu, X.; Liu, Y.; Fang, Z.; Guo, K. Enzymatic Continuous Flow Synthesis of Thiol-Terminated Poly(δ-Valerolactone) and Block Copolymers. *Macromol. Rapid Commun.* *39* (8), 1700807. https://doi.org/10.1002/marc.201700807.

(296) Domski, G. J.; Rose, J. M.; Coates, G. W.; Bolig, A. D.; Brookhart, M. Living Alkene Polymerization: New Methods for the Precision Synthesis of Polyolefins. *Prog. Polym. Sci.* **2007**, *32* (1), 30–92. https://doi.org/10.1016/j.progpolymsci.2006.11.001.

(297) Thomas, J. M.; Raja, R.; Lewis, D. W. Single-Site Heterogeneous Catalysts. *Angew. Chem. Int. Ed.* **2005**, *44* (40), 6456–6482. https://doi.org/10.1002/anie.200462473.

(298) Zhang, X.; Fevre, M.; Jones, G. O.; Waymouth, R. M. Catalysis as an Enabling Science for Sustainable Polymers. *Chem. Rev.* **2018**, *118* (2), 839–885. https://doi.org/10.1021/acs.chemrev.7b00329.

(299) Hawker, C. J.; Wooley, K. L. The Convergence of Synthetic Organic and Polymer Chemistries. *Science* **2005**, *309* (5738), 1200–1205. https://doi.org/10.1126/science.1109778.

(300) Ajellal, N.; Carpentier, J.-F.; Guillaume, C.; Guillaume, S. M.; Helou, M.; Poirier, V.; Sarazin, Y.; Trifonov, A. Metal-Catalyzed Immortal Ring-Opening Polymerization of Lactones, Lactides and Cyclic Carbonates. *Dalton Trans.* **2010**, *39* (36), 8363–8376. https://doi.org/10.1039/C001226B.

(301) Bochmann, M. The Chemistry of Catalyst Activation: The Case of Group 4 Polymerization Catalysts. *Organometallics* **2010**, *29* (21), 4711–4740. https://doi.org/10.1021/om1004447.

(302) Hou, Z.; Wakatsuki, Y. Recent Developments in Organolanthanide Polymerization Catalysts. *Coord. Chem. Rev.* **2002**, *231* (1), 1–22. https://doi.org/10.1016/S0010-8545(02)00111-X.

(303) Albertsson, A.-C.; Varma, I. K. Recent Developments in Ring Opening Polymerization of Lactones for Biomedical Applications. *Biomacromolecules* **2003**, *4* (6), 1466–1486.

(304) Hedrick, J. L.; Magbitang, T.; Connor, E. F.; Glauser, T.; Volksen, W.; Hawker, C. J.; Lee, V. Y.; Miller, R. D. Application of Complex Macromolecular Architectures for Advanced Microelectronic Materials. *Chem. – Eur. J.* **2002**, *8* (15), 3308–3319. https://doi.org/10.1002/1521-3765(20020802)8:15<3308::AID-CHEM3308>3.0.CO;2-D.

(305) Liu, S.; Ren, C.; Zhao, N.; Shen, Y.; Li, Z. Phosphazene Bases as Organocatalysts for Ring-Opening Polymerization of Cyclic Esters. *Macromol. Rapid Commun.* **2018**, *39* (24), 1800485. https://doi.org/10.1002/marc.201800485.

(306) Appel, R.; Halstenberg, M. A Diazadiphosphetidine with Ring-Stabilized "Pentaamidophosphorus." *Angew. Chem. Int. Ed. Engl.* **1977**, *16* (4), 263–264. https://doi.org/10.1002/anie.197702631.

© 2020 Tous droits réservés.

lilliad.univ-lille.fr

(307) Goldwhite, H.; Gysegem, P.; Schow, S.; Swyke, C. Phosphorimidates and Related Compounds. *J. Chem. Soc. Dalton Trans.* **1975**, No. 1, 12–15. https://doi.org/10.1039/DT9750000012.

(308) Haasemann, P.; Goubeau, J. Darstellung und Schwingungsspektren von Verbindungen des Typus X3PNCH3. *Z. Für Anorg. Allg. Chem.* **1974**, *408* (3), 293–303. https://doi.org/10.1002/zaac.19744080310.

(309) Millington, D. Chapter 11. The Typical Elements. Part II: Groups IV and V. *Annu. Rep. Prog. Chem. Sect. Phys. Inorg. Chem.* **1973**, *70* (0), 315–348. https://doi.org/10.1039/PR9737000315.

(310) Schwesinger, R.; Schlemper, H.; Hasenfratz, C.; Willaredt, J.; Dambacher, T.; Breuer, T.; Ottaway, C.; Fletschinger, M.; Boele, J.; Fritz, H. Extremely Strong, Uncharged Auxiliary Bases; Monomeric and Polymer-Supported Polyaminophosphazenes (P2–P5). *Liebigs Ann.* **1996**, *1996* (7), 1055–1081.

(311) Schwesinger, R.; Willaredt, J.; Schlemper, H.; Keller, M.; Schmitt, D.; Fritz, H. Novel, Very Strong, Uncharged Auxiliary Bases; Design and Synthesis of Monomeric and Polymer-Bound Triaminoiminophosphorane Bases of Broadly Varied Steric Demand. *Chem. Ber.* **1994**, *127* (12), 2435–2454. https://doi.org/10.1002/cber.19941271215.

(312) Zhao, N.; Ren, C.; Li, H.; Li, Y.; Liu, S.; Li, Z. Selective Ring-Opening Polymerization of Non-Strained γ-Butyrolactone Catalyzed by A Cyclic Trimeric Phosphazene Base. *Angew. Chem.* **2017**, *129* (42), 13167–13170. https://doi.org/10.1002/ange.201707122.

(313) Li, H.; Zhao, N.; Ren, C.; Liu, S.; Li, Z. Synthesis of Linear and Star Poly(ε-Caprolactone) with Controlled and High Molecular Weights via Cyclic Trimeric Phosphazene Base Catalyzed Ring-Opening Polymerization. *Polym. Chem.* **2017**, *8* (47), 7369–7374. https://doi.org/10.1039/C7PY01673E.

(314) Illy, N.; Boileau, S.; Penelle, J.; Barbier, V. Metal-Free Activation in the Anionic Ring-Opening Polymerization of Cyclopropane Derivatives. *Macromol. Rapid Commun.* **2009**, *30* (20), 1731–1735. https://doi.org/10.1002/marc.200900303.

(315) Zhao, J.; Schlaad, H. Controlled Anionic Graft Polymerization of Ethylene Oxide Directly from Poly(N-Isopropylacrylamide). *Macromolecules* **2011**, *44* (15), 5861–5864. https://doi.org/10.1021/ma2012392.

(316) Förster, S.; Krämer, E. Synthesis of PB- PEO and PI- PEO Block Copolymers with Alkyllithium Initiators and the Phosphazene Base t-BuP4. *Macromolecules* **1999**, *32* (8), 2783–2785.

(317) Zhao, J.; Pahovnik, D.; Gnanou, Y.; Hadjichristidis, N. A "Catalyst Switch" Strategy for the Sequential Metal-Free Polymerization of Epoxides and Cyclic Esters/Carbonate. *Macromolecules* **2014**, *47* (12), 3814–3822. https://doi.org/10.1021/ma500830v.

(318) Koppel, I. A.; Schwesinger, R.; Breuer, T.; Burk, P.; Herodes, K.; Koppel, I.; Leito, I.; Mishima, M. Intrinsic Basicities of Phosphorus Imines and Ylides: A Theoretical Study. *J. Phys. Chem. A* **2001**, *105* (41), 9575–9586. https://doi.org/10.1021/jp012168s.

(319) Kolomeitsev, A. A.; Koppel, I. A.; Rodima, T.; Barten, J.; Lork, E.; Röschenthaler, G.-V.; Kaljurand, I.; Kütt, A.; Koppel, I.; Mäemets, V.; Leito, I. Guanidinophosphazenes: Design, Synthesis, and Basicity in THF and in the Gas Phase. *J. Am. Chem. Soc.* **2005**, *127* (50), 17656–17666. https://doi.org/10.1021/ja053543n.

(320) Garrido, G.; Koort, E.; Ràfols, C.; Bosch, E.; Rodima, T.; Leito, I.; Rosés, M. Acid−Base Equilibria in Nonpolar Media. Absolute PKa Scale of Bases in

© 2020 Tous droits réservés.

lilliad.univ-lille.fr

Tetrahydrofuran. *J. Org. Chem.* **2006**, *71* (24), 9062–9067. https://doi.org/10.1021/jo061432g.

(321) Kaljurand, I.; Kütt, A.; Sooväli, L.; Rodima, T.; Mäemets, V.; Leito, I.; Koppel, I. A. Extension of the Self-Consistent Spectrophotometric Basicity Scale in Acetonitrile to a Full Span of 28 PKa Units: Unification of Different Basicity Scales. *J. Org. Chem.* **2005**, *70* (3), 1019–1028. https://doi.org/10.1021/jo048252w.

(322) Solladié-Cavallo, A.; Liptaj, T.; Schmitt, M.; Solgadi, A. Iso-Propyl Phenylacetate: Formation of a Single Enolate with TBuP4 as Base. *Tetrahedron Lett.* **2002**, *43* (3), 415–418. https://doi.org/10.1016/S0040-4039(01)02157-8.

(323) Hong, M.; Chen, E. Y.-X. Towards Truly Sustainable Polymers: A Metal-Free Recyclable Polyester from Biorenewable Non-Strained γ-Butyrolactone. *Angew. Chem.* **2016**, *128* (13), 4260–4265. https://doi.org/10.1002/ange.201601092.

(324) Ottou, W. N.; Sardon, H.; Mecerreyes, D.; Vignolle, J.; Taton, D. Update and Challenges in Organo-Mediated Polymerization Reactions. *Prog. Polym. Sci.* **2016**, *56*, 64–115. https://doi.org/10.1016/j.progpolymsci.2015.12.001.

(325) Pietzonka, T.; Seebach, D. The P4-Phosphazene Base as Part of a New Metal-Free Initiator System for the Anionic Polymerization of Methyl Methacrylate. *Angew. Chem. Int. Ed. Engl.* **1993**, *32* (5), 716–717. https://doi.org/10.1002/anie.199307161.

(326) Schmitt, M.; Falivene, L.; Caporaso, L.; Cavallo, L.; Chen, E. Y.-X. High-Speed Organocatalytic Polymerization of a Renewable Methylene Butyrolactone by a Phosphazene Superbase. *Polym. Chem.* **2014**, *5* (9), 3261–3270. https://doi.org/10.1039/C3PY01579C.

(327) Liu, S.; Zhang, J.; Zuo, W.; Zhang, W.; Sun, W.-H.; Ye, H.; Li, Z. Synthesis of Aluminum Complexes Bearing 8-Anilide-5,6,7-Trihydroquinoline Ligands: Highly Active Catalyst Precursors for Ring-Opening Polymerization of Cyclic Esters. *Polymers* **2017**, *9* (3), 83. https://doi.org/10.3390/polym9030083.

(328) Luo, W.; Shi, T.; Liu, S.; Zuo, W.; Li, Z. Well-Designed Unsymmetrical Salphen-Al Complexes: Synthesis, Characterization, and Ring-Opening Polymerization Catalysis. *Organometallics* **2017**, *36* (9), 1736–1742. https://doi.org/10.1021/acs.organomet.7b00106.

(329) Shi, T.; Zheng, Q.-D.; Zuo, W.-W.; Liu, S.-F.; Li, Z.-B. Bimetallic Aluminum Complexes Supported by Bis(Salicylaldimine) Ligand: Synthesis, Characterization and Ring-Opening Polymerization of Lactide. *Chin. J. Polym. Sci.* **2018**, *36* (2), 149–156. https://doi.org/10.1007/s10118-018-2039-5.

(330) Shi, T.; Luo, W.; Liu, S.; Li, Z. Controlled Random Copolymerization of Rac-Lactide and ε-Caprolactone by Well-Designed Phenoxyimine Al Complexes. *J. Polym. Sci. Part Polym. Chem.* **2018**, *56* (6), 611–617. https://doi.org/10.1002/pola.28932.

(331) Zhang, J.; Liu, S.; Zuo, W.; Ye, H.; Li, Z. Synthesis of Dinuclear Aluminum Complexes Bearing Bis-Phenolate Ligand and Application in Ring-Opening Polymerization of ε-Caprolactone. *New J. Chem.* **2017**, *41* (6), 2358–2363. https://doi.org/10.1039/C6NJ03818B.

(332) Goldys, A. M.; Dixon, D. J. Organocatalytic Ring-Opening Polymerization of Cyclic Esters Mediated by Highly Active Bifunctional Iminophosphorane Catalysts. *Macromolecules* **2014**, *47* (4), 1277–1284. https://doi.org/10.1021/ma402258y.

(333) Zhang, L.; Nederberg, F.; Pratt, R. C.; Waymouth, R. M.; Hedrick, J. L.; Wade, C. G. Phosphazene Bases: A New Category of Organocatalysts for the Living Ring-Opening Polymerization of Cyclic Esters. *Macromolecules* **2007**, *40* (12), 4154–4158. https://doi.org/10.1021/ma070316s.

(334) Zhang, L.; Nederberg, F.; Messman, J. M.; Pratt, R. C.; Hedrick, J. L.; Wade, C. G. Organocatalytic Stereoselective Ring-Opening Polymerization of Lactide with

© 2020 Tous droits réservés.

lilliad.univ-lille.fr

Dimeric Phosphazene Bases. *J. Am. Chem. Soc.* **2007**, *129* (42), 12610–12611. https://doi.org/10.1021/ja074131c.

(335) Dharmaratne, N. U.; Pothupitiya, J. U.; Bannin, T. J.; Kazakov, O. I.; Kiesewetter, M. K. Triclocarban: Commercial Antibacterial and Highly Effective H-Bond Donating Catalyst for Ring-Opening Polymerization. *ACS Macro Lett.* **2017**, *6* (4), 421–425. https://doi.org/10.1021/acsmacrolett.7b00111.

(336) Alamri, H.; Zhao, J.; Pahovnik, D.; Hadjichristidis, N. Phosphazene-Catalyzed Ring-Opening Polymerization of ε-Caprolactone: Influence of Solvents and Initiators. *Polym. Chem.* **2014**, *5* (18), 5471–5478. https://doi.org/10.1039/C4PY00493K.

(337) Ladelta, V.; Kim, J. D.; Bilalis, P.; Gnanou, Y.; Hadjichristidis, N. Block Copolymers of Macrolactones/Small Lactones by a "Catalyst-Switch" Organocatalytic Strategy. Thermal Properties and Phase Behavior. *Macromolecules* **2018**. https://doi.org/10.1021/acs.macromol.8b00153.

(338) Bozell, J. J.; Petersen, G. R. Technology Development for the Production of Biobased Products from Biorefinery Carbohydrates—the US Department of Energy's "Top 10" Revisited. *Green Chem.* **2010**, *12* (4), 539–554. https://doi.org/10.1039/B922014C.

(339) Zhang, C.-J.; Hu, L.-F.; Wu, H.-L.; Cao, X.-H.; Zhang, X.-H. Dual Organocatalysts for Highly Active and Selective Synthesis of Linear Poly(γ-Butyrolactone)s with High Molecular Weights. *Macromolecules* **2018**, *51* (21), 8705–8711. https://doi.org/10.1021/acs.macromol.8b01757.

(340) Hong, M.; Tang, X.; Newell, B. S.; Chen, E. Y.-X. "Nonstrained" γ-Butyrolactone-Based Copolyesters: Copolymerization Characteristics and Composition-Dependent (Thermal, Eutectic, Cocrystallization, and Degradation) Properties. *Macromolecules* **2017**, *50* (21), 8469–8479. https://doi.org/10.1021/acs.macromol.7b02174.

(341) Douka, A.; Vouyiouka, S.; Papaspyridi, L.-M.; Papaspyrides, C. D. A Review on Enzymatic Polymerization to Produce Polycondensation Polymers: The Case of Aliphatic Polyesters, Polyamides and Polyesteramides. *Prog. Polym. Sci.* **2018**, *79*, 1–25. https://doi.org/10.1016/j.progpolymsci.2017.10.001.

(342) Edlund, U.; Albertsson, A.-C. Polyesters Based on Diacid Monomers. *Adv. Drug Deliv. Rev.* **2003**, *55* (4), 585–609. https://doi.org/10.1016/S0169-409X(03)00036-X.

(343) Carothers, W. H. Studies on Polymerization and Ring Formation. I. An Introduction to the General Theory of Condensation Polymers. *J. Am. Chem. Soc.* **1929**, *51* (8), 2548–2559.

(344) Carothers, W. H.; Arvin, J. A. Studies on Polymerization and Ring Formation. II. Poly-Esters. *J. Am. Chem. Soc.* **1929**, *51* (8), 2560–2570.

(345) Kricheldorf, H. R. Star Shaped and Hyperbranched Aromatic Polyesters. *Pure Appl. Chem.* **1998**, *70* (6), 1235–1238.

(346) Nummelin, S.; Skrifvars, M.; Rissanen, K. Polyester and Ester Functionalized Dendrimers. In *Dendrimers II: Architecture, Nanostructure and Supramolecular Chemistry*; Vögtle, F., Ed.; Topics in Current Chemistry; Springer: Berlin, Heidelberg, 2000; pp 1–67. https://doi.org/10.1007/3-540-46577-4_1.

(347) Albertsson, A.-C.; Ljungquist, O. Degradable Polymers. I. Synthesis, Characterization, and Long-Term in Vitro Degradation of a 14C-Labeled Aliphatic Polyester. *J. Macromol. Sci. Part - Chem.* **1986**, *23* (3), 393–409. https://doi.org/10.1080/00222338608063402.

(348) Debuissy, T.; Sangwan, P.; Pollet, E.; Avérous, L. Study on the Structure-Properties Relationship of Biodegradable and Biobased Aliphatic Copolyesters Based on 1,3-Propanediol, 1,4-Butanediol, Succinic and Adipic Acids. *Polymer* **2017**, *122*, 105–116. https://doi.org/10.1016/j.polymer.2017.06.045.

© 2020 Tous droits réservés.

(349) Jian, J.; Xiangbin, Z.; Xianbo, H. An Overview on Synthesis, Properties and Applications of Poly(Butylene-Adipate-Co-Terephthalate)–PBAT. *Adv. Ind. Eng. Polym. Res.* **2020**, *3* (1), 19–26. https://doi.org/10.1016/j.aiepr.2020.01.001.

(350) Pakdeedachakiat, W.; Phruksaphithak, N.; Boontawan, A. Pretreatment of Mulberry Stem by Cholinium-Based Amino Acid Ionic Liquids for Succinic Acid Fermentation and Its Application in Poly(Butylene) Succinate Production. *Bioresour. Technol.* **2019**, *291*, 121873. https://doi.org/10.1016/j.biortech.2019.121873.

(351) Pasma, S. A.; Daik, R.; Maskat, M. Y. Enzymatic Synthesis of Biodegradable Polyesters Using Succinic Acid Monomer Derived from Cellulose of Oil Palm Empty Fruit Bunch. *J. Wood Chem. Technol.* **2018**, *38* (6), 445–459. https://doi.org/10.1080/02773813.2018.1533976.

(352) Buzin, P.; Lahcini, M.; Schwarz, G.; Kricheldorf, H. R. Aliphatic Polyesters by Bismuth Triflate-Catalyzed Polycondensations of Dicarboxylic Acids and Aliphatic Diols. *Macromolecules* **2008**, *41* (22), 8491–8495. https://doi.org/10.1021/ma8017662.

(353) Chandure, A. S.; Umare, S. S. Synthesis, Characterization and Biodegradation Study of Low Molecular Weight Polyesters. *Int. J. Polym. Mater. Polym. Biomater.* **2007**, *56* (3), 339–353. https://doi.org/10.1080/00914030600865093.

(354) Díaz, A.; Katsarava, R.; Puiggalí, J. Synthesis, Properties and Applications of Biodegradable Polymers Derived from Diols and Dicarboxylic Acids: From Polyesters to Poly(Ester Amide)s. *Int. J. Mol. Sci.* **2014**, *15* (5), 7064–7123. https://doi.org/10.3390/ijms15057064.

(355) Papaspyrides, C. D.; Vouyiouka, S.; Georgousopoulou, I.-N.; Marinkovic, S.; Estrine, B.; Joly, C.; Dole, P. Feasibility of Solid-State Postpolymerization on Fossil- and Bio-Based Poly(Butylene Succinate) Including Polymer Upcycling Routes. *Ind. Eng. Chem. Res.* **2016**, *55* (20), 5832–5842. https://doi.org/10.1021/acs.iecr.6b00588.

(356) Shirahama, H.; Kawaguchi, Y.; Aludin, M. S.; Yasuda, H. Synthesis and Enzymatic Degradation of High Molecular Weight Aliphatic Polyesters. *J. Appl. Polym. Sci.* **2001**, *80* (3), 340–347. https://doi.org/10.1002/1097-4628(20010418)80:3<340::AID-APP1105>3.0.CO;2-F.

(357) Jin, H.-J.; Park, J.-K.; Park, K.-H.; Kim, M.-N.; Yoon, J.-S. Properties of Aliphatic Polyesters with N-Paraffinic Side Branches. *J. Appl. Polym. Sci.* **2000**, *77* (3), 547–555. https://doi.org/10.1002/(SICI)1097-4628(20000718)77:3<547::AID-APP10>3.0.CO;2-E.

(358) Jovanović, D.; Nikolić, M. S.; Đonlagić, J. A. Synthesis and Characterization of Biodegradable Aliphatic Copolyesters with Hydrophilic Soft Segments. *J. Serbian Chem. Soc.* **2004**, *69* (12), 1013–1028.

(359) Coltelli, M.-B.; Savi, S.; Maggiore, I. D.; Liuzzo, V.; Aglietto, M.; Ciardelli, F. A Model Study of Ti(OBu)4 Catalyzed Reactions during Reactive Blending of Polyethylene (PE) and Poly(Ethylene Terephthalate) (PET). *Macromol. Mater. Eng.* **2004**, *289* (5), 400–412. https://doi.org/10.1002/mame.200300297.

(360) Kricheldorf, H. R.; Gao, Q.; Buzin, P.; Schwarz, G. Aliphatic Polyesters of Butyne-1,4-Diol. *Macromol. Chem. Phys.* **2008**, *209* (4), 385–392. https://doi.org/10.1002/macp.200700429.

(361) Shigemoto, I.; Kawakami, T.; Taiko, H.; Okumura, M. A Quantum Chemical Study on the Polycondensation Reaction of Polyesters: The Mechanism of Catalysis in the Polycondensation Reaction. *Polymer* **2011**, *52* (15), 3443–3450. https://doi.org/10.1016/j.polymer.2011.05.055.

© 2020 Tous droits réservés.

(362) Umare, S. S.; Chandure, A. S.; Pandey, R. A. Synthesis, Characterization and Biodegradable Studies of 1,3-Propanediol Based Polyesters. *Polym. Degrad. Stab.* **2007**, *92* (3), 464–479. https://doi.org/10.1016/j.polymdegradstab.2006.10.007.

(363) Jacquel, N.; Freyermouth, F.; Fenouillot, F.; Rousseau, A.; Pascault, J. P.; Fuertes, P.; Saint-Loup, R. Synthesis and Properties of Poly(Butylene Succinate): Efficiency of Different Transesterification Catalysts. *J. Polym. Sci. Part Polym. Chem.* **2011**, *49* (24), 5301–5312. https://doi.org/10.1002/pola.25009.

(364) Zhao, J. B.; Li, K. Y.; Yang, W. T. Chain Extension of Polybutylene Adipate and Polybutylene Succinate with Adipoyl- and Terephthaloyl-Biscaprolactamate. *J. Appl. Polym. Sci.* **2007**, *106* (1), 590–598. https://doi.org/10.1002/app.26635.

(365) Kobayashi, S.; Uyama, H. Synthesis of Polyesters I: Hydrolase as Catalyst for Polycondensation (Condensation Polymerization). In *Enzymatic Polymerization towards Green Polymer Chemistry*; Kobayashi, S., Uyama, H., Kadokawa, J., Eds.; Green Chemistry and Sustainable Technology; Springer: Singapore, 2019; pp 105–163. https://doi.org/10.1007/978-981-13-3813-7_5.

(366) Ishihara, K. Dehydrative Condensation Catalyses. *Tetrahedron* **2009**, *65* (6), 1085–1109. https://doi.org/10.1016/j.tet.2008.11.004.

(367) de Almeida, R. M.; Souza, F. T. C.; Júnior, M. A. C.; Albuquerque, N. J. A.; Meneghetti, S. M. P.; Meneghetti, M. R. Improvements in Acidity for TiO2 and SnO2 via Impregnation with MoO3 for the Esterification of Fatty Acids. *Catal. Commun.* **2014**, *46*, 179–182. https://doi.org/10.1016/j.catcom.2013.12.020.

(368) Lang, X.; Jia, W.; Wang, Y.; Zhu, Z. Novel Fluorination of Polystyrene Sulfonic Acid Resin by CF3SO3H for High Stability and Strong Acidity. *Catal. Commun.* **2015**, *70*, 58–61. https://doi.org/10.1016/j.catcom.2015.07.017.

(369) Leng, Y.; Wang, J.; Zhu, D.; Ren, X.; Ge, H.; Shen, L. Heteropolyanion-Based Ionic Liquids: Reaction-Induced Self-Separation Catalysts for Esterification. *Angew. Chem.* **2009**, *121* (1), 174–177. https://doi.org/10.1002/ange.200803567.

(370) Zhan, S.; Tao, X.; Cai, L.; Liu, X.; Liu, T. The Carbon Material Functionalized with NH2+ and SO3H Groups Catalyzed Esterification with High Activity and Selectivity. *Green Chem.* **2014**, *16* (11), 4649–4653. https://doi.org/10.1039/C4GC01395F.

(371) Fernandes, S. A.; Natalino, R.; Gazolla, P. A. R.; da Silva, M. J.; Jham, G. N. P-Sulfonic Acid Calix[n]Arenes as Homogeneous and Recyclable Organocatalysts for Esterification Reactions. *Tetrahedron Lett.* **2012**, *53* (13), 1630–1633. https://doi.org/10.1016/j.tetlet.2012.01.078.

(372) Koshikari, Y.; Sakakura, A.; Ishihara, K. N,N-Diarylammonium Pyrosulfate as a Highly Effective Reverse Micelle-Type Catalyst for Hydrolysis of Esters. *Org. Lett.* **2012**, *14* (12), 3194–3197. https://doi.org/10.1021/ol301290c.

(373) Minakawa, M.; Baek, H.; Yamada, Y. M. A.; Han, J. W.; Uozumi, Y. Direct Dehydrative Esterification of Alcohols and Carboxylic Acids with a Macroporous Polymeric Acid Catalyst. *Org. Lett.* **2013**, *15* (22), 5798–5801. https://doi.org/10.1021/ol4028495.

(374) Sakakura, A.; Koshikari, Y.; Akakura, M.; Ishihara, K. Hydrophobic N,N-Diarylammonium Pyrosulfates as Dehydrative Condensation Catalysts under Aqueous Conditions. *Org. Lett.* **2012**, *14* (1), 30–33. https://doi.org/10.1021/ol2027366.

(375) Tanemura, K.; Suzuki, T. Sulfonated Polypyrene (S-PPR) as Efficient Catalyst for Esterification of Carboxylic Acids with Equimolar Amounts of Alcohols without Removing Water. *Tetrahedron Lett.* **2013**, *54* (15), 1972–1975. https://doi.org/10.1016/j.tetlet.2013.01.126.

© 2020 Tous droits réservés.

(376) Zhou, Y.; Guo, Z.; Hou, W.; Wang, Q.; Wang, J. Polyoxometalate-Based Phase Transfer Catalysis for Liquid–Solid Organic Reactions: A Review. *Catal. Sci. Technol.* **2015**, *5* (9), 4324–4335. https://doi.org/10.1039/C5CY00674K.

(377) Ferré, M.; Pleixats, R.; Man, M. W. C.; Cattoën, X. Recyclable Organocatalysts Based on Hybrid Silicas. *Green Chem.* **2016**, *18* (4), 881–922. https://doi.org/10.1039/C5GC02579F.

(378) Gruttadauria, M.; Giacalone, F.; Noto, R. Supported Proline and Proline-Derivatives as Recyclable Organocatalysts. *Chem. Soc. Rev.* **2008**, *37* (8), 1666–1688. https://doi.org/10.1039/B800704G.

(379) Gao, L.; Liu, T.; Tao, X.; Huang, Y. 2,2,6,6-Tetramethylpiperidinium Triflate (TMPT): A Highly Selective and Self-Separated Catalyst for Esterification. *Tetrahedron Lett.* **2016**, *57* (44), 4905–4909. https://doi.org/10.1016/j.tetlet.2016.09.061.

(380) Ishihara, K.; Nakagawa, S.; Sakakura, A. Bulky Diarylammonium Arenesulfonates as Selective Esterification Catalysts. *J. Am. Chem. Soc.* **2005**, *127* (12), 4168–4169. https://doi.org/10.1021/ja050223v.

(381) Sakakura, A.; Nakagawa, S.; Ishihara, K. Bulky Diarylammonium Arenesulfonates as Mild and Extremely Active Dehydrative Ester Condensation Catalysts. *Tetrahedron* **2006**, *62* (2), 422–433. https://doi.org/10.1016/j.tet.2005.09.059.

(382) H, A.; M, B. DIPHENYLAMMONIUM TRIFLATE AS AN EFFECTIVE CATALYST FOR POLYESTERIFICATION REACTIONS. **2006**, *15* (975), 701–707.

(383) H, A.; M, B. POLYESTERIFICATION KINETICS BETWEEN ADIPIC ACID AND HEXAMETHYLENE GLYCOL USING DIPHENYLAMMONIUM TRIFLATE AS CATALYST. **2006**, *15* (1177), 921–928.

(384) Szwarc, M. Living Polymers and Mechanisms of Anionic Polymerization. In *Living Polymers and Mechanisms of Anionic Polymerization*; Springer, 1983; pp 1–177.

(385) Kamigaito, M.; Ando, T.; Sawamoto, M. Metal-Catalyzed Living Radical Polymerization. *Chem. Rev.* **2001**, *101* (12), 3689–3746. https://doi.org/10.1021/cr9901182.

(386) Melker, A.; Fors, B. P.; Hawker, C. J.; Poelma, J. E. Continuous Flow Synthesis of Poly(Methyl Methacrylate) via a Light-Mediated Controlled Radical Polymerization. *J. Polym. Sci. Part Polym. Chem.* **2015**, *53* (23), 2693–2698. https://doi.org/10.1002/pola.27765.

(387) Bou-Hamdan, F. R.; Seeberger, P. H. Visible-Light-Mediated Photochemistry: Accelerating Ru(Bpy)32+-Catalyzed Reactions in Continuous Flow. *Chem. Sci.* **2012**, *3* (5), 1612–1616. https://doi.org/10.1039/C2SC01016J.

(388) Tucker, J. W.; Zhang, Y.; Jamison, T. F.; Stephenson, C. R. J. Visible-Light Photoredox Catalysis in Flow. *Angew. Chem.* **2012**, *124* (17), 4220–4223. https://doi.org/10.1002/ange.201200961.

(389) Natalello, A.; Morsbach, J.; Friedel, A.; Alkan, A.; Tonhauser, C.; Müller, A. H. E.; Frey, H. Living Anionic Polymerization in Continuous Flow: Facilitated Synthesis of High-Molecular Weight Poly(2-Vinylpyridine) and Polystyrene. *Org. Process Res. Dev.* **2014**, *18* (11), 1408–1412. https://doi.org/10.1021/op500149t.

(390) Otsu, T.; Yoshida, M. Role of Initiator-Transfer Agent-Terminator (Iniferter) in Radical Polymerizations: Polymer Design by Organic Disulfides as Iniferters. *Makromol. Chem. Rapid Commun.* **1982**, *3* (2), 127–132. https://doi.org/10.1002/marc.1982.030030208.

© 2020 Tous droits réservés.

(391) Magenau, A. J. D.; Strandwitz, N. C.; Gennaro, A.; Matyjaszewski, K. Electrochemically Mediated Atom Transfer Radical Polymerization. *Science* **2011**, *332* (6025), 81–84. https://doi.org/10.1126/science.1202357.

(392) Caruso, M. M.; Davis, D. A.; Shen, Q.; Odom, S. A.; Sottos, N. R.; White, S. R.; Moore, J. S. Mechanically-Induced Chemical Changes in Polymeric Materials. *Chem. Rev.* **2009**, *109* (11), 5755–5798. https://doi.org/10.1021/cr9001353.

(393) Liu, X.; Zhang, L.; Cheng, Z.; Zhu, X. Metal-Free Photoinduced Electron Transfer–Atom Transfer Radical Polymerization (PET–ATRP) via a Visible Light Organic Photocatalyst. *Polym. Chem.* **2016**, *7* (3), 689–700. https://doi.org/10.1039/C5PY01765C.

(394) Otsu, T.; Yoshida, M.; Tazaki, T. A Model for Living Radical Polymerization. *Makromol. Chem. Rapid Commun.* **1982**, *3* (2), 133–140. https://doi.org/10.1002/marc.1982.030030209.

(395) McCarthy, B. G.; Pearson, R. M.; Lim, C.-H.; Sartor, S. M.; Damrauer, N. H.; Miyake, G. M. Structure–Property Relationships for Tailoring Phenoxazines as Reducing Photoredox Catalysts. *J. Am. Chem. Soc.* **2018**, *140* (15), 5088–5101. https://doi.org/10.1021/jacs.7b12074.

(396) Pearson, R. M.; Lim, C.-H.; McCarthy, B. G.; Musgrave, C. B.; Miyake, G. M. Organocatalyzed Atom Transfer Radical Polymerization Using N-Aryl Phenoxazines as Photoredox Catalysts. *J. Am. Chem. Soc.* **2016**, *138* (35), 11399–11407. https://doi.org/10.1021/jacs.6b08068.

(397) Theriot, J. C.; McCarthy, B. G.; Lim, C.-H.; Miyake, G. M. Organocatalyzed Atom Transfer Radical Polymerization: Perspectives on Catalyst Design and Performance. *Macromol. Rapid Commun.* **2017**, *38* (13), 1700040. https://doi.org/10.1002/marc.201700040.

(398) Theriot, J. C.; Lim, C.-H.; Yang, H.; Ryan, M. D.; Musgrave, C. B.; Miyake, G. M. Organocatalyzed Atom Transfer Radical Polymerization Driven by Visible Light. *Science* **2016**, *352* (6289), 1082–1086. https://doi.org/10.1126/science.aaf3935.

(399) Gromada, J.; Matyjaszewski, K. Simultaneous Reverse and Normal Initiation in Atom Transfer Radical Polymerization. *Macromolecules* **2001**, *34* (22), 7664–7671. https://doi.org/10.1021/ma010864k.

(400) Xia, J.; Matyjaszewski, K. Controlled/"Living" Radical Polymerization. Homogeneous Reverse Atom Transfer Radical Polymerization Using AIBN as the Initiator. *Macromolecules* **1997**, *30* (25), 7692–7696. https://doi.org/10.1021/ma9710085.

(401) Tsarevsky, N. V.; Matyjaszewski, K. "Green" Atom Transfer Radical Polymerization: From Process Design to Preparation of Well-Defined Environmentally Friendly Polymeric Materials. *Chem. Rev.* **2007**, *107* (6), 2270–2299. https://doi.org/10.1021/cr050947p.

(402) Jakubowski, W.; Matyjaszewski, K. Activators Regenerated by Electron Transfer for Atom-Transfer Radical Polymerization of (Meth)Acrylates and Related Block Copolymers. *Angew. Chem. Int. Ed.* **2006**, *45* (27), 4482–4486. https://doi.org/10.1002/anie.200600272.

(403) Matyjaszewski, K.; Jakubowski, W.; Min, K.; Tang, W.; Huang, J.; Braunecker, W. A.; Tsarevsky, N. V. Diminishing Catalyst Concentration in Atom Transfer Radical Polymerization with Reducing Agents. *Proc. Natl. Acad. Sci.* **2006**, *103* (42), 15309–15314.

(404) Prier, C. K.; Rankic, D. A.; MacMillan, D. W. C. Visible Light Photoredox Catalysis with Transition Metal Complexes: Applications in Organic Synthesis. *Chem. Rev.* **2013**, *113* (7), 5322–5363. https://doi.org/10.1021/cr300503r.

© 2020 Tous droits réservés.

lilliad.univ-lille.fr

(405) Guan, Z.; Smart, B. A Remarkable Visible Light Effect on Atom-Transfer Radical Polymerization. *Macromolecules* **2000**, *33* (18), 6904–6906.
(406) Dadashi-Silab, S.; Tasdelen, M. A.; Yagci, Y. Photoinitiated Atom Transfer Radical Polymerization: Current Status and Future Perspectives. *J. Polym. Sci. Part Polym. Chem.* **2014**, *52* (20), 2878–2888. https://doi.org/10.1002/pola.27327.
(407) Trotta, J. T.; Fors, B. P. Organic Catalysts for Photocontrolled Polymerizations. *Synlett* **2016**, *27* (5), 702–713. https://doi.org/10.1055/s-0035-1561264.
(408) Pan, X.; Lamson, M.; Yan, J.; Matyjaszewski, K. Photoinduced Metal-Free Atom Transfer Radical Polymerization of Acrylonitrile. *ACS Macro Lett.* **2015**, *4* (2), 192–196. https://doi.org/10.1021/mz500834g.
(409) Selsted, M. E.; Becker, H. W. Eosin Y: A Reversible Stain for Detecting Electrophoretically Resolved Protein. *Anal. Biochem.* **1986**, *155* (2), 270–274. https://doi.org/10.1016/0003-2697(86)90436-7.
(410) Salvador, A.; Chisvert, A. *Analysis of Cosmetic Products*; Elsevier, 2011.
(411) Sabnis, R. W. *Handbook of Acid-Base Indicators*; CRC Press, 2007.
(412) Dhingra, V. K. A., Sunita; Dhingra, S. *College Practical Chemistry*; Universities Press, 2005.
(413) Penzkofer, A.; Beidoun, A.; Speiser, S. Singlet Excited-State Absorption of Eosin Y. *Chem. Phys.* **1993**, *170* (1), 139–148. https://doi.org/10.1016/0301-0104(93)80099-U.
(414) Penzkofer, A.; Beidoun, A.; Daiber, M. Intersystem-Crossing and Excited-State Absorption in Eosin Y Solutions Determined by Picosecond Double Pulse Transient Absorption Measurements. *J Lumin.* **1992**, *51*, 297–314.
(415) Prasad Hari, D.; König, B. Synthetic Applications of Eosin Y in Photoredox Catalysis. *Chem. Commun.* **2014**, *50* (51), 6688–6699. https://doi.org/10.1039/C4CC00751D.
(416) Avens, H. J.; Bowman, C. N. Mechanism of Cyclic Dye Regeneration during Eosin-Sensitized Photoinitiation in the Presence of Polymerization Inhibitors. *J. Polym. Sci. Part Polym. Chem.* **2009**, *47* (22), 6083–6094. https://doi.org/10.1002/pola.23649.
(417) Kızılel, S.; Pérez-Luna, V. H.; Teymour, F. Photopolymerization of Poly(Ethylene Glycol) Diacrylate on Eosin-Functionalized Surfaces. *Langmuir* **2004**, *20* (20), 8652–8658. https://doi.org/10.1021/la0496744.
(418) Farsari, M.; Filippidis, G.; Sambani, K.; Drakakis, T. S.; Fotakis, C. Two-Photon Polymerization of an Eosin Y-Sensitized Acrylate Composite. *J. Photochem. Photobiol. Chem.* **2006**, *181* (1), 132–135. https://doi.org/10.1016/j.jphotochem.2005.11.025.
(419) Garlets, Z. J.; Nguyen, J. D.; Stephenson, C. R. J. The Development of Visible-Light Photoredox Catalysis in Flow. *Isr. J. Chem.* **2014**, *54* (4), 351–360. https://doi.org/10.1002/ijch.201300136.
(420) Steinbacher, J. L.; McQuade, D. T. Polymer Chemistry in Flow: New Polymers, Beads, Capsules, and Fibers. *J. Polym. Sci. Part Polym. Chem.* **2006**, *44* (22), 6505–6533. https://doi.org/10.1002/pola.21630.
(421) Hook, B. D. A.; Dohle, W.; Hirst, P. R.; Pickworth, M.; Berry, M. B.; Booker-Milburn, K. I. A Practical Flow Reactor for Continuous Organic Photochemistry. *J. Org. Chem.* **2005**, *70* (19), 7558–7564. https://doi.org/10.1021/jo050705p.
(422) Lu, H.; A. Schmidt, M.; F. Jensen, K. Photochemical Reactions and On-Line UV Detection in Microfabricated Reactors. *Lab. Chip* **2001**, *1* (1), 22–28. https://doi.org/10.1039/B104037P.
(423) Elliott, L. D.; Knowles, J. P.; Koovits, P. J.; Maskill, K. G.; Ralph, M. J.; Lejeune, G.; Edwards, L. J.; Robinson, R. I.; Clemens, I. R.; Cox, B. Batch versus Flow

© 2020 Tous droits réservés.

Photochemistry: A Revealing Comparison of Yield and Productivity. *Chem. Eur. J.* **2014**, *20* (46), 15226–15232.

(424) Enright, T. E.; Cunningham, M. F.; Keoshkerian, B. Nitroxide-Mediated Polymerization of Styrene in a Continuous Tubular Reactor. *Macromol. Rapid Commun.* **2005**, *26* (4), 221–225. https://doi.org/10.1002/marc.200400531.

(425) Fukuyama, T.; Kajihara, Y.; Ryu, I.; Studer, A. Nitroxide-Mediated Polymerization of Styrene, Butyl Acrylate, or Methyl Methacrylate by Microflow Reactor Technology. *Synthesis* **2012**, *44* (16), 2555–2559. https://doi.org/10.1055/s-0031-1290780.

(426) Chen, M.; Johnson, J. A. Improving Photo-Controlled Living Radical Polymerization from Trithiocarbonates through the Use of Continuous-Flow Techniques. *Chem. Commun.* **2015**, *51* (31), 6742–6745. https://doi.org/10.1039/C5CC01562F.

(427) Wenn, B.; Conradi, M.; Demetrio Carreiras, A.; M. Haddleton, D.; Junkers, T. Photo-Induced Copper-Mediated Polymerization of Methyl Acrylate in Continuous Flow Reactors. *Polym. Chem.* **2014**, *5* (8), 3053–3060. https://doi.org/10.1039/C3PY01762A.

(428) Zhang, G.; Song, I. Y.; Ahn, K. H.; Park, T.; Choi, W. Free Radical Polymerization Initiated and Controlled by Visible Light Photocatalysis at Ambient Temperature. *Macromolecules* **2011**, *44* (19), 7594–7599. https://doi.org/10.1021/ma201546c.

(429) Kutahya, C.; Aykac, F. S.; Yilmaz, G.; Yagci, Y. LED and Visible Light-Induced Metal Free ATRP Using Reducible Dyes in the Presence of Amines. *Polym. Chem.* **2016**, *7* (39), 6094–6098. https://doi.org/10.1039/C6PY01417H.

(430) Sharma, V.; Tepe, J. J. Diastereochemical Diversity of Imidazoline Scaffolds via Substrate Controlled TMSCl Mediated Cycloaddition of Azlactones. *Org. Lett.* **2005**, *7* (22), 5091–5094. https://doi.org/10.1021/ol052118w.

(431) Cornils, B.; Herrmann, W. A.; Xu, J.-H.; Zanthoff, H.-W. *Catalysis from A to Z: A Concise Encyclopedia*; John Wiley & Sons, 2020.

(432) Roos, S. G.; Müller, A. H. E.; Matyjaszewski, K. Copolymerization of N-Butyl Acrylate with Methyl Methacrylate and PMMA Macromonomers: Comparison of Reactivity Ratios in Conventional and Atom Transfer Radical Copolymerization. *Macromolecules* **1999**, *32* (25), 8331–8335. https://doi.org/10.1021/ma9819337.

(433) Yilmaz, G.; Yagci, Y. Photoinduced Metal-Free Atom Transfer Radical Polymerizations: State-of-the-Art, Mechanistic Aspects and Applications. *Polym. Chem.* **2018**, *9* (14), 1757–1762. https://doi.org/10.1039/C8PY00207J.

© 2020 Tous droits réservés.